Faculteit Wetenschappen

Departement Natuurkunde
Theory of Quantum Systems and Complex Systems

# A physical approach to financial derivatives: Pricing and the inverse pricing problem

# Een fysische benadering van financiële derivaten: Prijsbepaling en het inverse prijzingsprobleem

Proefschrift voorgelegd tot het behalen van de graad van

**Doctor in de Wetenschappen**

aan de Universiteit Antwerpen te verdedigen door

**Lingzhi Liang**

Promotor: Prof. Dr. Jacques Tempère

Antwerpen, June 14, 2012

## Doctoral committee:

Prof. Dr. Michèle Vanmaele (Ghent University)

Prof. Dr. Cornelis W. Oosterlee (Delft University of Technology)

Prof. Dr. Karel In't Hout (UA, dept. mathematics)

Prof. Dr. Dirk Lamoen (UA, Chairman)

Prof. Dr. Sabine Van Doorslaer (UA, Secretary)

Prof. Dr. Jacques Tempère (UA, Promotor)

# Acknowledgements

# Contents

# 1

# Introduction

Uncertainty is the dominant feature of the financial markets. Due to its random nature, trying to predict future prices of individual financial instruments makes little sense. One way to cope with financial risks and uncertainties is to construct optimal portfolios of different instruments based on the idea of diversification. Alternatively, one can introduce so called financial derivatives (the name emphasizes that their prices are derived from the prices of some underlying financial instruments). While some financial derivatives are fairly simple, others are quite complicated and require considerable mathematical background. The excellent power of financial derivatives to hedge risks has led to their widespread use and trade, both for hedging and for speculating. As a result, the size of the derivatives market has exploded from 3 trillion dollars in 1988 over 26 trillion dollars in 1995 to 439 trillion dollars in 2009. As such, it overtook the world GDP in goods and services, which stands at 63 trillion dollars. Also the complexity of financial derivatives has increased, as ever more specialized products are in demand.

Physics covers a wide range of phenomena, and it aims to connect the things observable to humans to root causes and then relate these causes together to generate general rules for these complex systems. Naturally, applying sophisticated methods from physics to the study of financial complex system is a significant attempt. In the present dissertation I show how to model the time evolution of financial derivatives in order to capture their empirical features, and based on these realistic models I focus on derivative pricing as well as risk management by using modern physical approaches.

In this very first chapter, I would like to start by giving three introductory parts intended to open the world of financial derivatives to non-specialist audiences. Part 1.1 provides an introduction to a variety of common financial derivatives and the market in which they trade. It also explores how these instruments appeared and their functions. In this chapter, some fundamentals of determining the price of derivatives are gradually introduced. Part 1.2 describes the famous Black-Scholes option pricing model, the Black-Scholes implied volatility and the model's limits. Part 1.3 concentrates on how to beyond the Black-Scholes model to meet the facts of the market by introducing stochastic volatility, jumps and their combinations. Part 1.4 turns to an overview of the pricing techniques. In particular, we will take a glance at the path integral approach. And finally, the key contributions of this thesis are listed after these introductory parts, together with an outline of this thesis, in part 1.5.

## 1.1 A tour of financial derivatives and markets

### 1.1.1 Forward and futures contracts

Recall that derivatives are financial instruments whose values are dependent on values of other assets, called underlying assets. Two of the simplest examples of derivatives are forward contracts and future contracts. A **forward** contract, and also a **future** contract, is a commitment by two parties to engage in a transaction, in which one party, the buyer, often called the "long", agrees to buy from the other party, the seller, often called the "short" [1], an underlying asset or other derivative at a future date with the price established at the start of the contract. For example, Alice may sign a contract that she will buy from Bob one tonne of copper for 8000 dollars exactly one year from now. This is a forward contract - if it were traded in a standardized form at an exchange, it would be called a futures contract.

Committing to the future purchase or sale of an asset at an $agreed-upon$ price, thus eliminating the uncertainty of future price fluctuation is the funda-

[1] Here words *long* and *short* are used not as adjectives but as nouns, which is a convention in the derivatives industry.

mental motivation of these two contracts. A very important aspect of them is that neither party pays any money at the start, while at later dates the buyer, the long, benefits from price increases, and the seller, the short, benefits from price decreases.

As an example, suppose an European subsidiary of Apple expects to send it €100 million in six months. When Apple receives the euros, it will then convert them to US dollars. In fact, Apple is effectively in a long-euro and short-dollar position, that is, it will have to sell euros and to buy dollars. Entering into a currency forward contract is especially useful in this situation, because it enables Apple to lock in the €/$ exchange rate at which it will sell euros and buy dollars in six months, thus protecting against a decrease in that exchange rate. For example, Apple goes to a bank and asks for a quote on a currency forward for €100 million in six months. The bank quotes a rate of $1.35. Now let us say that six months later, the spot rate for euros is $1.3. Apple is very pleased that it locked in a rate of $1.35. It delivers the €100 million and receives $135 million at the pre-specified rate of $1.35 rather than $1.3. This simplified example is a currency forward hedge. A **hedge** is an investment position designed to offset potential losses, in our case a short-euro and long-dollar position to offset its original long-euro and short-dollar position.

Various types of forward and future contracts exist according to the underlying asset groups on which these contracts are created. For instance, besides on currency, they can be on equity (individual stocks, stock portfolios, stock indices), on bond and interest rate (individual bonds, bond portfolios, forward rate agreements), and on fixed-income, etc. There is an extra group for futures contracts called commodity futures, which covers traditional agricultural, metal and petroleum products.

One may wonder how the bank in the previous example deals with the risk it takes from Apple. Typically, the bank does not want to hold this exposure, but rather lays it off by transacting with other parties. Thus, the bank is a wholesaler of risk - buying it, selling it, and trying to earn a profit off the spread between its buying price and selling price. By using its technical expertise, its vast network of contacts, and its access to critical financial market information, the bank provides a more efficient means for end users, like Apple.

When a forward or future contract expires, the two parties long and short can either engage in delivery of the asset, or settle the net cash equivalent, called the cash settlement. The possibility exists, however, that one party might wish to terminate the contract prior to expiration. That party can then create a new forward or future contract expiring at the same date as the original contract, taking the opposite position instead. It is apparent that that party has no further exposure to the price fluctuation.

There is always another possibility that one party could default. For example, in the aforementioned transition between Apple and the bank, suppose that perhaps because of bankruptcy or insolvency, the bank cannot come up with the $135 million, so Apple would purchase the US dollar in the open market at the prevailing spot rate $1.3, that is $130 million. The loss $5 million can be viewed as the credit risk Apple faces. Not surprisingly, this amount is just the market value of the contract at the point of expiration when the spot rate is $1.3. There are various methods of managing the credit risk. One particular method is called marking to market, i.e. Apple and the bank may agree in advance that they settle up the amount owed and restructure the contract so that it remains in force but with an updated price at whatever dates they feel are appropriate before the expiration of their contract. Marking to market avoids one party from becoming too deeply indebted to pay the other.

Forward contracts and **swaps**, which can be viewed as a series of forward contracts, are sometimes marked to market to mitigate credit risk, while the futures contracts are marked to market every day. Forward contracts are private created, over-the-counter customized instruments that carry credit risk. They are not created in any specific location but rather initiated between any two parties who wish to enter into such a contract. Though subjected to default risk, forward contracts offer the advantage of customization, the tailoring of a contract's terms, with target expiry dates, specific underlying assets and risks that parties involved, specifically large corporations and institutions, wish to reduce or take [1]. In contrast, futures contracts are publicly traded, exchange-listed standardized instruments that effectively have no credit risk. They are created on organized

[1]Some one may want risk because of the potential profits achieved by using their expertise in measuring the actual risk relative to the one perceived by the market.

trading facilities referred to as futures exchanges. In addition, futures contracts are standardized, meaning that it is the exchange, rather than the individual parties, that sets the terms and conditions, which makes a secondary market trading the preciously created contracts possible. Moreover, each futures exchange has a division or subsidiary called a clearinghouse that performs the specific responsibilities of paying and collecting daily gains and losses, thus guaranteeing the two parties against credit losses.

Both forwards and futures play a similar role: they provide price discovery and risk management, make the markets for the underlying assets more efficient, and permit trading at low transaction costs. These characteristics are also associated with other derivative markets. There are a variety of strategies and applications using forward and futures contracts. For a more thorough discussion about forwards and futures I refer to (1, 2).

I conclude this subsection with a question on our aforementioned currency forward contract - what if the exchange rate had risen, say the spot rate for euros is \$1.5 at expiry date? Apple would still have had to deliver €100 million and receive \$135 million, rather than \$150 million if it turns to the open market. This is due to the fact that Apple has the **obligation**, not the right, to buy dollars and sell euros in six months at a fixed exchange rate agreed, without paying cash at the start. To obtain such a right, in contrast to agreeing to an obligation, one must pay money at the initial time. These instruments, called options, are the subject of the next subsection.

### 1.1.2 Options

Now we turn to options. An **option** is a financial derivative contract that provides one party the right to buy or sell an underlying asset or other derivative at a prespecified price, called the exercise price, **strike price**, striking price or strike, by a certain future time, called the **expiration date**. The party holding the right is the option buyer, called the option holder or the "long"; the party granting the right is the option seller, called the option writer or the "short". There are two types of options, a **call**, an option granting the right to buy the underlying, and a **put**[1], an option granting the right to sell the underlying. This right to buy or sell is held by the "long". Taking the right but not the obligation to buy or sell an underlying asset at a fixed price in the future requires a cash payment from the "long" to the "short" up front. This amount of money is commonly referred to as the **option price**, also called the option premium or just the premium. Yet options can be privately created, over-the-counter, customized instruments that are subject to credit risk, just as forward contracts. Unlike the credit risk in forward contracts which is bilateral, meaning that the long assumes the risk of the short defaulting, and the short assumes the risk of the long defaulting, the credit risk in an option is unilateral - only the long who pays the premium up front faces credit risk. However, there is a large market for publicly traded, exchange-listed, standardized options, for which credit risk is essentially eliminated by the clearinghouse.

Almost anything with a random outcome can have an option on it. Identified by the nature of the underlying, options can be categorized as financial options (on stock, index, bond, interest rate, currency, etc.), options on futures, commodity options, and other types of options (on such underlying assets as electricity, various sources of energy, and even weather, etc.).

The use of the right to buy or sell the underlying by the long is referred to as exercise or exercising the option. There are two primary exercise styles associated with options. One type of option that can be exercised only on its expiration day is called a **European option**. The other type which can be exercised on any day through the expiration day is generally called an **American option**[2].

An important concept in the study of options is the notion of an option's moneyness, which can be classified into three groups, namely in-the-money, out-of-the-money, and at-the-money. **In-the-money** options are those in which exercising the option would produce a net cash inflow. Thus, calls are in-the-money

[1] The derivatives industry often uses nouns, verbs, adjectives, and adverbs as parts of speech different from their usual meaning (2). Just as *long* and *short* are used as nouns, here the words *call* and *put* denote other things than the corresponding verbs.

[2] These terms have nothing to do with Europe or America. There is no definitive history to explain how they came into use, and both types of options are found in Europe and America.

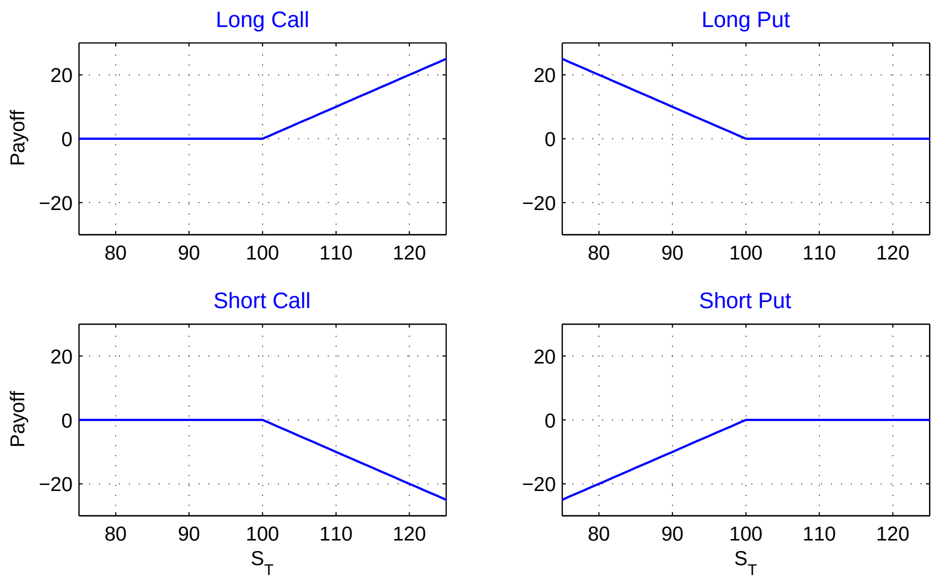


**Figure 1.1:** The option values at expiration (payoffs) as a function of the underlying price at expiration. The upper row panels represent the payoffs for the the long (option holder), the lower row panels for the short (option seller), for both European and American calls and puts. The strike price $K$ is assumed to be 100.

when the value of the underlying exceeds the strike price, whereas puts are in-the-money when the value of the strike price exceeds the underlying price. Conversely, when calls and puts are **out-of-the-money**, the long does not have the obligation to exercise the option. An option is called **at-the-money** when the underlying are exactly the same as the strike price.

An option's value at expiration is called its **payoff**. Denote the price of the underlying at time 0 (today) and time $T$ (expiration) by $S_0$ and $S_T$, the strike price by $K$, the price of European call and put by $c$ and $p$, the price of American call and put by $C$ and $P$, respectively. Obviously, only those options that are in-the-money would be exercised, the others simply expire. Therefore, the payoff of a call option is either the difference between the underlying price and the strike price or zero, whichever is greater: $\max(S_T - K, 0)$; the payoff of a put option is worth either the difference between the strike price and the underlying price or zero, whichever is greater: $\max(K - S_T, 0)$. Note that at expiration, a European option and an American option have the same payoff because they are equivalent instruments at that point. Figure 1.1 illustrates the payoffs as a function of $S_T$. Obviously, the shorts are the negative of the longs.

To obtain the option's value at present time from this payoff, which is a random value due to the uncertainty of the underlying price at expiration date, we should take its expectation value, and then discount this future value to the present value. This is due to the common knowledge and wisdom that when depositing a certain amount of money in a bank account, everybody expects that the amount grows as time goes by. The fact that receiving a given amount of money tomorrow is not equivalent to receiving exactly the same amount today leads to the European option's prices:

$$\begin{aligned} c &= \mathrm{PV}\left\{\mathbb{E}\left[\max\left(S_T - K, 0\right)\right]\right\}, \qquad (1.1) \\ p &= \mathrm{PV}\left\{\mathbb{E}\left[\max\left(K - S_T, 0\right)\right]\right\}. \qquad (1.2) \end{aligned}$$

Here I used the notation PV (an abbreviation of present value) as discounting the future value to the present value, and $\mathbb{E}$ as the expectation value. For the American option's price, we need to take the possibility of optimal early-exercise into account.

Without more information about the underlying, we cannot derive the accurate prices for options. However, we can already have some general results that are **underlying and model independent**. First of all, early exercise is not mandatory, the right to exercise early could never hurt the option holder but rather grants the long more flexibility, so intuitively, the prices of American options must be no less than the prices of European options:

$$C \geq c, \quad P \geq p. \qquad (1.3)$$

A call is a means of buying the underlying, so the value of a call can not exceed the current value of the underlying:

$$c \leq S_0, \quad C \leq S_0. \qquad (1.4)$$

To see the maximum value for a put, we simply consider its best possible outcome for the long. The best outcome is that the underlying goes to a value of zero, then the put holder could sell it for $K$. For an American put, the holder could sell it immediately, whereas for a European put the holder would have to wait until expiration:

$$p \leq \mathrm{PV}\{K\}, \quad P \leq K. \tag{1.5}$$

The minimum value for a European call can be obtained by applying Jensen's inequality to the convex function in expression (1.1):

$$\begin{aligned} c &= \mathrm{PV}\{\mathbb{E}[\max(S_T - K, 0)]\} \geq \mathrm{PV}\{\max(\mathbb{E}[S_T] - K, 0)\} \\ &= \max(S_0 - \mathrm{PV}\{K\}, 0). \end{aligned} \tag{1.6}$$

This result is not surprising. Consider, for example, a European call for less than $S_0 - \mathrm{PV}\{K\}$, one can buy the call at the start for $c$, exercise it at expiration, paying $K$, and sell the underlying for $S_T$, which gains a net present value of $S_0 - \mathrm{PV}\{K\} - c$. This value is positive and one assumes no risk, representing an **arbitrage** opportunity. Arbitrage opportunities appear when it is possible to make a profit in excess of the risk-free rate of return without bearing risk. Once such an arbitrage opportunity appears, a few people would do the previous transactions repeatedly to accumulate a profit. The increased demand in the call option would lead to it becoming more expensive until no risk-less profit exists. In general, when no-risk profit situations can occur, they will be taken advantage of until they disappear. This is called "arbitrage" and in general the reaction time of the market to remove such no-risk profit opportunities is very fast. For exchange, unequal exchange rates in different exchanges "relax" back to an equal exchange rate in a matter of minutes or less.

Similarly, from expression (1.2), we have the minimum values for a European put:

$$p \geq \max(\mathrm{PV}\{K\} - S_0, 0). \tag{1.7}$$

Incorporating the possibility of early-exercise into previous considerations, we have the lower bounds for American call and put:

$$C \geq \max(S_0 - \mathrm{PV}\{K\}, 0), \quad P \geq \max(K - S_0, 0). \tag{1.8}$$

We can already conclude that the price of an option relies on at least four factors, namely, the strike price, the interest rate for discounting, the volatility of the underlying and the time to maturity. Now consider the effects of these four factors by keeping all identical except one variable. Intuitively, the higher the *strike price*, the lower the value of a call and the higher the price of a put when fixing the other factors to be the same. When interest rates are higher, the call option holders save more money by not paying for the underlying until a later date; the put option holders, however, lose more interest while waiting to sell the underlying, i.e. higher opportunity cost of waiting. Therefore, the higher the *interest rate*, the higher the call option price and the lower the put option price. We will see in a later chapter that the interest rate does not have a very strong effect on option prices except when the underlying is a bond or the interest rate itself. Yet volatility has an extremely strong effect on the option price since it magnifies both the degree of out-of-the-money which does not contribute the option price and the degree of in-the-money which increases the option prices. So higher *volatility* increases both call and put option prices. For the effect of a difference in *time to expiration*, we see that when the shorter-term call with expiration date $T_1$ expires, the European call is worth $\max\left(S_{T_1} - K, 0\right)$ at $T_1$, but expression (1.6) tells us that the longer-term European call with expiration date $T_2 > T_1$ is worth at least $\max\left(S_{T_1} - \mathrm{PV}\left\{K\right\}, 0\right)$[1] at $T_1$, which is at least as greater as the previous amount. Thus, the longer-term European call is worth at least the value of the shorter-term European call. This also holds for an American call as can be seen by doing a similar analysis. The additional time is also beneficial to the holder of an American put option because an American put option can always be exercised; there is no penalty for waiting. However, in contrast to a European call holder who earns additional interest on the money by paying out the exercise price later, the European put holder loses interest on the money because of additional time. Analysis through expression (1.7) also supports the result that the the longer-term European put can be either greater or less than the value of the shorter-term European call, see in Table 1.1. Another way to look into this problem is though expression (1.5), that shows that the maximum European put price decreases as time goes by.

[1]Here the notation PV is used as discounting the future value at time $T_2$ to the present value at time $T_1$.

**Table 1.1:** The effect of a difference in time to expiration on option prices. Values are compared at time $T_1$ between the exact currently exercised one (at $T_1$) and the low bounds of the later exercised one (at $T_2$ with $T_2 > T_1$), as given by expressions (1.6), (1.7), and (1.8). The notation $(X)_+$ denotes max $(X, 0)$.

| Option | Value at $T_1$ | | Effect |
|---|---|---|---|
| | exercise at $T_1$ | exercise at $T_2$ | |
| Eur. call | $(S_{T_1} - K)_+$ | $\geq (S_{T_1} - \mathrm{PV}\{K\})_+$ | longer $T$, no less $c$ |
| Ame. call | $(S_{T_1} - K)_+$ | $\geq (S_{T_1} - \mathrm{PV}\{K\})_+$ | longer $T$, no less $C$ |
| Eur. put | $(K - S_{T_1})_+$ | $\geq (\mathrm{PV}\{K\} - S_{T_1})_+$ | longer $T$, greater or less $p$ |
| Ame. put | $(K - S_{T_1})_+$ | $\geq (K - S_{T_1})_+$ | longer $T$, no less $P$ |

Table 1.1 also helps us to understand the conditions under which early exercise of an American option might occur. Since the longer the time to expiration, the greater or the same prices for a European call and an American call, the American call would not exercise early and its price equals the European call price, except that there is an early exercise incentive. When the underlying makes cash payments during the life of the option, early exercise can be worthwhile and the American call price will be higher than the European call price. For instance, if the underlying is a stock and pays a dividend, then exercise just before the stock goes ex-dividend[1] is a good choice. Nevertheless the early exercise is not guaranteed beneficial unless the dividend is high enough. For puts, there is almost always a sufficient reason to exercise early. Once the underlying is very low, the American put holder would exercise immediately, which is not possible for a European call holder. So the American put is almost always worth more then the European put.

Now we move on to another interesting and important result for European options, called the **put-call parity**, which is nothing but a corollary of expressions

[1] After the declaration of a dividend by the stock issuer, the ex-dividend date is the the first day from which the buyer of a stock has no right to receive the next dividend payment. So just before the ex-dividend day is the last day that entitles the stock holder to receive the following dividend payment.

(1.1) and (1.2):

$$\begin{aligned} c - p &= \mathrm{PV}\{\mathbb{E}[\max(S_T - K, 0)]\} - \mathrm{PV}\{\mathbb{E}[\max(K - S_T, 0)]\} \\ &= \mathrm{PV}\{\mathbb{E}[S_T - K]\} = S_0 - \mathrm{PV}\{K\}. \end{aligned} \tag{1.9}$$

By rearranging the four terms, we have, for instance:

$$c + \mathrm{PV}\{K\} = p + S_0, \tag{1.10}$$

the left side of which constructs an option strategy referred to as a **fiduciary call**, which is long a call and a risk-free bond that matures on the option expiration day with its face value equal to the strike price of the call (we will discuss bonds in the next subsection); the right side constructs a **protective put**, which is long a put and the underlying. When one purchases a European call option, a smart way to cover the cost of exercising a stock at expiration is to invest the present value of the strike price in a risk-free interest bearing account if the person has the spare cash available. This is the motivation of a fiduciary call. A protective put is used as a **hedge**, a position invested in order to offset potential losses that might be incurred from a companion investment in the underlying. Buying a put protects one from a drop in the underlying price below the put's strike price. If the price of the underlying is above the strike price at expiration, the put expires worthless, the buyer has lost only the premium he paid for the put.

The portfolio strategy of protective put is useful for Apple's situation. In the aforementioned currency forward contract, no cash payment is needed up front, but Apple also assumes the substantial loss when the exchange rate for euros at expiration is higher than the strike rate \$1.35, i.e. Apple cannot sell euros in the open market for more dollars. In contrast, options offer the feature that, if one is willing to pay a cash fee (the option price) up front, one enjoys a unidirectional payoff, i.e. not only is the uncertainty eliminated, but also the potential gain is preserved. Thus, Apple can buy a European put on the USD/EUR exchange rate with a strike rate \$1.35. If the rate at expiration is greater than \$1.35, say \$1.5, Apple would not exercise the put, and sell the euros in the open market at a rate \$1.5. In this case, Apple only loses the put option price payed up front, which is relatively a small amount. This is an important characteristic of options called

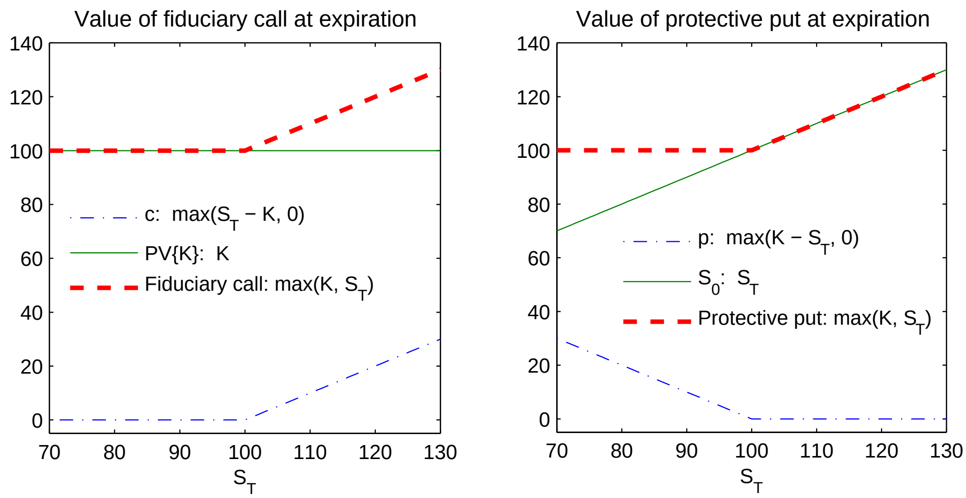


**Figure 1.2:** The payoffs of fiduciary call and protective put as a function of the underlying price at expiration. The strike price $K$ is assumed to be 100.

the leverage effect. If the rate at expiration is less than \$1.35, say \$1.3, Apple could still exercise the put and buy the dollars from the option seller at a rate \$1.35.

Both a fiduciary call and a protective put will end up worth $K$ or $S_T$ at expiration, whichever is greater, as illustrated in Figure 1.2. Note that their current values in the equation (1.10) are also equal. Does this imply that two portfolios of securities with exactly the same payoffs in all situations must have the same current price? The answer is yes, and it is one of the most essential principles in derivative pricing, which will be described more in detail in later sections. Here, we can still look into this problem from a perspective of an arbitrage opportunity. Suppose that the fiduciary call is underpriced, or equivalently the protective put is overpriced, e.g. the left-hand side of (1.10) is €105, while the right-hand side is €106. Then we can sell the overpriced combination, the protective put, by selling the put and selling short[1] the underlying, which generates a cash inflow of €106. Meanwhile, we buy the underpriced combination, the fiduciary call, paying out €105. These transactions net a cash inflow of €106 - €105 = €1. As seen

[1]Short selling is a practice of borrowing an underlying from a third party, selling it, and buying an identical underlying back at a later date to return to that third party.

in Figure 1.2, the values of these two portfolios at expiration exactly offset each other, so we receive €1 up front without bearing any risk nor paying anything out. The position is perfectly hedged and represents an arbitrage profit. This arbitrage opportunity disappears shortly once it is observed because other investors would follow the same scheme to make profit leading to a higher fiduciary call price and/or a lower protective put price. Of course, it is possible that transaction costs might consume any profit, so the possibility of a small discrepancy from put-call parity exists in the market.

In addition to the fiduciary call and the protective put, there are some other common derivative positions used in the market to increase the benefit and to reduce the risk, for example, the covered call, the straddle, the strangle, the risk reversal, the butterfly spread, the calendar spread, etc. For more details of these positions, I refer to (1). It is worth noting that our previous discussion of the put-call parity is based on European options, the put-call parity using American options is considerably more complicated. I would like not to explore it here but refer to (1) and references therein. Besides the existence of transaction costs and dividends mentioned above, there are commonly other cash flows on the underlying, for instance, stocks pay dividends, bonds pay interest, foreign currencies pay interest, commodities have carrying costs, etc. These factors together make the pricing of the derivatives more complicated. However, we are almost ready to study the pricing of options, and even the pricing of derivatives, which is the subject of the following sections.

I conclude this subsection with a discussion on the relationship between hedging and speculation, which are often thought of as opposites. Hedging is, as we have seen before, shedding of price risk through the use of derivatives, with the expectation that any risk exposure can be perfectly offset for a small fee (leverage). Speculation, on the other hand, is the taking on of financial risk that one previously did not possess for the simple purpose of achieving profits through the successful anticipation of which way prices will move. Speculators who expect prices to rise will enter into long call positions, while those expecting they will fall take long put positions. Speculators can be categorized by how they form their expectations as fundamental traders, namely those relying on basic economic conditions, or technical traders, namely those who base themselves on the analysis of price patterns and other market statistics. Speculators can also be classified by how they trade as day traders, who begin and end the day with no position in the market, or position traders, who hold positions over longer periods of time, perhaps days or weeks. In practice, though hedgers and speculators have different motivations for entering the derivatives markets, they are nevertheless closely dependent on each other. One can image that if markets relied solely on hedgers to trade in the market, a lack of liquidity would inevitably arise. It is the speculators who strive to profit from information and provide an important source of liquidity to the markets at the same time as hedgers seek to manage their price risk. The hedging of fuel purchases by airlines based on expectations that prices will rise is in fact somewhat a speculation because the airlines are trying to make profits from predicting fuel prices, i.e. they hedge it when they believe fuel price will rise and do not hedge it when they believe the price will fall. Meanwhile, speculators also use derivatives as an effective tool to reduce the overall risk of a portfolio, behaving just as hedgers. Therefore, in today's markets, practically all "hedgers" and "speculators" can be viewed as risk managers along the hedging-speculation continuum, see (3).

### 1.1.3 Bonds

One of the basic principles when we talk about finance is the **time value of money**. The same amount of money at a future date is worth less than at present. This is intuitively clear: do you prefer to receive €1.00 now, or €1.00 one year from now? To see how much more the current €1.00 is worth than the future €1.00's, consider placing it in a bank account that pays an interest rate $r$ per year. If the bank credits the interest once a year, the value of the account at year-end will be €(1+r). If the bank credits interest semi-annually, one would expects $€\left(1+\frac{r}{2}\right)^2$. What if the profit is accrued continuously? We know the existence of this limit:

$$€ \lim_{n\to\infty}\left(1+\frac{r}{n}\right)^n = €\, e^r, \tag{1.11}$$

where $e$ is Euler's number. If the bank account grows at each time $t$ at a rate $r(t)$ instead of the previous constant $r$, then the bank account values $€\, e^{\int_t^T r(s)ds}$ at time $T$ given its original **principal** amount €1 at the initial time $t$. This

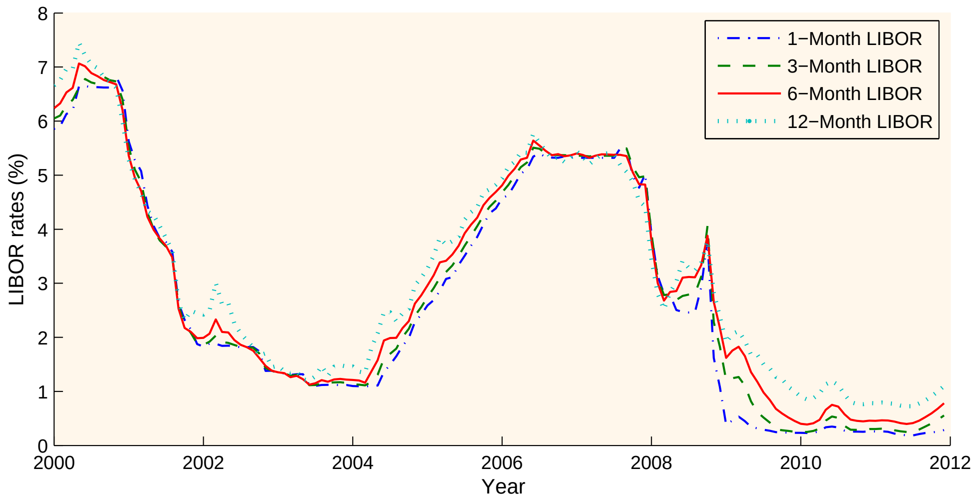


**Figure 1.3:** The historical LIBOR rates from January 2000 to December 2011.

instantaneous rate $r(t)$ is usually referred to as **instantaneous spot rate**. In real markets, this spot rate evolves stochastically as time goes by, as can been seen in for example Figure 1.3 for the historical LIBOR rates. LIBOR is an acronym for London InterBank Offered Rate, and it is a benchmark for finance all around the world. Banks borrowing money for one day, one month, two months, six months, one year, etc. pay interest to their lenders based on certain rates, and LIBOR is the average interest rate charged when leading to other banks by leading banks in London.

Depositing a certain amount of money in a bank account, everyone receives a supposedly risk-free return. This assurance of risk-free return makes the bank account a benchmark for financial investment. No surprisingly, no one would make an investment that returns less than in a bank account.

A quick question is: what is the value at time $t$ of one unit of currency available at time $T$. This is actually the inverse problem of the bank account, called the **(stochastic) discount factor**, which is given by: $e^{-\int_t^T r(s)ds}$. If $r(s)$ is a stochastic variable, so is the discount factor. Otherwise, they are deterministic variables.

A **bond** is a debt security, in which the authorized issuer (the borrower, or the debtor) owes the bondholder (the lender, or the creditor) a debt, and is obliged to repay the principal, or called the face amount - the amount on which the issuer pays interest, and the interest at a later date in any payment stream or pattern that the parties agree to. In essence, a bond is a promise for a certain sum of money in the future. As an example consider the Belgian government issued bonds (staatsbon): the state offers to pay you €1217 five years from now, and claims that this is worth €1000 now. The €1000 is the principal, hence the 4% interest rate cited on the "staatsbon", which results in the additional €$1000\times ((1.04)^5 - 1) =$ €217.

Various types of bonds exist in the market. According to the coupon rate structures, there are (1) **zero-coupon bonds**: bonds that do not pay periodic interest; (2) step-up notes: bonds have coupon rates that increase over time at a specified rate; (3) deferred-coupon bonds: bonds pay the initial coupon deferred for some period, and (4) floating-rate bonds: bonds carry coupons based on a specified interest rate or index. According to the way the principal will be repaid, there are (1) nonamortizing bonds: bonds only pay the entire par or face value and interest at maturity time; (2) amortizing bonds: bonds make periodic interest and principal payments over the life of the bonds.

There are some risks associated with investing in bonds. For example, (1) reinvestment risk: when interest rates fall, some options embedded bonds allow bond issuers to resort to other lower rate bonds, causing risks for bondholders to reinvest these prepayments at the new lower rate; (2) credit risk: worse creditworthiness, lower bond value, higher required yield; (3) liquidity risk: a decrease in a security's liquidity will decrease its price as the required yield will be higher; (4) exchange-rate risk, a depreciation of the foreign currency's value relative to the domestic currency will reduce a domestic investor's value who makes a foreign-based investment; (5) sovereign risk, essentially the credit risk of a sovereign bond issued by a country other than the investor's home country; (6) unexpected inflation risk or purchasing-power risk and event risk, almost for every investment; and of course (7) interest rate risk, i.e. when interest rate rise, bond values fall.

For more discussion about the bonds I refer to (4). Here I focus on the zero-coupon bond, also called pure discount bond, since the repayment of principal is only guaranteed at expiration, without any interest payed during the life of

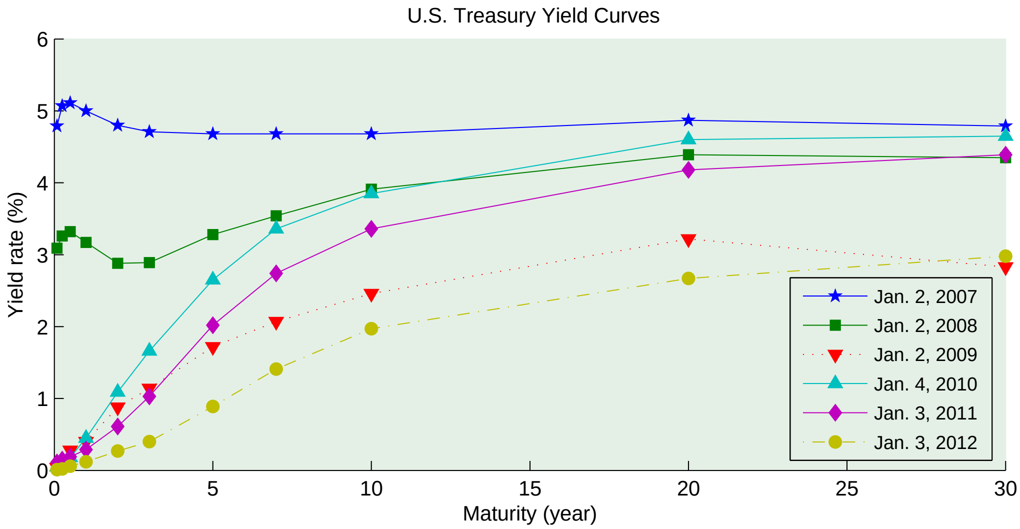


**Figure 1.4:** Daily U.S. treasury yield curves with maturities 1 month, 3 months, 6 months, 1 year, 2 years, 3 years, 5 years, 7 years, 10 years, 20 year and 30 years.

the bond. We know that the value at current time $t$ of a principal of €1 at maturity time $T$ is $e^{-\int_t^T r(s)ds}$, which can be a stochastic variable. The price of a zero-coupon bond is thus the expectation value of this value under a certain probability measure: $\mathbb{E}\left[e^{-\int_t^T r(s)ds}\right]$.

In the previous subsection, we introduced the discount function PV to bring the cash flow at time $T$ back to the beginning of the investment's life at time $t$. Now we can write the second term of expression (1.10) in a general formula as:

$$\mathrm{PV}\left\{K\right\} = \mathbb{E}\left[e^{-\int_t^T r(s)ds}\right] K. \tag{1.12}$$

Under some simple assumptions, the discounting factor reduces to $e^{-r(T-t)}$, or even $(1+r)^{-(T-t)}$. The circumstances under which such simpler assumptions can be made depends on the impact of the interest rate on the target financial instruments. As we mentioned before, for interest rate derivatives and bonds, the interest rate is of substantial importance, so no simplification is appropriate.

We can find zero-coupon bond prices in the market. One spontaneous question is: what is the equivalent continuously compounded rate of interest $Y(t,T)$ during this time interval $[t,T]$ such that $\mathbb{E}\left[e^{-\int_t^T r(s)ds}\right] = e^{-Y(t,T)(T-t)}$? This equivalent rate is called the zero-coupon yield. This yield as a function of time to maturity, i.e. $T-t$, constructs the so called **yield curve**, and it is used as a benchmark for other debt in the market, such as mortgage rates or bank lending rates. Figure 1.4 shows the daily U.S. treasury yield curves with different maturities. These curves can be also used to predict changes in economic growth.

### 1.1.4 Swaps

The Bank for International Settlements estimated the notional principal of the global over-the-counter derivatives market value as of 30 June 2011 at \$19518 billion. Of that amount, currency swaps account for \$1227 billion, and interest rate swaps represent \$11864 billion, see (5). In the race to see which derivative instrument is more popular, swaps have clearly won. A **swap** is an agreement between two parties to exchange a series of future cash flows. Usually one party makes payments that are floating, such as an interest rate, a currency rate, an equity return, or a commodity price, while the other party either makes other floating payments or makes fixed payments. Recall that it is acceptable to view a swap as a series of forward contracts, cf. 1.1.1. One reason why interest rate swaps have overwhelming success lie in the fact that interest rate swaps are simple and can usually be justified as nothing more than variations of loans. Moreover, given that risk often exists in a series, swaps are ideal instruments for managing it, i.e. a package of risk management tools all rolled up into one, which is surely over other instruments.

Let us now illustrate a plain vanilla swap, a simple interest rate swap, in which one party pays a fixed rate and the other pays a floating rate, with both sets of payments in the same currency. Suppose that on 1 January, Janssen Pharmaceutica borrows €10 million for one year from a bank such as KBC bank. The loan specifies that Janssen Pharmaceutica will pay the interest quarterly for one year at the rate of LIBOR observed at the end of each quarter plus 25 basis points (0.25 percent). Janssen Pharmaceutica believes that it is getting a good rate, but it fears a rise in interest rates and would prefer a fixed-rate loan. By engaging in a swap, Janssen Pharmaceutica converts the floating-rate loan to a fixed-rate loan. Suppose it approaches Goldman Sachs, a large investment bank, and requests a quote on a swap to pay a fixed rate and receive LIBOR, with payments on the dates of its loan payments. If Goldman Sachs quotes a fixed rate of 4 percent, then Janssen Pharmaceutica pays 4% to Goldman Sachs, receives LIBOR from Goldman Sachs, and pays LIBOR plus 0.25% to KBC bank on its loan. The net effect is that Janssen Pharmaceutica pays interest at a rate about $\frac{4\%+0.25\%}{4} = 1.06\%$ fixed per quarter.

While interest rate swaps are important in the interest rate derivatives market, **credit default swaps (CDS)** are the building blocks in the credit derivatives market and represent about half of its volume. A CDS is a contract between two parties to exchange the credit risk of a specific issuer. One party, the protection buyer, pays a premium to the other party, the protection seller, to assume the risk associated with a particular credit event. For example, I can buy protection from you, so that if Dexia bank owes me €1000, you will pay me that €1000 in case Dexia would go bankrupt in the meanwhile. Basically, this swap is an insurance against bankruptcy of one of my debtors. Rather than selling or buying such insurance, we can think about trading the *right* to buy or sell such insurance. This is a **swaption**: an option to enter into a swap. Swaptions have a variety of purposes, for instance, (1) swaptions are used by parties who anticipate the need for a swap at a later date but would like to establish the fixed rate today, while providing the flexibility to not engage in the swap later or engage in the swap at a more favorable rate in the market; (2) swaptions are used by parties entering into a swap to give them the flexibility to terminate the swap; (3) swaptions are used by parties to speculate on interest rates. More introduction about these instruments can be found in (2).

### 1.1.5 Historical charts

Our tour of financial derivatives and markets can already stop here. Of course there are other types of payoff functions that are different from the vanilla options' seen in subsection 1.1.2, leading to exotic derivatives. As I will analyse some common exotic derivative in later chapters, I would like to skip them here. But we should take a look at historical charts of underlying asset prices now since options as well as other derivatives are built on those underlying assets.

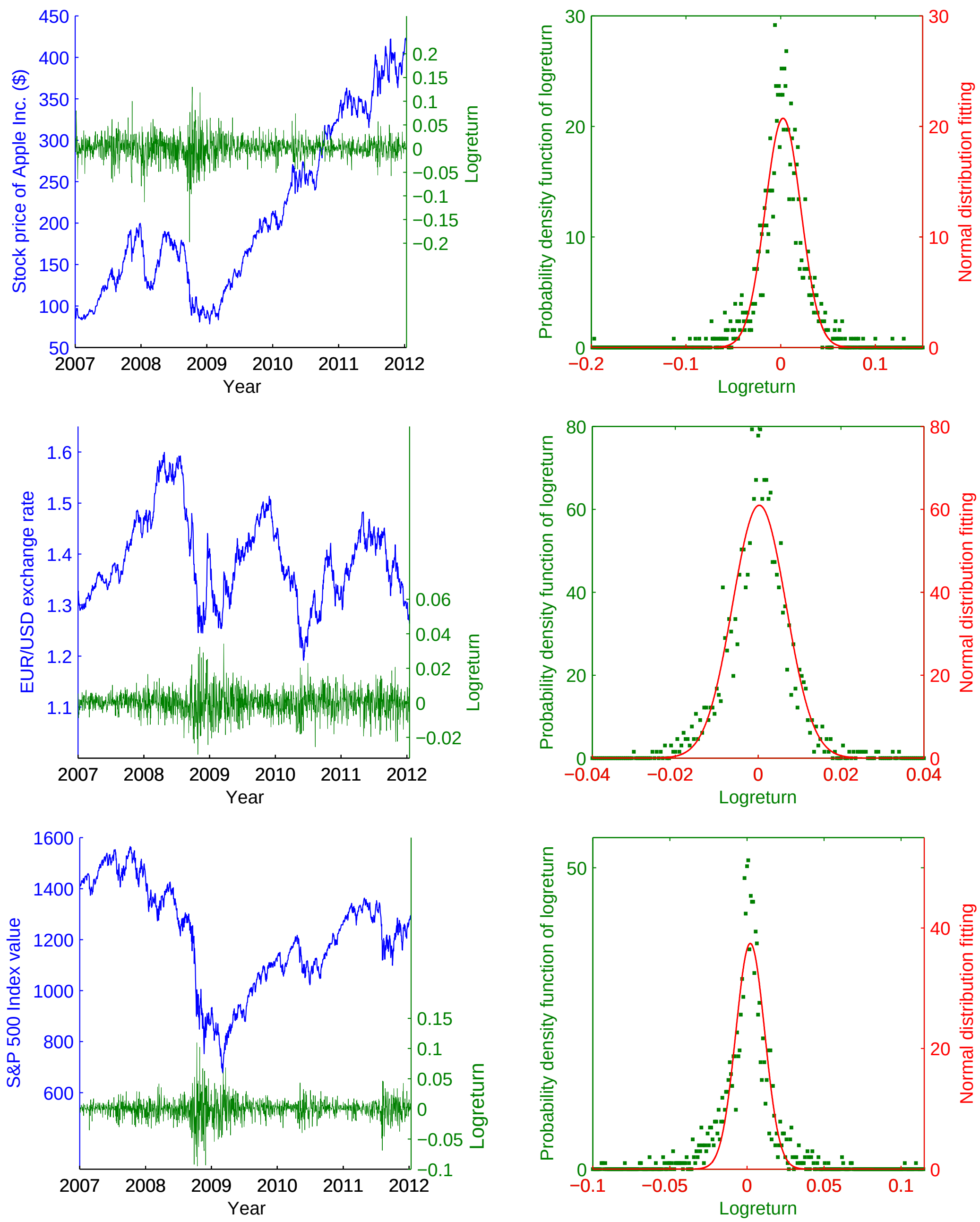


**Figure 1.5:** The left panels depict historical stock price of Apple Inc. (top), the Euro and US dollar exchange rate (middle) and the S&P 500 Index value (bottom), and their logreturns (dark green curves), over the last 5 years from January 2007 to January 2012. The right panels are the corresponding probability density functions of logreturns (square dots) as well as normal distribution fittings (red curves). The observed probability density functions are clearly leptokurtic.

Stock is the most basic financial security, and it represents a share of a corporation's ownership. Indices are created in order to master the market trend, typically these indices represent a weighted package of representative stocks. Eugene Farma devoloped the so called **efficient market hypothesis** into an academic concept in the 1960s, see (6). A market is defined as efficient if it is comprised of rational investors who strive to predict the future security prices and to maximize their profit, and all the important information is shared by the market. In such an efficient market, the current security prices reflect all existing information, and they will change only when new information comes out, so attempts to outperform the market are inappropriate. Though there are controversies about the efficient market hypothesis, it remains a basic principle for derivative pricing. New information appears and influences the underlying assets randomly, thus no one can predict the future price accurately, that is why we say the underlying prices are stochastic.

The blue curves in Figure 1.5 depict the behavior of the stock of Apple Inc. (top left), which is directly related to the earnings and dividends of Apple Inc, the Euro and US dollar exchange rate (middle left), which is determined by the market forces of supply and demand, and the S&P 500 Index value (bottom left), an equity index which is considered a bellwether for the American economy, over a representative 5-year period from January 1, 2007 to January 16, 2012. Denote these daily prices as $S(t)$. We can see that these underlying prices are quite different from each other. Nevertheless, there are some features in common. All of the prices are positive, and all evolve with apparent fluctuations and some trends. These features can be approximately captured by a Brownian motion with drift, called arithmetic Brownian motion.

It is well known that a Brownian motion with drift has independent increments with a normal distribution. Early in 1900, the French mathematician Louis Bachelier was historically the first who proposed the use of arithmetic Brownian motion (resulting in a normal distribution for the stock prices) to simulate stock options in his PhD thesis (7). His model results in a normal distribution, hence with non-zero probabilities for negative values, for the stock prices. Paul Samuelson introduced in 1965 a revised version of the Bachelier's model, called the

**geometric Brownian motion**, assuming that the return rates, instead of the stock prices, follow an arithmetic Brownian motion (8).

For this purpose, people usually look into the (daily) **logreturn** $x(t)$, defined by:

$$x(t) = \ln \frac{S(t + 1\text{day})}{S(t)}. \tag{1.13}$$

The daily logreturns corresponding to the displayed underlying prices are shown by dark green curves in Figure 1.5 (left column). Now we can see the similarity between them when ignoring their amplitudes. These logreturns are then binned and plotted to build their probability density functions (dark green square dots in Figure 1.5 right column). These densities show the probability distribution of continuously compounded returns over one trading day. We can see that these densities appear somewhat normal distributed, although they are more leptokurtic than the normal distribution. Their corresponding normal distribution fits are also plotted in Figure 1.5 right column by red curves.

## 1.2 The Black-Scholes world

### 1.2.1 Black-Scholes formula

Inspired by Samuelson's geometric Brownian motion and recognizing that underlying assets and options can be combined to construct a riskless portfolio, Fischer Black and Myron Scholes developed in 1973 an analytical model that provides a no-arbitrage value for options, see (9). In that paper, they proposed the well known Black-Scholes partial differential equation, and derived analytical European call and put option pricing formulas. As expected, the stock price dynamics in their model is described by a geometric Brownian motion with drift. However, their model does not assume that the investors agree on the expected return rate of the underlying, nor does it restrict the investors' risk preferences and their estimates for current and future returns. More explicitly, the option price depends on the risk-free interest rate. Robert Merton performed a rigorous analysis of the Black-Scholes model analyzing its assumptions (10). Scholes and Merton received the Nobel Prize in Economic Sciences in 1997; Black passed away in 1995.

The assumptions underpinning the Black-Scholes model include: (1) the underlying price follows a geometric log-normal diffusion process; (2) the risk-free interest rate and the volatility of the underlying are known and constant; (3) there are no taxes or transaction costs or cash flows on the underlying; (4) trades can be made instantaneously and at any time; (5) short selling is allowed.

Consider an asset whose price starts off at a known value $S_0$ and evolves over time according to the following stochastic differential equation (SDE):

$$\frac{dS(t)}{S(t)} = \mu dt + \sigma dW(t), \tag{1.14}$$

where $\mu$ and $\sigma$ are the known constants for the asset's expected return and volatility, and $W(t)$ is a standard Brownian motion. The increment $\Delta W(t) = W(t+\Delta t) - W(t)$ is Gaussian with mean 0 and variance $\Delta t$. Moments of $(\Delta W)^2$ include: (1) $\mathbb{E}\left[(\Delta W)^2\right] = \Delta t$; (2) $\mathrm{Var}\left[(\Delta W)^2\right] = 2\,(\Delta t)^2$. When the time increment $\Delta t \to 0$, the variance of $(dW)^2$ will approach zero as $2\,(dt)^2$, much faster than its expectation, $dt$. We known that the variance of a constant is zero, hence in the limit $\Delta t \to 0$ we have $(dW(t))^2 = dt$. Therefore, $(dS(t))^2 = \mu^2 S^2 (dt)^2 + 2\mu\sigma S^2 dt dW(t) + \sigma^2 S^2 dt + \cdots = \sigma^2 S^2 dt + \mathcal{O}\left((dt)^{\frac{3}{2}}\right)$.

Now consider two European derivatives depending on this underlying asset, denoted by $f[S(t)]$ and $g[S(t)]$, and a portfolio $\Pi[S(t)]$ combining these two derivatives, that is $\Pi[S(t)] = c_1 f[S(t)] + c_2 g[S(t)]$. Then to order $dt$ we have:

$$\begin{aligned} d\Pi &= \frac{\partial \Pi}{\partial t} dt + \frac{\partial \Pi}{\partial S} dS + \frac{1}{2}\frac{\partial^2 \Pi}{\partial S^2}(dS(t))^2 + \cdots \\ &= \left(\frac{\partial \Pi}{\partial t} + \frac{1}{2}\sigma^2 S^2 \frac{\partial^2 \Pi}{\partial S^2} + \mu S \frac{\partial \Pi}{\partial S}\right) dt + \sigma S \frac{\partial \Pi}{\partial S} dW(t). \end{aligned} \tag{1.15}$$

The uncertainty comes from term $dW(t)$. We can always make a portfolio such that all the associated risks are hedged away, then according to the non-arbitrage principle, the return of this portfolio is the constant risk-neutral interest rate $r$:

$$\frac{\partial \Pi}{\partial S} = 0, \tag{1.16}$$

$$d\Pi = \left(\frac{\partial \Pi}{\partial t} + \frac{1}{2}\sigma^2 S^2 \frac{\partial^2 \Pi}{\partial S^2}\right) dt = r\Pi dt, \tag{1.17}$$

that is:

$$\begin{aligned} c_1\frac{\partial f}{\partial S}+c_2\frac{\partial g}{\partial S}&=0,\\ c_1\left(\frac{\partial f}{\partial t}+\frac{1}{2}\sigma^2S^2\frac{\partial^2 f}{\partial S^2}-rf\right)+c_2\left(\frac{\partial g}{\partial t}+\frac{1}{2}\sigma^2S^2\frac{\partial^2 g}{\partial S^2}-rg\right)&=0. \end{aligned} \tag{1.18}$$

Collecting all $f$ terms on the left-hand side and all $g$ terms on the right-hand side, we get

$$\frac{\frac{\partial f}{\partial t}+\frac{1}{2}\sigma^2S^2\frac{\partial^2 f}{\partial S^2}+\mu S\frac{\partial f}{\partial S}-rf}{\sigma S\frac{\partial f}{\partial S}}=\frac{\frac{\partial g}{\partial t}+\frac{1}{2}\sigma^2S^2\frac{\partial^2 g}{\partial S^2}+\mu S\frac{\partial g}{\partial S}-rg}{\sigma S\frac{\partial g}{\partial S}}. \tag{1.19}$$

Note that the first three terms in the numerators are the returns of $f[S(t)]$ and $g[S(t)]$ if they bear a certain amount of risks corresponding to their volatilities as expressed in the respective denominators, while $rf$ and $rg$ are their returns if they do not bear any risk, respectively. Hence, both sides of expression (1.19) are the expected return in excess of the risk-free interest rate per unit of risk they are assuming. This quantity is used to value risk, called the **market price of risk**, and is the same for all derivatives in the market. The underlying itself of course obeys this market price of risk. Plugging $S$ into expression (1.19) gives the value $\frac{\mu-r}{\sigma}$. Therefore, for any derivatives $f[S(t)]$ depending on the underlying, we have the **Black-Scholes partial differential equation** (PDE):

$$\frac{\partial f}{\partial t}+rS\frac{\partial f}{\partial S}+\frac{1}{2}\sigma^2S^2\frac{\partial^2 f}{\partial S^2}=rf. \tag{1.20}$$

$c_1$ and $c_2$ can be solved from expression (1.18). They are not necessarily constant as a function of S or time. In practice, they are kept constant between adjustments during dynamic hedging. For example, if one holds a European call option, one should sell a certain amount of the underlying in order to hedge the exposure, i.e. $\Pi=c-c_2S(t)$. Expression (1.16) tells us how a construct a risk-free portfolio, just like the **Euler-Lagrange equation** in analytical mechanics, from which we have $c_2=\frac{\partial c}{\partial S}$. Thus $\Pi[S(t)]=c-\frac{\partial c}{\partial S}S(t)$ is risk-free portfolio for every time $t$. If $S(t)$ rises (falls), $\frac{\partial c}{\partial S}$ increases (decreases), one should sell (buy back) more of the underlying. In such circumstances, one always sells the underlying at higher prices and buys it at lower prices, so this dynamic hedging brings one profits. In principle, the quantity of profits should be the price of replicating the portfolio.

All derivatives should satisfy expression (1.20) in the Black-Scholes world, from which we see that derivative prices depend on the risk-free interest rate $r$ rather than on the return of the underlying $\mu$. As mentioned before, replication is the basic idea of derivative pricing. To determine the value of derivatives, one should construct a risk-free investment portfolio that depends on the underlying. Once the portfolio is risk-free, according to the non-arbitrage principle, its return is fixed, i.e. the risk-neutral interest rate. Hence, no matter what the underlying assets' returns are, the returns of the risk-free portfolios are the same. Consequently, we can surely assume that the return of the underlying is the the risk-neutral interest rate since the derivative prices will be the same. The Black-Scholes model is thus given by

$$dS(t) = rS(t)dt + \sigma S(t)dW(t). \tag{1.21}$$

Modeling the underlying's return by $r$ instead of $\mu$ involves a change of measures, i.e. from the physical measure $\mathbb{P}$ to the risk-neutral measure. The Black-Scholes market is said to be **complete**. A market is complete if and only if there exists a **unique** probability measure $\mathbb{Q}$ **equivalent** to $\mathbb{P}$ such that discounted assets are martingales with respect to $\mathbb{Q}$ (11). A stochastic variable is called a **martingale** if its expectation value is time-independent. More explicitly, for our stochastic variable $S(t)$ given in (1.21), the corresponding discount asset $X(t) = e^{-rt}S(t)$ follows:

$$dX(t) = \sigma X(t)dW(t). \tag{1.22}$$

From this SDE we have $\mathbb{E}[X(t)] = X_0$ for all $t$, thus $X(t)$ is a $\mathbb{Q}$-martingale.

There is a one-to-one correspondence between arbitrage-free pricing rules and equivalent martingale measure: in a market described by a probability measure $\mathbb{P}$ on scenarios, any arbitrage-free linear pricing rule $\Pi$ can be represented as

$$\Pi_t = e^{-r(T-t)}\mathbb{E}^{\mathbb{Q}}\left[\text{Payoff}\right], \tag{1.23}$$

where $\mathbb{Q}$ is an equivalent martingale measure. Due to the fact that the Black-Scholes market is complete, the unique equivalent measure is just the **risk-neutral measure** $\mathbb{Q}$. The argument including the expression (1.23) is thus called the **risk-neutral pricing theory** (11). Note that the existence of an equivalent martingale measure leads to absence of arbitrage while its uniqueness is related to market completeness. Unless otherwise stated, all the following probability distribution functions and expectations in this thesis will be with respect to the *risk-neutral measure*, and we drop the superscript $\mathbb{Q}$ in $\mathbb{E}^{\mathbb{Q}}$.

Expression (1.20) is a parabolic equation encountered in mathematical physics. It can be reduced to a heat equation by making some substitutions. Given different boundary conditions, i.e. the payoff functions for European call and put options with strike price $K$ and the time to maturity $T$, we can solve the equation explicitly. The derivation of the Black-Scholes formula by means of a hedging argument that yields the PDE (1.20) and the solution of the PDE constitute the **PDE pricing method**.

As we know, $S(t)$ follows a geometric Brownian motion. More explicitly, from (1.21) we have:

$$d\ln S(t) = \frac{1}{S}dS(t) - \frac{1}{2S^2}\left(dS(t)\right)^2 = \left(r - \frac{\sigma^2}{2}\right)dt + \sigma dW(t), \tag{1.24}$$

thus

$$S_T = S_0\, e^{\left(r-\frac{\sigma^2}{2}\right)T+\sigma W_T}, \tag{1.25}$$

where $W_T$ is a normal distributed stochastic variable with zero mean and variance $T$. Applying the risk-neutral pricing theory, we have the pricing formulas for European call and put options:

$$\begin{aligned}
c_{BS} &= e^{-rT}\mathbb{E}\left[\max\left(S_T - K, 0\right)\right] \\
&= e^{-rT}\left[\int_{S_T>K}\left(S_0\, e^{\left(r-\frac{\sigma^2}{2}\right)T+\sigma\sqrt{T}z} - K\right)\frac{1}{\sqrt{2\pi}}\, e^{-\frac{z^2}{2}}dz\right] \\
&= S_0 N(d_1) - e^{-rT}KN(d_2), \qquad (1.26)\\
p_{BS} &= e^{-rT}KN(-d_2) - S_0 N(-d_1), \qquad (1.27)
\end{aligned}$$

where

$$d_{1,2} = \frac{\ln\left(F/K\right)}{\sigma\sqrt{T}} \pm \frac{\sigma\sqrt{T}}{2}, \tag{1.28}$$

$N(\cdot)$ is the cumulative normal distribution function: $N(x) = \int_{-\infty}^{x}\frac{1}{\sqrt{2\pi}}\, e^{-\frac{1}{2}z^2}dz$, and $F = S_0\, e^{rT}$ is the future price. These results are the same as the ones by the PDE method, see (9). Especially, the term $N(d_2)$ represents the probability of exercise of a call option, while the term $N(-d_2)$ is the probability of exercise of a put option.

### 1.2.2 Implied volatility

Note that the Black-Scholes pricing formulas need two input variables, namely the risk free interest rate and the volatility of the underlying under the risk-neutral measure. There are some references for the risk free interest rate, for instance the US treasury rate. Given the market European call option price $c_{mark}$, we can define the **implied volatility** for strike $K$ and expiration $T$ as the volatility $\sigma_{imp}$ that through the Black-Scholes formula generates the market price:

$$c_{mark}\left(K,T\right) = c^{BS}\left(K,T,\sigma_{imp}(K,T)\right). \tag{1.29}$$

The solution of this equation is unique because $c^{BS}$ is strictly increasing in $\sigma$. If Black-Scholes model is correct, then the implied volatility should be the same for all strikes and expirations because this volatility uniquely describes the fluctuation of the underlying and should be independent of call option prices. However, this is in general not the case. Figure 1.6 illustrates the implied volatility for S&P 500 Index call option prices of September 3, 2010 with different expirations. We can see clearly that the implied volatility depends on both strike and time to maturity. There curves are called the **volatility smiles**, which exist in all derivative markets.

If the volatility of the underlying has a deterministic time dependence, denoted by $\sigma_d(t)$, then $\ln S_T$ is normal with mean $(r - \bar{\sigma}^2/2)\,T$ and variance $\bar{\sigma}^2 T$. Hence the implied volatility is simply given by $\bar{\sigma} = \left(\frac{1}{T}\int_0^T \sigma_d(t)dt\right)^{\frac{1}{2}}$.

Now we assume the volatility is stochastic, denoted by $\sigma_s(t)$. For this case, I follow Lee (12) and Gatheral (13), who derived a general path-integral representation of implied volatility by exploiting the work of Dupire (14). For every time $t$ in $[0,T]$, the actual realized volatility is stochastic $\sigma_s(t)$, and we assume that there exists an equivalent deterministic function, denoted by $\sigma_{eff}(t)$. If we can find this equivalent deterministic time dependent volatility $\sigma_{eff}(t)$, then we know from the previous discussion that the implied volatility is $\left(\frac{1}{T}\int_0^T \sigma_{eff}^2(t)dt\right)^{\frac{1}{2}}$.

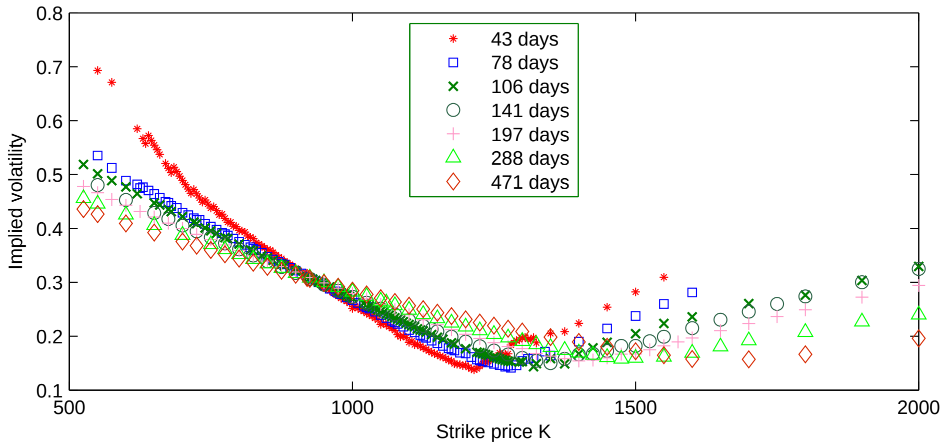


**Figure 1.6:** Implied volatility derived from S&P 500 Index call option prices of September 3, 2010 with different time to maturities. $S_0 = 1103.7, r = 0.49\%$.

We then introduce two functions:

$$C^{BS}(S(t),t) = e^{-r(T-t)}\mathbb{E}\left[(S_T - K)_+ \left| S(t)\right.\right], \tag{1.30}$$

$$\sigma_{imp}(t) = \left(\frac{1}{T-t}\int_t^T \sigma_{eff}^2(u)du\right)^{\frac{1}{2}}. \tag{1.31}$$

Note that for every time step $t$, $C^{BS}(S(t),t)$ is conditional on $S(t)$. Then $C^{BS}(S_T,T) = \mathbb{E}\left[(S_T - K)_+ \left| S_T\right.\right]$ is the payoff function of a European call option given the value $S_T$, and $C^{BS}(S_0,0) = e^{-rT}\mathbb{E}\left[(S_T - K)_+ \left| S_0\right.\right]$ is exactly the European call option price. Moreover, $\sigma_{imp}(0) = \left(\frac{1}{T}\int_0^T \sigma_{eff}^2(t)dt\right)^{\frac{1}{2}}$ is exactly the Black-Scholes implied volatility.

The value of a call option is given by the discounted expectation of the final payoff under the risk-neutral measure:

$$c_{mark}(K,T) = \mathbb{E}\left[e^{-rT}(S_T - K)_+\right] = \mathbb{E}\left[e^{-rT}C^{BS}(S_T,T)\right]. \tag{1.32}$$

Since $C^{BS}(S_t,t)$ is a smooth function of the random stock price $S(t)$ and random volatility $\sigma_s(t)$, we rewrite the previous equation as:

$$\begin{aligned} c_{mark}(K,T) &= \mathbb{E}\left[C^{BS}(S_0,0)\right] + \mathbb{E}\left[\int_0^T d\left(e^{-rt}C^{BS}(S(t),t)\right)\right] \\ &= C^{BS}(S_0,0) + \mathbb{E}\left[\int_0^T e^{-rt}\left(-rC^{BS}dt\right.\right. \\ &\quad \left.\left. + \frac{\partial C^{BS}}{\partial t}dt + \frac{\partial C^{BS}}{\partial S(t)}dS(t) + \frac{\sigma_s^2(t)}{2}S^2(t)\frac{\partial^2 C^{BS}}{\partial S^2(t)}dt\right)\right]. \end{aligned} \tag{1.33}$$

Of course, $C^{BS}(S(t),t)$ satisfies the Black-Scholes equation by using the equivalent deterministic time dependent volatility $\sigma_{eff}(t)$:

$$\frac{\partial C^{BS}}{\partial t} + rS(t)\frac{\partial C^{BS}}{\partial S(t)} + \frac{\sigma_{eff}^2(t)}{2}S^2(t)\frac{\partial^2 C^{BS}}{\partial S^2(t)} - rC^{BS}(S(t),t) = 0. \tag{1.34}$$

Plugging (1.34) into (1.33), we have (note that $\mathbb{E}\left[\int_0^T h(t)dW(t)\right] = 0$ for a non-random function $h(t)$)

$$c_{mark}(K,T) - C^{BS}(S_0,0) = \int_0^T e^{-rt}\,\mathbb{E}\left[\frac{1}{2}\left(\sigma_s^2(t) - \sigma_{eff}^2(t)\right)S^2(t)\frac{\partial^2 C^{BS}}{\partial S^2(t)}\right]dt. \tag{1.35}$$

This equation expresses the difference between the real call option price based on actual realized volatility and the call option price based on estimated volatility. In other words, trading a European call option is trading the volatility. That is why European options are often quoted in terms of volatility. According to the definition of implied volatility,$C^{BS}(S_0,0)$ is equal to the real call option price, so the left-hand side of equation (1.35) equals zero, leading to the so-called equivalent deterministic volatility $\sigma_{eff}(t)$ for every time step $t$ defined by:

$$\mathbb{E}\left[\left(\sigma_s^2(t) - \sigma_{eff}^2(t)\right)S^2(t)\frac{\partial^2 C^{BS}}{\partial S^2(t)}\right] = 0. \tag{1.36}$$

Denote the joint probability density function of the stochastic variables $S$ and $\sigma_s$ that have values $S(t)$ and $\sigma_s(t)$ at time $t$ given their initial values $S_0$ and $\sigma_s(0)$ at time $t=0$ as $\mathcal{P}\left(S(t),\sigma_s(t),t\middle|S_0,\sigma_s(0),0\right)$. The marginal probability density function of $S(t)$ is denoted as $\mathcal{P}\left(S(t),t\middle|S_0,0\right)$ and is related to the joint probability density function by $\int_0^\infty d\sigma_s(t)\mathcal{P}\left(S(t),\sigma_s(t),t\middle|S_0,\sigma_s(0),0\right)$. The previous risk-neutral expectation can be rewritten as:

$$
\begin{aligned}
&\mathbb{E}\left[\left(\sigma_s^2(t)-\sigma_{eff}^2(t)\right)S^2(t)\frac{\partial^2 C^{BS}}{\partial S^2(t)}\right]\\
=&\int_0^\infty dS(t)\int_0^\infty d\sigma_s(t)\mathcal{P}\left(S(t),\sigma_s(t),t\middle|S_0,\sigma_s(0),0\right)\left(\sigma_s^2(t)-\sigma_{eff}^2(t)\right)S^2(t)\frac{\partial^2 C^{BS}}{\partial S^2(t)}\\
=&\int_0^\infty dS(t)\int_0^\infty d\sigma_s(t)\mathcal{P}\left(S(t),\sigma_s(t),t\middle|S_0,\sigma_s(0),0\right)\sigma_s^2(t)S^2(t)\frac{\partial^2 C^{BS}}{\partial S^2(t)}\\
&-\sigma_{eff}^2(t)\int_0^\infty dS(t)\mathcal{P}\left(S(t),t\middle|S_0,0\right)S^2(t)\frac{\partial^2 C^{BS}}{\partial S^2(t)}\\
=&\,0,
\end{aligned}
\tag{1.37}
$$

from which we obtain

$$
\begin{aligned}
\sigma_{eff}^2(t) &= \frac{\int_0^\infty dS(t)\int_0^\infty d\sigma_s(t)\mathcal{P}\left(S(t),\sigma_s(t),t\middle|S_0,\sigma_s(0),0\right)\sigma_s^2(t)S^2(t)\frac{\partial^2 C^{BS}}{\partial S^2(t)}}{\int_0^\infty dS(t)\mathcal{P}\left(S(t),t\middle|S_0,0\right)S^2(t)\frac{\partial^2 C^{BS}}{\partial S^2(t)}}\\
&= \int_0^\infty dS(t)q\left(S(t)\right)\mathbb{E}\left[\sigma_s^2(t)\middle|S(t)\right],
\end{aligned}
\tag{1.38}
$$

where

$$
q\left(S(t)\right) = \frac{\mathcal{P}\left(S(t),t\middle|S_0,0\right)S^2(t)\frac{\partial^2 C^{BS}}{\partial S^2(t)}}{\int_0^\infty dS(t)\mathcal{P}\left(S(t),t\middle|S_0,0\right)S^2(t)\frac{\partial^2 C^{BS}}{\partial S^2(t)}}, \tag{1.39}
$$

$$
\mathbb{E}\left[\sigma_s^2(t)\middle|S(t)\right] = \frac{\int_0^\infty d\sigma_s^2(t)\mathcal{P}\left(S(t),\sigma_s(t),t\middle|S_0,\sigma_s(0),0\right)\sigma_s^2(t)}{\mathcal{P}\left(S(t),t\middle|S_0,0\right)}. \tag{1.40}
$$

The term $q\left(S(t)\right)$ looks like a Brownian Bridge density for the underlying price: $\mathcal{P}\left(S(t),t\middle|S_0,0\right)$ has a delta function peak at $S_0$ at time $t=0$, and $\frac{\partial^2 C^{BS}}{\partial S_T^2}$ has a delta function peak at $S_T=K$ at expiration time $t=T$. Indeed, at expiration, the Black-Scholes call option price is very close to $\max[S_T-K,0]$ which has zero second derivative everywhere except at $S_T=K$. The term $\mathbb{E}\left[\sigma_s^2(t)\middle|S(t)\right]$ is the local variance depending on the value $S(t)$. The Black-Scholes implied variance is thus given by

$$
\sigma_{imp}^2 T = \int_0^T \sigma_{eff}^2(t)dt. \tag{1.41}
$$

Brownnian Bridge density peaks on a line, which represents the most probable path. We now have a very simple picture for the implied variance: it is approximately the arithmetic average of the local variances over the option life along the most probable path for the underlying price from $S_0$ at today time 0 to $K$ at expiration $T$.

## 1.3 Beyond the Black-Scholes model

### 1.3.1 Facts of the market

The existence of the volatility smile challenges the Black-Scholes model. The fluctuation of the amplitude of logreturn indicates the volatility of the underlying asset. We see from logreturns depicted in Figure 1.5 that large moves follow large moves and small moves follow small moves. This feature is called volatility clustering, which implies that volatility is auto-correlated, thus has a long memory. Empirical studies agree that the autocorrelation function of the absolute value of the price movements, which is similar to its volatility, decreases only slowly with time, see for instance (15, 16, 17, 18, 19, 20). However, empirical studies show that the price movement itself has a short memory property, i.e. in liquid markets the logreturn is to a good approximation uncorrelated beyond a time scale of a few tens of minutes, though on shorter time scales strong correlation effects are observed, see for instance (21, 22, 23).

It is observed from the probability density functions of the logreturn in Figure 1.5 that these distributions are highly peaked and fat tailed relative to the normal distribution. From the perspective of mathematics, high central peak and fat tails is the feature of a mixture of distributions with different variances. In other words, the volatility correlation induces positive excess kurtosis, a measure of the peakedness of the logreturn over the Gaussian distribution. Several researchers have examined the shape of the logreturn distribution, see for instance (24, 25, 26, 27, 28, 29, 30, 31). We also note from Figure 1.5 the negative skewness of these logreturn distributions. This is explained by the fact that a decrease of asset price is typically accompanied by an increase of volatility, a phenomenon called the 'leverage' effect. That is to say, it is the price-volatility correlation that induces the skewness of the logreturn distribution. An account on this skewness can be found in references (32, 33, 34).

Since the volatility has long range correlations, the logreturn distributions of different time scales varies slowly. One can in principle chose a time scale which is long enough to measure some properties of the logreturn, but short compared to the time scale over which the distribution of the logreturn is expected to vary. Suppose for example that the distribution of logreturn over a small time scale $t$ is a Gaussian distribution of a variance, which is itself a random variable. The averaged distribution of the logreturn over a long time scale $T$ is apparent non-Gaussian even if each individual distribution of the logreturn over small time scale $t$ is Gaussian. This is the original idea of the so called superstatistics in econophysics, see (35, 36, 37). For example, in (35) the authors prefer a log-normal distribution for the volatility.

The scaling characteristic of logreturn distributions is investigated. If the log-return is independent and identically distributed (i.i.d.), then its distribution corresponding to a time scale of $n\tau$ should be the $n$th convolution of the elementary distribution of a time scale $\tau$. However, systematic deviations from this simple rule are observed in empirical studies. This is due to the correlated volatility fluctuations (38, 39). The slow decay of the volatility correlation function, together with the observed approximate log-normal distribution of the volatility, leads to a 'multifractal-like' behavior of the price variations, much as what is observed in turbulent hydrodynamical flows. More details can be found in books (40, 41, 42) and references therein.

From a mathematical point of view, the distributions of logreturn approach the Gaussian limit, though slowly, as the time horizon becomes large. However, the scale-free nature of the non-Gaussian logreturn distribution was observed near the black Monday crash in October 1987. This scale invariance suggests breaking of the law of large numbers and reflects persistent multiscale correlations at criticality, with large fluctuations at a longer time scale, indicating propagation of the heterogeneity and clustering of the local variances across scales (43). One possible explanation of the black Monday crash might be that a highly clustered behavior of traders was induced by large fluctuations at a short time scale (about 10 minutes), and rapidly grew through internal interactions in the stock market. Such almost sudden large price fluctuations can only be modeled by jumps (11).

### 1.3.2 Alternative models

It is clear that we need to alter the basic premises of the Black-Scholes theory. There are several alternative models, which can be roughly classified into six groups:

(I) Parametric local volatility model. Replacing geometric Brownian motion with a different process was the earliest approach. Several other possibilities have been considered, notably, (a) constant elasticity of variance (CEV) model (44, 45, 46); (b) displaced diffusion model (47); (c) hyperbolic diffusion (48, 49, 50, 51). In general, these models do not match market prices exactly.

(II) Non-parametric local volatility model. Alternatively, several researchers have considered processes with unknown local volatility to be calibrated to the market via implied trees (52, 53) or in terms of the partial differential equation method (54).

(III) **Stochastic volatility (SV) model**. The importance of a time-varying volatility has been known for a long time (22, 55, 56, 57). Unlike local volatility models that fit the smile, SV models assume realistic dynamics for the underlying asset. They are useful because they explain in a self-consistent way why the 'volatility smile' exists, i.e. Black-Scholes implied volatility in general depends on the strike and the maturity time of the option. To start with I refer to some books and review papers regarding this topic (13, 58, 59, 60, 61, 62, 63). In the early days, a popular approach to model stochastic volatility was through a Brownian motion subordinated to a random clock. This clock time, often referred to as trading time, may be identified with the volume of trades or the frequency of trading (64, 65, 66, 67, 68). The idea is that volatility varies as trading activity fluctuates. Taylor is the first who suggests a model in discrete time that results in volatility clustering (69). Nevertheless, the majority of SV models are in continuous time. Pioneering authors on continuous SV models are Vasicek, Johnson, Wiggins, Hull and Scott (70, 71, 72, 73, 74). In the 1990s, Stein and Stein modeled the volatility by an Gaussian Ornstein-Uhlenbeck process (Stein & Stein model) and derived analytic formulas for the option price (75); Heston constructed an analytic European option pricing formula for his famous Heston model (76). In that model, Heston made an popular assumption that the variance is driven by a square root process (77). The Stein & Stein model and the Heston model are generalized by Duffie etc. to construct a so called affine models (78, 79). More complicated SV models are proposed later on, and some of them are interlinked with interest rate models; for more details I refer to (80). The promise of being able to generate volatility smiles and logreturn skewness, especially for long term calibration, makes SV models very popular. However, they can not reproduce strong skews and smiles at short maturity (11, 13).

(IV) Add jumps. (a) **Jump-diffusion based models**. The idea is that events which have a great impact on the underlying price occur infrequently. Apart from these events, the price evolves as a regular diffusion. At unpredictable times, relatively large up or down jumps are added to this regular diffusion. Merton was the first to explore jump diffusion models. In 1976 he proposed to add a Gaussian distributed jumps to the standard Black-Scholes dynamics (81). Other jump distributions, such as exponential (82) and hyper-exponential (83) have been popular as well. A review of affine jump-diffusion models can be found in (84); (b) Lévy process based models. These models have infinitely many jumps in every time interval. Infinitely many small jumps work like a Brownian process. Consequently, it is not necessary to add a Brownian motion component to these models when infinitely many jumps exist (85). Lévy models without diffusion component but only possessing a finite activity (86), however, are said not to lead to realistic price dynamics (11). In general, Lévy models are supposed to model the underlying price at all relevant time scales well (85, 87). An intuitive approach to built a Lévy process is via a time changed Brownian motion. This random time is interpreted as a business time (88) just as the trading time mentioned before. Two infinite activity models built in this way are the variance gamma (VG) model (89, 90, 91, 92) and the normal inverse Gaussian (NIG) model (93, 94, 95). A second way to construct a Lévy model is to model it as a tempered stable process (96, 97). The well known CGMY model (85, 98) belongs to this class. More details about other truncated Lévy processes can be found in (99, 100). The third approach to construct a Lévy model is by specifying the probability density function of the increments directly. A well known model belonging to this class is the generalized hyperbolic (GH) model (101, 102, 103, 104, 105, 106). This model coves a wide variety of shapes. With chosen special parameter values, the

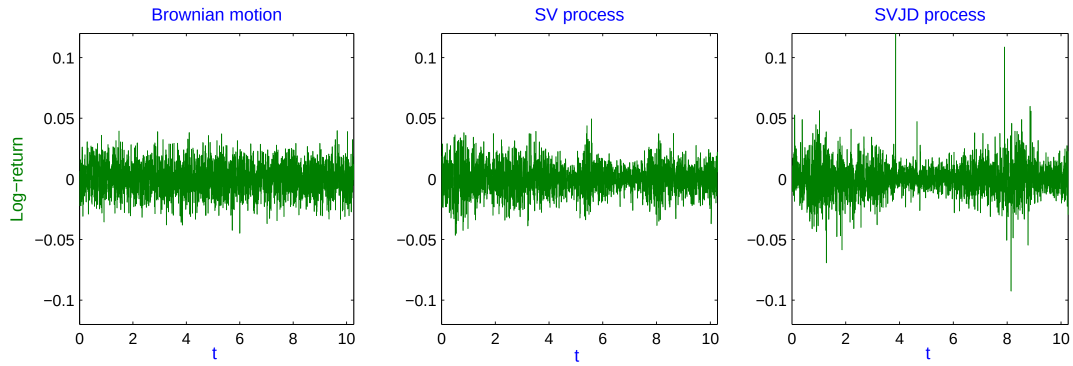


**Figure 1.7:** Samples of log-returns following a pure Brownian process (left panel), a stochastic volatility (SV) model (middle panel), and a stochastic volatility jump diffusion (SVJD) model (right panel), respectively.

GH model can reduce to the NIG model, the VG and the normal distribution. Recently, there are some papers about the time changed Lévy processes, see for instance (107, 108). The following are three excellent books, among others, about the application of Lévy process in finance: (11, 109, 110).

(V) Regime switching. Regime switching models have been less popular, see for instance (111) and references therein.

(VI) Various combinations of the above. Each of the models considered above has its own attractions as well as drawbacks. Hence several researchers tried to build combined models. Among others, popular models include: (1) the SV and stochastic interest rate model (112, 113, 114, 115); (2) the SV jump diffusion (SVJD) model (116, 117, 118, 119, 120, 121, 122). The need for such models is particularly strong in some markets where several exotics are liquid and can be used for calibration purposes. Figure 1.7 illustrates samples of log-returns under different models. No special parameter values are chosen. Comparing these samples with the real time evolution of log-returns shown in left panels of Figure 1.5, we see that the Brownian motion can not replicate the real log-returns well, the SV model performs well, and the SVJD model performs better.

## 1.4 A glance at the path integral approach

As seen before, a basic idea to solving the pricing problem of financial derivatives is through solving the partial differential equations, which forms the original mathematical method called the PDE approach. It is well known that in quantum mechanics the Schrödinger equation is commonly used to describe the quantum system. Solving a Schrödinger equation for a quantum system is analogous to solving a partial differential equation for the price of a financial derivative. Both the evolution of underlying assets' prices and the motion of microscopic particles are unpredictable. This shared uncertainty motivates the use of methods from theoretical physics for various financial derivative products, see for instance (41, 100, 123, 124) and references therein. Among them, the path integral method from quantum mechanics is most promising, among others, see (115, 125, 126, 127). This method is originally developed to calculate the probability amplitude of a particle evolving from an initial quantum state to a final quantum state directly without solving the Schrödinger equation. The application of the path integral approach to the pricing of financial derivatives inherits this superiority, i.e. one can derive the probability density functions of the underlying assets, and thus the derivatives' prices directly without solving the partial differential equation.

In this section, I will briefly introduce the path integral approach and show its equivalence to the PDE method. More details about the path integral method are given in the next chapter 2.2, and its applications to finance will be shown in chapters 3 to 6.

After the matrix mechanics, an algebraic formulation of quantum mechanics, created by Werner Heisenberg, Max Born, and Pascual Jordan in 1925 (128, 129, 130), as well as the wave mechanics, a partial differential equation formulation or a local description of quantum mechanics, created by Erwin Schrödinger in 1926 (131, 132), Richard Feynman proposed a third theoretical formulation of quantum mechanics, called the path integral in 1942 (133, 134, 135, 136), which is a global description of quantum mechanics. Heisenberg's matrix mechanics is a quantum correspondence of classical mechanics under the canonical formulation by replacing the classical Poisson bracket by a quantum commutator, and

Schrödinger's wave mechanics is closely related to the Hamilton-Jacobi equation in classical mechanics. Therefore, both of them have something to do with the classical Hamiltonian. However, Feynman's path integral involves the classical Lagrangian through the classical action. Path integration has shown its superiority in field quantization. Another merit of path integration lies in the fact that it can treat the time-dependent and time-independent problems in one framework. Furthermore, path integrals depict the relation between quantum mechanics and classical mechanics more vividly, and enable people to have a deeper understanding of some fundamental rules of classical mechanics, such as the principle of least action.

Nevertheless, these three formulations are equivalent to each other. By the Stone-von Neumann theorem, the Heisenberg picture and the Schrödinger picture are proved to be unitarily equivalent (137). We will prove briefly the equivalence of the formulations of Schrödinger and Feynman in the following context. For simplicity, we only consider the one dimensional case.

In Schrödinger's formulation, the quantum state of a particle is described by its wave function. For instance, we use $\psi(x,t)$ to characterize the probability amplitude of a one dimensional particle that appears in point $x$ at time $t$. In fact, people are not interested in the history of that particle, because all past information are included in $\psi(x,t)$. Given the wave function $\psi(x,t)$ at time $t$, then according to Schrödinger's equation (see the following context), one knows all the states of that particle at any later time. In contrast, the essence of path integration is to construct the **propagator** which includes all the information of the quantum system under consideration. The propagator, denoted by $\mathcal{K}\left(x'',t''|x',t'\right)$, gives the probability amplitude that the particle is located in $x''$ at time $t''$ given that it was in $x'$ at time $t'$, with $t'' \geq t'$. The relation between $\psi$ and $\mathcal{K}$ is given by:

$$\psi(x'',t'') = \int \mathcal{K}\left(x'',t''|x',t'\right)\psi(x',t')dx'. \tag{1.42}$$

According to Feynman's assumption, the propagator is given by

$$\mathcal{K}\left(x'',t''|x',t'\right) = C\sum_{\text{all paths}} e^{\frac{i}{\hbar}S[x(t)]} = C\sum_{\text{all paths}} e^{\frac{i}{\hbar}\int_{t'}^{t''}\mathcal{L}[x,\dot{x},t]dt}, \tag{1.43}$$

where $S[x]$ is the classical action, $\mathcal{L}[x, \dot{x}, t]$ is the classical Lagrangian, $\dot{x}$ is the time derivative of the position coordinate, i.e. the velocity, $i$ is the imaginary unit, and $\hbar$ is the reduced Planck constant. All paths contribute to the propagator with equal magnitude but varying phase according to $S[x(t)]$. Assume the action corresponding to one path from $x'$ to $x''$ is $S$ and to an adjacent path is $S + \delta S$. If these two paths are macro-distinguishable, i.e. $\delta S \gg \hbar$, then their contributions cancel because of destructive interference. Only the path which extremizes $S[x(t)]$, i.e. $\delta S = 0$, enhances the whole transition amplitude by coherent superposition. This is the quantum explanation of why macro-particles always follow the path given by the principle of least action. Note that minimizing the action functional $\delta S = 0$ involves the Euler-Lagrange equation. Recall that we mentioned the Euler-Lagrange equation in the previous section 1.2.1, where it is used to hedge the risk, thus to eliminate the arbitrage. Therefore the absence of arbitrage plays a fundamental role in finance similar to the least action principle in classical physics.

Return to the equation (1.43), which should be written as a functional integral due to the fact the all paths are changed continuously:

$$\mathcal{K}\left(x'', t'' | x', t'\right) = \int \mathcal{D}x(t)\, e^{\frac{i}{\hbar}\int_{t'}^{t''} \mathcal{L}[x,\dot{x},t]dt}. \tag{1.44}$$

Here $\int \mathcal{D}x(t)$ represents the integral over all possible continuous paths between two fixed endpoints $x'$ and $x''$. Feynman proposed a simple calculation scheme for this path integral via polygonal paths, writing the path integral as a limit of multi-dimensional Riemann integrals. A rigorous mathematical proof of this scheme can be found in (138, 139, 140).

Assume that the particle with mass $m$ evolves in a potential $V(x, t)$, then its classical Lagrangian is:

$$\mathcal{L}\left[x(t), \dot{x}(t), t\right] = \frac{1}{2}m\dot{x}^2 - V(x, t). \tag{1.45}$$

Now consider the case that $t'' - t' = \varepsilon \to 0^+$. According to Feynman's assumption, the propagator can be expressed as:

$$\mathcal{K}\left(x'', t' + \varepsilon | x', t'\right) = C\, e^{\frac{i\varepsilon}{\hbar}\mathcal{L}\left[\frac{x'+x''}{2}, \frac{x''-x'}{\varepsilon}, t'\right]}. \tag{1.46}$$

Therefore, expression (1.42) becomes (let $\eta = x' - x''$):

$$\psi(x'', t'+\varepsilon) = C\int_{-\infty}^{\infty} e^{\frac{i}{\hbar}\left[\frac{m\eta^2}{2\varepsilon} - \varepsilon V\left(x''+\frac{\eta}{2}, t\right)\right]}\psi(x''+\eta, t')d\eta. \tag{1.47}$$

Note that term $e^{\frac{im\eta^2}{2\hbar\varepsilon}}$ oscillates dramatically as $\varepsilon \to 0$, so the main contribution of the previous integral comes from the domain where $\eta \approx 0$. Seeing $\varepsilon$ and $\eta$ as infinitesimally small and taking the Taylor expansion of the previous equation with respect to $\eta$, we have:

$$\begin{aligned} \psi(x'', t') + \varepsilon\frac{\partial\psi}{\partial t'} &= C\int_{-\infty}^{\infty} e^{\frac{im\eta^2}{2\hbar\varepsilon}}\left[1 - \frac{i\epsilon}{\hbar}V\left(x'', t'\right)\right] \\ &\quad \times \left[\psi(x'', t') + \eta\frac{\partial\psi}{\partial x''} + \eta^2\frac{\partial^2\psi}{\partial(x'')^2} + \cdots\right]d\eta, \end{aligned} \tag{1.48}$$

which yields

$$C = \left(\int_{-\infty}^{\infty} e^{\frac{im\eta^2}{2\hbar\varepsilon}}d\eta\right)^{-1} = \sqrt{\frac{m}{2\pi i\hbar\varepsilon}}, \tag{1.49}$$

$$\psi(x'', t') + \varepsilon\frac{\partial\psi}{\partial t'} = \psi(x'', t') - \frac{i\varepsilon}{\hbar}\psi(x'', t') + \frac{i\hbar\varepsilon}{2m}\frac{\partial^2}{\partial(x'')^2}\psi(x'', t'). \tag{1.50}$$

The second equation is the **Schrödinger equation** (in one dimension):

$$i\hbar\frac{\partial}{\partial t}\psi\left(x, t\right) = \left(-\frac{\hbar^2}{2m}\frac{\partial^2}{\partial x^2} + V\right)\psi\left(x, t\right). \tag{1.51}$$

Thus we proved the equivalence between the Feynman path integral formulation and the Schrödinger equation.

As to the financial derivatives' pricing methods, besides the PDE method (by solving the partial differential equation analytically or numerically) and the path integral method (by calculating the probability density function), there are other methods such as the Monte Carlo simulations (141). We use differential equations when we model continuous processes. But if the processes are modeled discretely, then difference equations will be used. Moreover, when the model is complicated, the partial differential equation can be extended to a partial integro-differential equation. Even within the PDE method, in order to achieve high numerical efficiency, technically there are various ways including the Fast Fourier transform

(92), the generalized Fourier transform (79), the Laplace transform (142), the Fourier-Cosine expansion (143) and so on. I will not introduce them in detail here. In chapter 6, the method based on the Fourier-Cosine expansion, called the COS method (143), as well as a PDE method, call the finite difference method will be studied.

## 1.5 My contribution and the thesis' outline

Applying the path integral technique to the pricing of financial derivatives is the main goal of this thesis. How the path integral framework performs as an efficient alternative to the PDE method is first explained in chapter 2, including how to extract the Lagrangian from a stochastic differential equation, how to use the time slicing method to calculate the path integral (as well as its drawbacks), and how to improve it with the Duru-Kleinert time-space transformation. Besides this part, chapter 2 also provides other mathematical preliminaries that will be used in this thesis.

As far as I know, before the publication of our paper (144), path integral methods for the pricing of financial options in the literature are mostly based on models that can be recast in terms of a Fokker-Planck differential equation, i.e. neglect jumps and only describe drift and diffusion. I present in chapter 3, based on the article (144), a method to adapt formulas for both the path integral propagators and the option prices themselves, so that jump processes are taken into account in conjunction with the usual drift and diffusion terms. Therefore, the probability density function for a general stochastic volatility model with jumps can be calculated by the path integral now. This can be applied directed to the pricing of European vanilla options.

The price of a European vanilla option is quoted in the market by the implied volatility. However, the level of implied volatility often higher than the realized volatility in order to reflect the uncertainty of future market fluctuations. The fact that higher implied volatility gives higher European vanilla option price led to the development of the timer option. The principle of the timer option is remarkably simple: instead of fixing the maturity and letting the volatility float, the total realized volatility is fixed, and the expiry time is left floating. That is, the timer option can be viewed as a European option with random maturity, determined as the first time when the prespecified variance budget is exhausted. There are some benefits of introducing timer options. First of all, the holders of timer options only pay the realized variances, so no extra costs are payed for higher implied volatilities as with the European vanilla options. Secondly, it allows the pricing of call and put options whose implied volatilities are difficult to quote. Thirdly, the timer options will be terminated sooner or later according to the market realized variance, a feature that can be utilized to optimize the market timing. In chapter 4, the Duru-Kleinert method is applied to the pricing of timer options under general stochastic volatility models, based on our paper (145).

Chapter 5 is a collection of more applications of path integration over conditioned paths, an approach we already used in chapter 4. In particular, I derive closed-form pricing formulas for the continuous arithmetic and harmonic Asian option under the Black-Scholes model, for the variance options under Heston and 3/2 stochastic volatility with jump models, and for the VIX options under the 3/2 model. Asian options are path-dependent, i.e. its payoff function contains an average of the price of the underlying asset during the lifetime of the option. Consequently, their prices are normally not influenced so much by a single uncertain asset price at the expiry time (except for the floating Asian option that depends on the asset price at maturity). To price Asian options, first the set of all paths needs to be partitioned in subsets containing paths with the same average. Within each set, the option can be calculated just like a path-independent option. Then the results need to be averaged over the different partitions. This example well demonstrates the path integration over conditioned paths. The variance options as well as VIX futures and options are based on the calculation of the probability density function of the realized variance, which is defined as an integration of the stochastic variance. So the path integration over conditioned paths still performs distinctively for them. The last section of chapter 5 is retained for a topic outside of finance. It is related to radioactive decay. In that section, we investigate the radioactive dosimetry problem in an environment with fluctuating radioactivity. Fluctuating radioactivity is modeled by Poisson processes with stochastic intensity. The closed-form probability density functions of the maximum allowed exposure time for one receiving a predetermined dosimetry under six different models are obtained. All results shown in this chapter are part of (as yet unpublished) internal work notes.

So chapters 3 to 5 (and part of chapter 2) are exploring the path integral in finance. A method based on the Fourier Cosine expansion called the COS method (143) exhibited excellent performances recently in the pricing of both vanilla and some exotic options, especially under the Lévy process and for some options under the Heston model. This method relies on the availability of the characteristic function. Since the path integral technique allows to derive the probability density function, sometimes in a transformed form, efficiently for stochastic volatility jump-diffusion models, a combination of these two methods makes sense. I also note that the computational complexity for some exotic options is almost the same as that for vanilla options by using the finite difference method, so I also look into the finite difference method. These three methods are applied in chapter 6 to the pricing of some exotic options under the Heston stochastic volatility with uncorrelated Cox-Ingersoll-Ross stochastic interest rate. Reference values from literature or from Monte Carlo simulations are used, confirming our formulas. Nevertheless, the pricing of exotic options for three dimensional dynamics remains time consuming if we use the COS method directly. More effective implementations of the COS method and the finite difference method are the subject of further research.

Chapter 7 is devoted to the inverse problem of option pricing. We investigate how to extract the risk-neutral implied density of the underlying asset from observed market option prices. The option prices are only available for discrete sets of strikes in the real market, and moreover these prices contain errors. These two problems are tackled by our newly introduced rational interval interpolation method. This is a global and nonlinear method, and can retrieve the risk-neutral implied density thoroughly and quickly. We first use simulated option prices to demonstrate that our method outperforms some other common methods in the literature. We then look into real market data, and plug the risk-neutral implied density obtained by our method into the general European vanilla option pricing formulas to replicate the option prices, called the implied option prices. We checked that these implied option prices are mostly between the bid and ask intervals of the real market call and put options, confirming our method. Our method is efficient and robust, and the achieved risk-neutral implied density is promising to further applications, such as model calibration. This chapter is based on our newly submitted article (146).

Finally, a summary of this thesis as well as a list of my publications are given in chapter 8.

# 2

# Mathematical preliminaries

## 2.1 Stochastic processes, the Itô theorem and the Kolmogolov equations

Figure 1.5 illustrates typical time series of real market underlying assets, from which we can identify that these underlying assets evolve probabilistically in time, so they can be mathematically described as stochastic processes. For a stochastic process $X(t)$, we can measure values $x_0$, $x_1$, $x_2$, ..., $x_n$ at times $t_0$, $t_1$, $t_2$, ... $t_n$, and we assume that a set of joint probability densities exists $P\left(x_n, t_n; x_{n-1}, t_{n-1}; ...; x_0, t_0\right)$ which describes the process completely. We also define conditional probability densities ($0 \leq j-1 < n$):

$$P\left(x_n, t_n; ...; x_j, t_j | x_{j-1}, t_{j-1}; ...; x_0, t_0\right) = \frac{P\left(x_n, t_n; ...; x_j, t_j; ...; x_0, t_0\right)}{P\left(x_{j-1}, t_{j-1}; ...; x_1, t_1; x_0, t_0\right)}. \tag{2.1}$$

One type of stochastic processes is called the **Markov process**, in which knowledge of only the present determines the future. This process is preferred for financial modeling because of the fact that under the efficient market hypothesis only the current information contributes to future prices.

In a Markov process, the conditional probability is determined entirely by the knowledge of the most recent condition:

$$P\left(x_n, t_n; ...; x_j, t_j | x_{j-1}, t_{j-1}; ...; x_0, t_0\right) = P\left(x_n, t_n; ...; x_j, t_j | x_{j-1}, t_{j-1}\right). \tag{2.2}$$

From this Markov assumption, we have ($t_0 < t_1 < t_2$):

$$\begin{aligned}
P\left(x_2, t_2 | x_0, t_0\right) &= \int dx_1 P\left(x_2, t_2 | x_1, t_1; x_0, t_0\right) P\left(x_1, t_1 | x_0, t_0\right) \\
&= \int dx_1 P\left(x_2, t_2 | x_1, t_1\right) P\left(x_1, t_1 | x_0, t_0\right), \qquad (2.3)
\end{aligned}$$

which is the **Chapman-Kolmogorov equation**, see (147).

A general Markov process $Y(t)$ is introduced to model the time evolution of financial underlying assets by the following stochastic differential equation (SDE):

$$dY(t) = A\left(Y(t-), t\right) dt + B\left(Y(t-), t\right) dW(t) + j\left(Y(t-), J, t\right) dN(t), \qquad (2.4)$$

where the right terms represent the drift, diffusion and jumps processes respectively, $Y(t-)$ stands for the value of the process $Y(t)$ just before the jump $J$ occurs, $W(t)$ is a standard Wiener process (Brownian motion) and $N(t)$ is a Poisson process with stochastic intensity $\lambda\left(Y(t), t\right)$. The processes $W(t)$ and $N(t)$ are assumed to be independent. The random variable $J$ with probability density function (PDF) $\varpi(J)$ describes the magnitude of the jump when it occurs, and $j\left(Y(t-), J, t\right)$ maps the jump size to the post-jump value of $Y(t)$, see (79).

Note that $dW(t)$ is of order $\sqrt{dt}$, $dN(t)$ is of order $dt$, and recall that $\left(dW(t)\right)^2 = dt$. The Taylor series expansion for any twice differentiable function $F\left(Y(t), t\right)$ to the order $dt$ gives the so called **Itô lemma**:

$$\begin{aligned}
& dF\left(Y(t), t\right) \\
= \; & F_t\left(Y(t-), t\right) dt + F_Y\left(Y(t-), t\right) dY(t-) + \frac{1}{2} F_{YY}\left(Y(t-), t\right) \left(dY(t-)\right)^2 \\
= \; & \Big(F_t\left(Y(t-), t\right) + A\left(Y(t-), t\right) F_Y\left(Y(t-), t\right) \\
& + \frac{1}{2} B^2\left(Y(t-), t\right) F_{YY}\left(Y(t-), t\right)\Big) dt + B\left(Y(t-), t\right) F_Y\left(Y(t-), t\right) dW(t) \\
& + \left[F\left(Y(t-) + j\left(Y(t-), J, t\right), t\right) - F\left(Y(t-), t\right)\right] dN(t), \qquad (2.5)
\end{aligned}$$

where $F_t$, $F_Y$, $F_{YY}$ stand for partial derivatives with respect to $Y$ and $t$.

Denote the probability density of $Y(t)$ by $P\left(Y_T, T | Y_t, t\right)$, then the expectation value of $F\left(Y_T, T\right)$ is given by $\mathbb{E}\left[F\left(Y_T, T\right)\right] = \int F\left(Y_T, T\right) P\left(Y_T, T | Y_t, t\right) dY_T$. Now differentiate this expectation with respect to $T$:

$$
\begin{aligned}
&\frac{\partial}{\partial T}\int F(Y_T,T)\,P(Y_T,T|Y_t,t)\,dY_T \\
&= \lim_{\Delta T\to 0}\int dY_T\frac{F(Y_T,T+\Delta T)\,P(Y_T,T+\Delta T|Y_t,t)-F(Y_T,T)\,P(Y_T,T|Y_t,t)}{\Delta T} \\
&= \lim_{\Delta T\to 0}\frac{1}{\Delta T}\left\{\begin{array}{l}\int dY_T F(Y_T,T+\Delta T)\int P(Y_T,T+\Delta T|z,T)\,P(z,T|Y_t,t)\,dz \\ -\int dz F(z,T)\,P(z,T|Y_t,t)\end{array}\right\} \\
&= \int dz P(z,T|Y_t,t)\lim_{\Delta T\to 0}\frac{1}{\Delta T}\int dY_T P(Y_T,T+\Delta T|z,T) \\
&\quad\times\left(F(Y_T,T+\Delta T)-F(z,T)\right) \\
&= \int dz P(z,T|Y_t,t)\frac{1}{dT}\mathbb{E}\left[dF(z,T)\right] \\
&= \int dz P(z,T|Y_t,t)\left\{\begin{array}{l}A(z,T)F_z(z,T)+\frac{1}{2}B^2(z,T)F_{zz}(z,T) \\ +\int dJ\varpi(J)\left[F(z+j(z,J,T),T)-F(z,T)\right]\lambda(z,T)\end{array}\right\} \\
&= \int dz F(z,T)\left\{\begin{array}{l}-\frac{\partial}{\partial z}\left(P(z,T|Y_t,t)\,A(z,T)\right)+\frac{1}{2}\frac{\partial^2}{\partial z^2}\left(P(z,T|Y_t,t)\,A^2(z,T)\right) \\ +\int dJ\varpi(J)\lambda(z-j(z,J,T),T)P(z-j(z,J,T),T|Y_t,t) \\ -\lambda(z,T)P(z,T|Y_t,t)\end{array}\right\}.
\end{aligned}
$$

Hence

$$
\begin{aligned}
&\frac{\partial P(Y_T,T|Y_t,t)}{\partial T} \\
= \quad & -\frac{\partial}{\partial Y_T}\left(P(Y_T,T|Y_t,t)\,A(Y_T,T)\right)+\frac{1}{2}\frac{\partial^2}{\partial Y_T^2}\left(P(Y_T,T|Y_t,t)\,B^2(Y_T,T)\right) \\
&+\int dJ\varpi(J)\lambda(Y_T-j(Y_T,J,T),T)P(Y_T-j(Y_T,J,T),T|Y_t,t) \\
&-\lambda(Y_T,T)P(Y_T,T|Y_t,t)\,, \qquad (2.6)
\end{aligned}
$$

which is called the **Kolmogorov forward equation**. Similarly we have the **Kolmogorov backward equation**:

$$
\begin{aligned}
-\frac{\partial P(Y_T,T|Y_t,t)}{\partial t} \quad = \quad & A(Y_t,t)\frac{\partial}{\partial Y_t}P(Y_T,T|Y_t,t)+\frac{1}{2}B^2(Y_t,t)\frac{\partial^2}{\partial Y_t^2}P(Y_T,T|Y_t,t) \\
&+\lambda(Y_t,t)\int dJ\varpi(J)P(Y_T,T|Y_t+j(Y_t,J,t),t) \\
&-\lambda(Y_t,t)P(Y_T,T|Y_t,t)\,. \qquad (2.7)
\end{aligned}
$$

The initial condition for both equations is

$$P(Y_T,t|Y_t,t)=\delta(Y_T-Y_t) \quad \text{for all } t. \qquad (2.8)$$

In the case of the forward equation, we hold $(Y_t, t)$ fixed, and solutions exist for $T \geq t$, so that (2.8) is an initial condition for the forward equation. For the backward equation, solutions exist for $s \leq t$, so that (2.8) is a final condition in this case. The forward and the backward equations are equivalent to each other. The forward equation gives more directly the values of measurable quantities, so it tends to be used more commonly in European option pricing and model calibration. The backward equation is generally applied to option pricing with some optional features, such as American options which can be exercised by the holder at any time up to maturity time.

The mathematical definition of a continuous Markov process is through the Lindeberg condition (147), which requires that for any $\epsilon > 0$ we have

$$\lim_{\Delta t \to 0} \frac{1}{\Delta t} \int\limits_{|x - x_0| > \epsilon} P\left(x, t + \Delta t | x_0, t\right) dx = 0. \tag{2.9}$$

This means that the probability for the final position $x$ to be finitely different from $x_0$ goes to zero faster than $\Delta t$, as $\Delta t$ goes to zero.

We know from the definition of the Poisson process that for any infinitesimally small time step $\Delta t$, there is a finite probability that the path will jump. For this reason, the third term in (2.4) is known as the jump component. As to the second term in (2.4), we note that the transition probability of Wiener process, denoted by $P_W\left(x_T, T | x_t, t\right)$ satisfies the characteristic property $\lim\limits_{T-t \to 0} P_W\left(x_T, T | x_t, t\right) \to \delta\left(x_T - x_t\right)$. That is, after an infinitesimally small period of time the particle appears to be in the infinitesimally small vicinity of the initial point $x_t$. Brownian motions are thus continuous. On the other hand, recall that $\mathbb{E}\left[(\Delta W)^2\right] = \Delta t$, thus the shift during the period of time $\Delta t$ is of the order $\sqrt{\mathbb{E}\left[(\Delta W)^2\right]} \sim \sqrt{\Delta t}$ and the speed of the Brownian particle at any moment of time is infinite: $\lim\limits_{\Delta t \to 0} \frac{\sqrt{\Delta t}}{\Delta t} \to \infty$. Therefore, Brownian motions are in reality suns over fully 'zigzag-like' trajectories, which can be described more precisely in the framework of fractal theory, corresponding to non-differentiable continuous functions.

If we assume the quantities $\lambda\left(Y(t), t\right)$ to be zero, i.e. no jumps, the general Markov process (2.4) reduces to a Langevin process:

$$dY(t) = A\left(Y(t), t\right) dt + B\left(Y(t), t\right) dW(t), \tag{2.10}$$

thus the Kolmogorov forward equation (2.6) becomes the so called **Fokker-Planck equation**:

$$\begin{aligned}\frac{\partial P\left(Y_T, T|Y_t, t\right)}{\partial T} &= -\frac{\partial}{\partial Y_T}\left(P\left(Y_T, T|Y_t, t\right) A(Y_T, T)\right) \\ &+\frac{1}{2}\frac{\partial^2}{\partial Y_T^2}\left(P\left(Y_T, T|Y_t, t\right) B^2(Y_T, T)\right). \end{aligned} \tag{2.11}$$

The previous results (2.5), (2.6), (2.7) and (2.11) are based on a one-dimensional process $Y(t)$, for the multi-dimensional case, we have to replace $A$ by a drift vector and $B$ by a diffusion tensor, etc. Explicitly, the multi-dimensional Fokker-Planck equation is:

$$\begin{aligned}\frac{\partial P\left(\mathbf{Y}, T|\mathbf{X}, t\right)}{\partial T} &= -\sum_i \frac{\partial}{\partial Y_i}\left(P\left(\mathbf{Y}, T|\mathbf{X}, t\right) \mathbf{A}_i(\mathbf{Y}, T)\right) \\ &+\frac{1}{2}\sum_{i,j}\frac{\partial^2}{\partial Y_i \partial Y_j}\left(P\left(\mathbf{Y}, T|\mathbf{X}, t\right) \mathbf{B^2}_{ij}(\mathbf{Y}, T)\right), \end{aligned} \tag{2.12}$$

where $\mathbf{A}(\mathbf{Y}, T)$ is the drift vector and the matrix $\mathbf{B^2}(\mathbf{Y}, T)$ the diffusion matrix for the multi-dimensional Langevin process.

Similarly, without jumps, the Kolmogorov backward equation (2.7) reduces to:

$$\frac{\partial P\left(Y_T, T|Y_t, t\right)}{\partial t} + A(Y_t, t)\frac{\partial P\left(Y_T, T|Y_t, t\right)}{\partial Y_t} + \frac{1}{2}B^2(Y_t, t)\frac{\partial^2 P\left(Y_T, T|Y_t, t\right)}{\partial Y_t^2} = 0. \tag{2.13}$$

Especially, for the Black-Scholes model (1.14), $A = rS(t)$, $B = \sigma S(t)$, the transition probability density function of $S$ is given by:

$$\frac{\partial P\left(S_T, T|S_t, t\right)}{\partial t} + rS(t)\frac{\partial P\left(S_T, T|S(t), t\right)}{\partial S(t)} + \frac{1}{2}r^2 S^2(t)\frac{\partial^2 P\left(S_T, T|S(t), t\right)}{\partial S^2(t)} = 0. \tag{2.14}$$

Since the European call option price is expressed in the risk-neutral measure as $c = e^{-r(T-t)}\int_0^\infty dS_T\left(S_T - K\right)_+ P\left(S_T, T|S_t, t\right)$, we thus have:

$$\frac{\partial c}{\partial t} + rS(t)\frac{\partial c}{\partial S(t)} + \frac{1}{2}\sigma^2 S^2(t)\frac{\partial^2 c}{\partial S^2(t)} = rc, \tag{2.15}$$

which coincides with the Black-Scholes partial differential equation (1.20).

## 2.2 The path integral framework and probability density functions

Every Fokker-Planck equation has a corresponding path integral, because the Fokker-Planck equation is formally equivalent to the Schrödinger equation (with imaginary time) and we have proved in Chapter 1 that the Schrödinger equation is equivalent to the Feynman path integral.

As mentioned in section 1.4, the Feynman path integral originates from quantum mechanics, where it is used to describe the probability amplitude of quantum evolution between two fixed states, where each possible trajectory contributes a different phase. The probability for an event is given by the modulus squared of the probability amplitude. When using imaginary times, a Feynman path integral provides directly the transition probability density function between two fixed points, rather than the probability amplitude. From now on, we will use the "imaginary time" Feynman path integral which gives the probability density function, but for the sake of simplicity we will omit the "imaginary time" and refer to the probability density function as propagator.

In the Feynman path integral framework, the propagator is expressed as

$$P\left(Y_T, T|Y_t, t\right) = \int_{(Y_t,t)}^{(Y_T,T)} \mathcal{D}Y(s) \exp\left\{-\int_t^T \mathcal{L}\left[Y(s), \dot{Y}(s), s\right] ds\right\}. \tag{2.16}$$

Note that this expression is very similar to Feynman path integral expression in quantum mechanics, see (1.44), but now in an "imaginary time". The Lagrangian $\mathcal{L}\left[Y(s), \dot{Y}(s), s\right]$ for a general Langevin process (2.10) is given by (126, 148, 149):

$$\begin{aligned}\mathcal{L}\left[Y(s), \dot{Y}(s), s\right] &= \frac{1}{2B^2\left(Y(s), s\right)}\left[\dot{Y}(s) - h\left(Y(s), s\right)\right]^2 \\ &\quad + \frac{B\left(Y(s), s\right)}{2}\frac{\partial}{\partial Y(s)}\left(\frac{h\left(Y(s), s\right)}{B\left(Y(s), s\right)}\right),\end{aligned} \tag{2.17}$$

where

$$h\left(Y(s), s\right) = A\left(Y(s), s\right) - \frac{B\left(Y(s), s\right)}{2}\frac{\partial B\left(Y(s), s\right)}{\partial Y(s)}. \tag{2.18}$$

If $B$ does not depend on $Y(s)$ explicitly, then $h\left(Y(s), s\right) = A\left(Y(s), s\right)$ and the Lagrangian (2.17) reduces to:

$$\mathcal{L}\left[Y(s), \dot{Y}(s), s\right] = \frac{1}{2B^2(s)}\left[\dot{Y}(s) - A\left(Y(s), s\right)\right]^2 + \frac{1}{2}\frac{\partial A\left(Y(s), s\right)}{\partial Y(s)}. \tag{2.19}$$

Note that $\dot{Y}(s)$ is not well defined since $Y(s)$ is continuous but nowhere differentiable. But $\dot{Y}(s)$ in (2.16) has a meaning as velocity because the discretization rule is specified by the Wiener measure $\int_{(Y_t,t)}^{(Y_T,T)} \mathcal{D}Y(s)$. More explicitly, plugging (2.19) into (2.16), we see that the classical action $S = \int_t^T \mathcal{L}\left[Y(s), \dot{Y}(s), s\right] ds$ contains a term $\int_t^T \frac{A(Y(s),s)}{B(s)} dW(s)$, which is a $\theta-$stochastic integral. A $\theta-$stochastic integral is defined by

$$I^{(\theta)}(X) = \int_t^T X(s)_\theta dW(s) = \lim_{n\to\infty} \sum_{i=0}^{n-1} X(t_i^\theta)\left(W(t_{i+1}) - W(t_i)\right) \tag{2.20}$$

for any partition $t = t_0 < t_1 < \cdots < t_{n-1} < t_n = T$ and with $t_i^\theta$ equals to

$$t_i^\theta = t_i + \theta\left(t_{i+1} - t_i\right). \tag{2.21}$$

In the path integral framework, we use the mid-point formulation, i.e. $\theta = \frac{1}{2}$. The $\theta$-stochastic integral then reduces to a Stratonovich stochastic integral. The advantage of Stratonovich stochastic integral is that if we introduce a function $\phi(Y)$ such that $\frac{A(Y(s),s)}{B^2(s)} = \frac{d\phi}{dY}$, then the classical chain rule is formally satisfied:

$$\int_t^T \frac{A\left(Y(s), s\right)}{B^2(s)} \dot{Y}(s) ds = \int_t^T \frac{d\phi}{dY} dY = \phi(Y_T) - \phi(Y_t), \tag{2.22}$$

which is the same for all paths and depends only on the endpoints.

It is important to note that the result (2.22) is true only if we use the mid-point formulation (Stratonovich prescription). If we use the left-point formulation ($\theta = 0$), which is the Itô prescription, then

$$d\phi = \frac{d\phi}{dY} dY + \frac{B^2}{2} \frac{d^2\phi}{dY^2} ds = \frac{d\phi}{dY} dY + \frac{1}{2} \frac{\partial A(Y(s), s)}{\partial Y(s)} ds \tag{2.23}$$

according to Itô's lemma, thus

$$\int_t^T \frac{A\left(Y(s), s\right)}{B^2(s)} \dot{Y}(s) ds = \int_t^T \frac{d\phi}{dY} dY = \phi(Y_T) - \phi(Y_t) - \frac{1}{2} \int_t^T \frac{\partial A(Y(s), s)}{\partial Y(s)} ds. \tag{2.24}$$

In fact, if we use the left-point formulation, the term $\frac{1}{2}\frac{\partial A(Y(s),s)}{\partial Y(s)}$ should be dropped in (2.19), so the final classical action is the same in both the left-point and the mid-point cases. In conclusion, the reason why we adopt the mid-point formulation lies in the convenience of the classical chain rule of integral calculus.

According to Feynman's polygonal paths method, a procedure called time slicing is implemented. With two end points $Y_t$ at initial time $t$ and $Y_T$ at time $T$, we divide the time interval $[t, T]$ into $N$ equal infinitesimal segments with duration $\varepsilon = \frac{T-t}{N} \to 0$. That is $t_j = t + j\varepsilon$ for $j = 0, 1, \cdots, N$, while $t_0 = t$ and $t_N = T$. The infinite-dimensional functional integral (2.16) is therefore computed as the following limit ($Y_j = Y(t_j), j = 0, 1, \cdots, N$):

$$\begin{aligned} P\left(Y_T, T|Y_t, t\right) &= \int_{(Y_t,t)}^{(Y_T,T)} \mathcal{D}Y(s) \exp\left\{-\int_t^T \mathcal{L}\left[Y(s), \dot{Y}(s), s\right] ds\right\} \\ &= C \lim_{N\to\infty} \int dY_1 \int dY_2 \cdots \int dY_{N-1} \\ &\quad \times \exp\left\{-\varepsilon \sum_{j=1}^{N} \mathcal{L}\left[\frac{Y_j + Y_{j-1}}{2}, \frac{Y_j - Y_{j-1}}{\varepsilon}, \frac{t_j + t_{j-1}}{2}\right]\right\} \end{aligned} \quad (2.25)$$

where $C$ is a proper normalization factor. For the value of $C$, we resort to the infinitesimal propagator of process (2.10), which is known to be a normal distribution when $\varepsilon = t_j - t_{j-1} \to 0$:

$$P\left(Y_{t_j}, t_j|Y_{t_{j-1}}, t_{j-1}\right) = \frac{1}{\sqrt{2\pi B^2(Y_{t_{j-1}}, t_{j-1})\varepsilon}}\, e^{-\frac{\left[Y_{t_j} - Y_{t_{j-1}} - A(Y_{t_{j-1}}, t_{j-1})\varepsilon\right]^2}{2B^2(Y_{t_{j-1}}, t_{j-1})\varepsilon}} \quad (2.26)$$

In addition, the Chapman-Kolmogorov equation (2.3) holds for the propagator:

$$P\left(Y_T, T|Y_t, t\right) = \lim_{N\to\infty} \int dY_1 \int dY_2 \cdots \int dY_{N-1} \prod_{j=1}^{N} P\left(Y_{t_j}, t_j|Y_{t_{j-1}}, t_{j-1}\right). \quad (2.27)$$

Inserting (2.26) into (2.27) and comparing it with (2.25), we have the Wiener path integral measure for (2.16):

$$\mathcal{D}Y = \prod_{i=1}^{N-1} dY_i \prod_{j=1}^{N} \frac{1}{\sqrt{2\pi B^2\left(Y_{j-1}, t_{j-1}\right)\varepsilon}}. \quad (2.28)$$

In the rest of this section, I will give some examples to illustrate how propagators are derived by the path integral approach.

### 2.2.1 Examples of path integral propagators

#### 2.2.1.1 Propagator for the Black-Scholes model

The most simple example is for the Black-Scholes model (1.21). The substitution $x(t) = \ln S(t)$ leads to a SDE for $x(t)$ according to the Itô lemma (2.5):

$$dx(t) = \left(r - \frac{\sigma^2}{2}\right) dt + \sigma dW(t). \tag{2.29}$$

Since $B = \sigma$ does not depends on $x$, the Lagrangian (2.19) becomes

$$\mathcal{L}\left[x, \dot{x}, t\right] = \frac{1}{2\sigma^2}\left[\dot{x} - \left(r - \frac{\sigma^2}{2}\right)\right]^2. \tag{2.30}$$

The transition probability that $x(t)$ arrives in $x_T$ at time $T$ given its initial position $x_0$ at time 0, denoted by $\mathcal{P}\left(x_T, T|x_0, 0\right)$, is given by the path integral (2.16):

$$\begin{aligned}\mathcal{P}\left(x_T, T|x_0, 0\right) &= \int \mathcal{D}x(t)\, e^{-\int_0^T \frac{1}{2\sigma^2}\left[\dot{x} - \left(r - \frac{\sigma^2}{2}\right)\right]^2 dt} \\ &= e^{\left(r - \frac{\sigma^2}{2}\right)\frac{(x_T - x_0)}{\sigma^2} - \left(r - \frac{\sigma^2}{2}\right)^2 \frac{T}{2\sigma^2}} \int \mathcal{D}x(t)\, e^{-\frac{1}{2\sigma^2}\int_0^T \dot{x}^2 dt}. \end{aligned} \tag{2.31}$$

Applying (2.28) and (2.25), the previous expression can be written as the path integral for a free particle with mass $\frac{1}{\sigma^2}$:

$$\begin{aligned}\int \mathcal{D}x(t)\, e^{-\frac{1}{2\sigma^2}\int_0^T \dot{x}^2 dt} &= \int \prod_{i=1}^{N-1} dx_i \prod_{j=1}^{N} \frac{1}{\sqrt{2\pi\sigma^2\varepsilon}}\, e^{-\frac{\left(x_j - x_{j-1}\right)^2}{2\sigma^2\epsilon}} \\ &= \frac{1}{\sqrt{2\pi\sigma^2 N\varepsilon}}\, e^{-\frac{(x_N - x_0)^2}{2\sigma^2 N\varepsilon}}. \end{aligned} \tag{2.32}$$

Since $N\varepsilon = T$ and $x_N = x(t_N) = x(T) = x_T$, we finally get the well known result:

$$\begin{aligned}\mathcal{P}\left(x_T, T|x_0, 0\right) &= e^{\left(r - \frac{\sigma^2}{2}\right)\frac{(x_T - x_0)}{\sigma^2} - \left(r - \frac{\sigma^2}{2}\right)^2 \frac{T}{2\sigma^2}} \frac{1}{\sqrt{2\pi\sigma^2 T}}\, e^{-\frac{(x_T - x_0)^2}{2\sigma^2 T}} \\ &= \frac{1}{\sqrt{2\pi\sigma^2 T}} \exp\left\{-\frac{\left(x_T - x_0 - \left(r - \sigma^2/2\right)T\right)^2}{2\sigma^2 T}\right\}. \end{aligned} \tag{2.33}$$

The propagator of $S(t)$ is obtained by the relation that $\mathcal{P}\left(x_T, T|x_0, 0\right) dx_T = \mathcal{P}\left(S_T, T|S_0, 0\right) dS_T$:

$$\mathcal{P}\left(S_T, T|S_0, 0\right) = \frac{1}{\sqrt{2\pi\sigma^2 T}S_T} \exp\left\{-\frac{\left(\ln S_T - \ln S_0 - \left(r - \sigma^2/2\right)T\right)^2}{2\sigma^2 T}\right\}, \tag{2.34}$$

which is a log-normal distribution as expected. Inserting this propagator into the risk-neutral pricing formula, we can quickly obtain the Black-Scholes option prices through discounted expectation values with respect to $\mathcal{P}(S_T, T|S_0, 0)$. For instance the European vanilla call option price with strike price $K$ and time to maturity $T$ is given by

$$\begin{aligned}
\mathcal{C}(K,T) &= e^{-rT}\mathbb{E}\left[\max\left(S_T - K, 0\right)\right] \\
&= e^{-rT}\int_K^\infty \left(S_T - K\right)\mathcal{P}\left(S_T, T|S_0, 0\right) dS_T \\
&= e^{-rT}\int_{\ln K}^\infty \left(e^{x_T} - K\right)\mathcal{P}\left(x_T, T|x_0, 0\right) dx_T \\
&= S_0 \int_{\ln K-(x_0+(r+\sigma^2/2)T)}^\infty \frac{1}{\sqrt{2\pi\sigma^2 T}} \exp\left\{-\frac{z^2}{2\sigma^2 T}\right\} dz \\
&\quad -K \int_{\ln K-(x_0+(r-\sigma^2/2)T)}^\infty \frac{1}{\sqrt{2\pi\sigma^2 T}} \exp\left\{-\frac{z^2}{2\sigma^2 T}\right\} dz \\
&= S_0\, N\left(d_+\right) - K N\left(d_-\right),
\end{aligned} \tag{2.35}$$

where $N(\cdot)$ is the cumulative normal distribution function and

$$d_\pm = \frac{\ln\left(S_0 \exp\left\{rT\right\}/K\right)}{\sigma\sqrt{T}} \pm \frac{1}{2}\sigma\sqrt{T}, \tag{2.36}$$

in agreement with (1.26).

#### 2.2.1.2 Propagator for the Cox-Ingersoll-Ross model

The Cox-Ingersoll-Ross (CIR) model is originally created for the interest rate $r$ (150). The dynamics of $r$ in the CIR model is governed by the following SDE:

$$dr(t) = \kappa\left(\theta - r(t)\right) dt + \sigma\sqrt{r} dW(t). \tag{2.37}$$

This SDE is the same as the one used in the Heston stochastic volatility model to describe the time evolution of the volatility. Just as for the Black-Scholes model, first a substitution is made such that the diffusion term of the new variable does not depend on itself. Let $z(t) = \sqrt{r(t)}$, the Itô lemma (2.5) tells us that

$$dz = \left[\frac{\kappa\theta - \sigma^2/4}{2z} - \frac{\kappa}{2}z\right] dt + \frac{\sigma}{2} dW(t). \tag{2.38}$$

Its Lagrangian is then calculated, see (2.19):

$$\begin{aligned}\mathcal{L}[z,\dot{z},t] &= \frac{1}{2\left(\frac{\sigma}{2}\right)^2}\left[\dot{z}-\left(\frac{\kappa\theta-\sigma^2/4}{2z}-\frac{\kappa}{2}z\right)\right]^2+\frac{1}{2}\left(-\frac{\kappa\theta-\sigma^2/4}{2z^2}-\frac{\kappa}{2}\right)\\ &= \frac{2}{\sigma^2}\dot{z}^2+\frac{(\kappa\theta-\sigma^2/4)(\kappa\theta-3\sigma^2/4)}{2\sigma^2z^2}+\frac{\kappa^2}{2\sigma^2}z^2\\ &\quad -\frac{2(\kappa\theta-\sigma^2/4)}{\sigma^2}\frac{\dot{z}}{z}+\frac{2\kappa}{\sigma^2}z\dot{z}-\frac{\kappa^2\theta}{\sigma^2}.\end{aligned} \tag{2.39}$$

The propagator of $z$, denoted by $\mathcal{P}(z_T,T|z_0,0)$ is expressed as, see (2.16):

$$\begin{aligned}\mathcal{P}(z_T,T|z_0,0) &= \int\mathcal{D}z(t)\,e^{-\int_0^T\mathcal{L}[z,\dot{z},t]dt}\\ &= \left(\frac{z_T}{z_0}\right)^{\frac{2\kappa\theta}{\sigma^2}-\frac{1}{2}} e^{-\frac{\kappa}{\sigma^2}\left(z_T^2-z_0^2-\kappa\theta T\right)}\\ &\quad\times\int\mathcal{D}z(t)\,e^{-\int_0^T\left[\frac{2}{\sigma^2}\dot{z}^2+\frac{\kappa^2}{2\sigma^2}z^2+\frac{\left(\kappa\theta-\sigma^2/4\right)\left(\kappa\theta-3\sigma^2/4\right)}{2\sigma^2}\frac{1}{z^2}\right]dt}.\end{aligned} \tag{2.40}$$

Introducing new notations: $a=\frac{\sigma^2}{4}$, $b=\frac{\kappa}{2}$, and $\lambda=\frac{2\kappa\theta}{\sigma^2}-1$, we arrive at the one dimensional path integral for the radial harmonic oscillator:

$$\mathcal{P}_{RHO}=\int\mathcal{D}z(t)\exp\left\{-\int_0^T\left[\frac{1}{2a}\dot{z}^2+\frac{b^2}{2a}z^2+\frac{\left(\lambda^2-\frac{1}{4}\right)a}{2}\frac{1}{z^2}\right]dt\right\}. \tag{2.41}$$

The solution of this path integral is not trivial. The first step is time slicing, see (2.28) and (2.25):

$$\mathcal{P}_{RHO}=\lim_{N\to\infty}\int dz_1\cdots dz_{N-1}\left(\frac{1}{\sqrt{2\pi a\varepsilon}}\right)^N\prod_{j=1}^N e^{-\frac{\left(z_j-z_{j-1}\right)^2}{2a\varepsilon}-\frac{b^2\varepsilon}{4a}\left(z_j^2+z_{j-1}^2\right)-\frac{\left(\lambda^2-\frac{1}{4}\right)a}{2z_jz_{j-1}}\varepsilon}. \tag{2.42}$$

Note that to first order in $\Delta z=z_j-z_{j-1}$, $\left(\frac{z_j+z_{j-1}}{2}\right)^2=\frac{z_j^2+z_{j-1}^2}{2}=z_jz_{j-1}=z_{j-1}^2+z_{j-1}\Delta z$. In the limit of $x$ going to infinity, the asymptotic approximation holds for the modified Bessel function of the first kind:

$$I_\nu(x)=\frac{1}{\sqrt{2\pi x}}\exp\left\{x-\frac{\nu^2-\frac{1}{4}}{2x}\right\}\left(1+\mathcal{O}\left(\frac{1}{x^2}\right)\right). \tag{2.43}$$

Since $\frac{z_jz_{j-1}}{a\varepsilon}\to\infty$ as $\varepsilon\to 0$, to first order in $\varepsilon$ we have

$$e^{-\frac{\left(\lambda^2-\frac{1}{4}\right)a}{2z_jz_{j-1}}\varepsilon}=I_\lambda\left(\frac{z_jz_{j-1}}{a\varepsilon}\right)\sqrt{2\pi\frac{z_jz_{j-1}}{a\varepsilon}}\,e^{-\frac{z_jz_{j-1}}{a\varepsilon}}. \tag{2.44}$$

Thus

$$\begin{aligned}\mathcal{P}_{RHO} &= \sqrt{z_0 z_T}\lim_{N\to\infty}\int z_1 dz_1\cdots z_{N-1}dz_{N-1}\left(\frac{1}{a\varepsilon}\right)^N \\ &\times\prod_{j=1}^{N} e^{-\left(z_j^2+z_{j-1}^2\right)\left(\frac{1}{2a\varepsilon}+\frac{b^2\varepsilon}{4a}\right)} I_\lambda\left(\frac{z_j z_{j-1}}{a\varepsilon}\right).\end{aligned} \tag{2.45}$$

The substitutions $\alpha = \frac{1}{a\varepsilon}$, $\beta = \frac{1}{a\varepsilon}+\frac{b^2\varepsilon}{2a} = \alpha\left(1+\frac{1}{2}b^2\varepsilon^2\right)$ lead to:

$$\begin{aligned}\mathcal{P}_{RHO} &= \sqrt{z_0 z_T}\, e^{-\frac{\beta}{2}\left(z_0^2+z_T^2\right)}\lim_{N\to\infty}\alpha^N\int dz_1\cdots dz_{N-1} z_1\, e^{-\beta z_1^2}\cdots z_{N-1}\, e^{-\beta z_{j-1}^2} \\ &\times I_\lambda\left(\alpha z_1 z_0\right) I_\lambda\left(\alpha z_2 z_1\right)\cdots I_\lambda\left(\alpha z_T z_{N-1}\right).\end{aligned} \tag{2.46}$$

By using the identity ($\mathrm{Re}[p]>0, \mathrm{Re}[\nu]>-1$), see 6.633-4 in (151):

$$\int_0^\infty x\, e^{-px^2} I_\nu(c_1 x) I_\nu(c_2 x)dx = \frac{1}{2p}\, e^{\frac{c_1^2+c_2^2}{4p}} I_\nu\left(\frac{c_1 c_2}{2p}\right), \tag{2.47}$$

the integration over $z_1$ becomes

$$\int_0^\infty dz_1 z_1\, e^{-\beta z_1^2} I_\lambda\left(\alpha z_1 z_0\right) I_\lambda\left(\alpha z_2 z_1\right) = \frac{1}{2\gamma_1}\, e^{\frac{T_1^2 z_0^2+\alpha^2 z_2^2}{4\gamma_1}}\, I_\lambda\left(\frac{T_1 z_0 \alpha z_2}{2\gamma_1}\right), \tag{2.48}$$

where

$$\gamma_1 = \beta, \quad T_1 = \alpha; \tag{2.49}$$

and the integration over $z_2$ becomes

$$\int_0^\infty dz_2 z_2\, e^{-\left(\beta-\frac{\alpha^2}{4\gamma_1}\right)z_2^2} I_\lambda\left(\frac{\alpha T_1 z_0}{2\gamma_1} z_2\right) I_\lambda\left(\alpha z_3 z_2\right) = \frac{1}{2\gamma_2}\, e^{\frac{T_2^2 z_0^2+\alpha^2 z_3^2}{4\gamma_2}}\, I_\lambda\left(\frac{T_2 z_0 \alpha z_3}{2\gamma_2}\right), \tag{2.50}$$

where

$$\gamma_2 = \beta-\frac{\alpha^2}{4\gamma_1}, \quad T_2 = \frac{\alpha^2}{2\gamma_1}. \tag{2.51}$$

Next, the integration over $z_3$ yields

$$\int_0^\infty dz_3 z_3\, e^{-\left(\beta-\frac{\alpha^2}{4\gamma_2}\right)z_3^2} I_\lambda\left(\frac{\alpha T_2 z_0}{2\gamma_2} z_3\right) I_\lambda\left(\alpha z_4 z_3\right) = \frac{1}{2\gamma_3}\, e^{\frac{T_3^2 z_0^2+\alpha^2 z_4^2}{4\gamma_3}}\, I_\lambda\left(\frac{T_3 z_0 \alpha z_4}{2\gamma_3}\right), \tag{2.52}$$

where

$$\gamma_3 = \beta-\frac{\alpha^2}{4\gamma_2}, \quad T_3 = \frac{\alpha^3}{2\gamma_1 2\gamma_2}. \tag{2.53}$$

The successive integrations are performed in the same manner until the integration over $z_{N-1}$. Putting these terms into expression (2.46) yields

$$\begin{aligned}\mathcal{P}_{RHO} =& \sqrt{z_0 z_T}\exp\left\{-\frac{\beta}{2}\left(z_0^2+z_T^2\right)\right\}\lim_{N\to\infty}\alpha^N\frac{1}{2\gamma_1}\frac{1}{2\gamma_2}\cdots\frac{1}{2\gamma_{N-1}}\exp\left\{\frac{\alpha^2}{4\gamma_{N-1}}z_T^2\right\}\\ &\times\exp\left\{\left(\frac{T_1^2}{4\gamma_1}+\frac{T_2^2}{4\gamma_2}+\cdots+\frac{T_{N-1}^2}{4\gamma_{N-1}}\right)z_0^2\right\}I_\lambda\left(\frac{\alpha T_{N-1}}{2\gamma_{N-1}}z_0 z_T\right),\end{aligned} \tag{2.54}$$

where the coefficients $\gamma$ and $T$ are given by:

$$\gamma_1=\beta, T_1=\alpha, \gamma_k=\beta-\frac{\alpha^2}{4\gamma_{k-1}}, T_k=\frac{\alpha^k}{2\gamma_1 2\gamma_2\cdots 2\gamma_{k-1}}, (k=2,3,\cdots,N-1). \tag{2.55}$$

Now these quantities can be determined, starting with the evaluation of $\gamma_k$. Since $\gamma_k=\beta-\frac{\alpha^2}{4\gamma_{k-1}}$, that is $\frac{2}{\alpha}\gamma_k=\frac{2}{\alpha}\beta-\frac{1}{\frac{2}{\alpha}\gamma_{k-1}}$, we can let $C_k=\frac{2}{\alpha}\gamma_k$, then $C_k+\frac{1}{C_{k-1}}=\frac{2}{\alpha}\beta$ for $k=2,3,\cdots,N-1$ while $C_1=\frac{2}{\alpha}\beta$. Furthermore, let $C_k=\frac{y_{k+1}}{y_k}$, then $\frac{y_{k+1}+y_{k-1}}{y_k}=\frac{2}{\alpha}\beta=2+b^2\varepsilon^2$. Arranging the terms we have

$$\frac{y_{k+1}-2y_k+y_{k-1}}{\varepsilon^2}=b^2 y_k, \tag{2.56}$$

which in the limit $\varepsilon\to 0$ gives a differential equation $\ddot{y}-b^2y=0$, where $\ddot{y}$ means the second derivative with respect to time. For the boundary conditions for $y$, we extend $C_k$ to $C_0$, then $\frac{1}{C_0}=\frac{2}{\alpha}\beta-C_1=0=\frac{y_0}{y_1}$, so $y_0=0$. The solution of $y$ is thus $y(t)=\frac{d}{2}\left(e^{bt}-e^{-bt}\right)=d\sinh(bt)$, with $d$ being a constant. Therefore

$$\begin{aligned} y_k &= y(t_k)=y(k\varepsilon)=d\sinh\left(bk\varepsilon\right), &(2.57)\\ \dot{y}_k &= db\sinh(bt_k)=db\sinh(bk\varepsilon). &(2.58)\end{aligned}$$

Consequently

$$
\begin{aligned}
\lim_{N\to\infty} \alpha^N \frac{1}{2\gamma_1}\frac{1}{2\gamma_2}\cdots\frac{1}{2\gamma_{N-1}} &= \lim_{N\to\infty} \alpha \frac{y_1}{y_2}\frac{y_2}{y_3}\cdots\frac{y_{N-1}}{y_N} \\
&= \lim_{N\to\infty} \frac{1}{a\varepsilon}\frac{d\sinh(b\varepsilon)}{d\sinh(bN\varepsilon)} \\
&= \frac{b}{a}\frac{1}{\sinh(bT)}; \qquad (2.59) \\
\lim_{N\to\infty} \exp\left\{-\left(\frac{\beta}{2}-\frac{\alpha^2}{4\gamma_{N-1}}\right)z_T^2\right\} &= \lim_{N\to\infty} \exp\left\{-\frac{\alpha}{4}\left(C_N - \frac{1}{C_{N-1}}\right)z_T^2\right\} \\
&= \lim_{N\to\infty} \exp\left\{-\frac{1}{2a}\frac{\dot{y}_N}{y_N}z_T^2\right\} \\
&= \exp\left\{-\frac{b}{2a}\coth(bT)\,z_T^2\right\}; \qquad (2.60) \\
\lim_{N\to\infty} I_\lambda\left(\frac{\alpha T_{N-1}}{2\gamma_{N-1}}z_0 z_T\right) &= \lim_{N\to\infty} I_\lambda\left(\alpha\frac{y_1}{y_2}\frac{y_2}{y_3}\cdots\frac{y_{N-1}}{y_N}z_0 z_T\right) \\
&= I_\lambda\left(\frac{b z_0 z_T}{a\sinh(bT)}\right). \qquad (2.61)
\end{aligned}
$$

Similarly

$$
\begin{aligned}
&\lim_{N\to\infty} \exp\left\{-\left[\frac{\beta}{2}-\left(\frac{T_1^2}{4\gamma_1}+\frac{T_2^2}{4\gamma_2}+\cdots+\frac{T_{N-1}^2}{4\gamma_{N-1}}\right)\right]z_0^2\right\} \\
=\;& \lim_{N\to\infty} \exp\left\{-\left[\frac{\beta}{2}-\sum_{k=1}^{N-1}\frac{(\alpha y_1/y_k)^2}{2\alpha y_{k+1}/y_k}\right]z_0^2\right\} \\
=\;& \lim_{N\to\infty} \exp\left\{-\left[\frac{\beta}{2}-\frac{\alpha b^2\varepsilon}{2}\sum_{k=1}^{N-1}\frac{\varepsilon}{\sinh(bt_k)\sinh(bt_{k+1})}\right]z_0^2\right\} \\
=\;& \lim_{N\to\infty} \exp\left\{-\left[\frac{\beta}{2}-\frac{\alpha b^2\varepsilon}{2}\int_\varepsilon^T\frac{dt}{\sinh^2(bt)}\right]z_0^2\right\} \\
=\;& \lim_{N\to\infty} \exp\left\{-\left[\frac{\beta}{2}+\frac{b}{2a}\left(\coth(bT)-\coth(b\varepsilon)\right)\right]z_0^2\right\} \\
=\;& \exp\left\{-\frac{b}{2a}\coth(bT)\,z_0^2\right\}. \qquad (2.62)
\end{aligned}
$$

Plugging (2.59), (2.60), (2.61) and (2.62) into (2.46), we have finally for the path integral of the radial harmonic oscillator:

$$\begin{aligned} &\int \mathcal{D}z(t) \exp\left\{-\int_0^T \left[\frac{1}{2a}\dot{z}^2 + \frac{b^2}{2a}z^2 + \frac{\left(\lambda^2 - \frac{1}{4}\right)a}{2}\frac{1}{z^2}\right] dt\right\} \\ = &\frac{\sqrt{z_0 z_T} b}{a \sinh(bT)} \exp\left\{-\frac{b}{2a}\coth(bT)\left(z_0^2 + z_T^2\right)\right\} I_\lambda\left(\frac{b z_0 z_T}{a \sinh(bT)}\right). \quad (2.63) \end{aligned}$$

Proceeding with the calculation of expression (2.40), we obtain the propagator of the CIR model in the variable $z = \sqrt{r}$:

$$\begin{aligned} \mathcal{P}(z_T, T|z_0, 0) =& z_T^{\lambda+1} z_0^{-\lambda} \exp\left\{-\frac{\kappa}{\sigma^2}\left[\left(\coth\frac{\kappa T}{2} + 1\right) z_T^2 + \left(\coth\frac{\kappa T}{2} - 1\right) z_0^2\right]\right\} \\ &\times \exp\left\{\frac{\kappa^2 \theta T}{\sigma^2}\right\} \frac{2\kappa}{\sigma^2 \sinh\frac{\kappa T}{2}} I_\lambda\left(\frac{2\kappa z_0 z_T}{\sigma^2 \sinh\frac{\kappa T}{2}}\right), \quad (2.64) \end{aligned}$$

where $\lambda = \frac{2\kappa\theta}{\sigma^2} - 1$ as mentioned before. The propagator of $r$ is then

$$\begin{aligned} \mathcal{P}(r_T, T|r_0, 0) &= r_T^{\frac{\lambda}{2}} r_0^{-\frac{\lambda}{2}} \exp\left\{-\frac{\kappa}{\sigma^2}\left[\left(\coth\frac{\kappa T}{2} + 1\right) r_T + \left(\coth\frac{\kappa T}{2} - 1\right) r_0\right]\right\} \\ &\times \exp\left\{\frac{\kappa^2 \theta T}{\sigma^2}\right\} \frac{\kappa}{\sigma^2 \sinh\frac{\kappa T}{2}} I_\lambda\left(\frac{2\kappa\sqrt{r_0 r_T}}{\sigma^2 \sinh\frac{\kappa T}{2}}\right). \quad (2.65) \end{aligned}$$

### 2.2.2 The Duru-Kleinert transformation

Feynman's time-slicing procedure does not, however, directly work for one of the most important system of quantum mechanics, the hydrogen atom. This is due to the singularity of the Coulomb potential $\frac{1}{r}$ at the origin. In 1972, M. J. Goovaerts and J. T. Devreese performed a straightforward analytical calculation of the energy spectrum of the hydrogen atom entirely within Feynman's path integral formalism by using a perturbation expansion of the Coulomb potential (152). Their work developed calculation tools. In 1979, I. H. Duru and H. Kleinert derived from the path integral the full Feynman propagator of the Coulomb potential (153). They replaced the real time $t$ by another path-dependent pseudo-time parameter $\tau$ such that the singularity is removed and a time-sliced approximation exists. Furthermore, the path integral can be made harmonic by a coordinate transformation, thus being exactly integrable. This time transformation and coordinate transformation is an important tool to solve many path integrals and is called generically the Duru-Kleinert transformation, for details see Kleinert's book (100).

In this subsection I first demonstrate the main idea of this transformation, then propagators for the Kratzer potential, Morse potential and Liouville potential are treated as examples.

Consider a path integral for a particle evolving in a general potential $V(x)$ with constant mass $m$ during the time domain $t \in [0, T]$:

$$\int_{x(0)=x_0}^{x(T)=x_T} \mathcal{D}x(t) \exp\left\{-\int_0^T \left(\frac{m}{2}\dot{x}^2 + V(x)\right) dt\right\}, \tag{2.66}$$

where $\dot{x} = \frac{dx}{dt}$ and $\frac{m}{2}\dot{x}^2$ denote the particle's kinetic energy. Now introduce a path-dependent pseudo-time parameter $\tau$ and a new coordinate variable $q(\tau)$:

$$\tau(t) = \int_0^t \frac{1}{f(x(s))} ds, \tag{2.67}$$

$$x(t) = F(q(\tau)), \tag{2.68}$$

with suitable real, positive functions $f$ and $F$. Furthermore, we assume

$$f = (F')^2. \tag{2.69}$$

where $F' = \frac{dF}{dq}$ is the first derivative of $F$ with respect to $q$, and similarly $F''$ and $F'''$ are the second and the third derivative of $F$ with respect to $q$ respectively as we will need later. Since $f$ is positive, we can denote the domain of $\tau$ by $[\tau(0), \tau(T)] = [0, \tau_b]$. Apparently $\tau$ is path dependent; it is determined by the following constraint:

$$\int_0^{\tau_b} f[F(q(\tau))] = T. \tag{2.70}$$

Of course $f$ and $F$ should be such that for all possible paths, a unique solution $\tau_b > 0$ exists for the previous equation.

Let $\varepsilon = \frac{T}{N}$ be the lattice constant when doing the time slicing for $x$, and $\epsilon_j = \tau_j - \tau_{j-1}$ to be the $j^{th}$ lattice interval for $q$. While $\varepsilon$ is constant, $\epsilon_j$ varies from time to time; they are related by the following equation:

$$\epsilon_j = \frac{\varepsilon}{F'(q_j)F'(q_{j-1})}. \tag{2.71}$$

Therefore

$$\begin{aligned}\left(\frac{1}{2\pi\varepsilon}\right)^{\frac{N}{2}} \prod_{j=1}^{N-1} dx_j &= \left(F'(q_0)F'(q_b)\right)^{-\frac{1}{2}} \prod_{j=1}^{N} \left(\frac{1}{2\pi\epsilon_j}\right)^{\frac{1}{2}} \prod_{j=1}^{N-1} \left(\frac{1}{F'(q_j)} dx_j\right) \\ &= \left(f(x_0)f(x_T)\right)^{-\frac{1}{4}} \prod_{j=1}^{N} \left(\frac{1}{2\pi\epsilon_j}\right)^{\frac{1}{2}} \prod_{j=1}^{N-1} dq_j. \end{aligned} \tag{2.72}$$

To transform the original coordinates $x$ into the new coordinates $q$, we use the midpoint prescription expansion method. It means that one has to expand any dynamical quantity of $F(q)$ which is defined on the points $q_j$ and $q_{j-1}$ of the $j^{th}$ interval in the midpoints $\bar{q}_j = \frac{q_j+q_{j-1}}{2}$ up to order $\mathcal{O}\left((q_j - q_{j-1})^3 = (\Delta q_j)^3\right)$. Consequently

$$\begin{aligned} x_j - x_{j-1} &= F(q_j) - F(q_{j-1}) \\ &= F\left(\bar{q}_j + \frac{\Delta q_j}{2}\right) - F\left(\bar{q}_j - \frac{\Delta q_j}{2}\right) \\ &= F'\left(\bar{q}_j\right)\Delta q_j + \frac{1}{24} F'''\left(\bar{q}_j\right)\left(\Delta q_j\right)^3; \end{aligned} \tag{2.73}$$

$$\left(x_j - x_{j-1}\right)^2 = \left(F'\left(\bar{q}_j\right)\Delta q_j\right)^2 + \frac{1}{12} F'\left(\bar{q}_j\right) F'''\left(\bar{q}_j\right)\left(\Delta q_j\right)^4, \tag{2.74}$$

and similarly

$$\begin{aligned} \varepsilon &= \epsilon_j F'(q_j)F'(q_{j-1}) \\ &= \epsilon_j F'\left(\bar{q}_j + \frac{\Delta q_j}{2}\right) F'\left(\bar{q}_j - \frac{\Delta q_j}{2}\right) \\ &= \epsilon_j \left(F'(\bar{q}_j)\right)^2 \left[1 + \left(\frac{F'''(\bar{q}_j)}{F'(\bar{q}_j)} - \left(\frac{F''(\bar{q}_j)}{F'(\bar{q}_j)}\right)^2\right)\left(\frac{\Delta q_j}{2}\right)^2\right]. \end{aligned} \tag{2.75}$$

Therefore

$$\begin{aligned} \frac{\left(x_j - x_{j-1}\right)^2}{\varepsilon} &= \frac{\left(\Delta q_j\right)^2}{\epsilon_j}\left[1 + \left(-\frac{1}{6}\frac{F'''(\bar{q}_j)}{F'(\bar{q}_j)} + \frac{1}{4}\left(\frac{F''(\bar{q}_j)}{F'(\bar{q}_j)}\right)^2\right)\left(\Delta q_j\right)^2\right] \\ &= \frac{\left(q_j - q_{j-1}\right)^2}{\epsilon_j} + \frac{\left(\Delta q_j\right)^4}{12\epsilon_j}\left(3\left(\frac{F''(\bar{q}_j)}{F'(\bar{q}_j)}\right)^2 - 2\frac{F'''(\bar{q}_j)}{F'(\bar{q}_j)}\right). \end{aligned} \tag{2.76}$$

The term $(\Delta q_j)^4$ cannot be neglected here. The importance of such a term has already been stressed by Feynman in his basic paper (134), see also (154, 155) and references therein.

Plugging expressions (2.72) and (2.76) into (2.66), we then have, **conditional on** $\tau_b$, the following formula:

$$
\begin{aligned}
& \int\limits_{x(0)=x_0}^{x(T)=x_T} \mathcal{D}x(t) \exp\left\{-\int_0^T \left(\frac{m}{2}\dot{x}^2 + V(x)\right) dt\right\} \\
= \; & \left(\frac{m}{2\pi\varepsilon}\right)^{\frac{N}{2}} \prod_{j=1}^{N-1} dx_j \prod_{j=1}^{N} \exp\left\{-\frac{m\,(x_j - x_{j-1})^2}{2\varepsilon} - V\left(\frac{x_j + x_{j-1}}{2}\right)\varepsilon\right\} \\
= \; & (f(x_0)f(x_T))^{-\frac{1}{4}} \prod_{j=1}^{N-1} dq_j \prod_{j=1}^{N} \left[\left(\frac{m}{2\pi\epsilon_j}\right)^{\frac{1}{2}} \exp\left\{-\frac{m\,(q_j - q_{j-1})^2}{2\epsilon_j}\right.\right. \\
& \left.\left. -\frac{m\,(\Delta q_j)^4}{24\epsilon_j}\left(3\left(\frac{F''(\bar{q}_j)}{F'(\bar{q}_j)}\right)^2 - 2\frac{F'''(\bar{q}_j)}{F'(\bar{q}_j)}\right) - V(\bar{q}_j)\,\epsilon_j F'(q_j)F'(q_{j-1})\right\}\right] \\
\doteq \; & (f(x_0)f(x_T))^{-\frac{1}{4}} \prod_{j=1}^{N-1} dq_j \prod_{j=1}^{N} \left[\left(\frac{m}{2\pi\epsilon_j}\right)^{\frac{1}{2}} \exp\left\{-\frac{m\,(q_j - q_{j-1})^2}{2\epsilon_j}\right.\right. \\
& \left.\left. -\frac{\epsilon_j}{8m}\left(3\left(\frac{F''(\bar{q}_j)}{F'(\bar{q}_j)}\right)^2 - 2\frac{F'''(\bar{q}_j)}{F'(\bar{q}_j)}\right) - V(\bar{q}_j)\,\epsilon_j F'(q_j)F'(q_{j-1})\right\}\right],
\end{aligned}
\tag{2.77}
$$

where the symbol $\doteq$ denotes equivalence as far as use in the path integral is concerned (156). For more clear derivation about this equivalence I refer to books (155) and (100).

Recall that expression (2.77) holds conditional on $\tau_b$. In order to incorporate the constraint on $\tau$, see (2.70), we insert the following identity into the path integral (2.77)

$$
\begin{aligned}
& [f(x_0)f(x_T)]^{\frac{1}{2}} \int_0^\infty d\tau_b\, \delta\left(\int_0^{\tau_b} f[F(q(\tau))]d\tau - T\right) \\
= \; & [f(x_0)f(x_T)]^{\frac{1}{2}} \int_{\Phi_R - i\infty}^{\Phi_R + i\infty} \frac{d\Phi}{2\pi i}\, e^{\Phi T} \int_0^\infty d\tau_b\, e^{-\Phi \int_0^{\tau_b} f[F(q(\tau))]d\tau}
\end{aligned}
\tag{2.78}
$$

where $\Phi$ is a complex number with real part $\Phi_R$ and imaginary part $\Phi_I$.

Finally we arrive at the full formula under the Duru-Kleinert transformation:

$$\begin{aligned}
&\int_{x(0)=x_0}^{x(T)=x_T} \mathcal{D}x(t) \exp\left\{-\int_0^T \left(\frac{m}{2}\dot{x}^2 + V(x)\right) dt\right\} \\
&= \quad (F'(q_a)F'(q_b))^{\frac{1}{2}} \int_{-\infty}^{\infty} \frac{d\Phi_I}{2\pi}\, e^{\Phi T} \int_0^{\infty} d\tau_b \int_{q(0)=q_a}^{q(\tau_b)=q_b} \mathcal{D}q(\tau) \\
&\quad \times \exp\left\{-\int_0^{\tau_b} \left[\frac{m}{2}\dot{q}^2 + [V(q)+\Phi]\left(F'(q)\right)^2 + V_{eff}\right] d\tau\right\}, \qquad (2.79)
\end{aligned}$$

where $\dot{q} = \frac{dq}{d\tau}$, and the additional effective potential term due to the transformation, denoted by $V_{eff}$, is given by

$$V_{eff} = \frac{1}{8m}\left[3\left(\frac{F''(q)}{F'(q)}\right)^2 - 2\frac{F'''(q)}{F'(q)}\right]. \qquad (2.80)$$

This effective potential is caused by time slicing effects and it has the form of a Schwartz-derivative. The coordinate variables $x$ and $q$ are related by expression (2.68), i.e. $x = F(q)$, thus $x_0 = F(q_a)$, $x_T = F(q_b)$. The time variables $t$ and $\tau$ are related by expressions (2.67) and (2.69), i.e. $dt = f(x(t))d\tau = (F'[q(\tau)])^2 d\tau$.

This transformation formula will be used to find a number of path integrals. The following are three examples.

#### 2.2.2.1 Path integral for the Kratzer potential

A typical example of a path integral solved via the Duru-Kleinert method is the path integral for the Kratzer potential, given by:

$$\mathcal{P}_{KRA}\left(x_T, T|x_0, 0\right) = \int \mathcal{D}x(t) \exp\left\{-\int_0^T \left(\frac{1}{2}\dot{x}^2 + \frac{\lambda^2 - \frac{1}{4}}{2x^2} - \frac{\beta}{x}\right) dt\right\}, \qquad (2.81)$$

where $\lambda$ and $\beta$ are constants. This potential $V(x) = \frac{\lambda^2 - \frac{1}{4}}{2x^2} - \frac{\beta}{x}$ involves a singularity $\frac{1}{x}$, hence it does not lead to a time-sliced propagator of the Feynman type. The barrier is removed via a coordinate transformation with

$$x = F(q) = q^2, \qquad (2.82)$$

and a pseudotime $\tau$ satisfying

$$dt = (F'(q))^2 d\tau = 4q^2 d\tau. \tag{2.83}$$

Applying the Duru-Kleinert transformation formula (2.79), we have

$$\begin{aligned}
&\int\limits_{x(0)=x_0}^{x(T)=x_T} \mathcal{D}x(t) \exp\left\{-\int_0^T \left(\frac{1}{2}\dot{x}^2 + \frac{\lambda^2 - \frac{1}{4}}{2x^2} - \frac{\beta}{x}\right) dt\right\} \\
= \; & 2\left(q_a q_b\right)^{\frac{1}{2}} \int_{-\infty}^{\infty} \frac{d\Phi_I}{2\pi}\, e^{\Phi T} \int_0^{\infty} d\tau_b \exp\left\{4\beta\tau_b\right\} \\
& \times \int\limits_{q(0)=q_a}^{q(\tau_b)=q_b} \mathcal{D}q(\tau) \exp\left\{-\int_0^{\tau_b} \left[\frac{\dot{q}^2}{2} + \frac{(2\lambda)^2 - \frac{1}{4}}{2q^2} + 4\Phi q^2\right] d\tau\right\}.
\end{aligned} \tag{2.84}$$

The remaining path integral is the one for the radial harmonic oscillator. By using expression (2.63), we obtain the final path integral for the Kratzer potential $\left(\omega = \sqrt{8\Phi}\right)$:

$$\begin{aligned}
&\int \mathcal{D}x(t) \exp\left\{-\int_0^T \left(\frac{1}{2}\dot{x}^2 + \frac{\lambda^2 - \frac{1}{4}}{2x^2} - \frac{\beta}{x}\right) dt\right\} \\
= \; & 2\sqrt{x_0 x_T} \int_{-\infty}^{\infty} \frac{d\Phi_I}{2\pi} \exp\left\{\Phi T\right\} \int_0^{\infty} d\tau_b \exp\left\{4\beta\tau_b\right\} \\
& \times \frac{\omega}{\sinh\left(\omega\tau_b\right)} \exp\left\{-\frac{\omega}{2}\coth\left(\omega\tau_b\right)\left(x_0 + x_T\right)\right\} I_{2\lambda}\left(\frac{\omega\sqrt{x_0 x_T}}{\sinh\left(\omega\tau_b\right)}\right).
\end{aligned} \tag{2.85}$$

#### 2.2.2.2 Path integral for the Morse potential

The path integral for Morse potential reads

$$\mathcal{P}_{Mor}\left(x_T, T|x_0, 0\right) = \int \mathcal{D}x(t) \exp\left\{-\int_0^T \left[\frac{m}{2}\dot{x}^2 + \frac{V_0^2}{2m}\left(e^{2x} - 2\alpha\, e^{x}\right)\right] dt\right\}, \tag{2.86}$$

where $V_0$, $\alpha$, and $m$ are constants. This potential does not involve a singularity term, but no solution is known via direct time-slicing. Introducing new variables $q$ and $\tau$ with

$$x = F(q) = \ln q^2, \tag{2.87}$$

$$dt = \left(F'(q)\right)^2 d\tau = \frac{4}{q^2} d\tau, \tag{2.88}$$

and applying the Duru-Kleinert transformation formula (2.79) again, we similarly have

$$\int_{x(0)=x_0}^{x(T)=x_T} \mathcal{D}x(t)\exp\left\{-\int_0^T\left[\frac{m}{2}\dot{x}^2+\frac{V_0^2}{2m}\left(e^{2x}-2\alpha\, e^x\right)\right]dt\right\}$$
$$=2\left(\frac{1}{q_a q_b}\right)^{\frac{1}{2}}\int_{-\infty}^{\infty}\frac{d\Phi_I}{2\pi}\,e^{\Phi T}\int_0^\infty d\tau_b\exp\left\{\frac{4V_0^2\alpha}{m}\tau_b\right\}$$
$$\times\int_{q(0)=q_a}^{q(\tau_b)=q_b}\mathcal{D}q(\tau)\exp\left\{-\int_0^{\tau_b}\left[\frac{m}{2}\dot{q}^2+\frac{2V_0^2}{m}q^2+\left(4\Phi-\frac{1}{8m}\right)\frac{1}{q^2}\right]d\tau\right\}. \quad (2.89)$$

Let $\xi=\frac{2V_0}{m}\tau_b$, and with the help of (2.63), the propagator of Morse potential is finally obtained:

$$\int\mathcal{D}x(t)\exp\left\{-\int_0^T\left[\frac{m}{2}\dot{x}^2+\frac{V_0^2}{2m}\left(e^{2x}-2\alpha\, e^x\right)\right]dt\right\}$$
$$=\int_{-\infty}^{\infty}\frac{d\Phi_I}{2\pi}\,\exp\left\{\Phi T\right\}\int_0^\infty d\xi\,\exp\left\{2\alpha V_0\xi\right\}$$
$$\times\frac{2m}{\sinh\xi}\exp\left\{-V_0\coth\xi\left(e^{x_0}+e^{x_T}\right)\right\}I_{2\sqrt{2m\Phi}}\left(\frac{2V_0 e^{\frac{x_0+x_T}{2}}}{\sinh\xi}\right). \quad (2.90)$$

#### 2.2.2.3 Path integral for the Liouville potential

In the limit $\alpha=0$, the path integral for Morse potential reduces to the one for the Liouville potential:

$$\int\mathcal{D}x(t)\exp\left\{-\int_0^T\left[\frac{m}{2}\dot{x}^2+\frac{V_0^2}{2m}\,e^{2x}\right]dt\right\}$$
$$=\int_{-\infty}^{\infty}\frac{d\Phi_I}{2\pi}\,e^{\Phi T}\int_0^\infty d\xi\frac{2m}{\sinh\xi}\,e^{-V_0\coth\xi\left(e^{x_0}+e^{x_T}\right)}I_{2\sqrt{2m\Phi}}\left(\frac{2V_0 e^{\frac{x_0+x_T}{2}}}{\sinh\xi}\right). \quad (2.91)$$

Substituting $\eta=\frac{1}{\sinh\xi}$ gives

$$\int_0^\infty d\xi\frac{1}{\sinh\xi}\,e^{-V_0\coth\xi\left(e^{x_0}+e^{x_T}\right)}\,I_{2\sqrt{2m\Phi}}\left(\frac{2V_0 e^{\frac{x_0+x_T}{2}}}{\sinh\xi}\right)$$
$$=\int_0^\infty\frac{d\eta}{\sqrt{1+\eta^2}}\,e^{-V_0\left(e^{x_0}+e^{x_T}\right)\sqrt{1+\eta^2}}I_{2\sqrt{2m\Phi}}\left(2V_0 e^{\frac{x_0+x_T}{2}}\eta\right)$$
$$=I_{\sqrt{2m\Phi}}\left(V_0\,e^{x_<}\right)\,K_{\sqrt{2m\Phi}}\left(V_0\,e^{x_>}\right), \quad (2.92)$$

where $I_\nu(\cdot)$ and $K_\nu(\cdot)$ are the modified Bessel function of the first and the second kind, respectively, and $x_>(x_<)$ is the larger (smaller) of two variables $x_0$ and $x_T$. Since

$$\int_0^\infty \frac{dl}{l}\, e^{-\left(e^{2x_0}+e^{2x_T}\right)l-\frac{V_0^2}{4l}}\, I_{\sqrt{2m\Phi}}\left(2\, e^{x_0+x_T} l\right) = 2 I_{\sqrt{2m\Phi}}\left(V_0\, e^{x_<}\right)\, K_{\sqrt{2m\Phi}}\left(V_0\, e^{x_>}\right) \tag{2.93}$$

one obtains

$$\begin{aligned} &\int \mathcal{D}x(t) \exp\left\{-\int_0^T \left[\frac{m}{2}\dot{x}^2 + \frac{V_0^2}{2m}\, e^{2x}\right] dt\right\} \\ = &\int_{-\infty}^{\infty} \frac{d\Phi_I}{2\pi}\, e^{\Phi T} m \int_0^\infty \frac{dl}{l}\, e^{-\left(e^{2x_0}+e^{2x_T}\right)l-\frac{V_0^2}{4l}}\, I_{\sqrt{2m\Phi}}\left(2\, e^{x_0+x_T} l\right). \end{aligned} \tag{2.94}$$

Expression (2.94) is equivalent to (2.91). But the term including $V_0$ appears only once in (2.94).

Note that the transformation rule of the measure is

$$\mathcal{D}y(t) = \left|\frac{\partial y}{\partial x}\right|_{x,T}^{-1} \mathcal{D}x(t). \tag{2.95}$$

Thus for $y(t) = 2x(t)$, we have

$$\begin{aligned} &\int \mathcal{D}y(t) \exp\left\{-\int_0^T \left[\frac{m}{2}\dot{y}^2 + \frac{V_0^2}{2m}\, e^{y}\right] dt\right\} \\ = &\frac{1}{2}\int \mathcal{D}x(t) \exp\left\{-\int_0^T \left[\frac{4m}{2}\dot{x}^2 + \frac{4V_0^2}{2(4m)}\, e^{2x}\right] dt\right\} \\ = &\int_{-\infty}^{\infty} \frac{d\Phi_I}{2\pi}\, e^{\Phi T} 2m \int_0^\infty \frac{dl}{l}\, e^{-\left(e^{y_0}+e^{y_T}\right)l-\frac{V_0^2}{l}}\, I_{2\sqrt{2m\Phi}}\left(2\, e^{\frac{y_0+y_T}{2}} l\right). \end{aligned} \tag{2.96}$$

## 2.3 Lévy processes and characteristic functions

In this section, I follow (109). The **characteristic function** $\phi_X$ of a distribution of a random variable $X$ with probability density function $\mathcal{P}(x)$ is defined as:

$$\phi_X(u) = \mathbb{E}\left[\exp\left\{iux\right\}\right] = \int_{-\infty}^{\infty} e^{iux}\mathcal{P}(x)dx. \tag{2.97}$$

It is easy to see from the definition that $\phi(0) = 1$ and $|\phi(u)| \leq 1$, for all $u \in \mathbb{R}$. An important fact is that the characteristic function always exists and is continuous.

Moreover, $\phi$ determines the probability density function $\mathcal{P}(x)$ uniquely. The moments of $X$ can also easily be derived from $\phi$. Suppose $X$ has a $k$th moment, then

$$\mathbb{E}\left[x^k\right] = i^{-k} \left.\frac{d^k\phi(u)}{du^k}\right|_{u=0}. \tag{2.98}$$

If $X$ and $Y$ are two independent random variables with characteristic function $\phi_X$ and $\phi_Y$, respectively, then the characteristic function of $X+Y$ is given by $\phi_{X+Y}(u) = \phi_X(u)\phi_Y(u)$. That is, characteristic functions take convolutions into multiplications. If for every positive integer $n$, $\phi(u)$ is also the $n$th power of a characteristic function, we say that the distribution is **infinitely divisible**.

The definition and some properties of Lévy process are given as follows, see (109). We can define for every such infinitely divisible distribution a stochastic process, $X = \{X_t, t \geq 0\}$, called a **Lévy process**, which starts at zero and has independent and identical stationary increments such that the distribution of an increment over $[s, s+t]$, $s, t \geq 0$, i.e. $X_{t+s} - X_s$, has $(\phi(u))^t$ as its characteristic function (the increments are "i.i.d.", independent and identically distributed).

The cumulant characteristic function $\psi(u) = \ln\phi(u)$ is often called the **characteristic exponent**, which satisfies the following **Lévy-Khintchine formula**:

$$\psi(u) = i\gamma u - \frac{1}{2}\sigma^2 u^2 + \int_{-\infty}^{\infty} \left(e^{iux} - 1 - iux\Theta\left(1 - |x|\right)\right)\nu(dx), \tag{2.99}$$

where $\gamma \in \mathbb{R}$, $\sigma^2 \geq 0$, $\Theta(\cdot)$ is the Heaviside step function and $\nu$ is a measure on $\mathbb{R} - 0$ with

$$\int_{-\infty}^{\infty} \inf\left\{1, x^2\right\}\nu(dx) < \infty. \tag{2.100}$$

We say that our infinitely divisible distribution has a triplet of Lévy characteristics $[\gamma, \sigma^2, \nu(dx)]$. The measure $\nu$ is called the Lévy measure of $X$. We see from the Lévy-Khintchine formula that, in general, a Lévy process consists of three independent parts: a linear deterministic part, a Brownian part and a pure jump part. The Lévy measure $\nu(dx)$ specifies how the jumps occur.

### 2.3.1 Examples of Lévy processes

In this subsection I list a number of popular Lévy processes that appear in our later chapters.

#### 2.3.1.1 The Poisson process

Besides the Brownian motion, the homogeneous Poisson process with with constant intensity $\lambda > 0$ is the simplest Lévy process we can think of. It is based on the Poisson($\lambda$) distribution, which lives on the nonnegative integers $\{0, 1, 2, \cdots\}$ with the probability density function at point $j$ as:

$$P_{\text{Poisson}}(x = j) = \exp\{-\lambda\} \frac{\lambda^j}{j!}. \tag{2.101}$$

Thus its characteristic function is given by:

$$\phi_{\text{Poisson}}(u) = \sum_{j=0}^{\infty} \exp\{-\lambda\} \frac{\lambda^j}{j!} \exp\{iuj\} = \exp\{\lambda(\exp\{iu\} - 1)\}. \tag{2.102}$$

Since the Poisson($\lambda$) distribution is infinitely divisible, we can define a Poisson process $N = \{N_t, t \geq 0\}$ with intensity parameter $\lambda > 0$, which starts at zero and has independent and stationary increments, and where the increment over a time interval of length $s > 0$ follows a Poisson($\lambda s$) distribution.

#### 2.3.1.2 The compound Poisson process

Suppose $N = \{N_t, t \geq 0\}$ is a Poisson process with intensity parameter $\lambda > 0$ and that $Z_k, k = 1, 2, \cdots$ is an i.i.d. sequence of random variables independent of $N$ with probability density function $\varpi(z)$ and characteristic function $\phi_Z(u)$. Then we say that

$$X_t = \sum_{k=1}^{N_t} Z_k, \quad t \geq 0, \tag{2.103}$$

is a compound Poisson process. The value of the process at time $t$, $X_t$, is the sum of $N_t$ random numbers $Z_k$. This is the case in the jump diffusion model, where the number of infrequent price jumps within a time interval is modeled following a Poisson process with the jump amplitudes being random variables following a specific distribution. The ordinary Poisson process corresponds to the case where

$Z_k = 1, k = 1, 2, \cdots$. The characteristic function of $X_t$ is given by:

$$\begin{aligned}
\mathbb{E}\left[\exp\left\{iuX_t\right\}\right] &= \mathbb{E}\left[\exp\left\{iu\sum_{k=1}^{N_t} Z_k\right\}\right] = \sum_{j=0}^{\infty} \exp\left\{-\lambda t\right\} \frac{(\lambda t)^j}{j!} \left(\phi_Z(u)\right)^j \\
&= \exp\left\{\lambda t\left(\phi_Z(u) - 1\right)\right\} \\
&= \exp\left\{\lambda t \int_{-\infty}^{\infty} \left(e^{iuz} - 1\right) \varpi(z) dz\right\}. \qquad (2.104)
\end{aligned}$$

#### 2.3.1.3 The CGMY process

The CGMY$(C, G, M, Y)$ distribution is a four-parameter distribution, with characteristic function, see (85):

$$\phi_{\text{CGMY}}\left(u; C, G, M, Y\right) = \exp\left\{C\Gamma(-Y)\left((M - iu)^Y - M^Y + (G + iu)^Y - G^Y\right)\right\}, \qquad (2.105)$$

where $\Gamma(\cdot)$ is a gamma function. The CGMY distribution is infinitely divisible, so we can define the CGMY Lévy process

$$X^{(\text{CGMY})} = \left\{X_t^{(\text{CGMY})}, t \geq 0\right\} \qquad (2.106)$$

as the process that starts at zero and has independent and stationary distributed increments, and in which the increment over a time interval of length $t$ follows a CGMY$(tC, G, M, Y)$ distribution.

### 2.3.2 Market incompleteness and the equivalent Martingale measure

These more sophisticated infinitely divisible distributed Lévy processes give rise to the Lévy market model for risky assets as

$$S(t) = S_0 \exp\left\{X_t\right\}. \qquad (2.107)$$

The logreturn $\ln \frac{S(t+s)}{S(t)}$ of such a model follows the distribution of increment of length $s$ of the Lévy process $X$.

Recall that in the Black-Scholes world, both the properties of absence of arbitrage and of market completeness are satisfied. However, studies show that given a complete market model, the addition of even a small jump risk destroys market completeness (11). Thus, in models with jumps, market completeness is an exception rather than the rule. Except when $X$ is a Poisson process or a Brownian motion, the Lévy market model is an **incomplete** model (109).

The market completeness is related to the uniqueness of the equivalent martingale measures. So in the Lévy market there are many different equivalent martingale measures to choose. We focus on two ways to find an equivalent martingale measure.

#### 2.3.2.1 The Esscher transform

Let $P(x)$ be the probability density function of $X_t$ under the original physical measure $\mathbb{P}$. Following (157, 158) for some real number $\theta \in \mathbb{R}$ such that $\int_{-\infty}^{\infty} e^{\theta x} P(x)dx < \infty$, we can define a new density

$$P^{(\theta)}(x) = \frac{e^{\theta x} P(x)}{\int_{-\infty}^{\infty} e^{\theta x} P(x)dx}. \tag{2.108}$$

We then choose $\theta$ such that the discounted price process is a martingale, i.e.

$$\begin{aligned} \mathbb{E}^{(\theta)}\left[e^{-rt}S(t)\right] &= S_0\, e^{-rt}\,\mathbb{E}^{(\theta)}\left[e^{x_t}\right] = S_0\, e^{-rt}\int_{-\infty}^{\infty}\frac{e^{\theta x_t}P(x_t)}{\int_{-\infty}^{\infty} e^{\theta y}P(y)dy}dx_t \\ &= S_0\, e^{-rt}\,\frac{\mathbb{E}^{\mathbb{P}}\left[e^{(\theta+1)x_t}\right]}{\mathbb{E}^{\mathbb{P}}\left[e^{(\theta)x_t}\right]} = S_0\, e^{-rt}\left(\frac{\phi^{\mathbb{P}}\left(-i(\theta+1)\right)}{\phi^{\mathbb{P}}\left(-i\theta\right)}\right)^t \\ &= S_0, \end{aligned} \tag{2.109}$$

where $\phi^{\mathbb{P}} = \mathbb{E}^{\mathbb{P}}\left[e^{iuX_1}\right]$ is the characteristic function of $X_1$ under the physical measure $\mathbb{P}$. Then from (2.109) we have

$$\exp\{r\} = \frac{\phi^{\mathbb{P}}\left(-i(\theta+1)\right)}{\phi^{\mathbb{P}}\left(-i\theta\right)}. \tag{2.110}$$

The solution of this equation, say $\theta^*$ gives us the Esscher transform martingale measure through the density function $P^{(\theta^*)}(x)$. Under this new measure, the discount price process is a martingale, leading to an arbitrage-free pricing.

#### 2.3.2.2 The mean-correcting martingale measure

Another way to obtain an equivalent martingale measure $\mathbb{Q}$ is by mean correcting the exponential of a Lévy process. Assume we add an independent drift term $\varrho$

into the original non-drift price model, then the mean corrected characteristic function of $X_1$ becomes $\phi^{mc}(u) = \phi^{\mathbb{P}}(u)\, e^{iu\varrho}$. Now we choose the $\varrho$ parameter in an appropriate way such that the discounted price process becomes a martingale. That is:

$$\begin{aligned} \mathbb{E}^{mc}\left[e^{-rt}S(t)\right] &= S_0\, e^{-rt}\, \mathbb{E}^{mc}\left[e^{x_t}\right] = S_0\, e^{-rt}\left(\phi^{mc}(-i)\right)^t \\ &= S_0\, e^{-rt}\left(\phi^{\mathbb{P}}(-i)\, e^{\varrho}\right)^t = S_0, \end{aligned} \tag{2.111}$$

from which we have

$$\varrho = r - \ln \phi^{\mathbb{P}}(-i). \tag{2.112}$$

Therefore under the mean-correcting martingale measure, the characteristic function of $X_1$ becomes

$$\phi^{mc}(u) = \phi^{\mathbb{P}}(u)\, e^{iu\varrho} = e^{iur}\frac{\phi^{\mathbb{P}}(u)}{\left(\phi^{\mathbb{P}}(-i)\right)^{iu}}. \tag{2.113}$$

Especially, for the model including a compound Poisson process, see (2.104), we have the mean correcting drift parameter

$$\varrho = r - \lambda \int_{-\infty}^{\infty} (e^z - 1)\, \varpi(z) dz. \tag{2.114}$$

# 3

# Path integral approach to the European option pricing under the SV jump diffusion models

> This chapter is based on the article (144), which is joint work with Damiaan Lemmens and Jacques Tempère.

As seen in the previous chapter, path integral techniques for the pricing of financial options are mostly based on models that can be recast in terms of a Fokker-Planck differential equation (2.11) and that, consequently, neglect jumps and only describe drift and diffusion. We present in this chapter a method to adapt formulas for both the path integral propagators and the option prices themselves, so that jump processes are taken into account in conjunction with the usual drift and diffusion terms. In particular, we focus on stochastic volatility (SV) models, such as the exponential Vašiček model, and extend the pricing formulas and propagator of this model to incorporate jump diffusion with a given jump size distribution. This model is of importance to include non-Gaussian fluctuations beyond the Black-Scholes model, and moreover yields a log-normal distribution of the volatilities, in agreement with results from superstatistical analysis.

More explicitly, in this chapter we will present a method that makes it possible to extend the Fourier space propagator of a general SV model to the Fourier space propagator of that SV model where an arbitrary jump process has been added to the asset price dynamics. Thereby we contribute to the existing work on Fourier transform methods applied to option pricing. For example in (84) jump diffusions are treated and prices for some exotic options are obtained. In (159) the Heston model is extended with a jump process for the asset price. In (122) the Heston model is extended with arbitrary jump processes in both the asset price and the volatility process. As an application, we investigate a model where we assume that the stochastic volatility follows an exponential Vašiček model (15, 160). To the best of our knowledge, for this model no closed form formulas for the propagator or the vanilla option price exist yet. Making use of path integral methods (100, 115, 123, 124) we derive approximative closed form formulas for the propagator and for vanilla option prices for this model. Using Monte Carlo (MC) simulations we specify parameter ranges for which the approximation is valid. Using the above mentioned method we extend the propagator of this model to the propagator of this model including jumps in the asset price which leads also to closed form pricing formulas in this extended model. These last results are checked with MC simulations.

This chapter is organized as follows. In section 3.1 we present the method for extending the propagator of a general SV model to the propagator of that model with jumps in the asset price. In section 3.2, we present an approximative propagator for jump diffusion models where the volatility is assumed to follow an exponential Vašiček model. Section 3.3 is devoted to European vanilla option pricing, as well as comparisons with MC simulations. In this section we also give parameter ranges for the approximation made in the exponential Vašiček model to be valid. And finally a conclusion is given in section 3.4.

## 3.1 General Propagator Formulas

### 3.1.1 Arbitrary SV models

We assume that the asset price process $S(t)$ follows the Black-Scholes stochastic differential equation (SDE):

$$dS(t) = rS(t)dt + \sigma(t)S(t)dW_1(t), \tag{3.1}$$

in which $r$ is the constant interest rate and the volatility $\sigma(t)$ is behaving stochastically over time, following an arbitrary stochastic process:

$$d\sigma(t) = A(t,\sigma(t))dt + B(t,\sigma(t))dW_2(t). \tag{3.2}$$

Here and in the rest of the chapter $W_j = \{W_j(t), t \geq 0\}\,(j = 1,2)$ are two correlated Wiener processes such that $\mathrm{Cov}[\,dW_1(t)\,dW_2(t)\,] = \rho\,dt$. Equation (3.1) is commonly expressed as a function of the logreturn $x(t) = \ln S(t)$, which leads to a new SDE:

$$dx(t) = \left(r - \frac{1}{2}\sigma^2(t)\right)dt + \sigma(t)dW_1(t). \tag{3.3}$$

To deal with the pricing problem, we need to solve for the propagator of the joint dynamics of $x(t)$ and $\sigma(t)$. The propagator, denoted by $\mathcal{P}(x_T,\sigma_T,T|\,x_0,\sigma_0,0)$, describes the probability that $x$ has the value $x_T$ and $\sigma$ has the value $\sigma_T$ at a later time $T$ given the initial values $x_0$ and $\sigma_0$ respectively at time 0. It satisfies the following Fokker-Planck equation, see (2.12):

$$\begin{aligned}\frac{\partial\mathcal{P}}{\partial T} \;=\;& \frac{\partial}{\partial x_T}\left[-(r-\frac{1}{2}\sigma_T^2)\mathcal{P}\right] + \frac{1}{2}\frac{\partial^2}{\partial x_T^2}\left[\sigma_T^2\mathcal{P}\right] + \frac{\partial}{\partial\sigma_T}\left[-A(T,\sigma_T)\mathcal{P}\right]\\ &+\frac{1}{2}\frac{\partial^2}{\partial\sigma_T^2}\left[B^2(T,\sigma_T)\mathcal{P}\right] + \rho\frac{\partial^2}{\partial x_T\,\partial\sigma_T}\left[\sigma_T B(T,\sigma_T)\mathcal{P}\right],\end{aligned} \tag{3.4}$$

with initial condition

$$\mathcal{P}(x_T,\sigma_T,0|\,x_0,\sigma_0,0) = \delta(x_T - x_0)\,\delta(\sigma_T - \sigma_0). \tag{3.5}$$

### 3.1.2 SV jump diffusion models

A general SV jump diffusion model is obtained by adding an arbitrary jump process into the asset price process (see for instance (117)). That is, equation (3.1) becomes

$$dS(t) = \mu S(t)dt + \sigma(t)S(t)dW_1(t) + \left(e^J - 1\right)S(t)dN(t), \tag{3.6}$$

where $N = \{N(t), t \geq 0\}$ is an independent Poisson process with intensity parameter $\lambda > 0$, i.e. $\mathbb{E}[\,N(t)\,] = \lambda\,t$. The random variable $J$ with probability density $\varpi(J)$ describes the magnitude of the jump when it occurs.

Here the risk-neutral drift $\mu = r - \lambda\, m^j$ is no longer the constant interest rate $r$, rather it is adjusted by a compensator term $\lambda\, m^j$, with $m^j$ the expectation value of $e^J - 1$:

$$m^j = \mathbb{E}\left[e^J - 1\right] = \int_{-\infty}^{\infty} (e^J - 1)\varpi(J)dJ, \tag{3.7}$$

so that the asset price process constitutes a martingale under the risk-neutral measure, see expression (2.114). And the logreturn $x(t)$ follows a new SDE:

$$dx(t) = \left(r - \lambda m^j - \frac{1}{2}\sigma^2(t)\right) dt + \sigma(t)dW_1(t) + JdN(t). \tag{3.8}$$

Given the same arbitrary SV process (3.2), the new propagator of this model, denoted by $\mathcal{P}_J(x_T, \sigma_T, T|x_0, \sigma_0, 0)$, satisfies the new Kolmogorov forward equation, see (2.6) or (147):

$$\begin{aligned} \frac{\partial \mathcal{P}_J}{\partial T} \;=\; & \frac{\partial}{\partial x_T}\left[-\left(r - \lambda m^j - \frac{1}{2}\sigma_T^2\right)\mathcal{P}_J\right] + \frac{1}{2}\frac{\partial^2}{\partial x_T^2}\left[\sigma_T^2 \mathcal{P}_J\right] + \frac{\partial}{\partial \sigma_T}\left[-A(T, \sigma_T)\mathcal{P}_J\right] \\ & + \frac{1}{2}\frac{\partial^2}{\partial \sigma_T^2}\left[B^2(T, \sigma_T)\mathcal{P}_J\right] + \rho \frac{\partial^2}{\partial x_T\, \partial \sigma_T}\left[\sigma_T B(T, \sigma_T)\mathcal{P}_J\right] \\ & + \lambda \int_{-\infty}^{+\infty} \left[\mathcal{P}_J(x_T - J) - \mathcal{P}_J(x_T)\right]\varpi(J)dJ. \end{aligned} \tag{3.9}$$

If we write the propagator of the arbitrary SV model as a Fourier integral:

$$\mathcal{P}(x_T, \sigma_T, T|x_0, \sigma_0, 0) = \int_{-\infty}^{\infty} \frac{dp}{2\pi} e^{ip(x_T - x_0)} F(\sigma_T, \sigma_0, r, p, T), \tag{3.10}$$

then the propagator of arbitrary SV jump diffusion models can be written as

$$\mathcal{P}_J(x_T, \sigma_T, T|x_0, \sigma_0, 0) = \int_{-\infty}^{\infty} \frac{dp}{2\pi} e^{ip(x_T - x_0)} F(\sigma_T, \sigma_0, r, p, T)\, e^{U(p,T)}, \tag{3.11}$$

where

$$U(p, T) = \lambda T \int_{-\infty}^{\infty} \left[e^{-ipJ} - 1 + ip\left(e^J - 1\right)\right]\varpi(J)dJ. \tag{3.12}$$

The proof of this statement is given in the Appendix 3.5. Note the relation between propagators (3.10) and (3.11). The only difference between them is the factor $e^{U(p,T)}$.

If this is applied to the propagator of the Heston model (115), the propagator of the Heston model with jumps is obtained. This propagator is similar as the one derived in Ref. (122). Furthermore the above described method can be combined with the method described in Ref. (115) for finding the propagator of a model including both SV and stochastic interest rate. In particular extending the result of Ref. (115) for the Heston model with stochastic interest rate to include jumps again only involves multiplying the propagator with $e^{U(p,T)}$ as in (3.11). In the next section, as an example of the method of this section the volatility of the asset price will be assumed to follow an exponential Vašiček model.

## 3.2 Exponential Vašiček SV model with price jumps

The Heston model assumes that the squared volatility follows a CIR process which has a gamma distribution as stationary distribution. This assumption should be compared with market data. Attempts to reconstruct the stationary probability distribution of volatility from the time series data (among others, see Refs. (15, 35, 160)) generally agree that the central part of the stationary volatility distribution is better described by a log-normal distribution.

Reference (110) finds that due to the different structure in path-behavior between different models, the resulting exotic prices can vary significantly. So an investigation into an alternative model which fits market data better is meaningful. Furthermore the model will serve here both to demonstrate the use of path integral methods in finance and to illustrate the method of section 3.1.

When $\sigma(t)$ is assumed to be an exponential Vašiček process (used for example by Chesney and Scott (161)), this results in the following two SDEs

$$dS(t) = rS(t)\,dt + \sigma(t)\,S\,dW_1(t), \tag{3.13}$$

$$d\sigma(t) = \sigma(t)\left(\beta\left[\bar{a} - \ln\sigma(t)\right] + \frac{1}{2}\gamma^2\right)dt + \gamma\sigma(t)dW_2(t). \tag{3.14}$$

This model has a log-normal stationary volatility distribution and we will denote it by the LN model, the propagator for this model will be denoted by $\mathcal{P}_{LN}$. In this model $\ln\sigma(t)$ is a mean reverting process, with $\beta$ the spring constant of the force that attracts the logarithm of asset volatility to its mean reversion level $\bar{a}$. Again $\gamma$ is the volatility of the asset volatility. As far as we know, there is no closed form option pricing formula for this model. In this section, we will give an approximation for the propagator of this model. In the next section we will give an approximation for the vanilla option price and determine a parameter range for which the approximation is good. The derivation starts with the following substitutions:

$$y(t) = x(t) - \frac{\rho}{\gamma} e^{z(t)} - rt, \tag{3.15}$$

$$z(t) = \ln \sigma(t), \tag{3.16}$$

where $x(t)$ is defined as before. This leads to two uncorrelated equations:

$$dy = \left[ -\frac{1}{2} e^{2z} - \rho \left( \frac{\beta(\bar{a} - z)}{\gamma} + \frac{\gamma}{2} \right) e^{z} \right] dt + e^{z} \sqrt{1-\rho^2} dW_3(t), \tag{3.17}$$

$$dz = \beta\left(\bar{a} - z\right) dt + \gamma dW_4(t), \tag{3.18}$$

where $W_3$ and $W_4$ are two uncorrelated Wiener processes. Since these equations are uncorrelated, the propagator $\mathcal{P}_{LN}(y_T, z_T | \, y_0, z_0)$ is given by the following path integral

$$\mathcal{P}_{LN}(y_T, z_T | \, y_0, z_0) = \int \mathcal{D}z \left( \int \mathcal{D}y e^{-\int_0^T \mathcal{L}[\dot{y}, y, z, t] dt} \right) e^{-\int_0^T \mathcal{L}[\dot{z}, z, t] dt}, \tag{3.19}$$

where the Lagrangians are given by:

$$\mathcal{L}[\dot{y}, y, z, t] = \frac{\left[ \dot{y} + \frac{1}{2} e^{2z} + \rho \left( \frac{\beta(\bar{a}-z)}{\gamma} + \frac{\gamma}{2} \right) e^{z} \right]^2}{2(1-\rho^2)\, e^{2z}}, \tag{3.20}$$

$$\mathcal{L}[\dot{z}, z, t] = \frac{\left[\dot{z} - \beta\left(\bar{a} - z\right)\right]^2}{2\gamma^2} - \frac{\beta}{2}. \tag{3.21}$$

The first step in the evaluation of (3.19) is the integration over all $y$ paths. Because the action is quadratic in $y$, this path integration can be done analytically and yields

$$\mathcal{P}_{LN}(y_T, z_T | \, y_0, z_0) = \int \mathcal{D}z \, e^{-\int_0^T \mathcal{L}[\dot{z}, z, t] dt} \frac{1}{\sqrt{2\pi(1-\rho^2) \int_0^T e^{2z} dt}} \times e^{-\frac{\left[ y_T - y_0 + \frac{1}{2}\int_0^T e^{2z} dt + \rho \int_0^T \left( \frac{\beta(\bar{a}-z)}{\gamma} + \frac{\gamma}{2} \right) e^{z} dt \right]^2}{2(1-\rho^2) \int_0^T e^{2z} dt}}. \tag{3.22}$$

Note that the probability to arrive in $(y_T, z_T)$ only depends on the average value of the volatility along the path $z(t)$, in agreement with Ref. (161). With the help of a Fourier transform, we rewrite the preceding expression as follows

$$\mathcal{P}_{LN}(y_T, z_T | y_0, z_0) = \int_{-\infty}^{+\infty} \frac{dp}{2\pi} e^{ip(y_T - y_0)} \int \mathcal{D}z \, e^{-\int_0^T \mathcal{L}[\dot{z}, z, t] dt}$$
$$\times \exp\left\{ -\frac{(1-\rho^2)p^2 - ip}{2} \int_0^T e^{2z} dt + ip\rho \int_0^T \left( \frac{\beta(\bar{a} - z)}{\gamma} + \frac{\gamma}{2} \right) e^z dt \right\}. \quad (3.23)$$

If $\zeta(t) = z(t) - \bar{a}$, then $\zeta(t)$ is close to zero because $z(t)$ is a mean reverting process with mean reversion level $\bar{a}$, This motivates the approximation $e^{\zeta} \approx 1 + \zeta + \frac{\zeta^2}{2}$. This type of approximation is akin to expanding the path integral around the saddle point up to second order in the fluctuations, as in the Nozieres-Schmitt-Rink formalism (162) extended to path-integration by Sa de Melo, Randeria and Engelbrecht (163). Now we can work out the remaining path integral in (3.23)

$$\int \mathcal{D}z \, e^{-\int_0^T \left[ \mathcal{L}[\dot{z}, z, t] + \frac{(1-\rho^2)p^2 - ip}{2} e^{2z} - ip\rho \left( \frac{\beta(\bar{a} - z)}{\gamma} + \frac{\gamma}{2} \right) e^z \right] dt}$$
$$\approx \int \mathcal{D}\zeta \, e^{-\int_0^T \left\{ \frac{[\dot{\zeta} + \beta\zeta]^2}{2\gamma^2} - \frac{\beta}{2} + \frac{A}{2} e^{2\zeta} + B\beta\zeta \, e^{\zeta} - \frac{B\gamma^2}{2} e^{\zeta} \right\} dt}$$
$$= e^{\frac{\omega\left[ \left( \zeta_T + \frac{\gamma^2 M}{\omega^2} \right)^2 - \left( \zeta_0 + \frac{\gamma^2 M}{\omega^2} \right)^2 \right] - \beta\left( \zeta_T^2 - \zeta_0^2 \right)}{2\gamma^2} + \left[ \frac{\beta - \omega - A + B\gamma^2}{2} + \frac{\gamma^2 M^2}{2\omega^2} \right] T}$$
$$\times \sqrt{\frac{\omega}{\pi\gamma^2(1 - e^{-2\omega T})}} \, e^{-\frac{\omega\left[ \left( \zeta_T + \frac{\gamma^2 M}{\omega^2} \right) - \left( \zeta_0 + \frac{\gamma^2 M}{\omega^2} \right) e^{-\omega T} \right]^2}{\gamma^2 (1 - e^{-2\omega T})}}, \quad (3.24)$$

where

$$A = \left[ (1-\rho^2)p^2 - ip \right] e^{2\bar{a}}, \quad (3.25)$$
$$B = ip\rho \frac{1}{\gamma} e^{\bar{a}}, \quad (3.26)$$
$$\omega = \sqrt{\beta^2 + 2\gamma^2 \left( A + B\beta - \frac{B\gamma^2}{4} \right)}, \quad (3.27)$$
$$M = A + B\beta - \frac{B\gamma^2}{2}. \quad (3.28)$$

We see that also the integral over the final value $\zeta_T$ can be done, yielding the

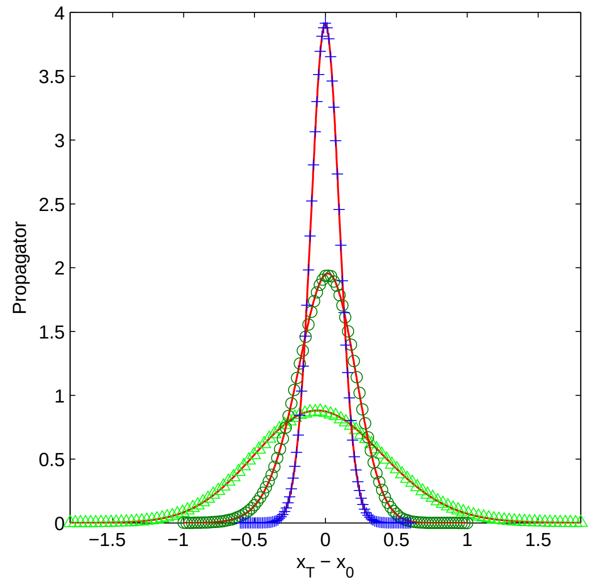


**Figure 3.1:** Propagator $\mathcal{P}(x_T|x_0, \zeta_0)$ as a function of $x_T - x_0$. The full curves are our analytical results, while the symbols represent Monte Carlo simulations. $T =$ 0.25y, $\rho = 0$ (crosses). $T =$ 1y, $\rho =$ -0.5 (circles). $T =$ 5y, $\rho =$ 0.5 (triangles). For the other parameters the following values are used for the three figures: $\beta = 5, \bar{a} = -1.6, \gamma = 0.5, r = 0.015$.

marginal probability distribution:

$$\mathcal{P}_{LN}(x_T|x_0,\zeta_0) = \int_{-\infty}^{+\infty} \frac{dp}{2\pi} e^{ip[x_T - x_0 - rT] + B\left(e^{\zeta_0}-1\right)}$$
$$\times\, e^{\frac{\beta\zeta_0^2 - \omega\left(\zeta_0 + \frac{\gamma^2 M}{\omega^2}\right)^2}{2\gamma^2} + \left[\frac{\beta-\omega-A+B\gamma^2}{2} + \frac{\gamma^2 M^2}{2\omega^2}\right]T} \frac{e^{\frac{\Xi}{\gamma^2[2\omega + (\beta-\omega+B\gamma^2)(1-e^{-2\omega T})]}}}{\sqrt{1 + \frac{1-e^{-2\omega T}}{2\omega}[\beta - \omega + B\gamma^2]}}, \tag{3.29}$$

where

$$\begin{aligned} \Xi &= \omega\left[2B\gamma^2 N + \omega(N - \frac{\gamma^2 M}{\omega^2})^2 - (\beta + B\gamma^2)N^2\right] \\ &\quad + (1 - e^{-2\omega T})\left[\frac{B^2\gamma^4}{2} - \frac{B\gamma^4 M}{\omega} + \frac{(\beta + B\gamma^2)\gamma^4 M^2}{2\omega^3}\right], \end{aligned} \tag{3.30}$$

$$N = \frac{\gamma^2 M}{\omega^2} - (\zeta_0 + \frac{\gamma^2 M}{\omega^2})e^{-\omega T}. \tag{3.31}$$

This approximative propagator was checked with MC simulations because of the lack of a closed form solution in literature. Figure 3.1 shows the propagators as a function of $x_T - x_0$, i.e., $\ln \frac{S_T}{S_0}$. The full curves come from expression (3.29), while the marked ones are MC simulation results, with time to maturity ranging from three months to five years, and correlation coefficients 0, −0.5 and 0.5 respectively. Here and in the rest of this chapter we will set $\sigma_0$ equal to the long time average of the volatility:

$$\sigma_0 = \lim_{t\to\infty} \mathbb{E}\left[\sigma(t)\right] = \exp\left\{\bar{a} + \frac{\gamma^2}{4\beta}\right\}, \tag{3.32}$$

which seems a reasonable choice. For these MC simulations 5,000,000 sample paths are used.

It is seen that our analytical results fit the MC simulations quite well. Actually, using the parameters of Figure 3.1, and putting expression (3.29) for those three cases into the left hand side of the Kolmogorov backward equation, see (2.7):

$$\begin{aligned} -\frac{\partial \mathcal{P}}{\partial T} &+ \left[r - \frac{1}{2}\, e^{2(\zeta_0+\bar{a})}\right] \frac{\partial \mathcal{P}}{\partial x_0} + \frac{1}{2}\, e^{2(\zeta_0+\bar{a})} \frac{\partial^2 \mathcal{P}}{\partial x_0^2} \\ -\beta\zeta_0 \frac{\partial \mathcal{P}}{\partial \zeta_0} &+ \frac{1}{2}\gamma^2 \frac{\partial^2 \mathcal{P}}{\partial \zeta_0^2} + \rho\, e^{\zeta_0+\bar{a}} \gamma \frac{\partial^2 \mathcal{P}}{\partial x_0 \zeta_0} = 0, \end{aligned} \tag{3.33}$$

we find that, for different $x_T$ values, the absolute deviations are all in the order of $10^{-7}$ or even smaller. In section 3.3.2 we come back to the discussion concerning the goodness of our approximation. According to the discussion of Section 3.1, an extension of this model to the one with price jumps is straightforward: the new marginal probability distribution is:

$$\begin{aligned} \mathcal{P}_{LNJ}(x_T|0,\zeta_0) = & \int_{-\infty}^{+\infty} \frac{dp}{2\pi} e^{ip[x_T - x_0 - rT] + B\left(e^{\zeta_0}-1\right)} \\ & \times e^{\frac{\beta\zeta_0^2 - \omega\left(\zeta_0 + \frac{\gamma^2 M}{\omega^2}\right)^2}{2\gamma^2} + \left[\frac{\beta-\omega-A+B\gamma^2}{2} + \frac{\gamma^2 M^2}{2\omega^2}\right] T} \\ & \times \frac{e^{\frac{\Xi}{\gamma^2\left[2\omega + \left(\beta-\omega+B\gamma^2\right)\left(1-e^{-2\omega T}\right)\right]}}}{\sqrt{1 + \frac{1-e^{-2\omega T}}{2\omega}\left[\beta - \omega + B\gamma^2\right]}} \\ & \times e^{\lambda T \int_{-\infty}^{+\infty}\left[e^{-ipJ} - 1 + ip\left(e^{J}-1\right)\right]\varpi(J)dJ}, \end{aligned} \tag{3.34}$$

where the same notations as in Eq.(3.29) are used.

## 3.3 European Vanilla Option Pricing

### 3.3.1 General Pricing Formulas

If we denote the general marginal propagator by

$$\mathcal{P}(x_T|x_0,\sigma_0) = \int_{-\infty}^{\infty} \frac{dp}{2\pi}\, e^{ip(x_T - x_0 - rT)} F(p,T)\, e^{U(p,T)}, \tag{3.35}$$

then the option pricing formula of a vanilla call option $\mathcal{C}$ with expiration date $T$ and strike price $K$ is given by the discounted expectation value of the payoff:

$$\begin{aligned} \mathcal{C} &= e^{-rT} \int_{-\infty}^{\infty} \max\left(e^{x_T} - K, 0\right)\, \mathcal{P}(x_T|x_0,\sigma_0) dx_T \\ &= \frac{\mathcal{G}(0)}{2} + i \int_{-\infty}^{\infty} \frac{dp}{2\pi} \frac{e^{ip\left(\ln \frac{K}{S_0} - rT\right)} \mathcal{G}(p)}{p}, \end{aligned} \tag{3.36}$$

where

$$\mathcal{G}(p) = S_0 F(p+i,T)\, e^{U(p+i,T)} - K\, e^{-rT} F(p,T)\, e^{U(p,T)}. \tag{3.37}$$

Here we have followed the derivation outlined in reference (164). In particular for the LN model $F(p,T)$ equals:

$$\begin{aligned} F(p,T) &= e^{\frac{\beta\zeta_0^2 - \omega\left(\zeta_0 + \frac{\gamma^2 M}{\omega^2}\right)^2}{2\gamma^2} + \left[\frac{\beta - \omega - A + B\gamma^2}{2} + \frac{\gamma^2 M^2}{2\omega^2}\right] T} \\ &\quad \times \frac{e^{B(e^{\zeta_0} - 1) + \frac{\Xi}{\gamma^2\left[2\omega + (\beta - \omega + B\gamma^2)(1 - e^{-2\omega T})\right]}}}{\sqrt{1 + \frac{1 - e^{-2\omega T}}{2\omega}\left[\beta - \omega + B\gamma^2\right]}}. \end{aligned} \tag{3.38}$$

At this stage one needs to specify the probability density function for the jump sizes. Merton (81) and Kou (82) proposed a normal distributed jump size, denoted by $\varpi_M(J)$, and a asymmetric double exponential distributed one, denoted by $\varpi_K(J)$, respectively:

$$\varpi_M(J) = \frac{1}{\sqrt{2\pi\delta^2}}\, e^{-\frac{(J-\nu)^2}{2\delta^2}}, \tag{3.39}$$

$$\varpi_K(J) = p_+ \frac{1}{\eta_+} e^{-\frac{1}{\eta_+} J} \Theta(J) + p_- \frac{1}{\eta_-} e^{\frac{1}{\eta_-} J}\, \Theta(-J). \tag{3.40}$$

For the Merton model $\nu$ is the mean jump size and $\delta$ is the standard deviation of the jump size. For Kou's model $0 < \eta_+ < 1$, $\eta_- > 0$ are means of positive and negative jumps respectively. $p_+$ and $p_-$ represent the probabilities of positive and negative jumps, $p_+ > 0$, $p_- > 0$, $p_+ + p_- = 1$ and $\Theta$ is the Heaviside function.

According to expression (3.12), it is easy to derive their corresponding $U(p,T)$'s:

$$U_M(p,T) = \lambda T\left[e^{-ip\nu-\frac{1}{2}\delta^2p^2} - 1 + ip\left(e^{\nu+\frac{1}{2}\delta^2} - 1\right)\right], \tag{3.41}$$

$$U_K(p,T) = \lambda T\left[\frac{p_+}{1+ip\eta_+} + \frac{p_-}{1-ip\eta_-} - 1 + ip\left(\frac{p_+}{1-\eta_+} + \frac{p_-}{1+\eta_-} - 1\right)\right]. \tag{3.42}$$

Using expression (3.38) and results (3.41), (3.42) in formulas (3.36), (3.37) allows to find the price of the vanilla call option for the exponential Vašiček stochastic volatility with price jumps model.

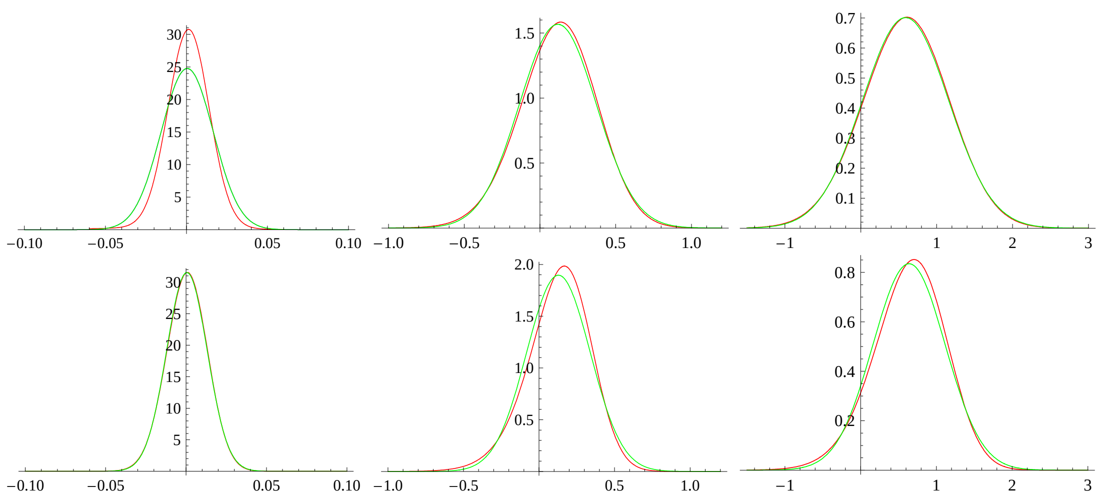


**Figure 3.2:** Comparison of propagators of Kou's jump diffusion model (Upper red curves), the LN SV model (Bottom red curves) and the corresponding Gaussian distributions with the same mean and variance (Green curves). Time to maturity is 1/250 year, 1 year and 5 years respectively from left panels to right panels. Parameter values used here are: $r = 0.15$, $\lambda = 10$, $p_+ = 0.3$, $p_- = 0.7$, $\eta_+ = 0.02$, $\eta_- = 0.04$, $\bar{a} = -1.6$, $\gamma = 0.5$, $\sigma_0 = 0.2$, $\rho = -0.5$.

As mentioned in chapter 1, jumps make it possible to reproduce strong skews and smiles for the implied volatility surface at short maturities while stochastic volatility provides for the calibration of the term structure, especially for long-term smiles (11, 13). Figure 3.2 illustrates these effects. Only a combination of the SV and jumps can calibrate the whole implied volatility surface well.

### 3.3.2 Monte Carlo simulations

To test our analytical pricing formula for the LN model, we focus on the parameters that most strongly influence the approximation. To satisfy the assumption that quadratic fluctuations around the mean reversion level $\bar{a}$ capture the behavior of the volatility well, the mean reversion speed $\beta$ and the volatility $\gamma$ of asset volatility are crucial. The substitution $\tau = \gamma^2 t$ transforms expression (3.18) into

$$dz(\tau) = \frac{\beta}{\gamma^2}\left[\bar{a} - z(\tau)\right] d\tau + dW_4(\tau), \tag{3.43}$$

showing that it is actually the parameter $c = \frac{\beta}{\gamma^2}$ which determines whether the approximation will be good. For bigger $c$ values the approximation $z\,(t) \approx \bar{a}$ will be better.

As the correlation parameter $\rho$ controls the skewness of spot returns, we will also consider the typical negative and positive skewed cases by taking values $-0.5$, 0 and 0.5 for this parameter. On the other hand, the constant interest rate $r$ and the mean reversion level $\bar{a}$ do not influence the accuracy of the result a lot, and we just assume them to be constant values: $r = 0.015$ and $\bar{a} = -1.6 \approx \ln 0.2$. These two parameters seem to be quite reasonable for the present European options.

To get an idea of what is a reasonable range for $c$, and since calibration values for the LN model are not available, we took calibration values from the literature (76, 165) for the Heston model and fitted our model to the volatility distribution of the Heston model with those parameters. For (76) we obtained $c \approx 7$ and for (165) $c \approx 18$. Therefore in Table 4.1 we used values for $\beta$ and $\gamma$ such that $c$ ranges from 4.08 up to 25. We calculated prices for $S_0 = 100$ and $K = 90$, 100 and 110.

The comparison of our analytical solution with the MC solution for a European call option in the LN model as shown in Table 4.1 suggests that for the above mentioned parameter values the relative errors are less than 3% and most of the time even less than 1%, which is acceptable when we take the typical bid-ask spread for European options into account. Here each MC simulation runs 20,000,000 times. For the basic LN model we can conclude that we found an approximation valid up to 3% for parameter values $c > 7$ (We only checked

**Table 3.1:** Comparison of our approximative analytic pricing result and the MC simulation value for the LN model.

| Parameter values | | | | | | |
|---|---|---|---|---|---|---|
| $K$ | $\rho$ | $\gamma$ | $\beta$ | MC value(a) | Approx.(b) | Relative error (b - a)/a (%) |
| 90 | -0.5 | 1.2 | 7 | 15.3947 | 15.2533 | -0.9185 |
| | | | 8 | 15.2979 | 15.1731 | -0.8166 |
| | | | 10 | 15.1630 | 15.0588 | -0.6869 |
| | | 0.8 | 5 | 15.1079 | 14.9995 | -0.7180 |
| | | | 6 | 15.0307 | 14.9337 | -0.6475 |
| | | | 7 | 14.9776 | 14.8855 | -0.6151 |
| | 0 | 0.7 | 2 | 15.2486 | 15.1982 | -0.3307 |
| | | | 3 | 15.0259 | 15.0024 | -0.1564 |
| | | | 4 | 14.9190 | 14.8992 | -0.1328 |
| | | 0.5 | 1 | 15.2061 | 15.1576 | -0.3187 |
| | | | 2 | 14.9030 | 14.8882 | -0.0996 |
| | | | 3 | 14.7951 | 14.7865 | -0.0577 |
| | 0.5 | 0.3 | 1 | 14.6051 | 14.5035 | -0.6953 |
| | | | 1.5 | 14.5524 | 14.4815 | -0.4872 |
| | | | 2 | 14.5354 | 14.4775 | -0.3986 |
| | | 0.2 | 0.5 | 14.6015 | 14.5398 | -0.4192 |
| | | | 0.75 | 14.5609 | 14.5098 | -0.3519 |
| | | | 1 | 14.5332 | 14.4981 | -0.2418 |
| 100 | -0.5 | 1.2 | 7 | 9.4541 | 9.2862 | -1.7762 |
| | | | 8 | 9.3720 | 9.2197 | -1.6253 |
| | | | 10 | 9.2599 | 9.1274 | -1.4310 |
| | | 0.8 | 5 | 9.1537 | 9.0346 | -1.3006 |
| | | | 6 | 9.0950 | 8.9869 | -1.1886 |
| | | | 7 | 9.0557 | 8.9534 | -1.1291 |
| | 0 | 0.7 | 2 | 9.5394 | 9.4975 | -0.4395 |
| | | | 3 | 9.2906 | 9.2704 | -0.2174 |
| | | | 4 | 9.1682 | 9.1513 | -0.1840 |
| | | 0.5 | 1 | 9.4915 | 9.4493 | -0.4480 |
| | | | 2 | 9.1445 | 9.1328 | -0.1285 |
| | | | 3 | 9.0235 | 9.0155 | -0.0887 |
| | 0.5 | 0.3 | 1 | 9.0168 | 8.9081 | -1.2051 |
| | | | 1.5 | 8.9302 | 8.8522 | -0.8737 |
| | | | 2 | 8.8886 | 8.8246 | -0.7195 |
| | | 0.2 | 0.5 | 8.9655 | 8.9023 | -0.7048 |
| | | | 0.75 | 8.9039 | 8.8509 | -0.5955 |
| | | | 1 | 8.8628 | 8.8247 | -0.4295 |
| 110 | -0.5 | 1.2 | 7 | 5.2749 | 5.1365 | -2.6237 |
| | | | 8 | 5.2209 | 5.0916 | -2.4758 |
| | | | 10 | 5.1507 | 5.0335 | -2.2756 |
| | | 0.8 | 5 | 5.0170 | 4.9219 | -1.8947 |
| | | | 6 | 4.9877 | 4.8986 | -1.7862 |
| | | | 7 | 4.9709 | 4.8849 | -1.7307 |
| | 0 | 0.7 | 2 | 5.6480 | 5.5989 | -0.8694 |
| | | | 3 | 5.3942 | 5.3705 | -0.4394 |
| | | | 4 | 5.2684 | 5.2503 | -0.3429 |
| | | 0.5 | 1 | 5.5967 | 5.5510 | -0.8173 |
| | | | 2 | 5.2475 | 5.2343 | -0.2519 |
| | | | 3 | 5.1253 | 5.1160 | -0.1821 |
| | 0.5 | 0.3 | 1 | 5.3151 | 5.2095 | -1.9860 |
| | | | 1.5 | 5.2048 | 5.1289 | -1.4589 |
| | | | 2 | 5.1427 | 5.0812 | -1.1966 |
| | | 0.2 | 0.5 | 5.2170 | 5.1576 | -1.1380 |
| | | | 0.75 | 5.1449 | 5.0954 | -0.9620 |
| | | | 1 | 5.0960 | 5.0595 | -0.7163 |

For the remaining parameters the values $S_0 = 100$, $r = 0.015$, $\bar{a} = -1.6$ and $T = 1$ are used here.

values of $c < 25$, but for bigger $c$ the approximation will only become better), $-0.5 < \rho < 0.5$, $T < 1$ and $0.9 < K/S_0 < 1.1$.

Finally we consider the vanilla call option pricing in LN model combined with Merton's and Kou's jumps, respectively. Since the jump process is independent from the approximation we made, we do not investigate the goodness of our approximation as thoroughly as in the basic LN model (assuming that, if it is good there it will be good here). Figure 3.3 illustrates our analytical results (curves) and the MC simulations (crosses), as well as the relative errors in percent. Each MC simulation runs 300,000,000 times. These results suggest that the approximation error is typically less than 2%. And due to the fact that whenever the degree of moneyness (the ratio of the strike price $K$ to the initial asset price $S_0$) is relatively high, the average bid-ask spread tends to be relatively high for call options (166), our analytical results can serve as an easy way to get a quick estimate that is normally accurate enough for many practical applications.

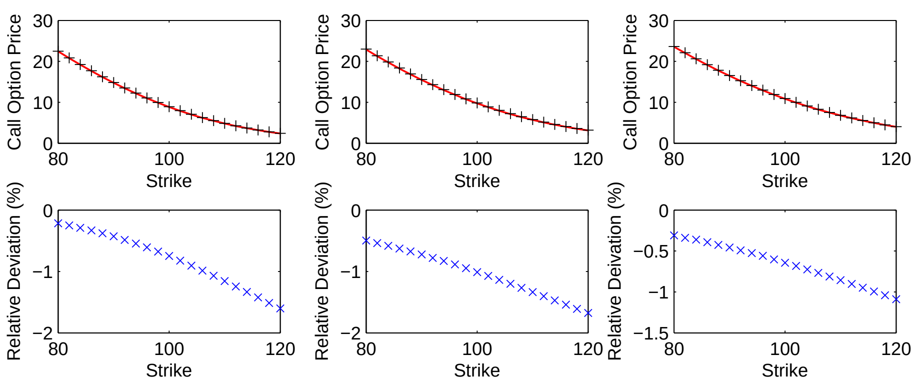


**Figure 3.3:** The upper figures show European call option prices in the LN model (left), the LN model with Merton's jump (middle) and the LN model with Kou's jump (right). The red curves are our analytical results and the black crosses are the Monte Carlo simulations. The corresponding lower figures give the relative deviations of our analytical results from the MC simulations in the unit of percent. Parameter values $S_0 = 100$, $r = 0.015$, $T = 1$, $\beta = 5$, $\bar{a} = -1.6$, $\gamma = 0.5$, $\rho = -0.5$, $\lambda = 10$, $\nu = -0.01$, $\delta = 0.03$, $p_+ = 0.3$, $p_- = 0.7$, $\eta_+ = 0.02$, $\eta_- = 0.04$ are used here.

## 3.4 Conclusion

We presented a method which makes it possible to extend the propagator for a general SV model to the propagator of that SV model extended with an arbitrary jump process in the asset price evolution. This procedure, applied to the Heston model, leads to similar results as those obtained in reference (122), which gives us confidence in the present treatment. The stationary volatility distribution of the Heston model, however, does not correspond to the observed log-normal distribution (15, 35, 160) in the market. The exponential Vašiček model does have the log-normal distribution as its stationary distribution. Therefore we used this model for the volatility to illustrate the method presented in section 3.1. For this model no closed form pricing formulas for the propagator or vanilla option prices exist. We first derive approximative formulas for the propagator and vanilla option prices for this model without jumps, using path integral methods. This result was checked with a Monte Carlo simulation, providing a parameter range for which the approximation is valid. We specified a parameter range for which our pricing formulas are accurate to within 3%. They become more accurate in the limit $\frac{\beta}{\gamma^2} >> 1$ where $\beta$ is the mean reversion rate and $\gamma$ is the volatility of the volatility. Finally we extended this result to the case where the asset price evolution contains jumps.

## 3.5 Appendix: Derivation of equations (3.11), (3.12).

The proof starts by assuming that a solution for $\mathcal{P}_J(x_T, \sigma_T, T|x_0, \sigma_0, 0)$ of the form (3.11) exists. Below we show that this assumption indeed leads to a solution, which in turn justifies the assumption.

Since $\int_{-\infty}^{+\infty} \frac{dp}{2\pi} e^{ip(x_T - x_0)} \frac{\partial F(\sigma_T, \sigma_0, r, p, T)}{\partial T}$ equals the right hand side of equation (3.4) and the derivative operators $\frac{\partial}{\partial x_T}$ and $\frac{\partial}{\partial \sigma_T}$ have no effect on $e^{U(p,T)}$, it follows that:

$$\begin{aligned}
&\frac{\partial}{\partial x_T}\left[-\left(r-\frac{1}{2}\sigma_T^2\right)\mathcal{P}_J\right]+\frac{1}{2}\frac{\partial^2}{\partial x_T^2}\left[\sigma_T^2\mathcal{P}_J\right]+\frac{\partial}{\partial \sigma_T}\left[-A(T,\sigma_T)\mathcal{P}_J\right]\\
&+\frac{1}{2}\frac{\partial^2}{\partial \sigma_T^2}\left[B^2(T,\sigma_T)\mathcal{P}_J\right]+\rho\frac{\partial^2}{\partial x_T\,\partial\sigma_T}\left[\sigma_T B(T,\sigma_T)\mathcal{P}_J\right]\\
=\;&\int_{-\infty}^{+\infty}\frac{dp}{2\pi}e^{ip(x_T-x_0)}\frac{\partial F(\sigma_T,\sigma_0,r,p,T)}{\partial T}\,e^{U(p,T)}. \qquad (3.44)
\end{aligned}$$

Adding the term $\lambda m^j\frac{\partial}{\partial x_T}\mathcal{P}_J$, which is given by

$$\lambda\int_{-\infty}^{+\infty}\frac{dp}{2\pi}ip\,e^{ip(x_T-x_0)}F(\sigma_T,\sigma_0,r,p,T)\,e^{U(p,T)}\int_{-\infty}^{+\infty}(e^J-1)\varpi(J)dJ, \qquad (3.45)$$

as well as the term $\lambda\int_{-\infty}^{+\infty}\left[\mathcal{P}_J(x_T-J)-\mathcal{P}_J(x_T)\right]\varpi(J)dJ$, which is given by

$$\lambda\int_{-\infty}^{+\infty}\frac{dp}{2\pi}e^{ip(x_T-x_0)}F(\sigma_T,\sigma_0,r,p,T)\,e^{U(p,T)}\int_{-\infty}^{+\infty}\left(e^{-ipJ}-1\right)\varpi(J)dJ, \qquad (3.46)$$

the right hand side of Eq.(3.9) is expressed as

$$\begin{aligned}
&\int_{-\infty}^{+\infty}\frac{dp}{2\pi}e^{ip(x_T-x_0)}\frac{\partial F}{\partial T}\,e^{U(p,T)}\\
&+\int_{-\infty}^{+\infty}\frac{dp}{2\pi}e^{ip(x_T-x_0)}F\,e^{U(p,T)}\lambda\int_{-\infty}^{+\infty}\left[e^{-ipJ}-1+ip(e^J-1)\right]\varpi(J)dJ. \qquad (3.47)
\end{aligned}$$

This, of course should equal the left hand side of Eq.(3.9), which is given by

$$\int_{-\infty}^{+\infty}\frac{dp}{2\pi}e^{ip(x_T-x_0)}\frac{\partial F}{\partial T}\,e^{U(p,T)}+\int_{-\infty}^{+\infty}\frac{dp}{2\pi}e^{ip(x_T-x_0)}F\frac{\partial e^{U(p,T)}}{\partial T}. \qquad (3.48)$$

Expression (3.47) equals (3.48) when

$$\frac{\partial U(p,T)}{\partial T}=\lambda\int_{-\infty}^{+\infty}\left[e^{-ipJ}-1+ip\left(e^J-1\right)\right]\varpi(J)dJ, \qquad (3.49)$$

from which the result (3.12) for $U(p,T)$ follows.

# 4

# Path integral approach to the pricing of timer options with the Duru-Kleinert transformation

> This chapter is based on the article (145), which is joint work with Damiaan Lemmens and Jacques Tempère.

In this chapter, the Duru-Kleinert transformation method, see section 2.2.2, is performed to price timer options under the stochastic volatility (SV) models.

Timer options, first introduced for sale by Société Générale Corporate and Investment Banking (SG CIB) in 2007 (167, 168), are relatively new products in the equity volatility market. The basic principle of this option is similar to the European vanilla option, with the key distinction being the uncertain expiration date. Rather than a fixed maturity time that is set at inception for the vanilla option, the expiry date of the timer option is a stopping time equals to the time needed for the realized variance of the underlying asset to reach a pre-specified level.

Stopping times, sometimes formulated as first passage or hitting times, have applications in various research fields. Traditional applications of stopping times in physics are for example the situation where internal fluctuations induce the current of an electric circuit to attain a critical value (169, 170) and Kramer's problem (171, 172). Recent applications of stopping times can be found in neuroscience, where a neuron emits a signal when its membrane voltage exceeds a certain threshold (173, 174, 175); in the research field of quantum hitting times of Markov chains and hitting times of quantum random walks (176, 177); and in econophysics (178, 179). For an introduction to first passage problems and an overview of possible applications see (180, 181).

When the expiration date is only determined by a stopping time that can theoretically become infinite the option is called a perpetual timer option. According to Hawkins and Krol (182), it is usual practice to specify a maximum expiry for the timer option, at which point the option expires in the same manner as vanilla options, to prevent excessively long maturity times. These options are called finite time-horizon timer options.

Timer options were first proposed in literature by Neuberger (183) as "mileage" options in 1990. In the middle 1990s, Bick emphasized the application of dynamic trading strategies with timer options to portfolio insurance as well as to hedging strategies (184). Recently, after timer options were traded in the market, the amount of research concerning the pricing of perpetual timer options has increased. Li studied the pricing and hedging under the Heston SV model (185). Bernard and Cui proposed a fast and accurate almost-exact simulation method in general SV models (186). Saunders developed an asymptotic approximation under fast mean-reverting SV models (187). We contribute to the existing literature by presenting analytical pricing results for both perpetual and finite time-horizon timer options for a general stochastic process. These general results are then applied to determine explicit closed-form formulas for the 3/2 (188) and the Heston (76) SV model. Especially for timer options it is relevant to investigate different SV models, since the price of these options is particularly sensitive to the behavior of the volatility.

We derive these results in the path integral framework. To derive our general results we will rely on the Duru-Kleinert space-time substitution method used by Duru and Kleinert to treat the hydrogen atom with path integrals (100, 153, 189), and explained in more detail in the chapter on mathematical preliminaries, section 2.2.2. This method has recently been used in finance by Decamps and De Schepper to derive asymptotic formulas for Black-Scholes implied volatilities (190).

The Duru-Kleinert space-time substitution approach serves here to translate the original stochastic processes to new ones behaving in a stochastic time horizon. Under this new time horizon, the random expiry time is expressed as a functional of the transformed SV. Then a method related to variational perturbation theory (100, 191) is applied to derive the joint propagator of the transformed SV process and the stopping time process in the new time horizon. Based on these transition probability density functions, we arrive at the pricing formulas for the perpetual timer option. In addition, we obtain pricing formulas for the finite time-horizon timer option by deriving the joint propagator of the log-return and the realized variance process.

For SV processes, we start by emphasizing the 3/2 SV model (188, 192, 193) not only in view of its analytical tractability but also because of the support from empirical evidence (194, 195, 196). The results for this model are obtained by making a connection with the Morse potential. Next we treat the Heston SV model (76) by relating it to the Kratzer potential. This leads to closed-form pricing formulas for perpetual and finite time-horizon timer options for both models. The result for the perpetual timer option under the Heston model corresponds to the one found by Li (185), confirming our approach.

This chapter is organized as follows. In section 4.1 we present general pricing formulas for perpetual and finite time-horizon timer call options under general SV models. Section 5.4.6 is devoted to deriving closed-form formulas for the 3/2 and the Heston SV model. In section 4.3 the closed-form formulas are compared with Monte Carlo simulations and some properties of timer options are discussed. And finally a conclusion is given in section 4.4.

## 4.1 General pricing formula of timer options

### 4.1.1 Model description

For conciseness of representation, in this chapter we only consider option pricing in a risk-neutral world. Moreover we assume that the initial time of the option is the current time $t = 0$ because the generalization to the case of a forward-start option is straightforward.

Let $\{S(t)\}$ denote the underlying asset price process following a Black-Scholes type stochastic differential equation (SDE), with a variance $v(t)$, which is stochastic variable itself. Conventionally, the time evolution of $S(t)$ is represented in terms of the log-return $x(t) = \ln \frac{S(t)}{S_0}$, with $S_0 = S(0)$. The realization of a stochastic process $Z$ at a special time $s$ will be denoted by $Z_s$, and we will use this notation throughout this chapter. After the transformation to the log-return, the system is governed by the SDEs:

$$
\begin{aligned}
dx(t) &= \left(r - \frac{v(t)}{2}\right) dt + \sqrt{v(t)} \left(\sqrt{1-\rho^2} dW_1(t) + \rho dW_2(t)\right), && (4.1) \\
dv(t) &= \alpha(v)dt + \beta(v)dW_2(t), && (4.2)
\end{aligned}
$$

where $r$ is the constant risk-neutral interest rate, $W_1(t)$ and $W_2(t)$ are two independent Wiener processes, $\rho \in [-1, 1]$ is the correlation coefficient between $x(t)$ and its variance $v(t)$.

Now we introduce the notion of the realized variance, which is a principal ingredient of timer options. In practice the realized variance is given by $\sum_{n=1}^{N} \left(x_{t_n} - x_{t_{n-1}}\right)^2$, where the set of evaluation times $t_n$ are for example daily closing times. In the literature (see (122, 185)), the realized variance of the underlying asset during a time period $[0, T]$, denoted by $I_T$, is usually approximated by:

$$
I_T = \int_0^T v(t)dt. \tag{4.3}
$$

Also in this chapter equation (4.3) will be used as the definition of the realized variance. Figure 4.1 shows samples of the time evolution of underlying asset processes $S(t)$ (top row), their corresponding variance processes $v(t)$ (middle row) and realized variances (bottom row). The left column is for perpetual timer options, while the right column is for finite time-horizon timer options ~~(right column)~~ with the maximum expiration time being 1.5. The pre-specified variance budget is assumed to be 0.875.

### 4.1.2 Pricing of perpetual timer options

The price of a perpetual timer call option with strike price $K$ can be expressed as the expectation of the discounted payoff:

$$
\mathcal{C}_{Perp} = \mathbb{E}\left[e^{-r\mathcal{T}_\mathcal{B}} \max\left(S_0\, e^{x_{\mathcal{T}_\mathcal{B}}} - K, 0\right)\right]. \tag{4.4}
$$

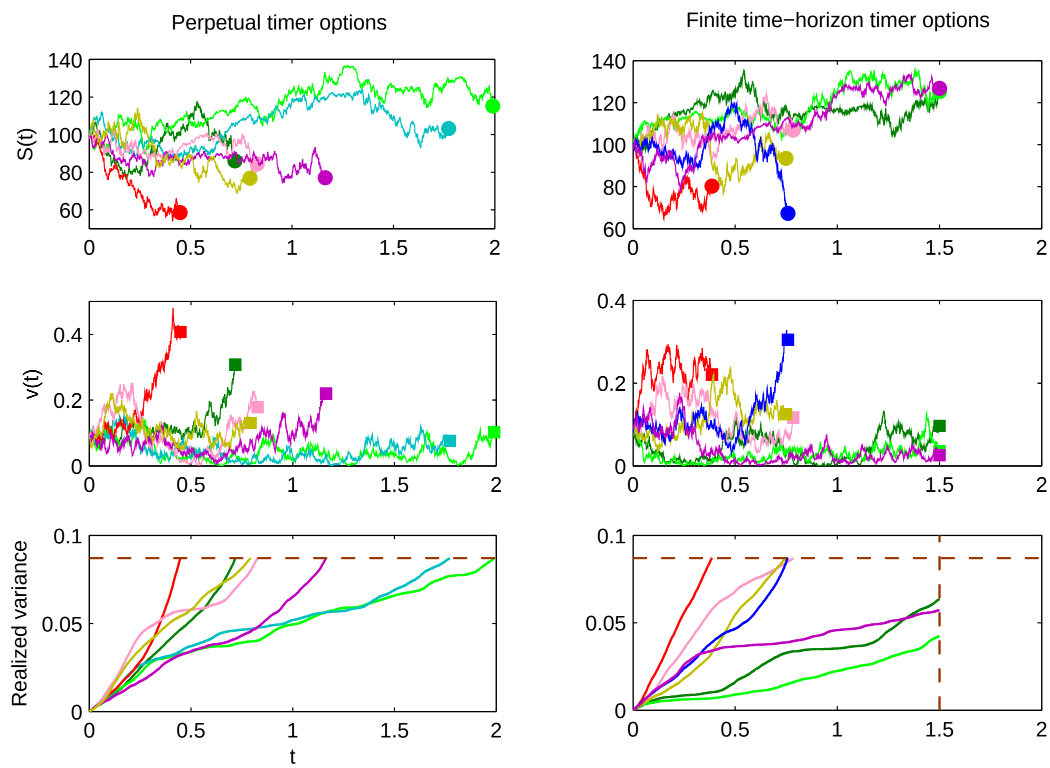


**Figure 4.1:** Samples of the time evolution of underlying asset processes $S(t)$ (top row), their corresponding variance processes $v(t)$ (middle row) and realized variances (bottom row). The left column is for perpetual timer options, while the right column is for finite time-horizon timer options (right column) with the maximum expiration time being 1.5. The pre-specified variance budget is assumed to be 0.875.

This expression is similar to the one for the vanilla call option, except for the uncertain expiry time $\mathcal{T}_{\mathcal{B}}$, which is the stopping time defined as

$$\mathcal{T}_{\mathcal{B}} = \inf \left\{ u > 0; \int_0^u v(t)dt = \mathcal{B} \right\}. \tag{4.5}$$

Here $\mathcal{B} = \sigma_0^2 T_0$ is the pre-specified variance budget with $T_0$ the expected investment horizon and $\sigma_0$ the forecasted volatility of the underlying asset during that period.

The dependence on the implicitly defined expiry time $\mathcal{T}_{\mathcal{B}}$ is inconvenient. We will now apply the Duru-Kleinert transformation method of quantum mechanics

(100), see also section 2.2.2, to construct variables in function of which $\mathcal{T}_{\mathcal{B}}$ is explicitly given. Define a time substitution $\tau(t)$ such that

$$\tau(t) = \int_0^t v(s)ds, \tag{4.6}$$

we will refer to $\tau$ as the pseudotime, following (100). The inverse function theorem gives us that

$$\frac{d\tau^{-1}(t)}{dt} = \frac{1}{v(\tau^{-1}(t))}, \tag{4.7}$$

from which it follows that $\tau^{-1}(t)$ is given by:

$$\tau^{-1}(t) = \int_0^t \frac{1}{v(\tau^{-1}(s))}ds. \tag{4.8}$$

Denote $v(\tau^{-1}(t))$ by $V(t)$ and $x(\tau^{-1}(t))$ by $X(t)$, which follow new SDEs:

$$dV(t) = \frac{\alpha(V)}{V}dt + \frac{\beta(V)}{\sqrt{V}}dW_2, \tag{4.9}$$

$$dX(t) = \left(\frac{r}{V} - \frac{1}{2}\right)dt + \left(\sqrt{1-\rho^2}dW_1 + \rho dW_2\right). \tag{4.10}$$

Given the timer call variance budget

$$\mathcal{B} = \int_0^{\mathcal{T}_{\mathcal{B}}} v(t)dt = \tau(\mathcal{T}_{\mathcal{B}}), \tag{4.11}$$

we obtain the explicit expression for the stopping time as

$$\mathcal{T}_{\mathcal{B}} = \tau^{-1}(\mathcal{B}) = \int_0^{\mathcal{B}} \frac{1}{v(\tau^{-1}(t))}dt = \int_0^{\mathcal{B}} \frac{1}{V(t)}dt. \tag{4.12}$$

Note that $(x(t), v(t)) = (X(\tau(t)), V(\tau(t)))$ , so as $(x(t), v(t))$ evolves in the period $[0, \mathcal{T}_{\mathcal{B}}]$, $(X(t), V(t))$ evolves in $[\tau(0), \tau(\mathcal{T}_{\mathcal{B}})]$, that is $[0, \mathcal{B}]$. Therefore $[0, \mathcal{B}]$ is now a fixed horizon in pseudotime, and not only do the processes $X$, $V$ and $\mathcal{T}$ evolve during that period, but also expression (4.4) can be written as

$$\mathcal{C}_{Perp} = \mathbb{E}\left[e^{-r\mathcal{T}_{\mathcal{B}}} \max\left(S_0\, e^{X_{\mathcal{B}}} - K, 0\right)\right]. \tag{4.13}$$

Hence, it is intuitive to study the joint transition probability density function of the dynamics of $(X, \mathcal{T})$. However, as $\mathcal{T}$ depends on $V$, we turn to the joint propagator of the dynamics of $(X, V, \mathcal{T})$.

The substitutions

$$z(t) = \int \frac{\sqrt{V}}{\beta(V)} dV(t), \tag{4.14}$$
$$y(t) = X(t) - \rho z(t), \tag{4.15}$$

help change the correlated dynamics of $(X, V)$ into two independent processes following

$$dy(t) = \left[\frac{r}{V(z)} - \frac{1}{2} - \rho \mathcal{A}(z)\right] dt + \sqrt{1-\rho^2} dW_1, \tag{4.16}$$
$$dz(t) = \mathcal{A}(z) dt + dW_2, \tag{4.17}$$

where

$$\mathcal{A}(z(t)) = \frac{\alpha(V)}{\beta(V)\sqrt{V}} + \frac{1}{2}\frac{d}{dV}\left(\frac{\sqrt{V}}{\beta(V)}\right)\frac{\beta^2(V)}{V} \tag{4.18}$$

is a function of $z(t)$ because $V(t)$ is expressed in terms of $z(t)$ according to expression (4.14).

To determine the price of the timer option, the propagator $\mathcal{P}(y_{\mathcal{B}}, z_{\mathcal{B}}, \mathcal{T}_{\mathcal{B}} \,|\, y_0, z_0, 0)$ is needed. This propagator describes the joint probability that $y$ has the value $y_{\mathcal{B}}$, $z$ has the value $z_{\mathcal{B}}$ and the stopping time has the value $\mathcal{T}_{\mathcal{B}}$ at a later pseudotime $\mathcal{B}$ given their initial value $y_0$, $z_0$ and 0 at pseudotime 0. Since the processes $y$ and $z$ are uncorrelated, the Lagrangian corresponding to their joint evolution can be written as $\mathcal{L}[\dot{y}, y, z] + \mathcal{L}[\dot{z}, z]$ with:

$$\mathcal{L}[\dot{y}, y, z] = \frac{\left[\dot{y} - \left(\frac{r}{V(z)} - \frac{1}{2} - \rho\mathcal{A}(z)\right)\right]^2}{2(1-\rho^2)}, \tag{4.19}$$
$$\mathcal{L}[\dot{z}, z] = \frac{1}{2}\left[\dot{z} - \mathcal{A}(z)\right]^2 + \frac{1}{2}\frac{\partial}{\partial z}\mathcal{A}(z), \tag{4.20}$$

Using the path integral framework, the joint propagator $\mathcal{P}(y_{\mathcal{B}}, z_{\mathcal{B}}, \mathcal{T}_{\mathcal{B}} \,|\, y_0, z_0, 0)$ can be determined by:

$$\mathcal{P}(y_{\mathcal{B}}, z_{\mathcal{B}}, \mathcal{T}_{\mathcal{B}} \,|\, y_0, z_0, 0) = \int \mathcal{D}y \int \mathcal{D}z \delta\left(\mathcal{T}_{\mathcal{B}} - \int_0^{\mathcal{B}} \frac{1}{V(z)} dt\right) e^{-\int_0^{\mathcal{B}}(\mathcal{L}[\dot{z},z] + \mathcal{L}[\dot{y},y,z])dt}, \tag{4.21}$$

where $\delta(\cdot)$ is the delta function. It serves here to select these paths of $V$, expressed in terms of $z$, such that $\int_0^{\mathcal{B}} \frac{1}{V(t)} dt$ equals $\mathcal{T}_{\mathcal{B}}$.

To proceed we introduce the Fourier transform of the delta function. Furthermore since the path integral corresponding to the $y$ variable is quadratic it can be solved analytically. After performing this path integral, we can return to the original $X_{\mathcal{B}}$ variable. Expression (4.21) then becomes:

$$\mathcal{P}\left(X_{\mathcal{B}}, z_{\mathcal{B}}, \mathcal{T}_{\mathcal{B}} \,|\, y_0, z_0, 0\right) = \int_{-\infty}^{\infty} \frac{dp}{2\pi} e^{ip\mathcal{T}_{\mathcal{B}}} \int \mathcal{D}z\, e^{-\int_0^{\mathcal{B}} \left(\mathcal{L}[\dot{z}, z] + ip\frac{1}{V(z)}\right) dt} \frac{e^{-\frac{\left[X_{\mathcal{B}} - \Upsilon(z)\right]^2}{2(1-\rho^2)\mathcal{B}}}}{\sqrt{2\pi\left(1-\rho^2\right)\mathcal{B}}}, \tag{4.22}$$

where

$$\Upsilon\left(z\right) = \rho\left(z_{\mathcal{B}} - z_0 - \int_0^{\mathcal{B}} \mathcal{A}\left(z(t)\right) dt\right) + r\mathcal{T}_{\mathcal{B}} - \frac{\mathcal{B}}{2}. \tag{4.23}$$

In order to add the $z$ dependent term $\Upsilon\left(z\right)$ to the Lagrangian of the $z$ path integral one can introduce another Fourier integral, and $\mathcal{P}\left(X_{\mathcal{B}}, z_{\mathcal{B}}, \mathcal{T}_{\mathcal{B}} \,|\, y_0, z_0, 0\right)$ then becomes:

$$\begin{aligned} \mathcal{P}\left(X_{\mathcal{B}}, z_{\mathcal{B}}, \mathcal{T}_{\mathcal{B}} \,|\, y_0, z_0, 0\right) &= \int_{-\infty}^{\infty} \frac{dl}{2\pi}\, e^{i\,l X_{\mathcal{B}} - \frac{\left(1-\rho^2\right)\mathcal{B}}{2} l^2} \int_{-\infty}^{\infty} \frac{dp}{2\pi}\, e^{ip\mathcal{T}_{\mathcal{B}}} \\ &\quad \times \int \mathcal{D}z(t)\, e^{-\int_0^{\mathcal{B}} \left[\mathcal{L}[z, \dot{z}] + ip\frac{1}{V(z)} + il\Upsilon(z)\right] dt}. \end{aligned} \tag{4.24}$$

Whether our approach will lead to closed-form pricing formulas for timer options will depend on the Lagrangian $\mathcal{L}[z, \dot{z}] + ip\frac{1}{V(z)} + il\Upsilon\left(z\right)$. More precisely this means that $\mathcal{A}\left(z(t)\right)$ and $\Upsilon\left(z\right)$ should be sufficiently well behaved in terms of $z$. For the two examples illustrated in this chapter, the functions $\alpha(V(t))$ and $\beta(V(t))$ are as such that $\Upsilon\left(z\right)$ is only a function of $z_{\mathcal{B}}$ and $\mathcal{T}_{\mathcal{B}}$, denoted by $\Upsilon\left(z_{\mathcal{B}}, \mathcal{T}_{\mathcal{B}}\right)$. Then it is not necessary to introduce the Fourier transform of expression (4.24) and we can proceed with expression (4.22). Now the price of a perpetual timer option which is given by

$$\mathcal{C}_{Perp} = \int dX_{\mathcal{B}} \int dz_{\mathcal{B}} \int d\mathcal{T}_{\mathcal{B}}\, \mathcal{P}\left(X_{\mathcal{B}}, z_{\mathcal{B}}, \mathcal{T}_{\mathcal{B}} \,|\, y_0, z_0, 0\right) \left[e^{-r\mathcal{T}_{\mathcal{B}}} \max\left(S_0\, e^{X_{\mathcal{B}}} - K, 0\right)\right], \tag{4.25}$$

can be written as:

$$\mathcal{C}_{Perp} = \int_0^{\infty} d\mathcal{T}_{\mathcal{B}} \int_{-\infty}^{\infty} dz_{\mathcal{B}} \mathcal{P}\left(z_{\mathcal{B}}, \mathcal{T}_{\mathcal{B}} \,|\, z_0, 0\right) \bar{\mathcal{C}}\left(z_{\mathcal{B}}, \mathcal{T}_{\mathcal{B}}\right), \tag{4.26}$$

with $\bar{\mathcal{C}}\left(z_{\mathcal{B}}, \mathcal{T}_{\mathcal{B}}\right)$ being the prices conditional on $z$:

$$\begin{aligned} \bar{\mathcal{C}}\left(z_{\mathcal{B}}, \mathcal{T}_{\mathcal{B}}\right) &= \int_{-\infty}^{\infty} dX_{\mathcal{B}} \, \frac{e^{-\frac{\left[X_{\mathcal{B}}-\Upsilon\left(z_{\mathcal{B}}, \mathcal{T}_{\mathcal{B}}\right)\right]^2}{2\left(1-\rho^2\right)\mathcal{B}}}}{\sqrt{2\pi\left(1-\rho^2\right)\mathcal{B}}} \left[e^{-r\mathcal{T}_{\mathcal{B}}} \max\left(S_0 \, e^{X_{\mathcal{B}}} - K, 0\right)\right] \\ &= S_0 \, e^{\Upsilon\left(z_{\mathcal{B}}, \mathcal{T}_{\mathcal{B}}\right) - r\mathcal{T}_{\mathcal{B}} + \frac{\left(1-\rho^2\right)\mathcal{B}}{2}} \mathcal{N}\left(d_+\right) - K \, e^{-r\mathcal{T}_{\mathcal{B}}} \mathcal{N}(d_-), \end{aligned} \tag{4.27}$$

where $\mathcal{N}(\cdot)$ is the cumulative distribution for the normal random variable and

$$d_+ = \frac{\ln\frac{S_0}{K} + \left(1-\rho^2\right)\mathcal{B} + \Upsilon\left(z_{\mathcal{B}}, \mathcal{T}_{\mathcal{B}}\right)}{\sqrt{\left(1-\rho^2\right)\mathcal{B}}}, \tag{4.28}$$

$$d_- = \frac{\ln\frac{S_0}{K} + \Upsilon\left(z_{\mathcal{B}}, \mathcal{T}_{\mathcal{B}}\right)}{\sqrt{\left(1-\rho^2\right)\mathcal{B}}}, \tag{4.29}$$

and $\mathcal{P}\left(z_{\mathcal{B}}, \mathcal{T}_{\mathcal{B}} \,|\, z_0, 0\right)$ is given by

$$\mathcal{P}\left(z_{\mathcal{B}}, \mathcal{T}_{\mathcal{B}} | z_0, 0\right) = \int_{-\infty}^{\infty} \frac{dp}{2\pi} e^{ip\mathcal{T}_{\mathcal{B}}} \int \mathcal{D}z e^{-\int_0^{\mathcal{B}}\left(\mathcal{L}[z,\dot{z}] + \frac{ip}{V(z)}\right)dt}. \tag{4.30}$$

Note that expression (4.27) is a Black-Scholes-Merton type pricing formula for perpetual timer options. To determine the price of a perpetual timer option for a particular model one needs to evaluate $\Upsilon\left(z_{\mathcal{B}}, \mathcal{T}_{\mathcal{B}}\right)$ in order to obtain $\bar{\mathcal{C}}\left(z_{\mathcal{B}}, \mathcal{T}_{\mathcal{B}}\right)$. Furthermore if we also have the analytical expression for the joint propagator $\mathcal{P}\left(z_{\mathcal{B}}, \mathcal{T}_{\mathcal{B}} \,|\, z_0, 0\right)$, formula (4.26) demonstrates that the closed-form perpetual timer option pricing formula can be derived through two trivial integrals.

### 4.1.3 Pricing of finite time-horizon timer options

In this subsection we consider the pricing of finite time-horizon timer option.

Let the maximum expiry time to be $T$, then the price of a finite time-horizon timer option, denoted by $\mathcal{C}_{Fini}$, of strike price $K$ can be expressed as a sum of two contributions:

$$\mathcal{C}_{Fini} = \mathcal{C}_1 + \mathcal{C}_2, \tag{4.31}$$

where

$$\mathcal{C}_1 = \int_0^T d\mathcal{T}_{\mathcal{B}} \int_{-\infty}^{\infty} dz_{\mathcal{B}} \mathcal{P}\left(z_{\mathcal{B}}, \mathcal{T}_{\mathcal{B}} \,|\, z_0, 0\right) \bar{\mathcal{C}}\left(z_{\mathcal{B}}, \mathcal{T}_{\mathcal{B}}\right) \tag{4.32}$$

is the contribution from paths that exhausted their variance budget before time $T$, and

$$\mathcal{C}_2 = e^{-rT} \int_{-\infty}^{\infty} \left(S_0\, e^{x_T} - K\right)_+ \mathcal{P}_{\mathcal{B}}\left(x_T \,|x_0\,\right) dx_T \tag{4.33}$$

is the contribution from paths that reach the preset finite time horizon. Note the integration range of $\mathcal{T}_{\mathcal{B}}$ in $\mathcal{C}_1$, which is truncated by the maximum expiry time $T$.

Denote the joint propagator of the log-return and the realized variance as $\mathcal{P}\left(x_T, I_T \,|\, x_0, 0\right)$, then

$$\mathcal{P}_{\mathcal{B}}\left(x_T \,|\, x_0\right) = \int_0^{\mathcal{B}} \mathcal{P}\left(x_T, I_T \,|\, x_0, 0\right) dI_T. \tag{4.34}$$

Note $\mathcal{P}_{\mathcal{B}}\left(x_T \,|\, x_0\right)$ is not the propagator of $x$ that should be used for the European vanilla option, which represents the probability that $x$ has the value $x_T$ at later time $T$ given the initial values $x_0$ at time 0. Instead $\mathcal{P}_{\mathcal{B}}\left(x_T \,|\, x_0\right)$ in $\mathcal{C}_2$ is the propagator of $x$ which is also conditioned on the fact that the realized variance budget of each path has not been exhausted before the maximum expiry time $T$.

Furthermore, if $\mathcal{P}_{\mathcal{B}}\left(x_T \,|\, x_0\right)$ can be written as a Fourier integral:

$$\mathcal{P}_{\mathcal{B}}\left(x_T \,|\, x_0\right) = \int_{-\infty}^{\infty} \frac{dl}{2\pi}\, e^{il(x_T - rT)} \mathcal{F}(l), \tag{4.35}$$

then by following the derivation outlined in (164), we can rewrite $\mathcal{C}_2$ explicitly, and thus the pricing formula of finite time-horizon Timer option as

$$\begin{aligned} \mathcal{C}_{Fini} &= \int_0^T d\mathcal{T}_{\mathcal{B}} \int_{-\infty}^{\infty} dz_{\mathcal{B}} \mathcal{P}\left(z_{\mathcal{B}}, \mathcal{T}_{\mathcal{B}} \,|\, z_0, 0\right) \bar{\mathcal{C}}\left(z_{\mathcal{B}}, \mathcal{T}_{\mathcal{B}}\right) \\ &\quad + \frac{\mathcal{G}(0)}{2} + i \int_{-\infty}^{\infty} \frac{dl}{2\pi} \frac{e^{il\left(\ln\frac{K}{S_0} - rT\right)} \mathcal{G}(l)}{l}, \end{aligned} \tag{4.36}$$

where

$$\mathcal{G}(l) = S_0 \mathcal{F}(l + i) - K\, e^{-rT} \mathcal{F}(l). \tag{4.37}$$

The integration of $\mathcal{P}_{\mathcal{B}}\left(x_T \,|\, x_0\right)$ over all possible $x_T$'s gives $\mathcal{F}(0)$, which is the "survival probability" describing the probability that the finite time-horizon timer option is executed at the maximum expiry time $T$. This survival probability can also be determined by $\int_T^{\infty} d\mathcal{T}_{\mathcal{B}} \int dz_{\mathcal{B}} \mathcal{P}\left(z_{\mathcal{B}}, \mathcal{T}_{\mathcal{B}} \,|\, z_0, 0\right)$, from which it is clear that this probability is independent from the evolution of $x$, thus does not depend on the correlation coefficient $\rho$.

For the finite time-horizon timer option, besides the evaluation of propagator $\mathcal{P}\left(z_{\mathcal{B}}, \mathcal{T}_{\mathcal{B}} \,|\, z_0, 0\right)$ as for the perpetual timer option, we must also calculate the propagator $\mathcal{P}\left(x_T, I_T \,|\, x_0, 0\right)$ to derive the formula of $\mathcal{F}(l)$.

## 4.2 Propagators for the 3/2 and the Heston model

In this section we focus on the derivations of joint propagators $\mathcal{P}\left(z_{\mathcal{B}}, \mathcal{T}_{\mathcal{B}} \,|\, z_0, 0\right)$ and $\mathcal{P}\left(x_T, I_T \,|\, x_0, 0\right)$. These are used in section 4.3 in conjunction with expressions (4.26) and (4.36) from the previous section to price perpetual and finite time-horizon timer options, respectively. Note that $\mathcal{P}\left(z_{\mathcal{B}}, \mathcal{T}_{\mathcal{B}} \,|\, z_0, 0\right)$ is evaluated in the pseudotime horizon and $\mathcal{P}\left(x_T, I_T \,|\, x_0, 0\right)$ in the original time horizon. The 3/2 and the Heston model are chosen both from mathematical and empirical considerations.

As mentioned in the previous section, it is convenient to choose models such that $\int_0^{\mathcal{B}} \mathcal{A}\left(z(t)\right) dt$ is a function of $z_{\mathcal{B}}$ and $\mathcal{T}_{\mathcal{B}}$. In addition, from the perspective of mathematics, the total Lagrangian in expression (4.30):

$$\mathcal{L}_{Tot}[\dot{z}, z] = \mathcal{L}[\dot{z}, z] + \frac{ip}{V(z)} \tag{4.38}$$

written in terms of $z$ and $\dot{z}$ should be sufficiently well behaved to achieve a closed-form solution with the path integral.

Furthermore there is substantial empirical evidence supporting the stochastic differential equation underlying the 3/2 model. The Heston model, on the other hand, is important because it is a standard model for the financial industry.

### 4.2.1 The 3/2 model and the Morse potential

The model dynamics of the 3/2 SV model (188) are given by:

$$dx(t) = \left(r - \frac{v(t)}{2}\right) dt + \sqrt{v(t)}\left(\sqrt{1-\rho^2}\, dW_1(t) + \rho\, dW_2(t)\right), \tag{4.39}$$

$$dv(t) = \kappa v(t)\left(\theta - v(t)\right) dt + \epsilon v^{3/2}(t)\, dW_2(t). \tag{4.40}$$

More properties of this model will be discussed in section 5.2.2. Relating this model to the general SV model used in (4.2), we have

$$\alpha(V) = \kappa V(\theta - V), \tag{4.41}$$

$$\beta(V) = \epsilon V^{3/2}. \tag{4.42}$$

For calculation convenience, we multiply $z(t)$ defined in expression (4.14) by a factor $-\epsilon$ to obtain

$$z(t) = -\ln V(t). \tag{4.43}$$

Thus, according to equations (4.12), (4.18) and (4.23), we have

$$\mathcal{T}_{\mathcal{B}} = \int_0^{\mathcal{B}} e^{z(t)} dt, \tag{4.44}$$

$$\int_0^{\mathcal{B}} \mathcal{A}(z(t))\, dt = \frac{\kappa\theta}{\epsilon}\mathcal{T}_{\mathcal{B}} - \left(\frac{\kappa}{\epsilon} + \frac{\epsilon}{2}\right)\mathcal{B} \tag{4.45}$$

$$\Upsilon(z_{\mathcal{B}}, \mathcal{T}_{\mathcal{B}}) = -\frac{\rho}{\epsilon}(z_{\mathcal{B}} + \ln v_0) + r\mathcal{T}_{\mathcal{B}} - \frac{\mathcal{B}}{2} - \rho\left(\frac{\kappa\theta}{\epsilon}\mathcal{T}_{\mathcal{B}} - \left(\frac{\kappa}{\epsilon} + \frac{\epsilon}{2}\right)\mathcal{B}\right), \tag{4.46}$$

Therefore the total Lagrangian is

$$\begin{aligned}\mathcal{L}_{Tot}[\dot{z}, z] = {} & \frac{1}{2\epsilon^2}\dot{z}^2 + \frac{\kappa^2\theta^2}{2\epsilon^2} e^{2z} - \left(\frac{\kappa^2\theta}{\epsilon^2} + \kappa\theta - ip\right) e^{z} \\ & + \frac{\kappa\theta}{\epsilon^2} e^{z}\dot{z} - \left(\frac{\kappa}{\epsilon^2} + \frac{1}{2}\right)\dot{z} + \frac{\left(\kappa + \epsilon^2/2\right)^2}{2\epsilon^2}.\end{aligned} \tag{4.47}$$

Note that the last three terms of $\mathcal{L}_{Tot}[z, \dot{z}]$ are trivial, and can be integrated directly, more precisely $\int_0^{\mathcal{B}} e^{z}\, \dot{z} dt = e^{z_{\mathcal{B}}} - e^{z_0}$ and $\int_0^{\mathcal{B}} \dot{z} dt = z_{\mathcal{B}} - z_0$. Plugging this total Lagrangian into expression (4.30), we have

$$\begin{aligned}\mathcal{P}(z_{\mathcal{B}}, \mathcal{T}_{\mathcal{B}} \,|\, z_0, 0) &= \int_{-\infty}^{\infty} \frac{dp}{2\pi} e^{ip\mathcal{T}_{\mathcal{B}}} \int \mathcal{D}z(t)\, e^{-\int_0^{\mathcal{B}} \mathcal{L}_{Tot}[\dot{z}, z] dt} \\ &= \exp\left\{-\frac{\kappa\theta}{\epsilon^2}\left(e^{z_{\mathcal{B}}} - e^{z_0}\right) + \left(\frac{\kappa}{\epsilon^2} + \frac{1}{2}\right)(z_{\mathcal{B}} - z_0) - \frac{\left(\kappa + \epsilon^2/2\right)^2 \mathcal{B}}{2\epsilon^2}\right\} \\ &\times \int_{-\infty}^{\infty} \frac{dp}{2\pi} e^{ip\mathcal{T}_{\mathcal{B}}} \int \mathcal{D}z(t)\, e^{-\int_0^{\mathcal{B}}\left[\frac{\dot{z}^2}{2\epsilon^2} + \frac{\kappa^2\theta^2}{2\epsilon^2} e^{2z} - \left(\frac{\kappa^2\theta}{\epsilon^2} + \kappa\theta - ip\right) e^{z}\right] dt}.\end{aligned} \tag{4.48}$$

The remaining nontrivial terms of $\mathcal{L}_{Tot}[\dot{z}, z]$ reveal that $z(t)$ is subjected to a Morse potential. By making use of the path integral for the Morse potential

(155), derived in chapter 2, see expression (2.90),the joint propagator becomes

$$\begin{aligned}\mathcal{P}\left(z_{\mathcal{B}},\mathcal{T}_{\mathcal{B}}\,|\,z_0,0\right)=&\frac{\kappa\theta}{\epsilon^2\sinh\frac{\kappa\theta\mathcal{T}_{\mathcal{B}}}{2}}\,e^{-\frac{\kappa\theta}{\epsilon^2}\left(e^{z_{\mathcal{B}}}-e^{z_0}\right)+\left(\frac{\kappa}{\epsilon^2}+\frac{1}{2}\right)\left(z_{\mathcal{B}}-z_0\right)}\\&\times\ e^{-\left(\frac{\kappa}{\epsilon^2}+\frac{1}{2}\right)^2\frac{\epsilon^2}{2}\mathcal{B}+\left(\frac{\kappa}{\epsilon^2}+1\right)\kappa\theta\mathcal{T}_{\mathcal{B}}-\frac{\kappa\theta}{\epsilon^2}\left(e^{z_{\mathcal{B}}}+e^{z_0}\right)\coth\frac{\kappa\theta\mathcal{T}_{\mathcal{B}}}{2}}\\&\times\int_0^\infty\frac{d\Phi_I}{\pi}\mathrm{Re}\left[e^{\Phi\mathcal{B}}\,I_{2\sqrt{\frac{2}{\epsilon^2}\Phi}}\left(\frac{\frac{2\kappa\theta}{\epsilon^2}\,e^{\frac{z_{\mathcal{B}}+z_0}{2}}}{\sinh\frac{\kappa\theta\mathcal{T}_{\mathcal{B}}}{2}}\right)\right],\end{aligned}\tag{4.49}$$

with $I_{\cdot}\left(\cdot\right)$ the modified Bessel function of the first kind.

Plugging expressions (4.46) and (4.49) into formula (4.26) yields the closed-form pricing formula for the perpetual timer call options under the 3/2 model.

The integral over all possible $z_{\mathcal{B}}$ can be done analytically, which leads to the marginal propagator for the stopping time $\mathcal{T}_{\mathcal{B}}$:

$$\begin{aligned}\mathcal{P}\left(\mathcal{T}_{\mathcal{B}}\,|\,0\right)\ =\ &\frac{\kappa\theta}{\epsilon^2}\left(1+\coth\frac{\kappa\theta\mathcal{T}_{\mathcal{B}}}{2}\right)\,e^{-\left(\frac{\kappa}{\epsilon^2}+\frac{1}{2}\right)^2\frac{\epsilon^2}{2}\mathcal{B}}\int_0^\infty\frac{d\Phi_I}{\pi}\,\mathrm{Re}\left[e^{\Phi\mathcal{B}}\left(\frac{\mathcal{N}}{v_0}\right)^{\mathcal{M}}\right.\\&\left.\times\frac{\Gamma\left(2\sqrt{\frac{2}{\epsilon^2}\Phi}-\mathcal{M}\right)}{\Gamma\left(2\sqrt{\frac{2}{\epsilon^2}\Phi}+1\right)}\,{}_1F_1\left(\mathcal{M}+1;\,2\sqrt{\frac{2}{\epsilon^2}\Phi}+1;\,-\frac{\mathcal{N}}{v_0}\right)\right],\end{aligned}\tag{4.50}$$

where $\Gamma\left(\cdot\right)$ is the Euler gamma function, ${}_1F_1\left(\cdot;\cdot;\cdot\right)$ is the confluent hypergeometric function, and

$$\mathcal{N}(\mathcal{T}_{\mathcal{B}})\ =\ \frac{\kappa\theta}{\epsilon^2}\left(\coth\frac{\kappa\theta\mathcal{T}_{\mathcal{B}}}{2}-1\right),\tag{4.51}$$

$$\mathcal{M}\left(\Phi\right)\ =\ \sqrt{\frac{2}{\epsilon^2}\Phi}-\left(\frac{\kappa}{\epsilon^2}+\frac{1}{2}\right).\tag{4.52}$$

Having obtained the results for the $z$-process (related to the variance, expression (4.40)), we next investigate the corresponding $x$-process (related to the underlying asset, expression (4.39)). We move on to the calculation of the propagator $\mathcal{P}\left(x_T,I_T\,|\,x_0,0\right)$ by performing the following substitutions

$$\chi(t)\ =\ x-\frac{\rho}{\epsilon}\left(\ln v-\kappa\theta t\right)-rt,\tag{4.53}$$

$$\zeta(t)\ =\ v^{-\frac{1}{2}},\tag{4.54}$$

which lead to two uncorrelated processes:

$$
\begin{aligned}
d\chi(t) &= \left(-\frac{1}{2}+\frac{\rho\kappa}{\epsilon}+\frac{\rho\,\epsilon}{2}\right)vdt+\sqrt{v}\sqrt{1-\rho^2}dW_1(t), && (4.55)\\
d\zeta(t) &= \left[-\frac{\kappa\theta}{2}\zeta+\left(\frac{\kappa}{2}+\frac{3}{8}\epsilon^2\right)\frac{1}{\zeta}\right]dt-\frac{\epsilon}{2}dW_2(t), && (4.56)
\end{aligned}
$$

and thus the corresponding Lagrangians:

$$
\begin{aligned}
\mathcal{L}[\dot{\chi},\chi,v] &= \frac{\left[\dot{\chi}-\left(-\frac{1}{2}+\frac{\rho\kappa}{\epsilon}+\frac{\rho\,\epsilon}{2}\right)v\right]^2}{2v\left(1-\rho^2\right)}, && (4.57)\\
\mathcal{L}[\dot{\zeta},\zeta] &= \mathcal{L}_1[\zeta]+\mathcal{L}_2[\zeta], && (4.58)
\end{aligned}
$$

where

$$
\begin{aligned}
\mathcal{L}_1[\zeta,\dot{\zeta}] &= \frac{2}{\epsilon^2}\left[\dot{\zeta}^2+\frac{\kappa^2\theta^2}{4}\zeta^2\right]+\frac{\left(2\kappa/\epsilon^2+1\right)^2-1/4}{8/\epsilon^2}\frac{1}{\zeta^2}, && (4.59)\\
\mathcal{L}_2[\zeta,\dot{\zeta}] &= \frac{2\kappa\theta}{\epsilon^2}\zeta\dot{\zeta}-\left(\frac{2\kappa}{\epsilon^2}+\frac{3}{2}\right)\frac{\dot{\zeta}}{\zeta}-\left(\frac{\kappa^2\theta}{\epsilon^2}+\kappa\theta\right). && (4.60)
\end{aligned}
$$

Since $\chi$ is independent from $\zeta$, the probability that $\chi$ goes to $\chi_T$, $\zeta$ goes to $\zeta_T$ and the realized variance reaches $I_T$ at a later time $T$ given the original positions $\chi_0$, $\zeta_0$ and $I_0 = 0$ at the initial time 0 is

$$
\begin{aligned}
&\mathcal{P}(\chi_T,\zeta_T,I_T\,|\,\chi_0,\zeta_0,0)\\
&=\int\mathcal{D}\zeta(t)\,\delta\left(I_T-\int_0^T v(t)\,dt\right)\,e^{-\int_0^T\mathcal{L}[\dot{\zeta},\zeta]dt}\int\mathcal{D}\chi(t)\,e^{-\int_0^T\mathcal{L}[\dot{\chi},\chi,v]dt}\\
&=\left(\frac{\zeta_T}{\zeta_0}\right)^{\frac{2\kappa}{\epsilon^2}+\frac{3}{2}}e^{-\frac{\kappa\theta}{\epsilon^2}(\zeta_T^2-\zeta_0^2)+\left(\frac{\kappa^2\theta}{\epsilon^2}+\kappa\theta\right)T}\int_{-\infty}^{\infty}\frac{dp}{2\pi}\,e^{ip\,I_T}\int_{-\infty}^{\infty}\frac{dl}{2\pi}\,e^{il\left[x_T+\frac{\rho\kappa\theta}{\epsilon}T-rT\right]}\left(\frac{\zeta_T}{\zeta_0}\right)^{2il\frac{\rho}{\epsilon}}\\
&\quad\times\int\mathcal{D}\zeta(t)\,e^{-\int_0^T\left[\mathcal{L}_1[\dot{\zeta},\zeta]+\frac{il\left(-\frac{1}{2}+\frac{\rho\kappa}{\epsilon}+\frac{\rho\epsilon}{2}\right)+(1-\rho^2)l^2/2+ip}{\zeta^2}\right]dt}, \qquad (4.61)
\end{aligned}
$$

where the remaining path integral over $\mathcal{D}\zeta(t)$ of the radial harmonic oscillator potential (154) is given by:

$$
\frac{2\kappa\theta\sqrt{\zeta_T\zeta_0}}{\epsilon^2\,\sinh(\frac{\kappa\theta T}{2})}\,e^{-\frac{\kappa\theta}{\epsilon^2}\left(\zeta_T^2+\zeta_0^2\right)\coth(\frac{\kappa\theta T}{2})}\,I_\lambda\left(\frac{2\kappa\theta\,\zeta_T\zeta_0}{\epsilon^2\,\sinh(\frac{\kappa\theta T}{2})}\right), \qquad (4.62)
$$

see expression (2.63), with

$$\lambda = \left( \left( \frac{2\kappa}{\epsilon^2} + 1 \right)^2 + \frac{8}{\epsilon^2} \left[ il \left( -\frac{1}{2} + \frac{\rho\kappa}{\epsilon} + \frac{\rho\epsilon}{2} \right) + \frac{(1-\rho^2)l^2}{2} + ip \right] \right)^{\frac{1}{2}}. \tag{4.63}$$

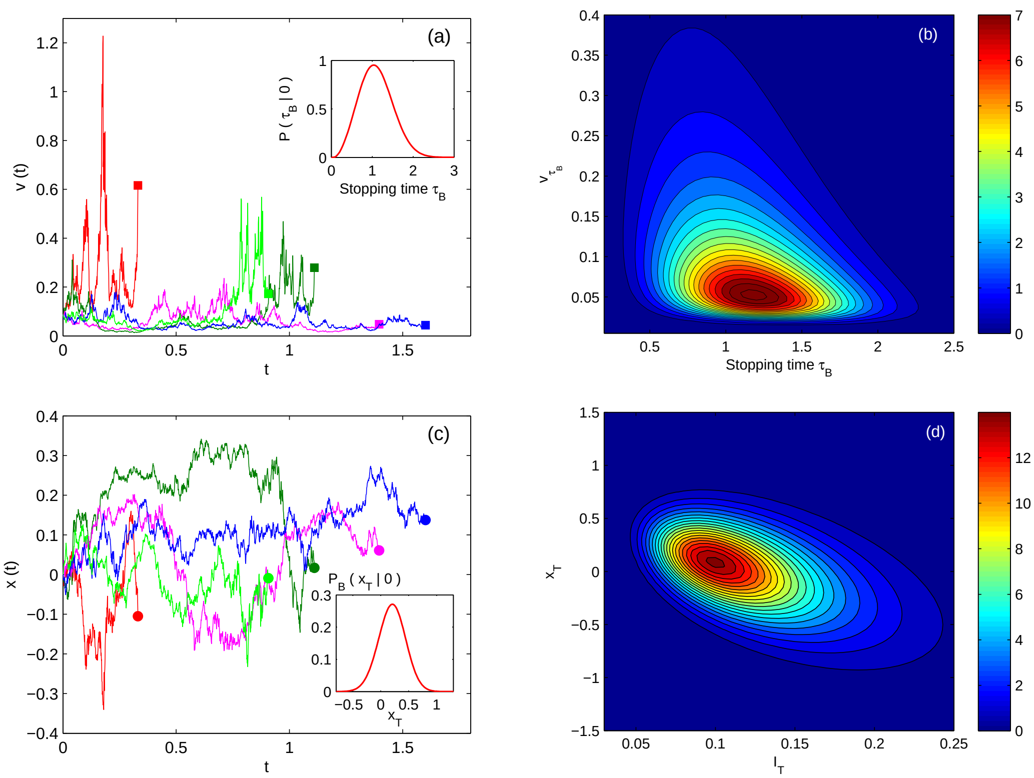


**Figure 4.2:** This figure shows several aspects of the time evolution of variables relevant for timer options under the 3/2 SV model. Panel (a) shows several simulated variance paths up to the point where the realized variance reached $\mathcal{B}$. Panel (c) shows corresponding log-return paths. The inset of panel (a) shows the probability distribution of the stopping time $\mathcal{T}_\mathcal{B}$. The inset of panel (c) shows the density $\mathcal{P}_\mathcal{B}\left(x_T \,|\, x_0\right)$ determined by expression (4.34). Panel (b) shows the joint probability distribution of the variance and the stopping time $\mathcal{P}\left(v_{\mathcal{T}_\mathcal{B}}, \mathcal{T}_\mathcal{B} | v_0, 0\right)$. Panel (d) shows the joint probability distribution of the log-return and the realized variance $\mathcal{P}\left(x_T, I_T | 0, 0\right)$. The parameters used here are: $v_0 = (0.295)^2, \kappa = 22.84, \theta = (0.4669)^2, \epsilon = 8.56, \mathcal{B} = v_0, r = 0.015, \rho = -0.5, T = 1.5$.

Integrating over $\zeta_T$ leads to $\mathcal{P}\left(\chi_T, I_T \,|\, \chi_0, 0\right)$:

$$\begin{aligned}
\mathcal{P}\left(\chi_T, I_T \,|\, \chi_0, 0\right) &= \int_0^\infty \mathcal{P}(\chi_T, \zeta_T, I_T \,|\, \chi_0, \zeta_0, 0)\, d\zeta_T \\
&= \int_{-\infty}^\infty \frac{dp}{2\pi}\, e^{ip\, I_T} \int_{-\infty}^{+\infty} \frac{dl}{2\pi}\, e^{il(x_T - rT)} \left(\frac{2}{\epsilon^2 N}\right)^M \\
&\quad \times \frac{\Gamma(\lambda+1-M)}{\Gamma(\lambda+1)}\, {}_1F_1\left(M; \lambda+1; -\frac{2}{\epsilon^2 N}\right), \qquad (4.64)
\end{aligned}$$

where

$$M = \frac{\lambda}{2} - \frac{\kappa}{\epsilon^2} - \frac{1}{2} - il\frac{\rho}{\epsilon}, \qquad (4.65)$$

$$N = \frac{2\sinh(\frac{\kappa\theta T}{2})}{\kappa\theta}\, e^{\frac{\kappa\theta T}{2}} v_0. \qquad (4.66)$$

Expression (4.64) agrees with expression (73) in (196).

According to (4.34), we have for the 3/2 model

$$\mathcal{P}_{\mathcal{B}}\left(x_T, T | x_0, 0\right) = \int_{-\infty}^{+\infty} \frac{dl}{2\pi}\, e^{il(x_T - rT)} \mathcal{F}(l), \qquad (4.67)$$

where

$$\mathcal{F}(l) = -i \int_{-\infty}^{\infty} \frac{dp}{2\pi} \frac{e^{ip\mathcal{B}} - 1}{p} \left(\frac{2}{\epsilon^2 N}\right)^M \frac{\Gamma(\lambda+1-M)}{\Gamma(\lambda+1)}\, {}_1F_1\left(M; \lambda+1; -\frac{2}{\epsilon^2 N}\right). \qquad (4.68)$$

The closed-form pricing formula for the finite time-horizon timer call options is derived by substituting (4.67) and (4.68) in expression (4.36).

### 4.2.2 The Heston model and the Kratzer potential

For Heston SV model (76), the model dynamics are written as:

$$dx(t) = \left(r - \frac{v(t)}{2}\right) dt + \sqrt{v(t)}\left(\sqrt{1-\rho^2} dW_1(t) + \rho dW_2(t)\right), \qquad (4.69)$$

$$dv(t) = \kappa\left(\theta - v\right) dt + \sigma\sqrt{v} dW_2(t). \qquad (4.70)$$

To relate this model to the general SV model (4.2), $\alpha\left(V\right)$ and $\beta\left(V\right)$ are given by

$$\alpha(V) = \kappa\left(\theta - V\right), \qquad (4.71)$$

$$\beta(V) = \sigma\sqrt{V}. \qquad (4.72)$$

From equation (4.14), we have the relation between $z(t)$ and $V(t)$:

$$z(t) = \frac{1}{\sigma} V(t). \tag{4.73}$$

thus the stopping time $\mathcal{T}_{\mathcal{B}}$ is a functional of $z(t)$:

$$\mathcal{T}_{\mathcal{B}} = \frac{1}{\sigma} \int_0^{\mathcal{B}} \frac{1}{z(t)} dt. \tag{4.74}$$

Plugging equations (4.70) and (4.2) into definition (4.18) gives

$$\int_0^{\mathcal{B}} \mathcal{A}\left(z(t)\right) dt = \frac{\kappa\theta}{\sigma} \mathcal{T}_{\mathcal{B}} - \frac{\kappa}{\sigma} \mathcal{B}, \tag{4.75}$$

therefore (written in original variable $v_0$)

$$\Upsilon\left(z_{\mathcal{B}}, \mathcal{T}_{\mathcal{B}}\right) = \rho\left(z_{\mathcal{B}} - \frac{v_0}{\sigma} - \frac{\kappa\theta}{\sigma}\mathcal{T}_{\mathcal{B}} + \frac{\kappa}{\sigma}\mathcal{B}\right) + r\mathcal{T}_{\mathcal{B}} - \frac{\mathcal{B}}{2}, \tag{4.76}$$

$$\mathcal{L}_{Tot}[\dot{z}, z] = \frac{1}{2}\dot{z}^2 + \frac{\lambda^2 - \frac{1}{4}}{2z^2} - \frac{\left(\lambda + \frac{1}{2}\right)\mu - \frac{ip}{\sigma}}{z} - \left(\lambda + \frac{1}{2}\right)\frac{\dot{z}}{z} + \mu\dot{z} + \frac{1}{2}\mu^2, \tag{4.77}$$

where

$$\lambda = \frac{\kappa\theta}{\sigma^2} - \frac{1}{2}, \qquad \mu = \frac{\kappa}{\sigma}. \tag{4.78}$$

The nontrivial terms of the total Lagrangian $\mathcal{L}_{Tot}[\dot{z}, z]$ manifest that $z(t)$ is subjected to a Kratzer potential. With the help of the path integral for Kratzer potential (155), derived in chapter 2, see expression (2.85), we obtain the joint propagator as:

$$\begin{aligned}
\mathcal{P}\left(z_{\mathcal{B}}, \mathcal{T}_{\mathcal{B}} \,|\, z_0, 0\right) &= \int \mathcal{D}z(t)\, \delta\left(\mathcal{T}_{\mathcal{B}} - \frac{1}{\sigma}\int_0^{\mathcal{B}} \frac{1}{z(t)} dt\right) e^{-\int_0^{\mathcal{B}} \mathcal{L}[z,\dot{z}] dt} \\
&= \left(\frac{z_{\mathcal{B}}}{z_0}\right)^{\lambda + \frac{1}{2}} e^{-\mu(z_{\mathcal{B}} - z_0) - \frac{1}{2}\mu^2\mathcal{B}} \int_{-\infty}^{\infty} \frac{dp}{2\pi}\, e^{ip\mathcal{T}_{\mathcal{B}}} \\
&\quad \times \int \mathcal{D}z(t)\, e^{-\int_0^{\mathcal{B}}\left[\frac{1}{2}\dot{z}^2 + \frac{\lambda^2 - \frac{1}{4}}{2z^2} - \frac{\left(\lambda+\frac{1}{2}\right)\mu - \frac{ip}{\sigma}}{z}\right] dt} \\
&= \frac{\sigma}{2}\frac{z_{\mathcal{B}}^{\lambda+1}}{z_0^{\lambda}}\, e^{-\mu(z_{\mathcal{B}} - z_0) - \frac{1}{2}\mu^2\mathcal{B} + \left(\lambda + \frac{1}{2}\right)\mu\sigma\mathcal{T}_{\mathcal{B}}} \int_0^{\infty} \frac{d\Phi_I}{\pi} \\
&\quad \times \mathrm{Re}\left[\begin{array}{l} e^{\Phi\mathcal{B}}\, e^{-\sqrt{2\Phi}(z_{\mathcal{B}} + z_0)\coth\left(\sqrt{\frac{\Phi}{2}}\sigma\mathcal{T}_{\mathcal{B}}\right)} \\ \times \frac{2\sqrt{2\Phi}}{\sinh\left(\sqrt{\frac{\Phi}{2}}\sigma\mathcal{T}_{\mathcal{B}}\right)}\, I_{2\lambda}\left(\frac{2\sqrt{2\Phi}\sqrt{z_{\mathcal{B}} z_0}}{\sinh\left(\sqrt{\frac{\Phi}{2}}\sigma\mathcal{T}_{\mathcal{B}}\right)}\right) \end{array}\right].
\end{aligned} \tag{4.79}$$

Again, plugging the expressions (4.76) and (4.79) into formula (4.26) yields the closed-form pricing formula for the perpetual timer call options under the Heston model. Expression (4.79) has a clear meaning as joint transition probability density function which illustrates the conciseness of physics; path integration allows to derive expression (4.79) without applying any previous results of Bessel processes as done in (185).

Li (185) computed the risk-neutral expected maturity in expression (5.2) by doing two numerical integrals. Actually, we can derive the marginal propagator of the stopping time $\mathcal{T}_{\mathcal{B}}$ by integrating over all possible $z_{\mathcal{B}}$ as follows

$$
\begin{aligned}
&\mathcal{P}\left(\mathcal{T}_{\mathcal{B}}\,|\,0\right)\\
=&\int_0^\infty \mathcal{P}\left(z_{\mathcal{B}},\mathcal{T}_{\mathcal{B}}\,|\,z_0,0\right)dz_{\mathcal{B}}\\
=&\sigma\, e^{-\frac{1}{2}\mu^2\mathcal{B}+\left(\lambda+\frac{1}{2}\right)\mu\sigma\mathcal{T}_{\mathcal{B}}}\int_0^\infty \frac{d\Phi_I}{\pi}\mathrm{Re}\left[\begin{array}{c}
\exp\left\{\Phi\mathcal{B}+\frac{\left(\mu^2-2\Phi\right)z_0}{\mu+\sqrt{2\Phi}\coth\left(\sqrt{\frac{\Phi}{2}}\sigma\mathcal{T}_{\mathcal{B}}\right)}\right\}\\
\times\frac{\left(\frac{\sqrt{2\Phi}}{\sinh\left(\sqrt{\frac{\Phi}{2}}\sigma\mathcal{T}_{\mathcal{B}}\right)}\right)^{2\lambda+1}}{\left(\mu+\sqrt{2\Phi}\coth\left(\sqrt{\frac{\Phi}{2}}\sigma\mathcal{T}_{\mathcal{B}}\right)\right)^{2\lambda+2}}\\
\times\left(2\lambda+1+\frac{\left(\frac{\sqrt{2\Phi}}{\sinh\left(\sqrt{\frac{\Phi}{2}}\sigma\mathcal{T}_{\mathcal{B}}\right)}\right)^{2}z_0}{\mu+\sqrt{2\Phi}\coth\left(\sqrt{\frac{\Phi}{2}}\sigma\mathcal{T}_{\mathcal{B}}\right)}\right)
\end{array}\right].
\end{aligned}
\tag{4.80}
$$

For the calculation of $\mathcal{P}\left(x_T, I_T|0,0\right)$, we follow the derivation in (115). Substitutions

$$\chi(t) = x-\frac{\rho}{\sigma}\left(v-\kappa\theta t\right)-rt, \tag{4.81}$$

$$\zeta(t) = \sqrt{v}, \tag{4.82}$$

give two uncorrelated processes:

$$d\chi(t) = \left(\frac{\rho\kappa}{\sigma}-\frac{1}{2}\right)v\,dt+\sqrt{v}\sqrt{1-\rho^2}dW_1(t), \tag{4.83}$$

$$d\zeta(t) = \left[\frac{\kappa\theta-\frac{\sigma^2}{4}}{2\zeta}-\frac{\kappa}{2}\zeta\right]dt+\frac{\sigma}{2}dW_2(t). \tag{4.84}$$

The corresponding Lagrangians are:

$$\begin{aligned} \mathcal{L}\left[\dot{\chi},\chi,v\right] &= \frac{1}{2v\left(1-\rho^2\right)}\left[\dot{\chi}-\left(\frac{\rho\kappa}{\sigma}-\frac{1}{2}\right)v\right]^2, &(4.85)\\ \mathcal{L}[\dot{\zeta},\zeta] &= \mathcal{L}_1[\dot{\zeta},\zeta]+\mathcal{L}_2[\dot{\zeta},\zeta], &(4.86)\end{aligned}$$

where

$$\begin{aligned} \mathcal{L}_1\left[\dot{\zeta},\zeta\right] &= \frac{2}{\sigma^2}\dot{\zeta}^2+\frac{(\kappa\theta-\frac{\sigma^2}{4})(\kappa\theta-\frac{3\sigma^2}{4})}{2\,\sigma^2\zeta^2}+\frac{\kappa^2}{2\sigma^2}\zeta^2, &(4.87)\\ \mathcal{L}_2\left[\dot{\zeta},\zeta\right] &= -\left(\frac{2\kappa\theta}{\sigma^2}-\frac{1}{2}\right)\frac{\dot{\zeta}}{\zeta}+\frac{2\kappa}{\sigma^2}\zeta\dot{\zeta}-\frac{\kappa^2\theta}{\sigma^2}. &(4.88)\end{aligned}$$

Since $\chi$ is independent from $\zeta$, we similarly have the joint propagator of the dynamics of $\chi$, $\zeta$ and $I$:

$$\begin{aligned} &\mathcal{P}(\chi_T,\zeta_T,I_T\,|\,\chi_0,\zeta_0,0)\\ &= \int\mathcal{D}\zeta(t)\,\delta\left(I_T-\int_0^T v(t)\,dt\right)\,e^{-\int_0^T\mathcal{L}[\dot{\zeta},\zeta]dt}\int\mathcal{D}\chi(t)\,e^{-\int_0^T\mathcal{L}[\dot{\chi},\chi,v]dt}\\ &= \left(\frac{\zeta_T}{\zeta_0}\right)^{\frac{2\kappa\theta}{\sigma^2}-\frac{1}{2}}\;e^{-\frac{\kappa}{\sigma^2}(\zeta_T^2-\zeta_0^2)+\frac{\kappa^2\theta}{\sigma^2}T}\int_{-\infty}^{\infty}\frac{dp}{2\pi}\,e^{ip\,I_T}\int_{-\infty}^{+\infty}\frac{dl}{2\pi}\,e^{il\left[x_T+\frac{\rho\kappa\theta}{\sigma}T-rT\right]}\,e^{-il\frac{\rho}{\sigma}\left(\zeta_T^2-\zeta_0^2\right)}\\ &\times\int\mathcal{D}\zeta(t)\,e^{-\int_0^T\left[\mathcal{L}_1[\dot{\zeta},\zeta]+\left(il\left(\frac{\rho\kappa}{\sigma}-\frac{1}{2}\right)+\frac{\left(1-\rho^2\right)l^2}{2}+ip\right)\zeta^2\right]dt}, \qquad (4.89)\end{aligned}$$

where the path integral for the radial harmonic oscillator potential is given by expression (2.63):

$$\frac{4\omega\sqrt{\zeta_T\zeta_0}}{\sigma^2\,\sinh(\omega T)}\,e^{-\frac{2\omega}{\sigma^2}\left(\zeta_T^2+\zeta_0^2\right)\coth(\omega T)}\,I_{\frac{2\kappa\theta}{\sigma^2}-1}\left(\frac{4\omega\,\zeta_T\zeta_0}{\sigma^2\,\sinh(\omega T)}\right), \qquad (4.90)$$

where

$$\omega=\frac{\sigma}{2}\sqrt{\frac{\kappa^2}{\sigma^2}+(1-\rho^2)\,l^2+il\left(\frac{2\rho\kappa}{\sigma}-1\right)+2ip}. \qquad (4.91)$$

Integrating over $\zeta_T$ leads to $\mathcal{P}\left(\chi_T,I_T\,|\,\chi_0,0\right)$:

$$\begin{aligned} \mathcal{P}\left(\chi_T,I_T\,|\,\chi_0,0\right) &= \int_0^{\infty}\mathcal{P}(x_T,\zeta_T,I_T\,|\,x_0,\zeta_0,0)\,d\zeta_T\\ &= e^{\frac{\kappa}{\sigma^2}v_0+\frac{\kappa^2\theta}{\sigma^2}T}\int_{-\infty}^{\infty}\frac{dp}{2\pi}\,e^{ip\,I_T}\int_{-\infty}^{\infty}\frac{dl}{2\pi}\,e^{il(x_T-rT)}\,e^{il\frac{\rho}{\sigma}(\kappa\theta T+v_0)}\\ &\quad\times N^{\frac{2\kappa\theta}{\sigma^2}}\,e^{-\frac{2\omega(\cosh(\omega T)-N)}{\sigma^2\sinh(\omega T)}v_0}, \qquad (4.92)\end{aligned}$$

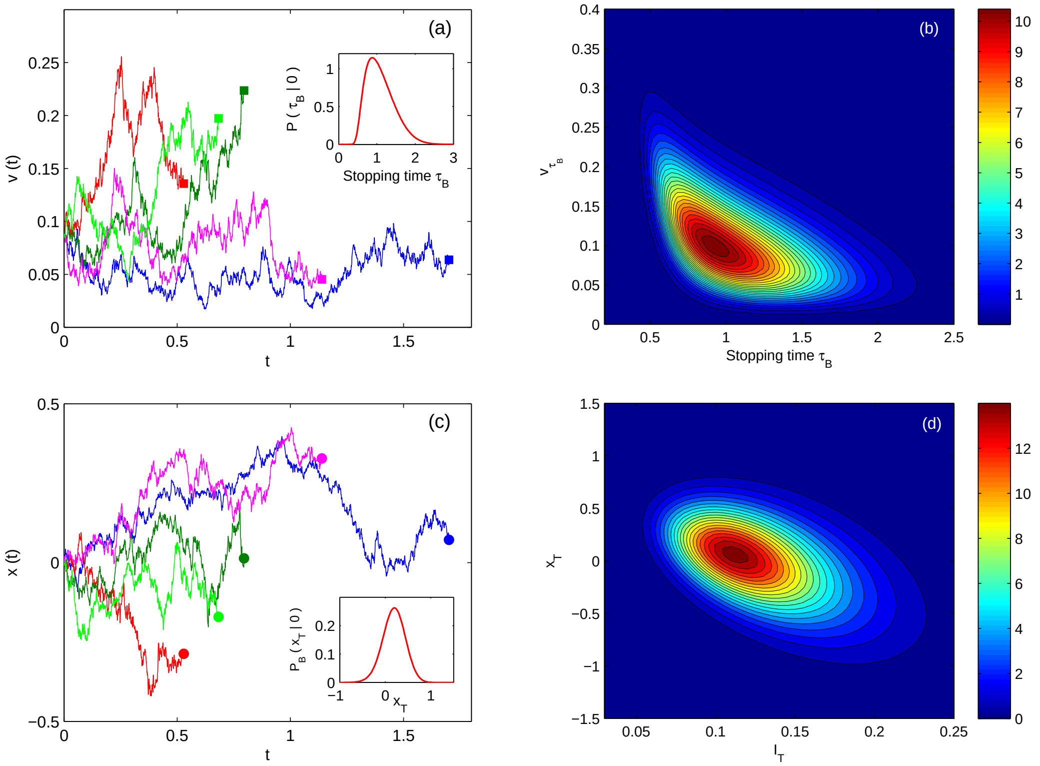

**Figure 4.3:** This figure is similar to Figure 4.2, but now for the Heston SV model. The parameters used here are: $v_0 = 0.087, \kappa = 2, \theta = 0.09, \sigma = 0.375, \mathcal{B} = v_0, r = 0.015, \rho = -0.5, T = 1.5$.

where

$$N = \left( \cosh(\omega T) + \frac{\kappa + il\rho\sigma}{2\omega} \sinh(\omega T) \right)^{-1}. \tag{4.93}$$

Note the similarity of expression (4.92) with the result obtained in (193).

According to (4.34), we have for the Heston model

$$\mathcal{P}_{\mathcal{B}}\left(x_T \,|\, x_0\right) = \int_{-\infty}^{+\infty} \frac{dl}{2\pi}\, e^{il(x_T - rT)} \mathcal{F}(l), \tag{4.94}$$

where

$$\mathcal{F}(l) = -i\, e^{\frac{\kappa}{\sigma^2} v_0 + \frac{\kappa^2 \theta}{\sigma^2} T} \int_{-\infty}^{\infty} \frac{dp}{2\pi} \frac{e^{ip\mathcal{B}} - 1}{p}\, e^{il\frac{\rho}{\sigma}(\kappa\theta T + v_0)} N^{\frac{2\kappa\theta}{\sigma^2}}\, e^{-\frac{2\omega(\cosh(\omega T) - N)}{\sigma^2 \sinh(\omega_2 T)} v_0}, \tag{4.95}$$

with which we obtain the closed-form pricing formula for the finite time-horizon timer call options according to formula (4.36).

## 4.3 Pricing results and discussion

In the previous sections explicit formulas concerning timer options are derived for the 3/2 and the Heston model. The analytical tractability of these formulas is demonstrated by Figures 4.2 and 4.3 and Tables 4.1 and 4.2. Figure 4.2 as well as Table 4.1 are devoted to the 3/2 model and Figure 4.3 as well as Table 4.2 to the Heston model. For the 3/2 model the parameters are based on reference (193), where they are calibrated on market prices of S&P500 European options to guarantee the relevance of these parameters. The parameters for the Heston model were chosen such that the two models are comparable.

The two tables compare timer option prices calculated with the formulas of the previous sections with prices obtained by Monte Carlo simulations. Results for both the perpetual and the finite time horizon timer option are presented for several strikes and correlation values. For all the Monte Carlo simulations presented here, we used 20 million samples and 3200 time steps per year. During the simulation for the Heston model, to avoid the negative values for variance, we set these to zero if we encounter negative values. The relative errors between the exact and the simulated prices are always less than 0.1%, and the exact prices are always within the corresponding simulated values' 95% confidence intervals, i.e. [mean - 1.96 standard error, mean + 1.96 standard error], confirming our formulas. More discussions about the Monte Carlo simulation techniques related to the 3/2 and the Heston stochastic models can be found, among other, in references (197, 198, 199).

Although the prices of the timer option presented in these tables vary only slightly as a function of the correlation coefficient $\rho$, the timer option does have different features for different correlation values. This can be seen in Figures 4.2 and 4.3. Panel (a) shows possible realizations of the variance up to the point where the realized variance reached $\mathcal{B}$. Panel (c) shows the corresponding log-returns. In these figures we used a negative correlation. As a consequence, paths with a low log-return are more likely to have a high volatility and the corresponding option will probably be exercised sooner than an option with a high log-return. This behavior is also seen in the inset of panel (c). This inset shows the density given by formula (4.34) when the maximum expiry time $T$ reached 1.5. Recall that this

**Table 4.1:** Comparison of the analytical and the Monte Carlo simulation values, indicated by MC with standard errors given in parentheses, for both perpetual ($\mathcal{C}_{Perp}$) and finite time-horizon ($\mathcal{C}_{Fini}$) timer call option prices under the 3/2 model. The columns indicated by RE show the relative errors (in %) between the analytical and simulated prices. Parameters used here are: $v_0 = (0.295)^2, \kappa = 22.84, \theta = (0.4669)^2, \epsilon = 8.56, \mathcal{B} = v_0, r = 0.015, T = 1.5$.

| $K$ | $\rho$ | $\mathcal{C}_{Perp}$ | | | $\mathcal{C}_{Fini}$ | | |
|---|---|---|---|---|---|---|---|
| | | Analytic | MC | RE(%) | Analytic | MC | RE(%) |
| | - 0.5 | 17.8064 | 17.8128 (0.0076) | -0.0359 | 17.6813 | 17.6790 (0.0073) | 0.0130 |
| 90 | 0 | 17.7046 | 17.7129 (0.0075) | -0.0469 | 17.5385 | 17.5510 (0.0075) | -0.0712 |
| | 0.5 | 17.5839 | 17.5853 (0.0075) | -0.0080 | 17.4260 | 17.4301 (0.0074) | -0.0235 |
| | - 0.5 | 12.5780 | 12.5784 (0.0067) | -0.0032 | 12.4089 | 12.3998 (0.0064) | 0.0734 |
| 100 | 0 | 12.4619 | 12.4683 (0.0066) | -0.0513 | 12.2780 | 12.2890 (0.0065) | -0.0895 |
| | 0.5 | 12.3300 | 12.3231 (0.0065) | 0.0560 | 12.2104 | 12.2032 (0.0065) | 0.0590 |
| | - 0.5 | 8.6518 | 8.6414 (0.0058) | 0.0486 | 8.4381 | 8.4301 (0.0054) | 0.0949 |
| 110 | 0 | 8.5339 | 8.5388 (0.0056) | -0.0574 | 8.3531 | 8.3611 (0.0055) | -0.0957 |
| | 0.5 | 8.4026 | 8.3943 (0.0056) | 0.0989 | 8.3229 | 8.3153 (0.0055) | 0.0914 |

**Table 4.2:** This table is similar to Table 4.1, but now for the Heston SV model. Parameters used here are: $v_0 = 0.087, \kappa = 2, \theta = 0.09, \sigma = 0.375, \mathcal{B} = v_0, r = 0.015, \rho = -0.5, T = 1.5$.

| $K$ | $\rho$ | $\mathcal{C}_{Perp}$ | | | $\mathcal{C}_{Fini}$ | | |
|---|---|---|---|---|---|---|---|
| | | Analytic | MC | RE(%) | Analytic | MC | RE(%) |
| | - 0.5 | 17.8095 | 17.7948 (0.0107) | 0.0826 | 17.6914 | 17.6851 (0.0071) | 0.0356 |
| 90 | 0 | 17.7249 | 17.7232 (0.0105) | 0.0096 | 17.5351 | 17.5330 (0.0074) | 0.0120 |
| | 0.5 | 17.6263 | 17.6146 (0.0105) | 0.0664 | 17.4627 | 17.4680 (0.0074) | -0.0303 |
| | - 0.5 | 12.5789 | 12.5668 (0.0094) | 0.0963 | 12.4034 | 12.4010 (0.0062) | 0.0194 |
| 100 | 0 | 12.4772 | 12.4763 (0.0092) | 0.0072 | 12.2675 | 12.2678 (0.0065) | -0.0024 |
| | 0.5 | 12.3691 | 12.3586 (0.0092) | 0.0842 | 12.2426 | 12.2464 (0.0065) | -0.0310 |
| | - 0.5 | 8.6515 | 8.6412 (0.0080) | 0.1192 | 8.4206 | 8.4218 (0.0053) | -0.0142 |
| 110 | 0 | 8.5449 | 8.5446 (0.0078) | 0.0035 | 8.3393 | 8.3405 (0.0055) | -0.0144 |
| | 0.5 | 8.4393 | 8.4317 (0.0078) | 0.0890 | 8.3522 | 8.3542 (0.0055) | -0.0239 |

is the distribution of log-returns whose realized variance has not yet reached $\mathcal{B}$. Due to the negative correlation, paths with a low log-return are more likely to have reached $\mathcal{B}$ and will therefore less likely contribute to this distribution than paths with a high log-return. Therefore this distribution is clearly shifted to the right. Panel (d) shows the joint density of the log-return $x_T$ and the realized variance $I_T$ when $T$ equals 1.5 and also illustrates this behavior.

Tables 4.1 and 4.2 illustrate that the prices for timer options are quite similar for the two SV models. Nevertheless there are important differences between the two models concerning timer options. This is illustrated by the upper panels of Figures 4.2 and 4.3. As already mentioned, panel (a) shows several possible time evolutions of the variance. The inset of this panel shows the probability distribution of the stopping time $\mathcal{T}_{\mathcal{B}}$. Panel (b) shows the joint density of the variance and the stopping time, which is useful for an intuitive understanding of the time evolution of the underlying processes. The explicit form of this density is not included in the text because it is not needed to calculate prices and because it can easily be derived from expression (4.30). For the 3/2 model, the probability that the variance reaches large values is larger than for the Heston model, while the probability that the variance reaches very small values is smaller than for the Heston model. Therefore the probability that the timer option will be exercised very fast is larger for the 3/2 model than for the Heston model. On the other hand for the Heston model there is a larger probability than for the 3/2 model that the timer option will only be exercised after a long time.

## 4.4 Conclusion

In this chapter we present a method to price both the perpetual and the finite time-horizon timer option for a general SV model. Pricing of such options is related to first passage time problems in that the stopping time for the option is determined by a boundary on a cumulative stochastic process. The method proposed here is based on the Duru-Kleinert time transformation and the path integral framework. Furthermore we discuss the conditions a SV model has to satisfy in order to be able to derive closed-form pricing formulas. These general results are then applied to derive closed-form formulas for the Heston and the 3/2 SV model. For the 3/2 model this involves the solution of the Morse potential, for the Heston model the Kratzer potential needs to be solved. Finally, our closed-form pricing formulas are shown to be computationally tractable and are validated by Monte Carlo simulation.

# 5

# Applications of path integration over conditioned paths

In expression (4.21), we have used an important technique in the path integral framework. More specifically, denote the propagator for a stochastic process $z(t)$ of the terminal state $z_T$ at expiration $T$ conditional on the initial state $z_0$ at time $t = 0$ by $\mathcal{P}\left(z_T, T|z_0, 0\right)$, that is:

$$\mathcal{P}\left(z_T, T|z_0, 0\right) = \int \mathcal{D}z(t)\, e^{-\int_0^T \mathcal{L}[\dot{z},z]dt}, \tag{5.1}$$

where $\mathcal{L}[\dot{z}, z]$ is its Lagrangian. We then define a function by

$$I(t) = \int_0^t f\left(z(t')\right) dt', \tag{5.2}$$

where $f\left(z(t)\right)$ is a function of $z(t)$. One interesting question is how to compute the joint propagator $\mathcal{P}\left(z_T, I_T, T|z_0, I_0, 0\right)$ of the joint dynamics $(z(t), I(t))$?

The key step to treat the joint propagator $\mathcal{P}\left(z_T, I_T, T|z_0, I_0, 0\right)$ within the path integral framework is to partition all pathes of $z(t)$ evolving from $z_0$ at time $t = 0$ to $z_T$ at time $T$ into (infinite) many subsets such that the quantity $\int_0^T f\left(z(t')\right) dt'$ achieved in each subset equals the same value $I_T$. Finally summing over all these possible subsets, we have the joint propagator. This technique was proposed by Feynman and Kleinert to reduce many complex path integrals to simple ordinary ones (191), and later was extended to a systematic and uniformly convergent variational perturbation theory in quantum mechanics (100, 200). Recently it was applied to the pricing of geometric Asian option under the Black-Scholes model (125, 201), and of course also to the pricing of timer options (145). The path integral representation of the joint propagator is given by:

$$\mathcal{P}\left(z_T, I_T, T|z_0, I_0, 0\right) = \int \mathcal{D}z(t)\delta\left(I_T - \int_0^T f\left(z(t)\right)dt\right) e^{-\int_0^T \mathcal{L}[\dot{z},z,t]dt}. \tag{5.3}$$

where $\delta(\cdot)$ is the delta function. Effectively, this propagator represents a sum over only those paths that satisfy a certain condition, and as such they appear in many problems related to exotic, path-dependent options. In this chapter, we will explore several of these applications, as well as an application outside of finance, relating to radioactive decay. These results are part of (unpublished) internal work notes, some of which are being prepared as manuscripts for publication.

## 5.1 Continuous arithmetic and harmonic Asian option under the Black-Scholes model

A quick application of the preceding technique is the pricing of Asian options under the Black-Scholes model. Asian options are path-dependent, in that the payoff function contains a (geometric, harmonic or arithmetic) average of the price of the underlying asset during the lifetime of the option. Thus, even for paths that end up in at the same final value, the option payoff can be different if a different route is taken. To price such options, the set of all paths needs to be partitioned in subsets containing paths with the same average. Within each set, the option can be calculated just like a path-independent option. The results then need to be averaged over the different partitions. As an example we will look at Asian arithmetic and harmonic call options. The pricing of geometric Asian options is relatively easier than the other two.

In the risk-neutral world, the call option prices of a continuous arithmetic and harmonic Asian option under the Black-Scholes model, with risk-neutral interest rate $r$, time to maturity $T$ and strike price $K$, denoted by $\mathcal{C}_A\left(K,T\right)$ and $\mathcal{C}_H\left(K,T\right)$

respectively, are given by:

$$\begin{aligned}\mathcal{C}_A(K,T) &= e^{-rT}\int_0^\infty \max\left(\frac{1}{T}A_T - K, 0\right)\mathcal{P}(A_T, T|A_0, 0)\, dA_T, &(5.4)\\ \mathcal{C}_H(K,T) &= e^{-rT}\int_0^\infty \max(H_T T - K, 0)\,\mathcal{P}(H_T, T|H_0, 0)\, dH_T, &(5.5)\end{aligned}$$

where

$$\begin{aligned}A(t) &= \int_0^t S(t')dt', \quad A_0 = A(0), \quad A_T = A(T), &(5.6)\\ H(t) &= \frac{1}{\int_0^t \frac{1}{S(t')}dt'}, \quad H_0 = H(0), \quad H_T = H(T), &(5.7)\\ dS(t) &= rS(t)dt + \sigma S(t)dW(t), &(5.8)\end{aligned}$$

and $\mathcal{P}(A_T, T|A_0, 0)$ and $\mathcal{P}(H_T, T|H_0, 0)$ are the propagator of $A(t)$ and $H(t)$ respectively. Let us derive the propagator $\mathcal{P}(A_T, T|A_0, 0)$ first. As usual, we make a substitution $x(t) = \ln S(t)$ for calculation convenience, thus $S(t) = e^{x(t)}$ and $A_T = \int_0^T e^{x(t)}dt$. Therefore $\mathcal{P}(A_T, T|A_0, 0)$ can be expressed as a marginal propagator of the joint propagator, say $\mathcal{P}(x_T, A_T, T|x_0, A_0, 0)$, for the joint dynamics $(x(t), A(t))$. Now we can apply the technique mentioned at the beginning of this chapter. The stochastic differential equation and the Lagrangian of $x(t)$ are given by:

$$\begin{aligned}dx(t) &= \left(r - \frac{\sigma^2}{2}\right)dt + \sigma dW(t), &(5.9)\\ \mathcal{L}[\dot{x}, x] &= \frac{1}{2\sigma^2}\left[\dot{x} - \left(r - \frac{\sigma^2}{2}\right)\right]^2. &(5.10)\end{aligned}$$

Thus the joint propagator of the joint dynamics $(x(t), A(t))$ can be expressed as:

$$\begin{aligned}&\mathcal{P}(x_T, A_T, T|x_0, A_0, 0) = \int \mathcal{D}x(t)\delta\left(A_T - \int_0^T e^{x(t)}dt\right)e^{-\int_0^T \mathcal{L}[\dot{x},x]dt}\\ &= \exp\left\{-\frac{(r-\sigma^2/2)^2}{2\sigma^2}T + \left(\frac{r}{\sigma^2} - \frac{1}{2}\right)(x_T - x_0)\right\}\\ &\quad\times\int_{-\infty}^\infty \frac{dp}{2\pi}e^{ipA_T}\int \mathcal{D}x(t)\exp\left\{-\int_0^T\left[\frac{\dot{x}^2}{2\sigma^2} + ip\,e^{x(t)}\right]dt\right\}. \qquad (5.11)\end{aligned}$$

The remaining path integral is the one for Liouville potential, see (2.96):

$$
\begin{aligned}
&\int_{-\infty}^{\infty} \frac{dp}{2\pi}\, e^{ipA_T} \int \mathcal{D}x(t) \exp\left\{-\int_0^T \left[\frac{\dot{x}^2}{2\sigma^2} + ip\, e^{x(t)}\right] dt\right\} \\
= &\int_{-\infty}^{\infty} \frac{dp}{2\pi}\, e^{ipA_T} \frac{2}{\sigma^2} \int_{-\infty}^{\infty} \frac{d\Phi_I}{2\pi}\, e^{\Phi T} \int_0^{\infty} \frac{dl}{l}\, e^{-(e^{x_0}+e^{x_T})l - ip\frac{2}{\sigma^2 l}}\, I_{2\sqrt{\frac{2}{\sigma^2}\Phi}} \left(2\, e^{\frac{x_0+x_T}{2}} l\right) \\
= &\int_{-\infty}^{\infty} \frac{d\Phi_I}{2\pi}\, e^{\Phi T} \frac{2}{\sigma^2 A_T}\, e^{-\frac{2}{\sigma^2 A_T}(e^{x_0}+e^{x_T})}\, I_{2\sqrt{\frac{2}{\sigma^2}\Phi}} \left(\frac{4\, e^{\frac{x_0+x_T}{2}}}{\sigma^2 A_T}\right). \qquad (5.12)
\end{aligned}
$$

with $I_{\cdot}(\cdot)$ the modified Bessel function of the first kind. Therefore, we obtain the joint propagator:

$$
\begin{aligned}
\mathcal{P}\left(x_T, A_T, T | x_0, A_0, 0\right) = &\, e^{-\frac{\left(r-\frac{\sigma^2}{2}\right)^2}{2\sigma^2} T + \left(\frac{r}{\sigma^2}-\frac{1}{2}\right)(x_T - x_0)} \int_0^{\infty} \frac{d\Phi_I}{\pi} \\
&\times \mathrm{Re}\left[e^{\Phi T} \frac{2}{\sigma^2 A_T}\, e^{-\frac{2}{\sigma^2 A_T}(e^{x_0}+e^{x_T})}\, I_{2\sqrt{\frac{2}{\sigma^2}\Phi}} \left(\frac{4\, e^{\frac{x_0+x_T}{2}}}{\sigma^2 A_T}\right)\right], \qquad (5.13)
\end{aligned}
$$

With the help of the identity that ($\mathrm{Re}\,(\alpha+\nu) > 0$)

$$
\begin{aligned}
&\int_0^{\infty} x^{\alpha-1}\, e^{-px^2}\, I_{\nu}\left(cx\right) dx \\
= &\; 2^{-\nu-1} c^{\nu} p^{-(\alpha+\nu)/2} \frac{\Gamma\left((\alpha+\nu)/2\right)}{\Gamma\left(\nu+1\right)}\, e^{\frac{c^2}{4p}}\, {}_1F_1\left(\frac{\nu-\alpha}{2}+1; \nu+1; -\frac{c^2}{4p}\right), \qquad (5.14)
\end{aligned}
$$

the integral over $x_T$ can be done analytically, leading to the marginal propagator $\mathcal{P}\left(A_T, T | A_0, 0\right)$:

$$
\begin{aligned}
\mathcal{P}\left(A_T, T | A_0, 0\right) &= \int_{-\infty}^{\infty} \mathcal{P}\left(x_T, A_T, T | x_0, A_0, 0\right) dx_T \\
&= \frac{1}{S_0}\, e^{-\frac{\left(r-\frac{\sigma^2}{2}\right)^2}{2\sigma^2} T} \int_0^{\infty} \frac{d\Phi_I}{\pi} \mathrm{Re}\left[e^{\Phi T} \left(\frac{2S_0}{\sigma^2 A_T}\right)^{\mathcal{M}} \frac{\Gamma\left(\mathcal{N}-\mathcal{M}\right)}{\Gamma\left(\mathcal{N}\right)}\right. \\
&\quad \left.\times\; {}_1F_1\left(\mathcal{M}; \mathcal{N}; -\frac{2S_0}{\sigma^2 A_T}\right)\right], \qquad (5.15)
\end{aligned}
$$

where $\Gamma(\cdot)$ is the Euler gamma function, ${}_1F_1\left(\cdot;\cdot;\cdot\right)$ is the confluent hypergeometric function and

$$
\mathcal{M}\left(\Phi\right) = \sqrt{\frac{2}{\sigma^2}\Phi} - \left(\frac{r}{\sigma^2} - \frac{1}{2}\right) + 1, \qquad (5.16)
$$

$$
\mathcal{N}\left(\Phi\right) = 2\sqrt{\frac{2}{\sigma^2}\Phi} + 1, \qquad (5.17)
$$

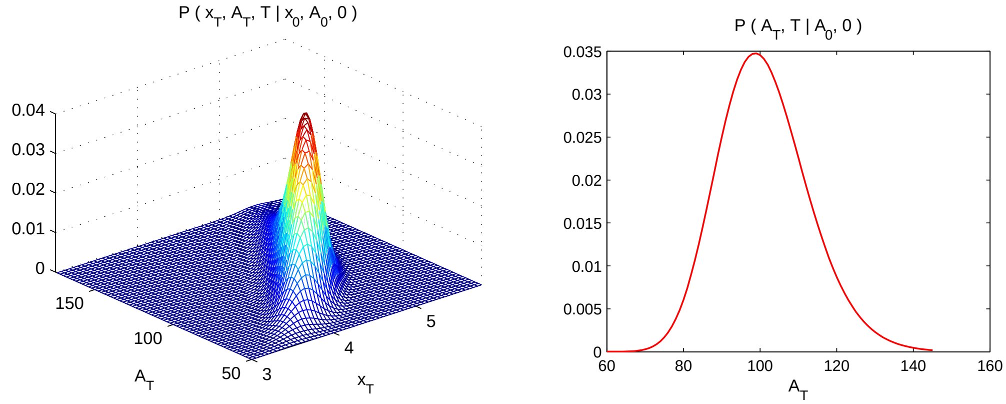


**Figure 5.1:** This figure shows the joint propagator $\mathcal{P}(x_T, A_T, T|x_0, A_0, 0)$ (left), see (5.13), as well as the marginal propagator $\mathcal{P}(A_T, T|A_0, 0)$ (right), see (5.15). The parameter values used here are $S_0 = 100$, $r = 2.25\%$, $\sigma = 0.36$, $T = 1$.

with the restriction of the real part of variable $\Phi$:

$$\Phi_R > \frac{\sigma^2}{2}\left(\frac{\kappa}{\sigma^2} + \frac{1}{2}\right)^2. \tag{5.18}$$

This propagator is shown in Figure 5.1, and with it the call option price can now be straightforwardly calculated from expression (5.4).

Now we move on to the calculation of $\mathcal{P}(H_T, T|H_0, 0)$. The idea is to introduce a new variable

$$Y(t) = \frac{1}{H(t)} = \int_0^t \frac{1}{S(u)} du, \tag{5.19}$$

then the propagator of $Y(t)$, denoted by $\mathcal{P}(Y_T, T|Y_0, 0)$, is related to the propagator of $H(t)$ by the following expression:

$$\mathcal{P}(H_T, T|H_0, 0) = \left|\frac{dY(t)}{dH(t)}\right|_{t=T} \mathcal{P}(Y_T, T|Y_0, 0) = \frac{1}{H_T^2}\mathcal{P}(Y_T, T|Y_0, 0)\Big|_{H_T}. \tag{5.20}$$

So we only need to investigate the propagator $\mathcal{P}(Y_T, T|Y_0, 0)$. Let $y(t) = -\ln S(t)$ $= -x(t)$, then

$$Y_T = \int_0^T e^{y(t)} dt, \tag{5.21}$$

$$dy(t) = -dx(t) = -\left(r - \sigma^2/2\right) dt - \sigma dW(t). \tag{5.22}$$

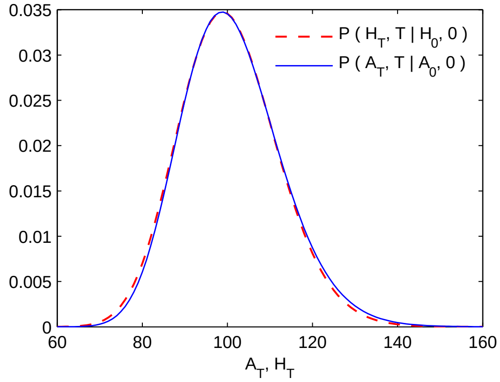


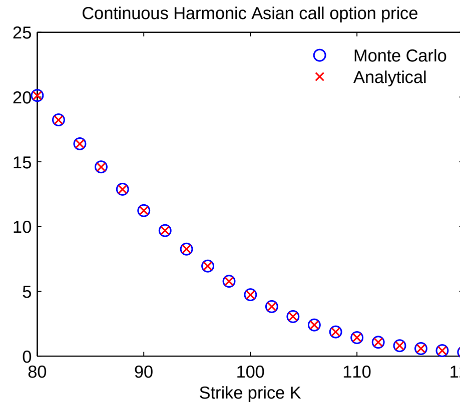


**Figure 5.2:** The left panel gives the comparison of $\mathcal{P}(H_T, T|H_0, 0)$ for the harmonic Asian option, see (5.25), and $\mathcal{P}(A_T, T|A_0, 0)$ for the arithmetic Asian option, see (5.15). The right panel shows that our analytical harmonic Asian call option prices fit the Monte Carlo results well. The parameter values used here are $S_0 = 100$, $r = 2.25\%$, $\sigma = 0.2$, $T = 1$.

Comparing (5.22) with (5.9), we see that $\mathcal{P}(Y_T, T|Y_0, 0)$ can easily be obtained by changing the signs of the terms $\left(r - \frac{\sigma^2}{2}\right)$ and $\sigma$ in expression (5.15):

$$\begin{aligned}\mathcal{P}(Y_T, T|Y_0, 0) \quad &= \quad S_0\, e^{-\frac{\left(r-\frac{\sigma^2}{2}\right)^2}{2\sigma^2}T} \int_0^\infty \frac{d\Phi_I}{\pi} \mathrm{Re}\left[ e^{\Phi T} \left(\frac{2}{S_0\sigma^2 Y_T}\right)^{\mathcal{M}_2} \frac{\Gamma(\mathcal{N} - \mathcal{M}_2)}{\Gamma(\mathcal{N})}\right.\\ &\quad \left.\times\ {}_1F_1\left(\mathcal{M}_2; \mathcal{N}; -\frac{2}{S_0\sigma^2 Y_T}\right)\right], \qquad (5.23)\end{aligned}$$

where

$$\mathcal{M}_2(\Phi) = \sqrt{\frac{2}{\sigma^2}\Phi + \left(\frac{r}{\sigma^2} - \frac{1}{2}\right)} + 1. \qquad (5.24)$$

Therefore

$$\begin{aligned}\mathcal{P}(H_T, T|H_0, 0) \quad &= \quad \frac{S_0}{H_T^2}\, e^{-\frac{\left(r-\frac{\sigma^2}{2}\right)^2}{2\sigma^2}T} \int_0^\infty \frac{d\Phi_I}{\pi} \mathrm{Re}\left[ e^{\Phi T} \left(\frac{2H_T}{S_0\sigma^2}\right)^{\mathcal{M}_2} \frac{\Gamma(\mathcal{N} - \mathcal{M}_2)}{\Gamma(\mathcal{N})}\right.\\ &\quad \left.\times\ {}_1F_1\left(\mathcal{M}_2; \mathcal{N}; -\frac{2H_T}{S_0\sigma^2}\right)\right]. \qquad (5.25)\end{aligned}$$

The left panel of Figure 5.2 compares $\mathcal{P}(H_T, T|H_0, 0)$ with $\mathcal{P}(A_T, T|A_0, 0)$. The distinction between them is due to the fact that the harmonic average value of a set of positive variables is not larger than their arithmetic average.

Plugging expressions (5.15) and (5.25) into (5.4) and (5.5), we have their corresponding Asian option prices respectively. As an example, the right panel of Figure 5.2 confirms our analytical continuous harmonic Asian call option prices.

## 5.2 Options on realized variance

The options we considered thusfar have a payoff that depends on the value of the underlying asset. However, options can be constructed with a payoff that depends on the realized variance of the underlying asset. To price such options, we again need the joint propagator (5.3), which sometimes can be simplified to a propagator for the realized variance only (rather than the propagator for the asset value only). In this section we consider these options on realized variance, starting from a stochastic volatility model with jumps.

The joint dynamics of the underlying asset price $S(t)$ (expressed in its logreturn $x(t) = \ln \frac{S(t)}{S_0}$) and its stochastic variance are generally assumed to evolve under the risk-neutral pricing measure as follows:

$$dx(t) = \left(r - \frac{v(t)}{2}\right) dt + \sqrt{v}\left(\sqrt{1-\rho^2}dW_1(t) + \rho dW_2(t)\right) + J^s dN(t), \quad (5.26)$$

$$dv(t) = \alpha\left(v(t)\right) + \beta\left(v(t)\right) dW_2(t) + J^v dN(t), \quad (5.27)$$

where $r$ is the constant interest rate, $W_1(t)$ and $W_2(t)$ are two independent Wiener processes, $\rho \in [-1,1]$ is the correlation coefficient between $x(t)$ and its variance $v(t)$. $N(t)$ is an independent Poisson process with constant intensity $\lambda$. We assume that the amplitudes of return jump $J^s$ and variance jump $J^v$ have respectively normal and exponential distribution:

$$\varpi(J^s) = \frac{1}{\sqrt{2\pi\nu^2}} e^{-\frac{(J^s-\mu)^2}{2\nu^2}}, \quad (5.28)$$

$$\varpi(J^v) = \frac{1}{\eta} e^{-\frac{1}{\eta}J^v}, \quad (5.29)$$

where $\mu$ is mean and $\nu$ is volatility of return jump $J^s$ and $\eta$ is mean of variance jump $J^v$.

This model is very similar to the one described in last chapter 4.1.1 except for the jumps. The realized variance of the underlying asset during a time period

$[0, T]$ under this model with price jumps is approximatively represented as, see (122, 185):

$$I_T = \int_0^T v(t)dt + \sum \left(J_k^s\right)^2, \tag{5.30}$$

where $\left(J_k^s\right)^2$ is the squared realization of $k - th$ jump $J_k^s$ that occurred at jump time $t_k$. Alternatively, the realized variance can be depicted by its stochastic differential equation (SDE):

$$dI(t) = v(t)dt + \left(J^s\right)^2 dN(t). \tag{5.31}$$

The pricing formulas of the options on realized variance rely on the propagator of the realized variance, which is denoted by $\mathcal{P}_{J^s}\left(I_T, T|I_0, 0\right)$. In order the derive $\mathcal{P}_{J^s}\left(I_T, T|I_0, 0\right)$ under the SDE (5.31), we first derive the propagator of the realized variance without price jumps, denoted by $\mathcal{P}\left(I_T, T|I_0, 0\right)$. When $J^s = 0$, $I_T$ reduces to $\int_0^T v(t)dt$, which is the case we solved in the previous chapter.

### 5.2.1 Realized variance in the Heston model with variance jumps

For the Heston SV model (76) with variance jumps, the model dynamics is written as:

$$dv(t) = \kappa\left(\theta - v(t)\right)dt + \sigma\sqrt{v(t)}dW_2(t) + J^v dN(t). \tag{5.32}$$

When $J^s = J^v = 0$, we already have the joint propagator of the joint dynamics $(x(t), I(t))$, see expression (4.92):

$$\begin{aligned}\mathcal{P}\left(x_T, I_T, T|x_0, I_0, 0\right) = &\; e^{\frac{\kappa}{\sigma^2}v_0 + \frac{\kappa^2\theta}{\sigma^2}T} \int_{-\infty}^{\infty} \frac{dp}{2\pi}\, e^{ip\,(I_T - I_0)} \int_{-\infty}^{\infty} \frac{dl}{2\pi}\, e^{il(x_T - rT)}\, e^{il\frac{\rho}{\sigma}(\kappa\theta T + v_0)} \\ &\times N^{\frac{2\kappa\theta}{\sigma^2}}\, e^{-\frac{2\omega(\cosh(\omega T) - N)}{\sigma^2\sinh(\omega T)}v_0},\end{aligned} \tag{5.33}$$

where

$$\omega = \frac{\sigma}{2}\sqrt{\frac{\kappa^2}{\sigma^2} + \left(1 - \rho^2\right)l^2 + il\left(\frac{2\rho\kappa}{\sigma} - 1\right) + 2ip}, \tag{5.34}$$

$$N = \left(\cosh(\omega T) + \frac{\kappa + il\rho\sigma}{2\omega}\sinh(\omega T)\right)^{-1}. \tag{5.35}$$

Of course, $I(t)$ does not depend on the process $x(t)$, so we do not need to calculate the joint propagator of $(x(t), I(t))$: it is trivial from (5.33) to get the marginal propagator of $I(t)$,

$$\mathcal{P}\left(I_T, T|I_0, 0\right) = \int_{-\infty}^{\infty} \frac{dp}{2\pi}\, e^{ip(I_T - I_0)} \frac{\exp\left\{\frac{\kappa^2\theta}{\sigma^2}T - \left(\frac{2ip}{\kappa+2\omega_2\coth(\omega_2 T)}\right)v_0\right\}}{\left(\cosh(\omega_2 T) + \frac{\kappa}{2\omega_2}\sinh(\omega_2 T)\right)^{\frac{2\kappa\theta}{\sigma^2}}}, \tag{5.36}$$

where

$$\omega_2 = \frac{1}{2}\sqrt{\kappa^2 + 2ip\sigma^2}. \tag{5.37}$$

Now consider the model with price jumps and variance jumps. The propagator of the realized variance $\mathcal{P}_{J^s}\left(I_T, T|I_0, 0\right)$ satisfies the Kolmogorov backward equation:

$$\begin{aligned} \frac{\partial \mathcal{P}_{J^s}}{\partial T} &= \kappa(\theta - v_0)\frac{\partial \mathcal{P}_{J^s}}{\partial v_0} + \frac{1}{2}\sigma^2 v_0 \frac{\partial^2 \mathcal{P}_{J^s}}{\partial v_0^2} + v_0\frac{\partial \mathcal{P}_{J^s}}{\partial I_0} \\ &+ \lambda \int_0^{\infty}\int_{-\infty}^{\infty}\left[\mathcal{P}_{J^s}(v_0 + J^v, I_0 + (J^s)^2) - \mathcal{P}_{J^s}(v_0, I_0)\right]\varpi(J^s)\varpi(J^v)dJ^s dJ^v. \end{aligned} \tag{5.38}$$

Given the propagator $\mathcal{P}\left(I_T, T|I_0, 0\right)$ for the model without jumps, which satisfies the previous Kolmogorov backward equation provided $\lambda = 0$, we thus write the propagator $\mathcal{P}_{J^s}\left(I_T, T|I_0, 0\right)$ for the model with jumps in a similar way:

$$\mathcal{P}_{J^s}(I_T, T|I_0, 0) = \int_{-\infty}^{\infty} \frac{dp}{2\pi}\, e^{ip(I_T - I_0)}\, \frac{\exp\left\{\frac{\kappa^2\theta}{\sigma^2}T - \left(\frac{2ip}{\kappa+2\omega_2\coth(\omega_2 T)}\right)v_0\right\}}{\left[\sinh(\omega_2 T)\left(\frac{\kappa}{2\omega_2} + \coth(\omega_2 T)\right)\right]^{\frac{2\kappa\theta}{\sigma^2}}} \times e^{U(p,T)}, \tag{5.39}$$

where $U(p, T)$ can be calculated as:

$$\frac{\partial U(p,T)}{\partial T} = \lambda \int_0^{\infty}\int_{-\infty}^{\infty}\left[e^{-ip(J^s)^2}\, e^{-\left(\frac{2ip}{\kappa+2\omega_2\coth(\omega_2 T)}\right)J^v} - 1\right]\varpi(J^s)\varpi(J^v)dJ^s dJ^v. \tag{5.40}$$

By using the jump size distributions (5.28) and (5.29), and taking the boundary condition $U(p, 0) = 0$ into account, we finally obtain

$$\begin{aligned} U(p,T) = \lambda &\frac{e^{-\frac{ip\mu^2}{1+2ip\nu^2}}}{\sqrt{1+2ip\nu^2}}\, \frac{-2\eta\ln\left[\frac{2ip\eta+\kappa}{2\omega_2}\sinh(\omega_2 T) + \cosh(\omega_2 T)\right] + \left(\sigma^2 - \eta\kappa\right)T}{\sigma^2 - 2\eta\kappa - 2ip\eta^2} \\ &- \lambda T. \end{aligned} \tag{5.41}$$

Substituting (5.41) into (5.39), we obtain the final propagator for the realized variance under the Heston model with jumps in asset price and variance, which is the same as the result obtained in reference (122), confirming our derivation.

### 5.2.2 Realized variance in the 3/2 model with deterministic mean-reverting level

The model dynamics of the 3/2 stochastic volatility model (188) with deterministic mean-reverting level reads:

$$\begin{aligned} dv(t) &= \kappa v(t)\left(\theta(t) - v(t)\right)dt + \epsilon v^{3/2}(t) dW_2(t) \\ &= v(t)\left[\kappa\left(\theta(t) - v(t)\right)dt + \epsilon\sqrt{v(t)}dW_2(t)\right]. \end{aligned} \tag{5.42}$$

This model is the same as the one given in (4.40) except that the mean-reverting level $\theta(t)$ is now a time dependent deterministic variable.

Inspection of equation (5.42) shows that this 3/2 model, in contrast to the Heston model, has a proportional structure, i.e. the mean reversion and the diffusion coefficient all depend on the current level of $v(t)$. The proportional structure of this model also exists in the exponential Vašiček model, see (3.14). Note that when $v(t)$ increases, its diffusion coefficient increases nonlinearly, so some of the large values of $v(t)$ can be captured by the diffusion part instead of the jump part. This makes it possible to drop the variance jumps in these models. Moreover, the larger the $v(t)$, the larger the effect of the mean reversion is. Thus these models are able to produce "spikes" rather than jumps, which is consistent with some underlying assets dynamics, such as the time evolution of a foreign exchange. So these models are capable of describing some underlying assets directly. The deterministic function of time $\theta(t)$ makes model (5.42) even more flexible.

To derive the propagator of the realized variance $\mathcal{P}_{J^s}\left(I_T, T|I_0, 0\right)$ for the model (5.42), we start by the derivation of a related joint propagator without price jumps $J^s$. The substitution

$$z(t) = \left(v(t)\right)^{-1/2}, \tag{5.43}$$

leads to the SDE for $z(t)$ and thus its Lagrangian:

$$\begin{aligned} dz(t) &= \left[-\frac{\kappa\theta(t)}{2}z+\left(\frac{\kappa}{2}+\frac{3}{8}\epsilon^2\right)\frac{1}{z}\right]dt-\frac{\epsilon}{2}dW_2(t), & (5.44)\\ \mathcal{L}[\dot z, z] &= \frac{2}{\epsilon^2}\left[\dot z^2+(\kappa\,\theta(t)/2)^2 z^2\right]+\frac{\left(2\kappa/\epsilon^2+1\right)^2-1/4}{(8/\epsilon^2)\,z^2} \\ &\quad +\frac{2\kappa\theta(t)}{\epsilon^2}z\dot z-\left(\frac{2\kappa}{\epsilon^2}+\frac{3}{2}\right)\frac{\dot z}{z}-\left(\frac{\kappa^2\theta(t)}{\epsilon^2}+\kappa\theta(t)\right). & (5.45)\end{aligned}$$

Denote the joint propagator of the joint dynamics $(z(t), I(t))$ without price jumps by $\mathcal{P}\left(z_T, I_T, T|z_0, I_0, 0\right)$. Applying the technique described at the beginning of this chapter, we have:

$$\begin{aligned} & \mathcal{P}\left(z_T, I_T, T|z_0, I_0, 0\right) \\ =& \int \mathcal{D}z(t)\,\delta\left(I_T-\int_0^T\frac{1}{z^2(t)}dt\right)\,e^{-\int_0^T\mathcal{L}[\dot z,z]dt} \\ =& \left(\frac{z_T}{z_0}\right)^{\frac{2\kappa}{\epsilon^2}+\frac{3}{2}}\;e^{-\frac{\kappa}{\epsilon^2}(\theta_T z_T^2-\theta_0 z_0^2)}\,e^{\kappa\left(\frac{\kappa}{\epsilon^2}+1\right)\int_0^T\theta(t)dt}\int_{-\infty}^{\infty}\frac{dp}{2\pi}e^{ip(I_T-I_0)} \\ & \times\int\mathcal{D}z(t)\,e^{-\int_0^T\left[\frac{2}{\epsilon^2}\left[\dot z^2+\left(\frac{\kappa^2\theta^2(t)}{4}-\frac{\kappa}{2}\dot\theta(t)\right)z^2\right]+\left(\frac{\left(\frac{2\kappa}{\epsilon^2}+1\right)^2-\frac{1}{4}}{8/\epsilon^2}+ip\right)\frac{1}{z^2}\right]dt}. \qquad (5.46)\end{aligned}$$

Make the substitutions

$$\begin{aligned}\omega^2(t) &= \frac{\kappa^2\theta^2(t)}{2}-\frac{\kappa}{2}\dot\theta(t), & (5.47)\\ \chi &= \sqrt{\left(\frac{2\kappa}{\epsilon^2}+1\right)^2+ip\frac{8}{\epsilon^2}}, & (5.48)\end{aligned}$$

then the rest propagator becomes

$$\int\mathcal{D}z(t)\exp\left\{-\int_0^T\left[\frac{2}{\epsilon^2}\left(\dot z^2+\omega^2(t)z^2\right)+\frac{\chi^2-\frac{1}{4}}{8/\epsilon^2}\frac{1}{z^2}\right]dt\right\}. \qquad (5.49)$$

This is the path integral of a time-dependent radial harmonic oscillator. Solution of this path integral can be found, for instance, in (155):

$$(5.49)=\frac{4\sqrt{z_0z_T}}{\epsilon^2\,\zeta(T)}\exp\left\{-\frac{2}{\epsilon^2}\left(\frac{\xi(T)}{\zeta(T)}z_0^2+\frac{\dot\zeta(T)}{\zeta(T)}z_T^2\right)\right\}\,I_\chi\left(\frac{4z_0z_T}{\epsilon^2\,\zeta(T)}\right). \qquad (5.50)$$

The quantities $\zeta(T)$ and $\xi(T)$, respectively, are determined by the differential equations:

$$\ddot{\zeta} - \omega^2(t)\zeta = 0, \qquad \zeta(0) = 0, \qquad \dot{\zeta}(0) = 1, \tag{5.51}$$

$$\ddot{\xi} - \omega^2(t)\xi = 0, \qquad \xi(0) = 1, \qquad \dot{\xi}(0) = 0. \tag{5.52}$$

To find the solutions of $\zeta$ and $\xi$, we consider the general differential equation

$$\ddot{\Upsilon}(t) = \omega^2(t)\Upsilon(t) = \left[\frac{\kappa^2\theta^2(t)}{2} - \frac{\kappa}{2}\dot{\theta}(t)\right]\Upsilon(t). \tag{5.53}$$

Assume

$$\dot{\Upsilon}(t) = -\frac{\kappa}{2}\theta(t)\Upsilon(t) + f(t), \tag{5.54}$$

then

$$\ddot{\Upsilon}(t) = \left[\frac{\kappa^2\theta^2(t)}{2} - \frac{\kappa}{2}\dot{\theta}(t)\right]\Upsilon(t) + \frac{d}{dt}f(t) - \frac{\kappa}{2}\theta(t)f(t), \tag{5.55}$$

from which we see that equation (5.53) can be satisfied with (5.54) if the function $f(t)$ satisfies

$$\frac{d}{dt}f(t) - \frac{\kappa}{2}\theta(t)f(t) = 0, \tag{5.56}$$

hence

$$f(t) = c_1\, e^{\int_0^t \frac{\kappa}{2}\theta(u)du}. \tag{5.57}$$

Now that

$$\dot{\Upsilon}(t) = -\frac{\kappa}{2}\theta(t)\Upsilon(t) + c_1\, e^{\int_0^t \frac{\kappa}{2}\theta(u)du}, \tag{5.58}$$

the general solution of differential equation (5.53) is

$$\Upsilon(t) = e^{-\int_0^t \frac{\kappa}{2}\theta(u)du}\left[c_1\int_0^t e^{\int_0^s \kappa\theta(u)du}ds + c_2\right]. \tag{5.59}$$

Given the boundary conditions of $\zeta$ and $\xi$, see (5.51) and (5.52), respectively, we find the their solutions as follows:

$$\zeta(t) \;=\; e^{-\int_0^t \frac{\kappa}{2}\theta(u)du}\int_0^t e^{\int_0^s \kappa\theta(u)du}ds, \tag{5.60}$$

$$\xi(t) \;=\; e^{-\int_0^t \frac{\kappa}{2}\theta(u)du}\left[\frac{\kappa\theta_0}{2}\int_0^t e^{\int_0^s \kappa\theta(u)du}ds + 1\right]. \tag{5.61}$$

So $(\theta(t) \dashrightarrow \theta)$

$$\begin{array}{rcll} \zeta(T) & = & e^{-\int_0^T \frac{\kappa}{2}\theta(u)du} \int_0^T e^{\int_0^s \kappa\theta(u)du} ds & \dashrightarrow \quad \frac{2}{\kappa\theta} \sinh \frac{\kappa\theta T}{2}, \\ \frac{\xi(T)}{\zeta(T)} & = & \frac{\kappa\theta_0}{2} + \frac{1}{\int_0^T e^{\int_0^s \kappa\theta(u)du} ds} & \dashrightarrow \quad \frac{\kappa\theta}{2} \coth \frac{\kappa\theta T}{2}, \\ \frac{\dot{\zeta}(T)}{\zeta(T)} & = & -\frac{\kappa\theta_T}{2} + \frac{e^{\int_0^T \kappa\theta(u)du}}{\int_0^T e^{\int_0^s k\theta(u)du} ds} & \dashrightarrow \quad \frac{\kappa\theta}{2} \coth \frac{\kappa\theta T}{2}. \end{array} \tag{5.62}$$

Especially, when $\theta(t) = \theta$, that is $\omega(t) = \omega = \frac{\kappa\theta}{2}$, we obtain our earlier result for the propagator of the normal radial harmonic oscillator

$$\begin{aligned} & \int \mathcal{D}z(t)\, e^{-\int_0^T \left[\frac{2}{\epsilon^2}\left(\dot{z}^2+\omega^2 z^2\right)+\frac{\chi^2-\frac{1}{4}}{8/\epsilon^2}\frac{1}{z^2}\right]dt} \\ = & \frac{4\omega\sqrt{z_T z_0}}{\epsilon^2 \sinh(\omega T)}\, e^{-\frac{2\omega}{\epsilon^2}\left(z_T^2+z_0^2\right)\coth(\omega T)}\, I_\chi\left(\frac{4\omega z_T z_0}{\epsilon^2 \sinh(\omega T)}\right). \end{aligned} \tag{5.63}$$

Note the relation that

$$\begin{aligned} \Xi(0,T) &= \int_0^T e^{\int_0^s \kappa\theta(u)du} ds \\ &= \zeta(T)\, e^{\int_0^T \frac{\kappa}{2}\theta(u)du} = \left(\frac{\xi(T)}{\zeta(T)} - \frac{\kappa\theta_0}{2}\right)^{-1} = \zeta^2(T)\left(\frac{\dot{\zeta}(T)}{\zeta(T)} + \frac{\kappa\theta_T}{2}\right), \end{aligned} \tag{5.64}$$

which is useful for further calculation.

Now we have the joint propagator $\mathcal{P}\left(z_T, I_T, T|z_0, I_0, 0\right)$, (5.46). Integrating it over $z_T$ yields the propagator of the realized variance for model (5.42) without price jumps:

$$\begin{aligned} \mathcal{P}\left(I_T, T|I_0, 0\right) &= \int_0^\infty \mathcal{P}\left(z_T, I_T, T|z_0, I_0, 0\right) dz_T \\ &= \int_{-\infty}^\infty \frac{dp}{2\pi}\, e^{ip(I_T-I_0)} \frac{\Gamma\left(\chi+1-\widetilde{M}\right)}{\Gamma\left(\chi+1\right)} \left(\frac{2}{\epsilon^2 \Xi(0,T)\, v_0}\right)^{\widetilde{M}} \\ &\quad \times {}_1F_1\left(\widetilde{M}; \chi+1; -\frac{2}{\epsilon^2\Xi(0,T)\, v_0}\right), \end{aligned} \tag{5.65}$$

where

$$\widetilde{M} = \frac{\chi}{2} - \frac{\kappa}{\epsilon^2} - \frac{1}{2}. \tag{5.66}$$

The propagator of the realized variance for model model (5.42) with price jumps $J^s$, following (5.28), can be obtained by using a similar procedure shown in section

(5.2.1), which is:

$$\mathcal{P}_{J^s}\left(I_T, T|I_0, 0\right) = \int_{-\infty}^{\infty} \frac{dp}{2\pi} e^{ip(I_T-I_0)} \frac{\Gamma\left(\chi+1-\widetilde{M}\right)}{\Gamma\left(\chi+1\right)} \left(\frac{2}{\epsilon^2 \Xi(0,T)\, v_0}\right)^{\widetilde{M}} \times {}_1F_1\left(\widetilde{M}; \chi+1; -\frac{2}{\epsilon^2 \Xi(0,T)\, v_0}\right) \exp\left\{U\left(p,T\right)\right\}, \quad (5.67)$$

where

$$U(p,T) = \lambda T \left[\frac{e^{-\frac{ip\mu^2}{1+2ip\nu^2}}}{\sqrt{1+2ip\nu^2}} - 1\right]. \quad (5.68)$$

Figure 5.3 illustrates the propagators of (5.67) and (5.65), and they are confirmed by Monte Carlo simulation results.

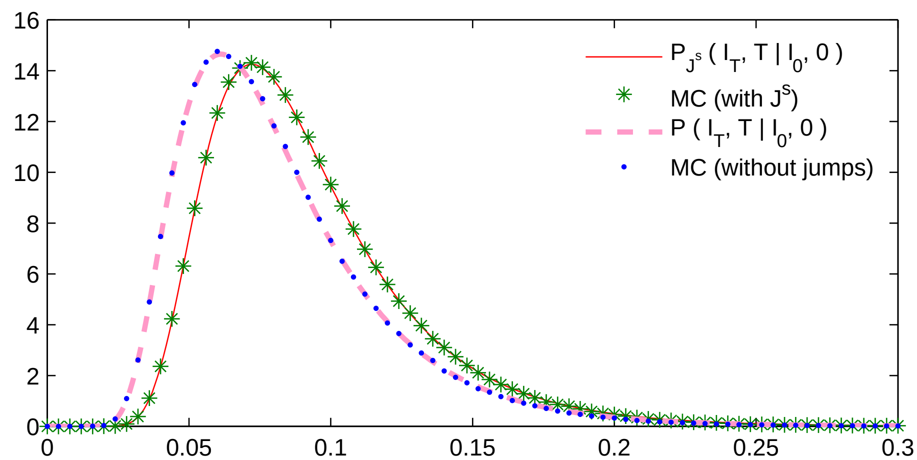


**Figure 5.3:** Propagators of the realized variance of the 3/2 model with price jumps from expression (5.67) (the red curve), and the one without price jumps from expression (5.65) (the pink dashed line). They fit their corresponding Monte Carlo (MC) simulations well. The parameter values used here are $v_0 = 0.245^2$, $\kappa = 22.84$, $\theta = 0.4669^2$, $\epsilon = 8.56$, $T = 1$, $\lambda = 10$, $\mu = -0.01$, $\nu = 0.03$.

### 5.2.3 Pricing derivative options on realized variance

Rewrite the previous two propagators of the realized variance $\mathcal{P}_{J^s}\left(I_{t_2}, t_2|I_{t_1}, t_1\right)$, $t_2 > t_1$, given in expressions (5.39) and (5.67), in a general form

$$\mathcal{P}_{J^s}\left(I_{t_2}, t_2|I_{t_1}, t_1\right) = \int_{-\infty}^{\infty} \frac{dp}{2\pi}\, e^{ip\left(I_{t_2}-I_{t_1}\right)} F\left(p, v_{t_1}, t_1, t_2\right), \tag{5.69}$$

where $F\left(p, v_{t_1}, t_1, t_2\right)$ is given by, for instance for the 3/2 model:

$$\begin{aligned} F\left(p, v_{t_1}, t_1, t_2\right) =& \frac{\Gamma\left(\chi+1-\widetilde{M}\right)}{\Gamma\left(\chi+1\right)} \left(\frac{2}{\epsilon^2 \Xi(t_1,t_2)\, v_{t_1}}\right)^{\widetilde{M}} \\ & \times {}_1F_1\left(\widetilde{M}; \chi+1; -\frac{2}{\epsilon^2 \Xi(t_1,t_2)\, v_{t_1}}\right) \exp\left\{U\left(p, t_2-t_1\right)\right\}. \end{aligned} \tag{5.70}$$

Then under the risk-neutral measure, we can compute option prices by calculating its expected payoff ($I_0 = 0$):

$$\begin{aligned} \text{Price} &= e^{-rT} \int_0^{\infty} \mathcal{P}_{J^s}\left(I_T, T|I_0, 0\right) \text{Payoff}\left(I_T - I_0\right) dI_T \\ &= e^{-rT} \int_{-\infty}^{\infty} \frac{dp}{2\pi} F(p, v_0, 0, T) \int_0^{\infty} dI_T\, e^{ipI_T}\, \text{Payoff}\left(I_T\right). \end{aligned} \tag{5.71}$$

In practice, a small imaginary part of $p$ is sometimes necessary. For example, a swap on the realized variance with the payoff $I_T - K$:

$$\int_0^{\infty} dI_T\, e^{ipI_T}\left(I_T - K\right) = -\frac{1+ipK}{p^2}. \tag{5.72}$$

A call option on the realized variance with the payoff $\left(I_T - K\right)_+$:

$$\int_0^{\infty} dI_T\, e^{ipI_T}\left(I_T - K\right)_+ = -\frac{e^{ipK}}{p^2}, \tag{5.73}$$

and so on. The option pricing formulas are then given straightforwardly.

The options discussed above are all current-start options, which means that the option life is from current time $t = 0$ to a maturity time $T$. For forward-start options on the realized variance, whose life is between two future times $t_F$ and $T$, with $0 < t_F < T$, the value of $v(t)$ at the option's initial time $t_F$, $v_{t_F}$, is unknown. So a propagator of $v(t)$, say $\mathcal{P}\left(v_{t_F}, t_F|v_0, 0\right)$, will be applied to eliminate this uncertainty. We know the computation of $\mathcal{P}\left(z_T, T|z_0, 0\right)$ is even easier than the one of $\mathcal{P}\left(z_T, I_T, T|z_0, I_0, 0\right)$, that is for the 3/2 model (5.42):

$$\begin{aligned}
\mathcal{P}\left(z_T, T|z_0, 0\right) &= \int \mathcal{D}z(t)\, e^{-\int_0^T \mathcal{L}[\dot{z},z]dt} \\
&= \left(\frac{z_T}{z_0}\right)^{\frac{2\kappa}{\epsilon^2}+\frac{3}{2}} e^{-\frac{\kappa\left(\theta_T z_T^2-\theta_0 z_0^2\right)}{\epsilon^2}+\left(\frac{\kappa^2}{\epsilon^2}+\kappa\right)\int_0^T \theta(t)dt} \\
&\quad \times \frac{4\sqrt{z_0 z_T}}{\epsilon^2 \zeta(T)}\, e^{-\frac{2}{\epsilon^2}\left(\frac{\xi(T)}{\zeta(T)}z_0^2+\frac{\dot{\zeta}(T)}{\zeta(T)}z_T^2\right)} I_{\frac{2\kappa}{\epsilon^2}+1}\left(\frac{4z_0 z_T}{\epsilon^2\zeta(T)}\right), \qquad (5.74)
\end{aligned}$$

therefore the propagator of $v(t)$ is

$$\begin{aligned}
\mathcal{P}\left(v_{t_F}, t_F|v_0, 0\right) &= \left|\frac{dz}{dv}\right|_{t_F} \mathcal{P}\left(z_{t_F}, t_F|z_0, 0\right) = \frac{z_{t_F}^3}{2}\mathcal{P}\left(z_{t_F}, t_F|z_0, 0\right) \\
&= \left(\frac{\Xi(0,t_F)}{\zeta(t_F)}\right)^{\frac{2\kappa}{\epsilon^2}+2} v_0^{\frac{\kappa}{\epsilon^2}+\frac{1}{2}}\, e^{-\frac{2}{\epsilon^2\Xi(0,t_F)}\frac{1}{v_0}}\, v_{t_F}^{-\left(\frac{\kappa}{\epsilon^2}+\frac{5}{2}\right)}\, e^{-\frac{2\,\Xi(0,t_F)}{\epsilon^2\zeta^2(t_F)}\frac{1}{v_T}} \\
&\quad \times \frac{2}{\epsilon^2\zeta(t_F)}\, I_{\frac{2\kappa}{\epsilon^2}+1}\left(\frac{4}{\epsilon^2\zeta(t_F)}\frac{1}{\sqrt{v_0 v_{t_F}}}\right). \qquad (5.75)
\end{aligned}$$

The stationary distribution of the 3/2 model can be calculated:

$$\begin{aligned}
\lim_{T\to\infty}\mathcal{P}\left(v_T, T|v_0, 0\right) &= \frac{\left(\frac{2\kappa\theta_T}{\epsilon^2}\right)^{\frac{2\kappa}{\epsilon^2}+2}}{\Gamma\left(\frac{2\kappa}{\epsilon^2}+2\right)} v_T^{-\left(\frac{2\kappa}{\epsilon^2}+3\right)} e^{-\frac{2\kappa\theta_T}{\epsilon^2}\frac{1}{v_T}} \\
&= \frac{\alpha^\beta}{\Gamma\left(\beta\right) v_T^{\beta+1}} \exp\left\{-\frac{\alpha}{v_T}\right\}, \qquad (5.76)
\end{aligned}$$

where $\alpha = \frac{2\kappa\theta_T}{\epsilon^2}$, $\beta = \frac{2\kappa}{\epsilon^2}+2$. Expression (5.76) tells us that the stationary density of the 3/2 stochastic volatility model follows an inverse gamma distribution. This distribution gives a very good fit for the probability density of the high frequency volatility proxy for the S&P500 index (41).

Now under the risk-neutral measure, the forward-start option prices on the realized variance are expressed as:

$$\begin{aligned}
\text{Price} &= e^{-rT}\mathbb{E}\left[\int_{I_{t_F}}^{\infty} \mathcal{P}_{J^s}\left(I_T, T|I_{t_F}, t_F\right) \text{Payoff}\left(I_T - I_{t_F}\right) dI_T\right] \\
&= e^{-rT}\mathbb{E}\left[\int_{-\infty}^{\infty}\frac{dp}{2\pi}F(p, v_{t_F}, t_F, T)\int_0^\infty d\mathcal{I}\, e^{ip\mathcal{I}}\, \text{Payoff}\left(\mathcal{I}\right)\right] \\
&= e^{-rT}\int_0^\infty dv_{t_F}\mathcal{P}\left(v_{t_F}, t_F|v_0, 0\right)\int_{-\infty}^{\infty}\frac{dp}{2\pi}F(p, v_{t_F}, t_F, T)\int_0^\infty d\mathcal{I}\, e^{ip\mathcal{I}}\, \text{Payoff}\left(\mathcal{I}\right).
\end{aligned}$$

(5.77)

## 5.3 VIX futures and options under the 3/2 model

The VIX stands for Chicago Board Options Exchange (CBOE) Volatility Index, a popular measure of the implied volatility of S&P500 index options with maturity 30 days. It represents the market's expectation of the annualized volatility of the S&P500 index over the next 30 day period, and it is often referred to as the fear index or the fear gauge.

The VIX is calculated and disseminated in real-time by the CBOE. More details on the VIX calculation can be found in the VIX white paper (CBOE 2009). Here, we model the VIX by assuming that the variance of returns on the S&P500 index is driven by dynamics (5.42). According to the market convention, the VIX is scaled by the factor of 100, which is omitted here for brevity.

The spot value of the VIX at current time $t_0$ with variance $v_0$, denoted by $X(t_0)$, measures the square root of the expected annualized realized variance for S&P500 index options with tenor $\tau_T = \frac{30}{365}$:

$$
\begin{aligned}
X(t_0) &= \sqrt{\mathbb{E}\left[\frac{1}{\tau_T}\left(I_{t_0+\tau_T} - I_{t_0}\right)\right]} \\
&= \left(\frac{1}{\tau_T}\int_{-\infty}^{\infty}\frac{dp}{2\pi}F(p, v_0, t_0, t_0+\tau_T)\int_0^{\infty} d\mathcal{I}\, e^{ip\mathcal{I}}\,\mathcal{I}\right)^{\frac{1}{2}} \\
&= \left(-\frac{1}{\tau_T}\int_{-\infty}^{\infty}\frac{dp}{2\pi}F(p, v_0, t_0, t_0+\tau_T)\frac{1}{p^2}\right)^{\frac{1}{2}}, \qquad (5.78)
\end{aligned}
$$

where $F(p, v_0, t_0, t_0+\tau_T)$ is given in (5.70). The futures value of the VIX, denoted by $X(t_0, t_F)$, $t_F > t_0$, is the expectation of the VIX at time $t_F$:

$$
\begin{aligned}
X(t_0, t_F) &= \mathbb{E}\left[\sqrt{\mathbb{E}\left[\frac{1}{\tau_T}\left(I_{t_F+\tau_T} - I_{t_F}\right)\middle| v_{t_F}\right]}\right] \\
&= \mathbb{E}\left[\left(-\frac{1}{\tau_T}\int_{-\infty}^{\infty}\frac{dp}{2\pi}F(p, v_{t_F}, t_F, t_F+\tau_T)\frac{1}{p^2}\right)^{\frac{1}{2}}\right] \\
&= \int_0^{\infty} dv_{t_F}\mathcal{P}\left(v_{t_F}, t_F | v_0, 0\right)\left(-\frac{1}{\tau_T}\int_{-\infty}^{\infty}\frac{dp}{2\pi}F(p, v_{t_F}, t_F, t_F+\tau_T)\frac{1}{p^2}\right)^{\frac{1}{2}}. \qquad (5.79)
\end{aligned}
$$

The forward-start option value on the VIX spot value $X(t_F)$ at a future time $t_F$ is:

$$\begin{aligned}
\text{Price} &= e^{-r(t_F-t_0)}\mathbb{E}\left[\text{Payoff}\left(X(t_F)\right)\right] \\
&= e^{-r(t_F-t_0)}\mathbb{E}\left[\text{Payoff}\left(\sqrt{\mathbb{E}\left[\frac{1}{\tau_T}\left(I_{t_F+\tau_T}-I_{t_F}\right)\right]}\right)\right] \\
&= e^{-r(t_F-t_0)}\int_0^{\infty} dv_{t_F}\mathcal{P}\left(v_{t_F},t_F|v_0,0\right) \\
&\quad\times\text{Payoff}\left(\sqrt{-\frac{1}{\tau_T}\int_{-\infty}^{\infty}\frac{dp}{2\pi}F(p,v_{t_F},t_F,t_F+\tau_T)\frac{1}{p^2}}\right). \qquad (5.80)
\end{aligned}$$

We see that the futures is a special option with payoff:

$$\text{Payoff}\left(\mathcal{E}\right)=\mathcal{E}. \qquad (5.81)$$

Also note that no discounting is applied for time $[t_F, t_F+\tau_T]$ because the payoff occurs at time $t_F$.

### 5.3.1 Expectation value of the realized variance

We already have the pricing formula for the froward-start options on the VIX, see expression (5.80), based on the computation of the realized variance's expectation value:

$$\mathbb{E}\left[I_{t_F+\tau_T}-I_{t_F}\right]=-\int_{-\infty}^{\infty}\frac{dp}{2\pi}F(p,v_{t_F},t_F,t_F+\tau_T)\frac{1}{p^2}. \qquad (5.82)$$

Actually, there is another way to calculate this value, i.e. ($\varpi(J^s)$ is given in (5.28))

$$\begin{aligned}
\mathbb{E}\left[I_{t_F+\tau_T}-I_{t_F}\right] &= \mathbb{E}\left[\int_{t_F}^{t_F+\tau_T}v(t)dt+\int_{t_F}^{t_F+\tau_T}(J^s)^2dN(t)\right] \\
&= \int_{t_F}^{t_F+\tau_T}\mathbb{E}\left[v(t)\right]dt+\lambda\int_{t_F}^{t_F+\tau_T}dt\int_{-\infty}^{\infty}(J^s)^2\varpi(J^s)dJ^s \\
&= \int_{t_F}^{t_F+\tau_T}\mathbb{E}\left[v(t)\right]dt+\lambda\left(\mu^2+\nu^2\right)\tau_T. \qquad (5.83)
\end{aligned}$$

Given the propagator of $v(t)$, see expression (5.75), we have:

$$
\begin{aligned}
\mathbb{E}\left[v(t)\right] &= \int_0^\infty v(t)\mathcal{P}\left(v_t, t | v_{t_F}, t_F\right) dv(t) \\
&= \frac{\frac{2}{\epsilon^2}}{\frac{2\kappa}{\epsilon^2}+1} \frac{\frac{d}{dt}\Xi(t_F, t)}{\Xi(t_F, t)} \; {}_1F_1\left(1; \frac{2\kappa}{\epsilon^2}+2; -\frac{2}{\epsilon^2 \Xi(t_F, t)} \frac{1}{v_{t_F}}\right). \qquad (5.84)
\end{aligned}
$$

Then it is not difficult to obtain:

$$
\mathbb{E}[v_T] \to \begin{cases} \frac{\frac{2}{\epsilon^2}}{\frac{2\kappa}{\epsilon^2}+1} \frac{1}{\int_0^T e^{\int_0^s \kappa\theta(u)du} ds} \frac{(-1)\left(\frac{2\kappa}{\epsilon^2}+1\right)}{(-1)\frac{2}{\epsilon^2 \int_0^T e^{\int_0^s \kappa\theta(u)du} ds} \frac{1}{v_0}} \to v_0, & \text{as} \quad T \to t_0; \\ \frac{\frac{2}{\epsilon^2}}{\frac{2\kappa}{\epsilon^2}+1} \frac{e^{\int_0^T \kappa\theta(u)du} \kappa\theta_T}{e^{\int_0^T \kappa\theta(u)du}} \to \frac{\theta_T}{1+\frac{\epsilon^2}{2\kappa}}, & \text{as} \quad T \to \infty, \end{cases}
$$

from which we see that the expectation value of $v(t)$ at large time is determined by $\theta(t)$. By using (5.84), we then have:

$$
\begin{aligned}
&\int_{t_F}^{t_F+\tau_T} \mathbb{E}\left[v(t)\right] dt \\
&= \int_{t_F}^{t_F+\tau_T} \frac{\frac{2}{\epsilon^2}}{\frac{2\kappa}{\epsilon^2}+1} \frac{\frac{d}{dt}\Xi(t_F, t)}{\Xi(t_F, t)} \; {}_1F_1\left(1; \frac{2\kappa}{\epsilon^2}+2; -\frac{2}{\epsilon^2 \Xi(t_F, t)} \frac{1}{v_{t_F}}\right) dt \\
&= \frac{\frac{2}{\epsilon^2}}{\frac{2\kappa}{\epsilon^2}+1} \int_0^{\Xi(t_F, t_F+\tau_T) v_{t_F}} \frac{1}{\Lambda} \; {}_1F_1\left(1; \frac{2\kappa}{\epsilon^2}+2; -\frac{2}{\epsilon^2 \Lambda}\right) d\Lambda. \qquad (5.85)
\end{aligned}
$$

In short, an alternative expression for (5.82) is

$$
\begin{aligned}
\mathbb{E}\left[I_{t_F+\tau_T} - I_{t_F}\right] &= \frac{2}{2\kappa+\epsilon^2} \int_0^{\Xi(t_F, t_F+\tau_T) v_{t_F}} \frac{1}{\Lambda} \; {}_1F_1\left(1; \frac{2\kappa}{\epsilon^2}+2; -\frac{2}{\epsilon^2 \Lambda}\right) d\Lambda \\
&\quad +\lambda\left(\mu^2+\nu^2\right)\tau_T. \qquad (5.86)
\end{aligned}
$$

Expression (5.86) is equivalent to but numerically simpler than equation (5.82).

## 5.4 Dosimetry in an environment with fluctuating radioactivity

This section is based on the joint work with Jacques Tempère and Maarten Baeten. Jacques Tempère is the initiator.

The disaster of Japanese Fukushima nuclear plant prompts people to be concerned about the dangers of radiation exposure. Indeed, radiation and radioactivity, though harmless at normal levels, are ubiquitous. Apart from the radiation hormesis, a controversial hypothesis, which states that radiation exposure comparable to and just above the natural background level of radiation is not harmful but beneficial (202, 203, 204), it is reported that an increase in the risk of tumor induction proportionate to the radiation dose is consistent with developing knowledge (205). Both these two radiation dose-risk relationships stimulate our research on the stopping time problems, such as the radioactive dosimetry problem. That is finding the probability distribution for the times when having received a predetermined total dose, under different circumstances.

We know from basic radioactivity theory that the number of radioactive decays in a given time interval can be very-well described by a Poisson distribution. However, this is only the case when the time of observation is much smaller than the half-life time of the isotopes. Otherwise, some corrections need to be made (206). Moreover, when residing in a natural environment, Nero et al. (207) proposed that indoor radon levels could be modeled well with a log-normal distribution. Ever since, much progress has been made in the field of radon mapping in many countries, see for instance (208, 209, 210, 211, 212). Other probability distributions have also been considered, for instance Janssen et al. modeled radon measurements with the gamma distribution (213, 214). For exposure to radiation leaked from a nuclear plant, it was found that the distribution of radioactive particles over Europe after the Chernobyl disaster could be fairly well modeled by a stochastic process where the particles, starting from Kiev, underwent a Lévy flight (with drift) rather than Brownian motion through the atmosphere (215). So the number of radioactive decays that one subjected to, can varies from a Poisson distribution in one case to a Lévy distribution in another case as one is traveling across contaminated land.

To capture these crucial empirical features of radioactive decays, i. e. exponentially decay with random fluctuations and occasional jumps, we model the complicated Poisson process by incorporating an arbitrary stochastic process into the basic Poisson intensity variable. In particular, we focus on the log-normal model and the Cox-Ingersoll-Ross (CIR) jump-diffusion model. The log-normal stochastic process gives a stationary log-normal distribution, while the CIR process gives a stationary gamma distribution (216). These two models will let us in agreement with literature findings (207, 213). The probability density of stopping times can be derived by taking the derivative of the cumulative distribution function, which is the death probability that in a time span, at least a given number of decays will have occurred. Therefore, the solution of the stopping time problem relies on the transition probability density of the number of decays.

The notion of stopping time in the context of radioactive decay is analogous to the notion of the expiry date of a timer option in the financial market, where the expiry date equals the time needed for the realized variance of the underlying asset to reach a prespecified level, see (145, 167) and references therein. This analogy inspires us to apply the techniques used in previous chapter.

### 5.4.1 Poisson distributions

We first investigate a Poisson process for radioactive decay, with an intensity parameter $\lambda_{n,t}$ that depends both on the time $t$ and on the number of decays $n(t)$, for example because the concentrations of radionuclides vary as a function of time. To start with, we assume that $\lambda_{n,t}$ represents the probability that a radioactive decay has occurred in the time window $[t, t+\Delta t]$ with $\Delta t$ infinitesimal.

We want to calculate the probability that in a (macroscopic) given time span $T$, $n$ decays have occurred. This can be written as a transition probability, starting with $n_0$ decays at time $t = t_0$ and ending up with $n$ decays at time $t_0 + T$. We denote this transition probability by $P(n_0, t_0 \to n, t_0 + T)$. With this notation, we can define $\lambda_{n,t}$ as

$$P(n, t \to n+1, t+\Delta t) = \lambda_{n,t}\Delta t. \tag{5.87}$$

If the time $\Delta t$ is short enough (indeed it is infinitesimal), not more than one decay will have occurred so that

$$P(n, t \to n, t+\Delta t) = 1 - \lambda_{n,t}\Delta t. \tag{5.88}$$

We can write the transition probability from $t_0$ to $t + \Delta t$ as a transition up to $t$ and then a transition from $t$ to $t + \Delta t$. Since in the short time span $\Delta t$ there can be either one or zero decays, but nothing else, we find

$$\begin{aligned}
& P\left(n_0, t_0 \rightarrow n, t+\Delta t\right) \\
= \; & P\left(n_0, t_0 \rightarrow n, t\right) P\left(n, t \rightarrow n, t+\Delta t\right) \\
& + P\left(n_0, t_0 \rightarrow n-1, t\right) P\left(n-1, t \rightarrow n, t+\Delta t\right) \\
= \; & \left(1-\lambda_{n,t} \Delta t\right) P\left(n_0, t_0 \rightarrow n, t\right)+\lambda_{n-1,t} \Delta t P\left(n_0, t_0 \rightarrow n-1, t\right), \quad (5.89)
\end{aligned}$$

from which

$$\frac{\partial P\left(n_0, t_0 \rightarrow n, t\right)}{\partial t}=-\lambda_{n,t} P\left(n_0, t_0 \rightarrow n, t\right)+\lambda_{n-1,t} P\left(n_0, t_0 \rightarrow n-1, t\right). \quad (5.90)$$

The number of decays between $t_0$ and $t$ is a Poisson stochastic variable. The number of decays as a function of time, is the Poisson stochastic process. We want to find the time $T_{\mathcal{B}}$ it takes, starting at $t_0$ , to get a dose of $\mathcal{B}$ decays. This time will by necessity also be a stochastic variable. So, to be precise, we want to find the probability density function $f\left(T_{\mathcal{B}}\right)$ associated with $T_{\mathcal{B}}$.

We can start by looking at the cumulative distribution function $F\left(T_{\mathcal{B}}\right)$ for $T_{\mathcal{B}}$. This is the probability that in a time span $T_{\mathcal{B}}$ (still staring at $t_0$), at least $\mathcal{B}$ decays will have occurred, in other words

$$F\left(T_{\mathcal{B}}\right)=\sum_{j=\mathcal{B}}^{N_{Tot}} P\left(n_0, t_0 \rightarrow n_0+j, t_0+T_{\mathcal{B}}\right). \quad (5.91)$$

We can also find this through its complement

$$F\left(T_{\mathcal{B}}\right)=1-\sum_{j=0}^{\mathcal{B}-1} P\left(n_0, t_0 \rightarrow n_0+j, t_0+T_{\mathcal{B}}\right). \quad (5.92)$$

Taking the derivative of $F\left(T_{\mathcal{B}}\right)$ yields the final stopping time distribution, i.e. the probability density function of the maximum exposure time:

$$f\left(T_{\mathcal{B}}\right)=\frac{dF\left(T_{\mathcal{B}}\right)}{dT_{\mathcal{B}}}. \quad (5.93)$$

Note that this final formula of stopping time relies in the probability distribution $P\left(n_0, t_0 \rightarrow n_0+j, t\right)$, which depends on the Poisson intensity parameter $\lambda_{n,t}$. Hence, we will focus on the modeling of $\lambda_{n,t}$ in the remaining of this section.

### 5.4.2 Basic n-dependent Poisson distribution

Here we assume that $\lambda_{n,t}$ depends on time by the number of decays $n(t)$. This assumption is essential if we have a finite stock of $N_{Tot}$ radionuclides and wait a long time. Indeed, one expects

$$\lambda_{n,t} = \lambda_0 \left( N_{Tot} - n(t) \right). \tag{5.94}$$

Note that usually $N_{tot}$ is deemed large enough so that $\lambda_{n,t}$ is assumed constant. This cannot hold for small amounts of randomly released radioactivity, as in the case of radon concentrations in mountainous regions. As time grows, $n(t)$ grows, and at some point it can no longer be neglected with respect to $N_{Tot}$.

Since $n(t) \leq N_{Tot}$, we define the generating function of $P\left(n_0, t_0 \to n, t\right)$ as

$$G\left(n_0, t_0; s, t\right) = \sum_{n=n_0}^{N_{Tot}} s^{n-n_0} \, P\left(n_0, t_0 \to n, t\right) = \sum_{j=0}^{N_{Tot}-n_0} s^j \, P\left(n_0, t_0 \to n_0 + j, t\right). \tag{5.95}$$

Plugging (5.95) into (5.90) gives

$$\begin{aligned}
\frac{\partial G\left(n_0, t_0; s, t\right)}{\partial t} &= \sum_{n=n_0}^{N_{Tot}} s^{n-n_0} \, \frac{\partial P\left(n_0, t_0 \to n, t\right)}{\partial t} \\
&= -\sum_{n=n_0}^{N_{Tot}} s^{n-n_0} \lambda_{n,t} P(n_0, t_0 \to n, t) + s \sum_{n=n_0}^{N_{Tot}-1} s^{n-n_0} \lambda_{n,t} P(n_0, t_0 \to n, t).
\end{aligned} \tag{5.96}$$

Considering our basic model $\lambda_{n,t} = \lambda_0 \left( N_{Tot} - n(t) \right)$, which yields

$$\begin{aligned}
& \sum_{n=n_0}^{N_{Tot}} s^{n-n_0} \, \lambda_{n,t} P\left(n_0, t_0 \to n, t\right) \\
= \; & \lambda_0 N_{Tot} \sum_{n=n_0}^{N_{Tot}} s^{n-n_0} \, P\left(n_0, t_0 \to n, t\right) - \lambda_0 \sum_{n=n_0}^{N_{Tot}} s^{n-n_0} \, n P\left(n_0, t_0 \to n, t\right) \\
= \; & \lambda_0 N_{Tot} \, G\left(n_0, t_0; s, t\right) - \lambda_0 \left( s \frac{\partial G\left(n_0, t_0; s, t\right)}{\partial s} + n_0 \, G\left(n_0, t_0; s, t\right) \right),
\end{aligned} \tag{5.97}$$

and also noting that

$$\lambda_{N_{Tot},t} = 0, \tag{5.98}$$

we have

$$\frac{\partial G\left(n_0,t_0;s,t\right)}{\partial t} = \lambda_0\left(N_{Tot}-n_0\right)(s-1)\,G\left(n_0,t_0;s,t\right) -\lambda_0 s(s-1)\frac{\partial G\left(n_0,t_0;s,t\right)}{\partial s}, \tag{5.99}$$

with boundary conditions:

$$G\left(n_0,t_0;s,t_0\right)=1, \qquad G\left(n_0,t_0;1,t\right)=1. \tag{5.100}$$

The solution of this equation is

$$\begin{aligned} G\left(n_0,t_0;s,t\right) &= \left(s-(s-1)\,e^{-\lambda_0(t-t_0)}\right)^{N_{Tot}-n_0} \\ &= e^{-\lambda_0(t-t_0)(N_{Tot}-n_0)}\left[1+\left(e^{\lambda_0(t-t_0)}-1\right)s\right]^{N_{Tot}-n_0} \\ &= e^{-\lambda_0(t-t_0)(N_{Tot}-n_0)}\sum_{j=0}^{N_{Tot}-n_0}\binom{N_{Tot}-n_0}{j}\left(e^{\lambda_0(t-t_0)}-1\right)^j s^j, \end{aligned} \tag{5.101}$$

where $\binom{\cdot}{\cdot}$ is the binomial coefficient. Comparing this result with expression (5.95), we obtain

$$P\left(n_0,t_0\to n_0+j,t\right) = e^{-\lambda_0(t-t_0)(N_{Tot}-n_0)}\binom{N_{Tot}-n_0}{j}\left(e^{\lambda_0(t-t_0)}-1\right)^j. \tag{5.102}$$

Straightforwardly, we have the mean and variance of the number of decays as follows:

$$\mathbb{E}_{t_0,t}(j) = \left.\frac{\partial G\left(n_0,t_0;s,t\right)}{\partial s}\right|_{s=1} = \left(1-e^{-\lambda_0(t-t_0)}\right)\left(N_{Tot}-n_0\right), \tag{5.103}$$

$$\begin{aligned} \mathrm{Var}_{t_0,t}(j) &= \left.\frac{\partial^2 G\left(n_0,t_0;s,t\right)}{\partial s^2}\right|_{s=1} + \left.\frac{\partial G\left(n_0,t_0;s,t\right)}{\partial s}\right|_{s=1} - \left(\left.\frac{\partial G\left(n_0,t_0;s,t\right)}{\partial s}\right|_{s=1}\right)^2 \\ &= e^{-\lambda_0(t-t_0)}\left(1-e^{-\lambda_0(t-t_0)}\right)\left(N_{Tot}-n_0\right). \end{aligned} \tag{5.104}$$

Note that the variance (5.104) first expands then converges to zero as time $t$ goes.

Plugging expression (5.102) into (5.92), we get

$$F(T_{\mathcal{B}}) = \binom{N_{Tot}-n_0}{\mathcal{B}}\left(e^{\lambda_0 T_{\mathcal{B}}}-1\right)^{\mathcal{B}}\,{}_2F_1\left(\mathcal{B},1+N_{Tot}-n_0;\,\mathcal{B}+1;\,1-e^{\lambda_0 T_{\mathcal{B}}}\right), \tag{5.105}$$

where ${}_2F_1\left(\cdot,\cdot;\cdot;\cdot\right)$ is the hypergeometric function.

Finally the probability density function of the stopping time is obtained by taking the derivative of the previous cumulative distribution function, see (5.93):

$$f(T_{\mathcal{B}}) = \lambda_0\mathcal{B}\binom{N_{Tot}-n_0}{\mathcal{B}}\left(e^{\lambda_0 T_{\mathcal{B}}}-1\right)^{\mathcal{B}-1}e^{-\lambda_0\,T_{\mathcal{B}}(N_{Tot}-n_0)}. \tag{5.106}$$

### 5.4.3 Time changed n-dependent Poisson distribution

Now we extend the previous Poisson intensity model (5.94) to a more general one that incorporates an arbitrary stochastic process $v(t)$:

$$\lambda_{n,t} = \lambda_0 \left(N_{Tot} - n(t)\right) v(t). \tag{5.107}$$

Due to the flexibility of the stochastic process $v(t)$, given a feasible process $v(t)$, this model enables us to capture the empirical features of the radioactive decays. In particular for the aforementioned case of radon concentrations in mountainous regions, the release of radon is a stochastic process where empirical indications are that it follows a distribution with non-Gaussian tails. Using the formalism developed in this thesis, we are in a unique position to investigate dosimetry in such an environment with fluctuating activity.

In order to find the transition probability function of decays under this model, we apply the Duru-Kleinert method of quantum mechanics by defining a pseudo-time $\tau(t)$ such that

$$\tau(t) = \int_0^t v(s)ds. \tag{5.108}$$

The inverse function theorem tells that

$$\frac{d\tau^{-1}(t)}{dt} = \frac{1}{v\left(\tau^{-1}(t)\right)}. \tag{5.109}$$

Denote $n\left(\tau^{-1}(t)\right)$ by $\widetilde{N}(t)$, then

$$\lambda_{\widetilde{N}(t),t}\, dt = \lambda_{n(\tau^{-1}(t)),\tau^{-1}(t)}\, d\tau^{-1}(t), \tag{5.110}$$

from which it follows

$$\begin{aligned} \lambda_{\widetilde{N}(t),t} &= \lambda_0 \left(N_{Tot} - n\left(\tau^{-1}(t)\right)\right) v\left(\tau^{-1}(t)\right) \frac{d\tau^{-1}(t)}{dt} \\ &= \lambda_0 \left(N_{Tot} - \widetilde{N}(t)\right). \end{aligned} \tag{5.111}$$

Consequently, $\widetilde{N}(t)$ is nothing but a basic n-dependent Poisson intensity process as described in subsection 5.4.2. In respect that $n(t) = \widetilde{N}\left(\tau(t)\right)$, therefore $n(t)$ is actually a time changed n-dependent Poisson intensity process. As the process $n(t)$ evolves in the real time period $[t_0, t_0 + T]$, the new process $\widetilde{N}(t)$

evolves in $[\tau(t_0), \tau(t_0+T)]$. Notably, while $[t_0, t_0+T]$ is a fixed time period, $[\tau(t_0), \tau(t_0+T)]$ is now an uncertain horizon in pseudotime.

In short, we reduce the time changed model's problem to the one under the basic Poisson intensity process, which we have solved in subsection 5.4.2, at the expense that the time horizon is now random in pseudotime. We can link this work with our work on timer options (145), presented in the previous chapter, where we fixed the uncertain expiration date at the cost of introducing more complicated processes.

Keeping the uncertainty of the pseudotime horizon in mind, we can, conditioning on $\tau(t)$, obtain the transition probability function of the number of decays under the $\widetilde{N}(t)$ process straightforwardly, see expression (5.102) and also note that $\widetilde{N}(\tau(t_0)) = n(t_0) = n_0$:

$$\begin{aligned} & P\left(\widetilde{N}(\tau(t_0)), \tau(t_0) \to \widetilde{N}(\tau(t_0)) + j, \tau(t)\right) \\ = \quad & e^{-\lambda_0(\tau(t)-\tau(t_0))(N_{Tot}-n_0)} \binom{N_{Tot}-n_0}{j} \left(e^{\lambda_0(\tau(t)-\tau(t_0))} - 1\right)^j . \end{aligned} \tag{5.112}$$

Denote the transition probability density function of the random variable $\tau(t)$ by $\mathcal{P}(\tau(t), t|\tau(t_0), t_0)$. The probability density function of $n(t)$ can be written as:

$$\begin{aligned} & \mathcal{P}(n_0, t_0 \to n_0 + j, t) \\ = \quad & \int_{\tau(t_0)}^{\infty} e^{-\lambda_0(\tau(t)-\tau(t_0))(N_{Tot}-n_0)} \binom{N_{Tot}-n_0}{j} \left(e^{\lambda_0(\tau(t)-\tau(t_0))} - 1\right)^j \\ & \times \mathcal{P}(\tau(t), t|\tau(t_0), t_0)\, d\tau(t). \end{aligned} \tag{5.113}$$

Then the cumulative distribution function defined in expression (5.92) is given by

$$\begin{aligned} F(T_{\mathcal{B}}) \quad = \quad & \binom{N_{Tot}-n_0}{\mathcal{B}} \int_{\tau(t_0)}^{\infty} d\tau(t)\, \mathcal{P}(\tau(t), t|\tau(t_0), t_0) \left(e^{\lambda_0(\tau(t)-\tau(t_0))} - 1\right)^{\mathcal{B}} \\ & \times {}_2F_1\left(\mathcal{B}, 1 + N_{Tot} - n_0; \mathcal{B}+1; 1 - e^{\lambda_0(\tau(t)-\tau(t_0))}\right)\Big|_{t=t_0+T_{\mathcal{B}}}. \end{aligned} \tag{5.114}$$

We thus arrive at the probability density function of the stopping time $f(T_{\mathcal{B}})$:

$$\begin{aligned} f(T_{\mathcal{B}}) \quad = \quad & \binom{N_{Tot}-n_0}{\mathcal{B}} \frac{d}{dT_{\mathcal{B}}} \int_{\tau(t_0)}^{\infty} d\tau(t)\, \mathcal{P}(\tau(t), t|\tau(t_0), t_0) \left(e^{\lambda_0(\tau(t)-\tau(t_0))} - 1\right)^{\mathcal{B}} \\ & \times {}_2F_1\left(\mathcal{B}, 1 + N_{Tot} - n_0; \mathcal{B}+1; 1 - e^{\lambda_0(\tau(t)-\tau(t_0))}\right)\Big|_{t=t_0+T_{\mathcal{B}}}. \end{aligned} \tag{5.115}$$

### 5.4.4 The limit $N_{Tot} \to \infty$

As a special case, one sometimes simply assume that the stock of radionuclides is infinite. Mathematically, we would express $(N_{Tot} - n(t)) \to \infty$ and $\lambda_0 \to 0$ such that $\lambda_0 N_{Tot}$ is finite. Denote the finite constant $\lambda_0 N_{Tot}$ by $\lambda$, then the binomial distribution expressed in (5.102) for the basic Poisson distribution converges to the well known Poisson distribution:

$$\begin{aligned} P\left(n_0, t_0 \to n_0 + j, t\right) &\to e^{-\lambda_0 (t-t_0) N_{Tot}} \frac{\left(N_{Tot}\right)^j}{j!} \left(\lambda_0 \left(t - t_0\right)\right)^j \\ &= e^{-\lambda (t-t_0)} \frac{\left(\lambda \left(t - t_0\right)\right)^j}{j!}, \end{aligned} \tag{5.116}$$

in agreement with reference (217). Moreover, the variance of the number of decays (5.104) reduces to $\mathrm{Var}_{t_0,t}(j) = \lambda\left(t - t_0\right)$, which only diverges as time $t$ goes. This describes a never exhausted source of radionuclides, in contrast with the case in (5.104), where a finite undecayed source is considered.

Still in the limit $N_{Tot} \to \infty$, the radioactivity can have a stochastic component modulating this background. The model (5.107) for the time-changed Poisson distribution now reduces to

$$\lambda_{n,t} = \lambda_0 \left(N_{Tot} - n(t)\right) v(t) \to \lambda_0 N_{Tot} v(t) = \lambda v(t). \tag{5.117}$$

Under this simplified model, the cumulative distribution function (5.114) becomes

$$\begin{aligned} F(T_{\mathcal{B}}) \to & \frac{\left(N_{Tot}\right)^{\mathcal{B}}}{\Gamma\left(\mathcal{B}+1\right)} \int_{\tau(t_0)}^{\infty} d\tau(t)\, \mathcal{P}\left(\tau(t), t | \tau(t_0), t_0\right) \left(\lambda_0 \left(\tau(t) - \tau(t_0)\right)\right)^{\mathcal{B}} \\ & \times {}_1F_1\left(\mathcal{B};\, \mathcal{B}+1;\, -\lambda_0\, \left(\tau(t) - \tau(t_0)\right) N_{Tot}\right) \Big|_{t=t_0+T_{\mathcal{B}}} \\ = & 1 - \int_{\tau(t_0)}^{\infty} d\tau(t)\, \mathcal{P}\left(\tau(t), t | \tau(t_0), t_0\right) \frac{\Gamma\left(\mathcal{B}, \lambda\left(\tau(t) - \tau(t_0)\right)\right)}{\Gamma\left(\mathcal{B}\right)} \Big|_{t=t_0+T_{\mathcal{B}}}, \end{aligned} \tag{5.118}$$

where ${}_1F_1\left(\cdot;\cdot;\cdot\right)$ is the confluent hypergeometric function, $\Gamma\left(\cdot\right)$ is the gamma function. Thus the probability density function of the stopping time is:

$$f(T_{\mathcal{B}}) = -\frac{1}{\Gamma\left(\mathcal{B}\right)} \frac{d}{dT_{\mathcal{B}}} \int_{\tau(t_0)}^{\infty} \Gamma\left(\mathcal{B},\, \lambda\left(\tau(t) - \tau(t_0)\right)\right) \mathcal{P}\left(\tau(t), t | \tau(t_0), t_0\right) d\tau(t)\, \Big|_{t=t_0+T_{\mathcal{B}}}, \tag{5.119}$$

where $\Gamma\left(\cdot,\cdot\right)$ is the upper incomplete gamma function.

### 5.4.5 The maximum exposure time formulas

It is worth noting that if $v(t)$ evolves in a deterministic way, then the transition probability density function of $\tau(t)$ defined in expression (5.108) reduces to a delta function:

$$\mathcal{P}\left(\tau(t), t | \tau(t_0), t_0\right) = \delta\left(\tau(t) - \tau(t_0) - \int_{t_0}^{t} v(s)ds\right). \tag{5.120}$$

Therefore, for the time changed n-dependent model (5.107), the transition probability function of the stopping time (5.115) becomes:

$$\begin{aligned} f(T_\mathcal{B}) &= \binom{N_{Tot} - n_0}{\mathcal{B}} \frac{d}{dT_\mathcal{B}} \left[ \left( e^{\lambda_0 \int_{t_0}^{t_0+T_\mathcal{B}} v(s)ds} - 1 \right)^{\mathcal{B}} \right. \\ &\quad \left. \times\ {}_2F_1\left(\mathcal{B}, 1 + N_{Tot} - n_0; \mathcal{B}+1; 1 - e^{\lambda_0 \int_{t_0}^{t_0+T_\mathcal{B}} v(s)ds}\right) \right] \\ &= \binom{N_{Tot} - n_0}{\mathcal{B}} \mathcal{B}\, \lambda_0\, v(t_0 + T_\mathcal{B}) \exp\left\{ -\lambda_0 (N_{Tot} - n_0) \int_{t_0}^{t_0+T_\mathcal{B}} v(s)ds \right\} \\ &\quad \times \left( \exp\left\{ \lambda_0 \int_{t_0}^{t_0+T_\mathcal{B}} v(s)ds \right\} - 1 \right)^{\mathcal{B}-1}. \end{aligned} \tag{5.121}$$

And for the n-independent model (5.117), the stopping time density function (5.119) becomes

$$f(T_\mathcal{B}) = \lambda \frac{1}{\Gamma(\mathcal{B})} v(t_0 + T_\mathcal{B}) \exp\left\{ -\lambda \int_{t_0}^{t_0+T_\mathcal{B}} v(s)ds \right\} \left( \lambda \int_{t_0}^{t_0+T_\mathcal{B}} v(s)ds \right)^{\mathcal{B}-1}. \tag{5.122}$$

Especially, when $v(t) = 1$, i.e. in the most simple model $\lambda_{n,t} = \lambda$, the stopping time density can even be simplified as:

$$f(T_\mathcal{B}) = \lambda \frac{(\lambda T_\mathcal{B})^{\mathcal{B}-1}}{\Gamma(\mathcal{B})} e^{-\lambda T_\mathcal{B}}; \tag{5.123}$$

while in the basic n-dependent model (5.94), the distribution of maximum exposure time, as mentioned before, is given by (5.106).

When $v(t)$ is behaving stochastically over time, we have to find the explicit $\mathcal{P}\left(\tau(t), t | \tau(t_0), t_0\right)$'s under different stochastic $v(t)$ processes in order to obtain the final probability distributions of stopping time, see formulas (5.115) and (5.119).

Table 5.1 summarizes these maximum exposure time distributions. This is the main contribution of this section.

**Table 5.1:** Summary of the distributions of the maximum exposure time $f(T_B)$ under different Poisson intensity models.

| | $n$-independent (5.117): $\lambda_{n,t} = \lambda v(t)$ | $n$-dependent (5.107): $\lambda_{n,t} = \lambda_0 (N_{Tot} - n(t))\, v(t)$ |
|---|---|---|
| $v(t) = 1$ | (5.123) | (5.106) |
| deterministic $v(t)$ | (5.122) | (5.121) |
| stochastic $v(t)$ | (5.119) | (5.115) |

### 5.4.6 Fluctuating $v(t)$-process

Since $\tau(t) = \int_0^t v(s)ds$, the derivation of the transition probability function of $\tau(t)$ is analogous to the solution of an arithmetic Asian option when $v(t)$ represents an underlying asset process (218, 219), or it is analogous to the calculation of the density function of the realized variance for variance options when $v(t)$ represents the variance process of an underlying asset process (122).

#### 5.4.6.1 The log-normal process for $v(t)$

The first model we use for the $v(t)$-process is the log-normal model:

$$dv(t) = -\kappa v(t)dt + \sigma v(t)dW(t), \tag{5.124}$$

where $W(t)$ is a Wiener process. This model is similar to the Black-Scholes model, but with negative drift coefficient. Rather than a positive expectation of the underlying's evolving trend, the Poisson intensity of the radioactivity is expected to decay as time goes. We can apply the result (5.15) directly if we replace $r$ in that case to $-\kappa$ , which gives the propagator of $\tau(t)$ ($e^{x(t_0)} = v_{t_0}$):

$$\begin{aligned}\mathcal{P}\left(\tau(t), t|\tau(t_0), t_0\right) = \frac{1}{v_{t_0}} \exp\left\{-\left(\kappa + \frac{\sigma^2}{2}\right)^2 \frac{(t-t_0)}{2\sigma^2}\right\} \int_0^\infty \frac{d\Phi_I}{\pi} \operatorname{Re}\Big[ e^{\Phi(t-t_0)} \\ \times \left(\frac{2\, v_{t_0}}{\sigma^2\left(\tau(t) - \tau(t_0)\right)}\right)^{\mathcal{M}} \frac{\Gamma\left(\mathcal{N} - \mathcal{M}\right)}{\Gamma\left(\mathcal{N}\right)}\, {}_1F_1\left(\mathcal{M}; \mathcal{N}; -\frac{2\, v_{t_0}}{\sigma^2\left(\tau(t) - \tau(t_0)\right)}\right)\Big].\end{aligned} \tag{5.125}$$

where

$$\mathcal{M}\left(\Phi\right) = \sqrt{\frac{2}{\sigma^2}\Phi + \frac{\kappa}{\sigma^2} + \frac{3}{2}}, \quad \mathcal{N}\left(\Phi\right) = 2\sqrt{\frac{2}{\sigma^2}\Phi} + 1. \tag{5.126}$$

So for the time changed n-dependent model (5.107), with $v(t)$ being a log-normal process, the transition probability function of the stopping time can be obtained by plugging the previous formula into expression (5.115):

$$f(T_\mathcal{B}) = \binom{N_{Tot}-n_0}{\mathcal{B}} \int_0^\infty dY \left(e^{\lambda_0 Y}-1\right)^{\mathcal{B}} {}_2F_1\left(\mathcal{B}, 1+N_{Tot}-n_0; \mathcal{B}+1; 1-e^{\lambda_0 Y}\right) \\ \times \frac{1}{v_{t_0}} \int_0^\infty \frac{d\Phi_I}{\pi} \mathrm{Re}\left[\left(\Phi - \frac{(\kappa+\sigma^2/2)^2}{2\sigma^2}\right) \exp\left\{\left(\Phi - \frac{(\kappa+\sigma^2/2)^2}{2\sigma^2}\right) T_\mathcal{B}\right\} \\ \times \left(\frac{2\,v_{t_0}}{\sigma^2 Y}\right)^{\mathcal{M}} \frac{\Gamma(\mathcal{N}-\mathcal{M})}{\Gamma(\mathcal{N})} {}_1F_1\left(\mathcal{M};\mathcal{N};-\frac{2\,v_{t_0}}{\sigma^2 Y}\right)\right]. \tag{5.127}$$

As for the n-independent model (5.117), the stopping time density function is given by rewriting expression (5.119):

$$f(T_\mathcal{B}) = -\frac{1}{v_{t_0}} \int_0^\infty dY \frac{\Gamma(\mathcal{B}, \lambda Y)}{\Gamma(\mathcal{B})} \int_0^\infty \frac{d\Phi_I}{\pi} \mathrm{Re}\left[\left(\Phi - \frac{(\kappa+\sigma^2/2)^2}{2\sigma^2}\right) \left(\frac{2\,v_{t_0}}{\sigma^2 Y}\right)^{\mathcal{M}} \\ \times \exp\left\{\left(\Phi - \frac{(\kappa+\sigma^2/2)^2}{2\sigma^2}\right) T_\mathcal{B}\right\} \frac{\Gamma(\mathcal{N}-\mathcal{M})}{\Gamma(\mathcal{N})} {}_1F_1\left(\mathcal{M};\mathcal{N};-\frac{2\,v_{t_0}}{\sigma^2 Y}\right)\right]. \tag{5.128}$$

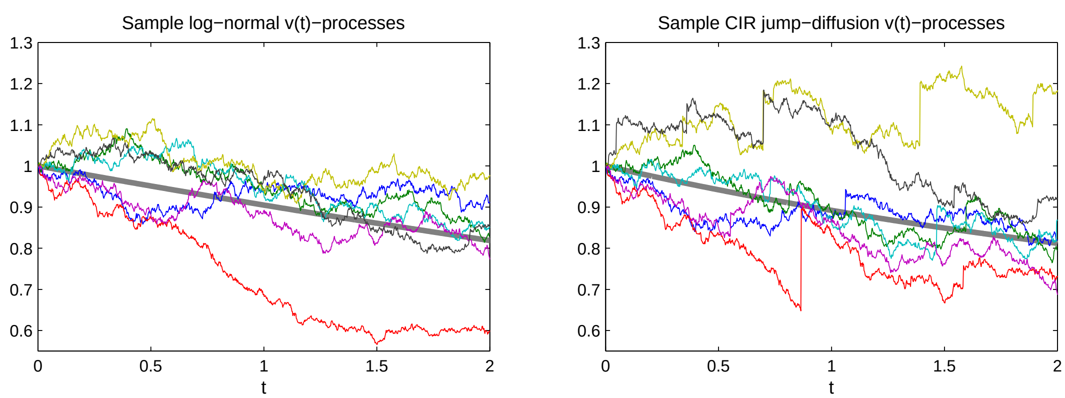


**Figure 5.4:** Sample $v(t)$-processes. The two gray curves are the expectation values of $v(t)$, i.e. $\mathbb{E}_{\mathrm{LN}}[v(t)]$, see (5.134), and $\mathbb{E}_{\mathrm{CIRJ}}[v(t)]$, see (5.135), respectively. Parameter values are chosen to make these two expectation values close to each other: $\kappa = 0.1$, $\sigma = 0.1$, $\kappa_v = 0.3$, $\theta_v = 0.25$, $\sigma_v = 0.1$, $\gamma = 2$, $\eta = 0.05$, $v_{t_0} = 1$.

#### 5.4.6.2 The CIR jump-diffusion process for $v(t)$

The second model we investigate is the CIR jump-diffusion model, defined by:

$$dv(t) = \kappa_v \left(\theta_v - v(t)\right) dt + \sigma_v \sqrt{v(t)} dW(t) + J^v dN(t), \tag{5.129}$$

where $N(t)$ is an independent Poisson process with intensity parameter $\gamma > 0$. We assume the jump density of $J^v$ is given by (5.29): $\varpi(J^v) = \frac{1}{\eta} \exp\left\{-\frac{1}{\eta} J^v\right\}$ with $\eta$ as the mean of the positive jumps. We then can use (5.39) directly ($J^s = 0$) to obtain the propagator of $\tau(t)$, that is:

$$\begin{aligned}\mathcal{P}\left(\tau(t), t | \tau(t_0), t_0\right) = \int_{-\infty}^{\infty} \frac{dp}{2\pi} e^{ip(\tau(t)-\tau(t_0))} \frac{\exp\left\{\frac{\kappa_v^2\theta_v}{\sigma_v^2} T - \left(\frac{2ip}{\kappa_v + 2\omega_v \coth(\omega_v T)}\right) v_{t_0}\right\}}{\left[\sinh(\omega_v T)\left(\frac{\kappa_v}{2\omega_v} + \coth(\omega_v T)\right)\right]^{\frac{2\kappa_v\theta_v}{\sigma_v^2}}} \\ \times \gamma \left[\frac{-2\eta \ln\left[\frac{2ip\eta + \kappa_v}{2\omega_v} \sinh(\omega_v T) + \cosh(\omega_v T)\right] + \left(\sigma_v^2 - \eta\kappa_v\right) T}{\sigma_v^2 - 2\eta\kappa_v - 2ip\eta^2} - T\right],\end{aligned} \tag{5.130}$$

where

$$T = t - t_0, \quad \omega_v = \frac{1}{2}\sqrt{\kappa_v^2 + 2ip\sigma_v^2}. \tag{5.131}$$

Inserting (5.130) into (5.119) and (5.115), we have the target distributions of the stopping times for the CIR jump-diffusion $v(t)$-process.

### 5.4.7 Results and discussion

We now introduce a deterministic $v(t)$-process as

$$v(t) = v_{t_0} \exp\left\{-t/\mathcal{T}\right\} = v_{t_0} \exp\left\{-\kappa t\right\}. \tag{5.132}$$

From which we can interpret $\mathcal{T}$ as the decay time. The previous expression would follow from

$$dv(t) = -\mathcal{T}^{-1} v(t) dt = -\kappa v(t) dt. \tag{5.133}$$

Here we let $\kappa = 1/\mathcal{T}$. Compare (5.133) with (5.124) and we see that the deterministic $v(t)$-process is just the deterministic part of the stochastic log-normal $v(t)$-process. Moreover, the deterministic $v(t)$ (5.132) has the same value as the maximum possible paths of the log-normal $v$-process. Actually the expectation value of $v(t)$ of the log-normal process (5.124) is

$$\mathbb{E}_{\mathrm{LN}}\left[v(t)\right] = \mathbb{E}\left[e^{-\kappa t}\left(v_{t_0} + \int_{t_0}^{t} e^{\kappa u}\sigma v(u)dW(u)\right)\right] = v_{t_0}\exp\left\{-\kappa t\right\}. \tag{5.134}$$

A background 'supply' of radioactive nuclei is modeled by a Wiener process in the log-normal model. This is also the case in the CIR jump-diffusion model (5.129). Furthermore, in the later model, the occasional release of a radioactive material is modeled by the jump process. We can also calculate the expectation value of $v(t)$ under the CIR jump-diffusion model:

$$\begin{aligned}
\mathbb{E}_{\mathrm{CIRJ}}\left[v(t)\right] &= \mathbb{E}\left[e^{-\kappa t}\left(v_{t_0} + \int_{t_0}^{t} e^{\kappa_v u}\left(\left(\kappa_v\theta_v + \gamma J^v\right)du + \sigma_v\sqrt{v(u)}dW(u)\right)\right)\right] \\
&= e^{-\kappa t}\left(v_{t_0} + \int_{t_0}^{t} e^{\kappa_v u}\left(\kappa_v\theta_v + \gamma\eta\right)du\right) \\
&= \left(\theta_v + \frac{\gamma\eta}{\kappa_v}\right) + \left(v_{t_0} - \left(\theta_v + \frac{\gamma\eta}{\kappa_v}\right)\right)\exp\left\{-\kappa_v t\right\}.
\end{aligned} \tag{5.135}$$

Unlike $\mathbb{E}_{\mathrm{LN}}\left[v(t)\right]$ that decreases exponentially from $v_{t_0}$ to zero as time goes, $\mathbb{E}_{\mathrm{CIRJ}}\left[v(t)\right]$ will decrease exponentially from $v_{t_0}$ when $v_{t_0} > \left(\theta_v + \frac{\gamma\eta}{\kappa_v}\right)$, and the asymptotic value is $\theta_v + \frac{\gamma\eta}{\kappa_v}$. This long-term level is positive, but it is not a problem if the model for $\lambda_{n,t}$ is $n$-dependent, since $N_{tot} - n(t)$ trends zero given a very long time. Note also that both $\mathbb{E}_{\mathrm{LN}}\left[v(t)\right]$ and $\mathbb{E}_{\mathrm{CIRJ}}\left[v(t)\right]$ do not dependent on their diffusion coefficients $\sigma$ and $\sigma_v$, respectively.

Figure 5.4 illustrates some samples of both the log-normal and CIR jump-diffusion $v(t)$-processes. The two solid gray curves are the expectation values $\mathbb{E}_{\mathrm{LN}}\left[v(t)\right]$, which equals the deterministic $v(t)$-process, and $\mathbb{E}_{\mathrm{CIRJ}}\left[v(t)\right]$. Parameter values are chosen such that these two expectation values are close to each other during the time region $t - t_0 \in [0, 2]$. One can image that given feasible parameter values, these stochastic $v(t)$-processes will hopefully make the description of $\lambda_{n,t}$ more accurate. The left panel of Figure 5.5 represents $\mathcal{P}\left(\tau(1), 1|\tau(0), 0\right)$ under the deterministic, the log-normal and the CIR jump-diffusion $v(t)$-processes, see (5.120), (5.125) and (5.130) respectively. Since the expectation values of $v(t)$ are given close to each other, the expectation values of $\tau(1) - \tau(0) = \int_0^1 v(t)dt$ are also close to each other for these three cases, which can be seen from the left panel of

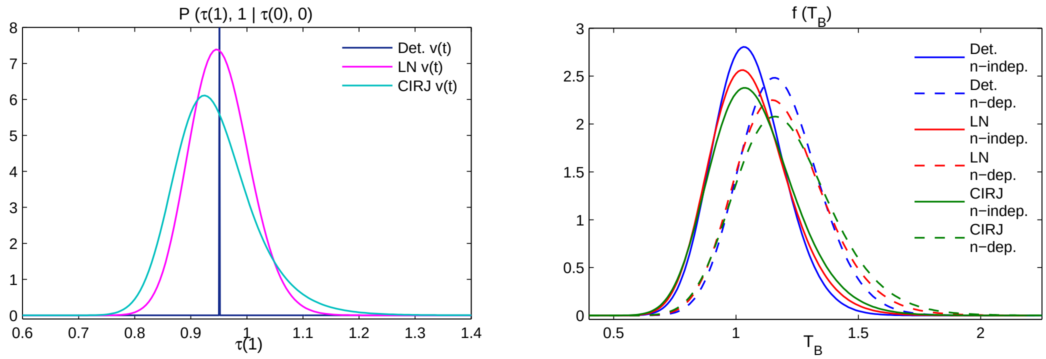


**Figure 5.5:** The left panel represents the propagators of $\tau(t)$ for the deterministic (Det.), the log-normal (LN), and the CIR jump-diffusion (CIRJ) $v(t)$-processes at time $t = 1$. The right panel shows the corresponding stopping time distributions for the n-independent and n-dependent models. The same parameter values are used as in Figure 5.4, and $\lambda_0 = 0.2$, $N_{Tot} - n_0 = 300$, $\lambda = \lambda_0 (N_{Tot} - n_0) = 60$, $\mathcal{B} = 60$.

Figure 5.5. The $\mathcal{P}(\tau(1), 1|\tau(0), 0)$ for deterministic $v(t)$ is a delta function, with a zero variance. The variance of the log-normal case is determined by $\sigma$, and the CIR jump-diffusion case is determined by $\sigma_v$ as well as jump parameters, which also make its $\mathcal{P}(\tau(1), 1|\tau(0), 0)$ strongly negative skewed due to positive jumps.

The right panel of Figure 5.5 shows the distributions of the maximum exposure time under these 3 (three $v(t)$-processes) times 2 (n-independent and -dependent) models. If we focus on the three n-independent results, we see that similar expectation values of $v(t)$ lead to similar expected maximum exposure time, and the more fluctuating the $v(t)$-process, the larger the variance of the density of $\tau(t)$, thus the wider the range of the maximum exposure time. In other words, the fluctuation of the radioactive decay strengths the possibility of both very short and very long maximum exposure time. The parameter values chosen in Figure 5.5 are such that $\lambda_0 (N_{Tot} - n(t))$ equals $\lambda$ only at the initial time $t = t_0$. At later times, $\lambda_0 (N_{Tot} - n(t)) < \lambda$, that is why the expected maximum exposure times for the $n$-dependent models are larger than those for the $n$-independent models, but their results for three different $v(t)$-processes are similar. Nevertheless, these three results for $n$-dependent models in the right panel of Figure 5.5 are not a simple parallel shift of the results for the $n$-independent models, their shapes are also widened. This can be explained by the fact that comparing to a constant $\lambda$, the effect of a time changing $\lambda_0 \left(N_{Tot} - n(t)\right)$ to $\lambda_{n,t}$ is similar to the effect of jumps, both of which widens the variance of $\lambda_{n,t}$, thus lengthen the allowed exposure time. The importance of $n$-dependent model also lies in the binomial distribution, which rules out the possibility of decaying more number of radionuclides than that available at $t = t_0$.

Next we exam the effects of different parameters on the allowed exposure time. For ease of presentation, we consider here the $n$-independent models. Figure 5.6 demonstrates their effects. The default parameter values are those used in Figure 5.4. We then increase one parameter value in each case while keeping the others to be the same. As seen before, $\kappa$ in the log-normal process has a meaning of the inverse of the decay time $\mathcal{T}$, so an increase of the value of $\kappa$ makes the expected allowed exposure time longer than the default one. The parameter $\kappa_v$ in the CIR jump-diffusion has a similar effect. The parameters $\sigma$ and $\sigma_v$ determine the fluctuation, but have nothing to do with the mean, of their processes. So larger values of $\sigma$ and $\sigma_v$ do not change the expected maximum exposure time, but mainly widen the range of allowed exposure time. The parameters $\theta_v$, $\gamma$ and $\eta$ dominant both the speed of approaching the long-term level of $\mathbb{E}_{\mathrm{CIRJ}}\left[v(t)\right]$ and the long-term level itself, see expression (5.135). An increase of these three parameter values keeps the values of $v(t)$ in a high level, thus shorten the allowed exposure time.

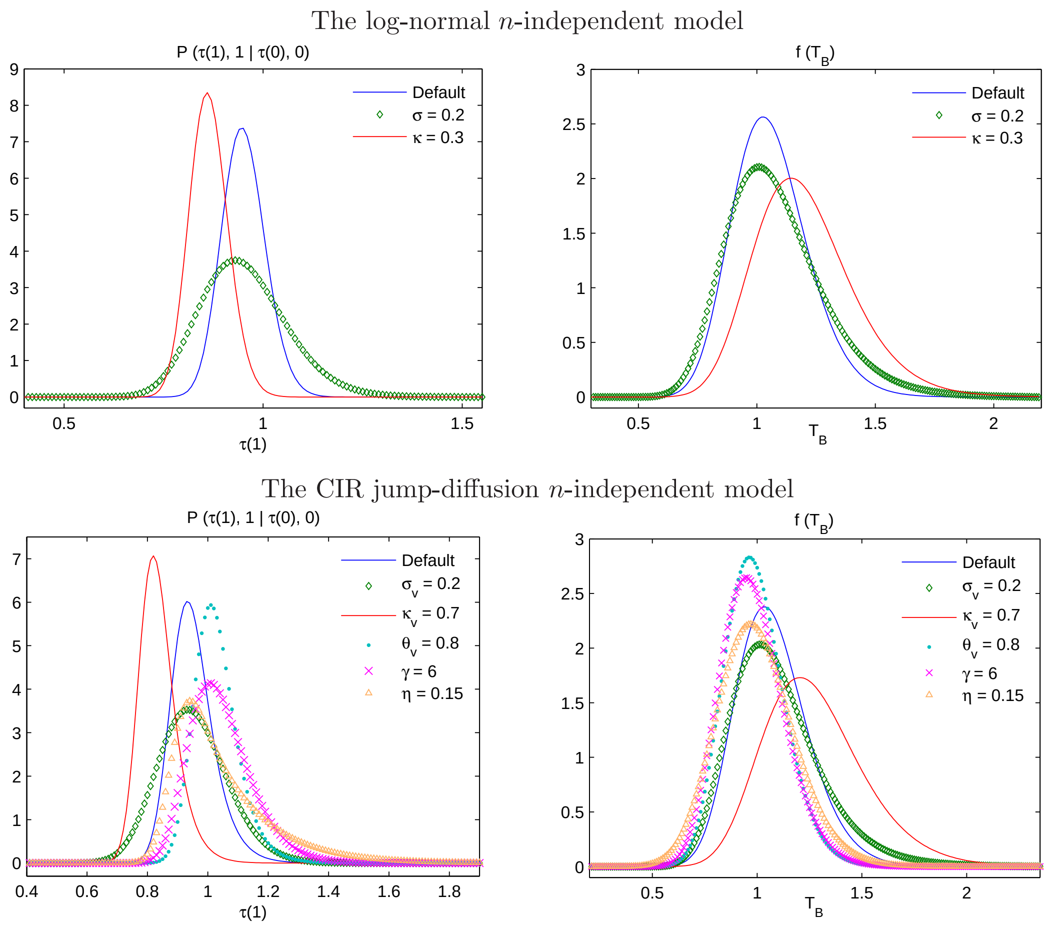


**Figure 5.6:** The upper panels represent the propagators of $\tau(t)$ for the log-normal $v(t)$-processes at time $t = 1$ (left), and the corresponding stopping time distributions for the n-independent models (right). The bottom panels are those for the CIR jump-diffusion $v(t)$-processes. The default parameter values are the same as those used in Figure 5.4. For others, only one parameter value is changed in each case.

# 6

# COS and PDE approaches to the pricing of some common exotic options under the HCIR model

In this chapter, I price some common exotic options, namely the discretely-monitored arithmetic Asian option, the Bermudan option (discrete barrier option as a special case) and the American option, under the Heston stochastic volatility (76) with uncorrelated Cox-Ingersoll-Ross (150) stochastic interest rate model. I will call it the HCIR model for short. As mentioned in Chapter 1, models with stochastic interest rate processes are essential for interest rate sensitive derivatives. In the HCIR model, the uncertainty stemming from interest rate is taken into account. However, the stochastic interest rate process is assumed to be uncorrelated with both the underlying asset and the volatility process, which fits the model in the class of affine diffusion processes (84) and a closed-form propagator as well as the characteristic function are available, see (115, 220). The analytical tractability of this model allows us to get efficient pricing formulas. For the hybrid Heston model with correlated stochastic interest rates, as far as I know, no analytical formula exists in literature, whereas approximate solutions for these models can be found, among others, in (221, 222, 223, 224).

The closed-form joint propagator of the HCIR model is the basis of the derivation of exotic option pricing formulas in this chapter. I derive this propagator in the framework of path integral, following Lemmens (115). These three-dimensional pricing problems are then treated by a generalization of the COS method developed by Oosterlee and co-workers (143, 225, 226, 227, 228). Zhang and Oosterlee recently proposed a pricing method based on the COS method for both the European-style discrete geometric and arithmetic Asian options under Lévy processes (227), which can be seen as an efficient alternative to our paper on pricing up and low bounds for discrete arithmetic Asian options under Lévy models (229). Efficient pricing formulas for Bermudan and discrete barrier options by COS method are developed by Fang and Oosterlee under both the exponential Lévy aset price models (225) and the Heston model (226). The price of American options are obtained in (225) by applying a Richardson extrapolation (230) on the prices of a few Bermudan options with small early-exercise dates. Another pricing approach based on the finite difference method can be found in (231). In that paper, Haentjens, In't Hout and Volders priced American put option in the Heston model by combining the Ikonen-Toivanen splitting approach (232, 233) with alternating direction implicit (ADI) schemes (234). Recently, ADI finite difference schemes for the Heston-Hull-White model was investigated by Haentjens and In't Hout for both the European vanilla call options and the up-and-out call barrier options (224).

This chapter is based on part of my work notes. I will study both the COS method and the FD method for exotic options under the HCIR model. Nevertheless, neither error analysis for the application of the COS method nor the testing of the stability of the FD method performed in this chapter is given. For the European vanilla options, not surprisingly, the COS method performs outstanding. For the discrete arithmetic Asian options, I focus on the COS method and the results are checked by Monte-Carlo simulations. For the Bermudan options, results from the COS method and FD method are compared. For the American put options, I focus on the FD method, and compare the performances of the Ikonen-Toivanen splitting approach and the Richardson extrapolation approach.

The chapter is organized as follows. In section 6.1, we derive the joint propagator of our model by the path integral approach. In section 6.2, the COS method is introduced, and the European vanilla option pricing formula is obtained as an quick example. Section 6.3 is devoted to the pricing of the discretely-monitored arithmetic Asian option. Discretely-monitored Bermudan options are priced in section 6.4, which is followed by the discussion of the pricing problems of barrier and American options in section 6.5. In section 6.6, a ADI finite difference scheme is introduced, and the numerical results of American put options with the Ikonen-Toivanen splitting as well as the Richardson extrapolation are shown. Section 6.7 gives a short discussion about the reason why it is time consuming to solve three-dimensional pricing problems by using the COS method directly.

## 6.1 The joint propagators of the HCIR model

In this section, following the derivation outlined in (115), we express the essential propagators in the path integral treatment. The HCIR model is specified by the following system of SDEs:

$$\begin{aligned} dS(t) &= r(t)S(t)dt + \sqrt{v(t)}S(t)dW_1(t), && (6.1)\\ dv(t) &= \kappa\left(\theta - v(t)\right)dt + \sigma\sqrt{v(t)}\left(\rho dW_1(t) + \sqrt{1-\rho^2}dW_2(t)\right), && (6.2)\\ dr(t) &= \kappa_r\left(\theta_r - r(t)\right)dt + \sigma_r\sqrt{r(t)}dW_3(t), && (6.3) \end{aligned}$$

where $S(t)$ represents the underlying asset process with its variance $v(t)$ and the risk free interest rate $r(t)$, both of which evolve stochastically over time. $W_i(t)\,\{i = 1, 2, 3\}$ are independent Brownian processes. Other parameters in this model are constants. Especially, the parameter $\rho \in [-1, 1]$ is the correlation coefficient. The substitutions (with $c$ being a constant)

$$\begin{aligned} x(t) &= \ln S(t) + c, && (6.4)\\ y(t) &= x(t) - \frac{\rho}{\sigma}\left(v(t) - \kappa\theta t\right), && (6.5)\\ z(t) &= \sqrt{v(t)}, && (6.6)\\ \zeta(t) &= \sqrt{r(t)}, && (6.7) \end{aligned}$$

lead to three new independent processes as follows:

$$\begin{aligned} dy &= \left[\zeta^2 + \left(\frac{\rho\kappa}{\sigma} - \frac{1}{2}\right)z^2\right]dt + z\sqrt{1-\rho^2}dW_1(t), && (6.8)\\ dz &= \left[\frac{\kappa\theta - \sigma^2/4}{2z} - \frac{\kappa}{2}z\right]dt + \frac{\sigma}{2}dW_2(t), && (6.9)\\ d\zeta &= \left[\frac{\kappa_r\theta_r - \sigma_r^2/4}{2r} - \frac{\kappa_r}{2}\zeta\right]dt + \frac{\sigma_r}{2}dW_3(t). && (6.10) \end{aligned}$$

Their Lagrangians are then calculated according to (2.19):

$$\begin{aligned}
\mathcal{L}[\dot{y}, z, \zeta] &= \frac{\left[\dot{y} - \left(\zeta^2 + (\rho\kappa/\sigma - 1/2)\, z^2\right)\right]^2}{2\,(1-\rho^2)\, z^2}, && (6.11)\\
\mathcal{L}[\dot{z}, z] &= \frac{2}{\sigma^2}\dot{z}^2 - \frac{2\,(\kappa\theta - \sigma^2/4)}{\sigma^2}\frac{\dot{z}}{z} + \frac{2\kappa}{\sigma^2} z\dot{z} \\
&\quad + \frac{(\kappa\theta - \sigma^2/4)\,(\kappa\theta - 3\sigma^2/4)}{2\sigma^2 z^2} + \frac{\kappa^2}{2\sigma^2} z^2 - \frac{\kappa^2\theta}{\sigma^2}, && (6.12)\\
\mathcal{L}[\dot{\zeta}, \zeta] &= \frac{2}{\sigma_r^2}\dot{\zeta}^2 - \frac{2\,(\kappa_r\theta_r - \sigma_r^2/4)}{\sigma_r^2}\frac{\dot{\zeta}}{\zeta} + \frac{2\kappa_r}{\sigma_r^2}\zeta\dot{\zeta} \\
&\quad + \frac{(\kappa_r\theta_r - \sigma_r^2/4)\,(\kappa_r\theta_r - 3\sigma_r^2/4)}{2\sigma_r^2 \zeta^2} + \frac{\kappa_r^2}{2\sigma_r^2}\zeta^2 - \frac{\kappa_r^2\theta_r}{\sigma_r^2}. && (6.13)
\end{aligned}$$

The joint propagator of these three independent processes $(y, z, \zeta)$ for $y = y_T$, $z = z_T$, $\zeta = \zeta_T$ at time $t = T$ given the initial values $y_0$, $z_0$ and $\zeta_0$ at time $t = 0$ is denoted by $\mathcal{P}\left(y_T, z_T, \zeta_T | y_0, z_0, \zeta_0\right)$, and can be written in the path integral treatment as:

$$\begin{aligned}
&\mathcal{P}\left(y_T, z_T, \zeta_T | y_0, z_0, \zeta_0\right) \\
&= \int \mathcal{D}y(t) \int \mathcal{D}z(t) \int \mathcal{D}\zeta(t) \exp\left\{-\int_0^T \left(\mathcal{L}[\dot{y}, z, \zeta] + \mathcal{L}[\dot{z}, z] + \mathcal{L}[\dot{\zeta}, \zeta]\right) dt\right\}.
\end{aligned} \tag{6.14}$$

This joint propagator is normalized, which means that

$$\int_{-\infty}^{\infty}\int_0^{\infty}\int_0^{\infty} \mathcal{P}\left(y_T, z_T, \zeta_T | y_0, z_0, \zeta_0\right) dz_T d\zeta_T dy_T = 1. \tag{6.15}$$

However, for risk-neutral option pricing, the discount factor $e^{-\int_0^T r(t)dt} = e^{-\int_0^T \zeta^2(t)dt}$ has to be taken into account. Consequently, we focus on the derivation of the so called modified joint propagator:

$$\begin{aligned}
\bar{\mathcal{P}}\left(y_T, z_T, \zeta_T | y_0, z_0, \zeta_0\right) &= \int \mathcal{D}y(t) \int \mathcal{D}z(t) \int \mathcal{D}\zeta(t) \\
&\quad \times \exp\left\{-\int_0^T \left(\mathcal{L}[\dot{y}, z, \zeta] + \mathcal{L}[\dot{z}, z] + \mathcal{L}[\dot{\zeta}, \zeta] + \zeta^2(t)\right) dt\right\}.
\end{aligned} \tag{6.16}$$

Direct calculation yields the following expression:

$$
\begin{aligned}
& \bar{\mathcal{P}}\left(y_T, z_T, \zeta_T | y_0, z_0, \zeta_0\right) \\
= \; & \left(\frac{z_T}{z_0}\right)^{\frac{2\kappa\theta}{\sigma^2}-\frac{1}{2}} e^{-\frac{\kappa}{\sigma^2}\left(z_T^2 - z_0^2 - \kappa\theta T\right)} \left(\frac{\zeta_T}{\zeta_0}\right)^{\frac{2\kappa_r\theta_r}{\sigma_r^2}-\frac{1}{2}} e^{-\frac{\kappa_r}{\sigma_r^2}\left(\zeta_T^2 - \zeta_0^2 - \kappa_r\theta_r T\right)} \\
& \times \int_{-\infty}^{\infty} \frac{dl}{2\pi}\, e^{-il(x_T - x_0)}\, e^{il\frac{\rho}{\sigma}\left(z_T^2 - z_0^2 - \kappa\theta T\right)} \\
& \times \frac{4\omega\sqrt{z_T z_0}}{\sigma^2 \sinh\left(\omega T\right)}\, e^{-\frac{2\omega\coth(\omega T)}{\sigma^2}\left(z_T^2 + z_0^2\right)}\, I_{\frac{2\kappa\theta}{\sigma^2}-1}\left(\frac{4\omega z_0 z_T}{\sigma^2 \sinh\left(\omega T\right)}\right) \\
& \times \frac{4\omega_r\sqrt{\zeta_T \zeta_0}}{\sigma_r^2 \sinh\left(\omega_r T\right)}\, e^{-\frac{2\omega_r\coth(\omega_r T)}{\sigma_r^2}\left(\zeta_T^2 + \zeta_0^2\right)}\, I_{\frac{2\kappa_r\theta_r}{\sigma_r^2}-1}\left(\frac{4\omega_r \zeta_0 \zeta_T}{\sigma_r^2 \sinh\left(\omega_r T\right)}\right), \qquad (6.17)
\end{aligned}
$$

where

$$
\omega(l) = \frac{\sigma}{2}\sqrt{\left(\frac{\kappa}{\sigma} - il\rho\right)^2 + l\left(l+i\right)}, \qquad (6.18)
$$

$$
\omega_r(l) = \frac{\sigma_r}{2}\sqrt{\left(\frac{\kappa_r}{\sigma_r}\right)^2 + 2\left(1 - il\right)}, \qquad (6.19)
$$

Note that the original propagator $\mathcal{P}\left(y_T, z_T, \zeta_T | y_0, z_0, \zeta_0\right)$ has the same formula as the risk-neutral propagator $\bar{\mathcal{P}}\left(y_T, z_T, \zeta_T | y_0, z_0, \zeta_0\right)$ except for the term $\omega_r(l)$, which in the original joint propagator would be:

$$
\omega_r(l) = \sqrt{\frac{\sigma_r^2}{2}\left(\frac{\kappa_r^2}{2\sigma_r^2} - il\right)} = \frac{\sigma_r}{2}\sqrt{\left(\frac{\kappa_r}{\sigma_r}\right)^2 - 2il}. \qquad (6.20)
$$

Expression (6.17) is expressed in the original variable $x$ rather than in $y$, we can write the modified propagator $\bar{\mathcal{P}}\left(y_T, z_T, \zeta_T | y_0, z_0, \zeta_0\right)$ as $\bar{\mathcal{P}}\left(x_T, z_T, \zeta_T | x_0, z_0, \zeta_0\right)$. Furthermore, we write the expression (6.17) in the form of a Fourier transform:

$$
\bar{\mathcal{P}}\left(x_T, z_T, \zeta_T | x_0, z_0, \zeta_0\right) = \int_{-\infty}^{\infty} \frac{dl}{2\pi}\, e^{-il(x_T - x_0)}\, \Phi(l, T, z_T, \zeta_T | z_0, \zeta_0), \qquad (6.21)
$$

where $\Phi(l, T, z_T, \zeta_T | z_0, \zeta_0)$ represents the characteristic function of $x_T$ given $z_T$ and $\zeta_T$ as final points, and $z_0$ and $\zeta_0$ as initial points over the time interval $[0, T]$, that is $\Phi(l, T, z_T, \zeta_T | z_0, \zeta_0) = \mathbb{E}\left[e^{il(x_T - x_0)} | z_T, \zeta_T, z_0, \zeta_0\right]$.

The integrals over $z_T$ and $\zeta_T$ can be done analytically, leading to the modified marginal propagator of $x$:

$$\begin{aligned}
& \bar{\mathcal{P}}\left(x_T|x_0, z_0, \zeta_0\right) \\
= & \int_0^\infty dz_T \int_0^\infty d\zeta_T \bar{\mathcal{P}}\left(x_T, z_T, \zeta_T|x_0, z_0, \zeta_0\right) \\
= & \int_{-\infty}^\infty \frac{dl}{2\pi}\, e^{-il(x_T-x_0)}\, e^{\left(\frac{\kappa}{\sigma^2}-il\frac{\rho}{\sigma}\right)(v_0+\kappa\theta T)}\, H^{\frac{2\kappa\theta}{\sigma^2}}\, e^{\frac{2\omega}{\sigma^2}\left(\frac{N}{\sinh(\omega T)}-\coth(\omega T)\right)v_0} \\
& \times e^{\frac{\kappa_r}{\sigma_r^2}(r_0+\kappa_r\theta_r T)}\, H_r^{\frac{2\kappa_r\theta_r}{\sigma_r^2}}\, e^{\frac{2\omega_r}{\sigma_r^2}\left(\frac{N_r}{\sinh(\omega_r T)}-\coth(\omega_r T)\right)r_0},
\end{aligned} \tag{6.22}$$

where

$$H(l) = \left(\cosh(\omega T) + \frac{\kappa - il\rho\sigma}{2\omega}\sinh(\omega T)\right)^{-1}, \tag{6.23}$$

$$H_r(l) = \left(\cosh(\omega_r T) + \frac{\kappa_r}{2\omega_r}\sinh(\omega_r T)\right)^{-1}. \tag{6.24}$$

Expression (6.22) can be written as

$$\bar{\mathcal{P}}\left(x_T|x_0, z_0, \zeta_0\right) = \int_{-\infty}^\infty \frac{dl}{2\pi}\, e^{-il(x_T-x_0)}\, \phi(l, T|z_0, \zeta_0), \tag{6.25}$$

then $\phi(l, T|z_0, \zeta_0)$ is the characteristic function of $x_T$ given initial values $z_0$ and $\zeta_0$ over the time interval $[0, T]$, that is $\phi(l, T|z_0, \zeta_0) = \mathbb{E}\left[e^{il(x_T-x_0)}|z_0, \zeta_0\right]$.

## 6.2 European vanilla options

In this section, we derive the European vanilla put option pricing formula under the HCIR model as an illustration of the COS method originally introduced by Fang and Oosterlee (143).

Define the transition probability density function a random variable $x$ by $\mathcal{P}(x|\mathcal{F})$, where $\mathcal{F}$ is the set of conditional variables, and the corresponding conditional characteristic function by

$$\mathrm{ChF}(u|\mathcal{F}) = \mathbb{E}\left[e^{iu(x-x_0)}\right] = \int_{-\infty}^\infty e^{iu(x-x_0)}\, \mathcal{P}(x|\mathcal{F})\, dx, \tag{6.26}$$

where $x_0$ is the value of $x$ at initial time.

The COS method is based on Fourier cosine series expansions. One starts by truncating the integration range of the probability density function $\mathcal{P}(x|\mathcal{F})$ from $[-\infty, \infty]$ to a feasible range $[a, b]$ without loosing accuracy. One then recovers this probability density by a Fourier cosine series expansion ($L = b - a$):

$$\mathcal{P}(x|\mathcal{F}) = \sum_{n=0}^{\infty}{}' P_n(\mathcal{F}) \cos\left(n\pi \frac{x-a}{L}\right), \tag{6.27}$$

where $\sum'$ indicates that the first element in the summation is multiplied by one-half. The essence of the COS method lies in the insight that the Fourier cosine coefficients $P_n$ can be accurately retrieved from the corresponding characteristic function $\mathrm{ChF}(u|\mathcal{F})$. More explicitly,

$$\begin{aligned}
P_n(\mathcal{F}) &= \frac{2}{L}\int_a^b \mathcal{P}(x|\mathcal{F}) \cos\left(n\pi\frac{x-a}{L}\right) dx \\
&\approx \frac{2}{L}\int_{-\infty}^{\infty} \mathcal{P}(x|\mathcal{F}) \cos\left(n\pi\frac{x-a}{L}\right) dx \\
&= \frac{2}{L}\int_{-\infty}^{\infty} \mathcal{P}(x|\mathcal{F}) \,\mathrm{Re}\left\{e^{in\pi\frac{x-a}{L}}\right\} dx \\
&= \frac{2}{L}\mathrm{Re}\left\{\int_{-\infty}^{\infty} \mathcal{P}(x|\mathcal{F})\, e^{in\pi\frac{x-x_0}{L}}\, e^{in\pi\frac{x_0-a}{L}} dx\right\} \\
&= \frac{2}{L}\mathrm{Re}\left\{\mathrm{ChF}\left(\frac{n\pi}{L}\middle|\mathcal{F}\right) e^{in\pi\frac{x_0-a}{L}}\right\}.
\end{aligned} \tag{6.28}$$

Substituting $P_n$ in (6.28) into (6.27) and truncating the series by a feasible finite number of terms, say $N$ terms, one obtains a semi-analytic formula which accurately approximates the probability density:

$$\mathcal{P}(x|\mathcal{F}) \approx \frac{2}{L}\sum_{n=0}^{N-1}{}' \mathrm{Re}\left[\mathrm{ChF}\left(\frac{n\pi}{L}\middle|\mathcal{F}\right) \exp\left\{in\pi\frac{x_0-a}{L}\right\}\right] \cos\left(n\pi\frac{x-a}{L}\right). \tag{6.29}$$

Note that the probability density function of variable $x$ is now decomposed into a linear combination of cosine functions, where $x$ is treated separately from other variables $\mathcal{F}$. The strength of the method is precisely this factorization: the expected payoff will often be an integral over $x$ involving the cosine factor and often analytically calculatable for any given $n$. This can be demonstrated with European vanilla options.

**Table 6.1:** European vanilla put option prices. The rows closed-form are from reference (223), whereas the rows COS are from expression (6.30). Parameter values used here are the same as those used in Table 3 of reference (223): $S_0 = 100$, $r_0 = 0.04$, $\theta = 0.02$, $\kappa_r = 0.3$, $\theta_r = 0.04$, $\sigma_r = 0.1$. Parameters for COS method are: $a = -1.5$, $b = 1.5$, $N = 128$.

| Method | $K = 90$ | | | $K = 100$ | | | $K = 110$ | | |
|---|---|---|---|---|---|---|---|---|---|
| | $T = \frac{1}{12}$ | $T = \frac{1}{4}$ | $T = \frac{1}{2}$ | $T = \frac{1}{12}$ | $T = \frac{1}{4}$ | $T = \frac{1}{2}$ | $T = \frac{1}{12}$ | $T = \frac{1}{4}$ | $T = \frac{1}{2}$ |
| | | | | $v_0 = 0.01,\ \kappa = 1.5,\ \sigma = 0.15,\ \rho = 0.1$ | | | | | |
| closed-form | 0.0001 | 0.0335 | 0.1965 | 1.0160 | 1.6492 | 2.2254 | 9.6358 | 9.0701 | 8.6410 |
| COS | 0.0001 | 0.0335 | 0.1965 | 1.0160 | 1.6492 | 2.2254 | 9.6358 | 9.0701 | 8.6410 |
| | | | | $v_0 = 0.04,\ \kappa = 0.75,\ \sigma = 0.3,\ \rho = 0.1$ | | | | | |
| closed-form | 0.0603 | 0.5205 | 1.1439 | 2.1009 | 3.3156 | 4.1999 | 9.7904 | 10.0156 | 10.3200 |
| COS | 0.0603 | 0.5205 | 1.1439 | 2.1009 | 3.3156 | 4.1999 | 9.7904 | 10.0156 | 10.3200 |
| | | | | $v_0 = 0.04,\ \kappa = 1.5,\ \sigma = 0.3,\ \rho = 0.1$ | | | | | |
| closed-form | 0.0577 | 0.4849 | 1.0383 | 2.0844 | 3.2441 | 4.0467 | 9.7850 | 9.9594 | 10.1657 |
| COS | 0.0577 | 0.4849 | 1.0383 | 2.0844 | 3.2441 | 4.0467 | 9.7850 | 9.9594 | 10.1657 |
| | | | | $v_0 = 0.04,\ \kappa = 1.5,\ \sigma = 0.15,\ \rho = -0.5$ | | | | | |
| closed-form | 0.0767 | 0.5903 | 1.2490 | 2.0998 | 3.3147 | 4.2085 | 9.7405 | 9.8073 | 9.9877 |
| COS | 0.0767 | 0.5903 | 1.2490 | 2.0998 | 3.3147 | 4.2085 | 9.7405 | 9.8073 | 9.9877 |

Denoting the European vanilla put option with strike price $K$ and time to maturity $T$ by $\mathscr{P}_{Eur}(K)$, and applying the COS method, we have the risk-neutral pricing formula ($x(t) = \ln S(t)/K$):

$$
\begin{aligned}
\mathscr{P}_{Eur}(K) =& \mathbb{E}\left[e^{-\int_0^T r(t)dt} \max\{K - S_T, 0\}\right] \\
\approx& \int_a^0 \left(K - K\, e^{x_T}\right) \bar{\mathcal{P}}\left(x_T | x_0, z_0, \zeta_0\right) dx_T \\
\approx& \int_a^0 dx_T K \left(1 - e^{x_T}\right) \\
& \times \frac{2}{L} \sum_{n=0}^{N-1}{}' \operatorname{Re}\left\{\phi\left(\frac{n\pi}{L}, T | z_0, \zeta_0\right) e^{in\pi\frac{x_0 - a}{L}}\right\} \cos\left(n\pi \frac{x_T - a}{L}\right) \\
=& \frac{2}{L} K \sum_{n=0}^{N-1}{}' \left[\psi_n(a, 0) - \chi_n(a, 0)\right] \operatorname{Re}\left\{\phi\left(\frac{n\pi}{L}, T | z_0, \zeta_0\right) e^{in\pi\frac{x_0 - a}{L}}\right\},
\end{aligned}
\tag{6.30}
$$

where

$$\begin{aligned}\psi_n(c,d) &= \int_c^d \cos\left(n\pi\frac{y-a}{L}\right) dy \\ &= \begin{cases} \left[\sin\left(n\pi\frac{d-a}{L}\right) - \sin\left(n\pi\frac{c-a}{L}\right)\right]\frac{L}{n\pi} & \text{for} \quad n \neq 0, \\ d-c & \text{for} \quad n = 0. \end{cases}\end{aligned} \tag{6.31}$$

and

$$\begin{aligned}\chi_n(c,d) &= \int_c^d e^y \cos\left(n\pi\frac{y-a}{L}\right) dy \\ &= \frac{1}{1+\left(\frac{n\pi}{L}\right)^2}\left[\begin{array}{l} \cos\left(n\pi\frac{d-a}{L}\right) e^d - \cos\left(n\pi\frac{c-a}{L}\right) e^c \\ +\frac{n\pi}{L}\sin\left(n\pi\frac{d-a}{L}\right) e^d - \frac{n\pi}{L}\sin\left(n\pi\frac{c-a}{L}\right) e^c \end{array}\right].\end{aligned} \tag{6.32}$$

By using the same parameter values as those used in Table 3 of reference (223), we calculated our pricing formula (6.30) by choosing $a = -1.5$, $b = 1.5$, $N = 128$. In Table 6.1, results from (6.30) are presented in rows COS, while those given in (223) are presented in rows closed-form. We see that they are exactly the same. MATLAB 7.10.0 is used, and the average CPU time cost for every case (with three different strike prices) is about 0.005 second in my computer. For the closed-form calculations, the average CPU time is about 0.1 second.

## 6.3 Discrete Arithmetic Asian options

For $M$ equally spaced monitoring dates at times $\{t_m, t_m < t_{m+1} | m = 0, 1, \cdots, M\}$ with $t_M = T$ and $\Delta t = t_{m+1} - t_m$, the price of an discrete arithmetic Asian put option with a fixed strike price $K$, denoted by $\mathscr{P}_{Asi}(K)$, is expressed as

$$\mathscr{P}_{Asi}(K) = \mathbb{E}\left[e^{-\int_0^T r(t)dt}\max\left\{K - \frac{1}{M+1}\sum_{j=0}^{M} S_j, 0\right\}\right]. \tag{6.33}$$

where $S_m = S(t_m)$. The dependence of the term $\sum_{j=0}^{M} S_j$ on the whole set of monitoring dates is inconvenient, so a set of variables to split this term into $M$ related parts is introduced, see (227) and references therein:

$$Y_0 = 0, \quad Y_j = \ln\frac{S_{M+1-j}}{S_{M-j}} + \ln\left(1 + e^{Y_{j-1}}\right) \text{ for } j = 1, 2, \cdots, M. \tag{6.34}$$

More explicitly

$$\begin{aligned}
Y_1 &= \ln \frac{S_M}{S_{M-1}} \\
Y_2 &= \ln \frac{S_{M-1}}{S_{M-2}} + \ln \frac{S_M + S_{M-1}}{S_{M-1}} = \ln \frac{S_M + S_{M-1}}{S_{M-2}} \\
&\vdots \\
Y_M &= \ln \frac{S_M + S_{M-1} + \cdots + S_1}{S_0}. \qquad (6.35)
\end{aligned}$$

Therefore, $\sum_{j=0}^{M} S_j = S_0 \left(1 + e^{Y_M}\right)$ and

$$\begin{aligned}
\mathscr{P}_{Asi}(K) &= \mathbb{E}\left[e^{-\int_0^T r(t)dt} \max\left\{K - \frac{S_0}{M+1}\left(1 + e^{Y_M}\right), 0\right\}\right] \\
&= \int_{-\infty}^{\infty} \left(K - \frac{S_0}{M+1}\left(1 + e^{Y_M}\right)\right)_+ \bar{\mathcal{P}}(Y_M)\, dY_M \\
&\approx \frac{2}{L} {\sum_{n=0}^{N-1}}' \left[\left(K - \frac{S_0}{M+1}\right) \psi_n(a, y^*) - \frac{S_0}{M+1} \chi_n(a, y^*)\right] \\
&\quad \times \mathrm{Re}\left\{\varphi_{Y_M}\left(\frac{n\pi}{L}\Big| z_0, \zeta_0\right) e^{-in\pi\frac{a}{L}}\right\}, \qquad (6.36)
\end{aligned}$$

where $\bar{\mathcal{P}}(Y_M)$ is the propagator of $Y_M$ when taking the discount factor $e^{-\int_0^T r(t)dt}$ into account with $\varphi_{Y_M}$ as its (modified) characteristic function. $[a, b]$ is the feasible truncated integration region for all $Y_j$ $(j = 1, 2, \cdots, M)$ with $L = b - a$, and $y^* = \ln\left(\frac{M+1}{S_0}K - 1\right)$. Let $x_m = \ln S_m = \ln S(t_m)$. We now focus on the derivation of $\varphi_{Y_j}$ for $j = 1, 2, \cdots, M$. We first look at the (modified) characteristic function of $Y_1 = x_M - x_{M-1}$:

$$\begin{aligned}
\varphi_{Y_1}(u|z_{M-1}, \zeta_{M-1}) &= \int_{-\infty}^{\infty} e^{iuY_1} \bar{\mathcal{P}}(Y_1)\, dY_1 \\
&= \mathbb{E}\left[e^{-\int_{t_{M-1}}^{t_M} r(t)dt} e^{iu(x_M - x_{M-1})}\right] \\
&= \int_0^{\infty} dz_M \int_0^{\infty} d\zeta_M \int_{-\infty}^{\infty} d(x_M - x_{M-1})\, e^{iu(x_M - x_{M-1})} \\
&\quad \times \bar{\mathcal{P}}(x_M, z_M, \zeta_M | x_{M-1}, z_{M-1}, \zeta_{M-1}) \\
&= \int_0^{\infty} dz_M \int_0^{\infty} d\zeta_M\, \Phi(u, \Delta t, z_M, \zeta_M | z_{M-1}, \zeta_{M-1}) \\
&= \phi(u, \Delta t | z_{M-1}, \zeta_{M-1}). \qquad (6.37)
\end{aligned}$$

Then the (modified) characteristic function of $Y_2 = x_{M-1} - x_{M-2} + \ln\left(1+e^{Y_1}\right)$ is given by:

$$\begin{aligned}
& \varphi_{Y_2}\left(u|z_{M-2},\zeta_{M-2}\right) \\
= & \int_{-\infty}^{\infty} e^{iuY_2}\,\bar{\mathcal{P}}\left(Y_2\right)dY_2 \\
= & \mathbb{E}\left[e^{-\int_{t_{M-2}}^{t_M} r(t)dt}\,e^{iuY_2}\right] \\
= & \mathbb{E}\left[e^{-\int_{t_{M-2}}^{t_{M-1}} r(t)dt}\,e^{iu(x_{M-1}-x_{M-2})}\,e^{-\int_{t_{M-1}}^{t_M} r(t)dt}\,\left(1+e^{Y_1}\right)^{iu}\right] \\
= & \int_0^{\infty} dz_{M-1}\int_0^{\infty} d\zeta_{M-1}\int_{-\infty}^{\infty} d\left(x_{M-1}-x_{M-2}\right)\,e^{iu(x_{M-1}-x_{M-2})} \\
& \times\bar{\mathcal{P}}\left(x_{M-1},z_{M-1},\zeta_{M-1}|x_{M-2},z_{M-2},\zeta_{M-2}\right) \\
& \times\int_{-\infty}^{\infty}\left(1+e^{Y_1}\right)^{iu}\bar{\mathcal{P}}\left(Y_1\right)dY_1 \\
\approx & \int_0^{\infty} dz_{M-1}\int_0^{\infty} d\zeta_{M-1}\Phi\left(u,\Delta t,z_{M-1},\zeta_{M-1}|z_{M-2},\zeta_{M-2}\right)\int_{-\infty}^{\infty}\left(1+e^{Y_1}\right)^{iu} \\
& \times\sum_{n=0}^{N-1}{}'\,\frac{2}{L}\,\mathrm{Re}\left\{\varphi_{Y_1}\left(\frac{n\pi}{L}\middle|z_{M-1},\zeta_{M-1}\right)\,e^{-in\pi\frac{a}{L}}\right\}\cos\left(n\pi\frac{Y_1-a}{L}\right)dY_1 \\
= & \int_0^{\infty} dz_{M-1}\int_0^{\infty} d\zeta_{M-1}\Phi\left(u,\Delta t,z_{M-1},\zeta_{M-1}|z_{M-2},\zeta_{M-2}\right) \\
& \times\frac{2}{L}\sum_{n=0}^{N-1}{}'\,\mathrm{Re}\left\{\varphi_{Y_1}\left(\frac{n\pi}{L}\middle|z_{M-1},\zeta_{M-1}\right)\,e^{-in\pi\frac{a}{L}}\right\}\mathcal{M}\left(u,n\right),
\end{aligned}\tag{6.38}$$

where $\mathcal{M}\left(u,n\right)$ is defined by:

$$\mathcal{M}\left(u,n\right) = \int_{-\infty}^{\infty}\left(1+e^{X}\right)^{iu}\cos\left(n\pi\frac{X-a}{L}\right)dX. \tag{6.39}$$

We apply the J-point Gauss-Legendre quadrature integration rule to the outer integrals with respect to $z_m$ and $\zeta_m$ $(m = M-1, M-2, \cdots, 1)$ in this chapter. Then we can rewrite expression (6.38) as:

$$\begin{aligned}
\varphi_{Y_2}\left(u|z_{M-2},\zeta_{M-2}\right) = & \frac{2}{L}\sum_{j_z=0}^{J_z-1} w_{j_z}\sum_{j_\zeta=0}^{J_\zeta-1} w_{j_\zeta}\Phi\left(u,\Delta t,z_{j_z},\zeta_{j_\zeta}|z_{M-2},\zeta_{M-2}\right) \\
& \times\sum_{n=0}^{N-1}{}'\,\mathrm{Re}\left\{\varphi_{Y_1}\left(\frac{n\pi}{L}\middle|z_{j_z},\zeta_{j_\zeta}\right)\,e^{-in\pi\frac{a}{L}}\right\}\mathcal{M}\left(u,n\right),
\end{aligned}\tag{6.40}$$

where the $w_{j_z}$ and $w_{j_\zeta}$ are the weights of the quadrature nodes $z_{j_z}$ and $\zeta_{j_\zeta}$, respectively. Moreover, for $Y_3 = x_{M-2} - x_{M-3} + \ln\left(1 + e^{Y_2}\right)$, we similarly have:

$$
\begin{aligned}
& \varphi_{Y_3}\left(u|z_{M-3},\zeta_{M-3}\right) \\
= & \int_{-\infty}^{\infty} e^{iuY_3}\,\bar{\mathcal{P}}\left(Y_3\right)dY_3 \\
= & \mathbb{E}\left[e^{-\int_{t_{M-3}}^{t_M} r(t)dt}\, e^{iuY_3}\right] \\
= & \mathbb{E}\left[e^{-\int_{t_{M-3}}^{t_{M-2}} r(t)dt}\, e^{iu(x_{M-2}-x_{M-3})}\, e^{-\int_{t_{M-2}}^{t_M} r(t)dt}\, \left(1+e^{Y_2}\right)^{iu}\right] \\
= & \int_0^{\infty} dz_{M-2}\int_0^{\infty} d\zeta_{M-2}\int_{-\infty}^{\infty} d\left(x_{M-2}-x_{M-3}\right)\, e^{iu(x_{M-2}-x_{M-3})} \\
& \times\bar{\mathcal{P}}\left(x_{M-2},z_{M-2},\zeta_{M-2}|x_{M-3},z_{M-3},\zeta_{M-3}\right) \\
& \times\int_{-\infty}^{\infty}\left(1+e^{Y_2}\right)^{iu}\bar{\mathcal{P}}\left(Y_2\right)dY_2 \\
\approx & \int_0^{\infty} dz_{M-2}\int_0^{\infty} d\zeta_{M-2}\Phi\left(u,\Delta t,z_{M-2},\zeta_{M-2}|z_{M-3},\zeta_{M-3}\right)\int_{-\infty}^{\infty}\left(1+e^{Y_2}\right)^{iu} \\
& \times\sum_{n=0}^{N-1}{}'\,\frac{2}{L}\,\mathrm{Re}\left\{\varphi_{Y_2}\left(\frac{n\pi}{L}\Big|z_{M-2},\zeta_{M-2}\right)\, e^{-in\pi\frac{a}{L}}\right\}\cos\left(n\pi\frac{Y_2-a}{L}\right)dY_2 \\
= & \frac{2}{L}\sum_{j_z=0}^{J_z-1} w_{j_z}\sum_{j_\zeta=0}^{J_\zeta-1} w_{j_\zeta}\Phi\left(u,\Delta t,z_{j_z},\zeta_{j_\zeta}|z_{M-3},\zeta_{M-3}\right) \\
& \times\sum_{n=0}^{N-1}{}'\,\mathrm{Re}\left\{\varphi_{Y_2}\left(\frac{n\pi}{L}\Big|z_{j_z},\zeta_{j_\zeta}\right)\, e^{-in\pi\frac{a}{L}}\right\}\mathcal{M}\left(u,n\right),
\end{aligned}
\tag{6.41}
$$

Deriving $\varphi_{Y_j}\left(u|z_{M-j},\zeta_{M-j}\right)$ from $\varphi_{Y_{j-1}}\left(u|z_{M-j+1},\zeta_{M-j+1}\right)$ for $j = 2, 3, \cdots, M$ iteratively, we finally obtain the (modified) characteristic function of $Y_M$:

$$
\begin{aligned}
\varphi_{Y_M}\left(u|z_0,\zeta_0\right) &= \int_{-\infty}^{\infty} e^{iuY_M}\,\bar{\mathcal{P}}\left(Y_M\right)dY_M \\
&= \frac{2}{L}\sum_{j_z=0}^{J_z-1} w_{j_z}\sum_{j_\zeta=0}^{J_\zeta-1} w_{j_\zeta}\Phi\left(u,\Delta t,z_{j_z},\zeta_{j_\zeta}|z_0,\zeta_0\right) \\
&\quad\times\sum_{n=0}^{N-1}{}'\,\mathrm{Re}\left\{\varphi_{Y_{M-1}}\left(\frac{n\pi}{L}\Big|z_{j_z},\zeta_{j_\zeta}\right)\, e^{-in\pi\frac{a}{L}}\right\}\mathcal{M}\left(u,n\right).
\end{aligned}
\tag{6.42}
$$

Plugging expression (6.42) into pricing formula (6.36) yields the discrete arithmetic Asian put option prices. Table 6.2 compares results from (6.36) in rows

**Table 6.2:** Pricing results for discrete arithmetic Asian put options. The rows "MC" are Monte-Carlo simulations, the rows "COS" are results from expression (6.36), and the rows RE represent their relative errors in %. Parameter values used here are from Table 3 of reference (223): $S_0 = 100$, $r_0 = 0.04$, $\theta = 0.02$, $\kappa_r = 0.3$, $\theta_r = 0.04$, $\sigma_r = 0.1$, $v_0 = 0.01$, $\kappa = 1.5$, $\sigma = 0.15$, $\rho = 0.1$, $T = 1/12$.

| | Method | $K = 90$ | $K = 95$ | $K = 100$ | $K = 105$ | $K = 110$ |
|---|---|---|---|---|---|---|
| | MC | 0.0000 | 0.0001 | 0.5357 | 4.8180 | 9.8003 |
| $M = 2$ | COS | 0.0000 | 0.0001 | 0.5362 | 4.8220 | 9.8082 |
| | RE | 0% | 0% | 0.09% | 0.08% | 0.08% |
| | MC | 0.0000 | 0.0002 | 0.5580 | 4.8183 | 9.8003 |
| $M = 4$ | COS | 0.0000 | 0.0002 | 0.5583 | 4.8204 | 9.8044 |
| | RE | 0% | 0% | 0.05% | 0.04% | 0.04% |
| | MC | 0.0000 | 0.0003 | 0.5762 | 4.8186 | 9.8003 |
| $M = 10$ | COS | 0.0000 | 0.0003 | 0.5763 | 4.8196 | 9.8020 |
| | RE | 0% | 0% | 0.02% | 0.02% | 0.02% |
| | MC | 0.0000 | 0.0004 | 0.5858 | 4.8189 | 9.8003 |
| $M = 30$ | COS | 0.0000 | 0.0004 | 0.5860 | 4.8194 | 9.8012 |
| | RE | 0% | 0% | 0.03% | 0.01% | 0.01% |

indicated by "COS" with Monte Carlo simulations given in rows "MC". Monte Carlo simulations run 15 000 000 times with 240 time steps for time to maturity $T = 1/12$ year. I choose a domain $[a, b] = [-0.5, 5]$ for all $Y_j$, and $N = 380$ terms are calculated for the COS approximation. An integration domain $[0, 0.35]$ with $J = 180$ points is used for both $z$ and $\zeta$ as applying the Gauss-Legendre integration. It may seem that these values are not sufficiently wide or large, but they are chosen such that the implementation in MATLAB does not cause my computer to run out of memory. In addition, I use the asymptotic formula (2.43) for the modified Bessel function of the first kind $I_{\cdot}(\cdot)$ that appears in $\Phi\left(u, \Delta t, z_{j_z}, \zeta_{j_\zeta} | z_0, \zeta_0\right)$ in MATLAB, since $I_{\cdot}(\cdot)$ becomes extremely large as $\Delta t = T/M$ becomes small. The relative errors defined as 100(COS - MC)/MC (in %) are also shown in Table 6.2. All absolute relative errors are less than 0.1%, confirming our pricing formula (6.36). We see that the larger the monitoring date $M$, the better the performance of the approximation (2.43). However, the COS method with Gauss-Legendre quadrature integration is time consuming for the discretely monitored arithmetic Asian option under the HCIR model. The typical CPU time cost in my computer is about 20 minutes for the case $M = 30$.

## 6.4 Bermudan options

A Bermudan option is an option where the option holder has the right to exercise at multiple pre-specified discrete exercise dates over the option's lifetime. This is between a European option, which allows to exercise at a single expiry data, and an American option, which allows to exercise at any time. The holder of a Bermudan option receives the payoff when he/she exercises the option. Between two consecutive exercise dates, the valuation process can be regarded as that for a European option, which is priced by using the risk-neutral valuation formula.

For $M$ equally spaced early-exercise dates $\{t_m, t_{m-1} < t_m \,|\, m = 1, \cdots, M\}$ with $t_M = T$, $\Delta t = t_{m+1} - t_m$, and $t_0$ being the initial time, the Bermudan put option pricing formula with strike price $K$ and maturity time $T$, denoted by $\mathscr{P}_{Ber}(x_m, z_m, \zeta_m, t_m)$, is given by ($x_m = \ln(S_m/K) = \ln(S(t_m)/K)$):

$$\begin{cases} g(x_m, t_m) & \text{for} \quad m = M; \\ \max\left[c(x_m, z_m, \zeta_m, t_m), g(x_m, t_m)\right] & \text{for} \quad m = 1, 2, \cdots, M-1; \\ c(x_m, z_m, \zeta_m, t_m) & \text{for} \quad m = 0, \end{cases} \tag{6.43}$$

where $g(x_m, t_m)$ is the payoff function at time $t_m$:

$$g(x_m, t_m) = \max(K - S_{t_m}, 0) = K \max(1 - e^{x_m}, 0), \tag{6.44}$$

and $c(x_m, z_m, \zeta_m, t_m)$ is called the continuation value at time $t_m$ (225, 226), which is the expectation value of the option at time $t_m$ if the option is exercised at the next early-exercise time $t_{m+1}$:

$$\begin{aligned} & c(x_m, z_m, \zeta_m, t_m) \\ = & \mathbb{E}\left[e^{-\int_{t_m}^{t_{m+1}} r(t)dt} \mathscr{C}(x_{m+1}, z_{m+1}, \zeta_{m+1}, t_{m+1})\right] \\ = & \int_{-\infty}^{\infty} dx_{m+1} \int_0^{\infty} dz_{m+1} \int_0^{\infty} d\zeta_{m+1}\, \mathscr{P}_{Ber}(x_{m+1}, z_{m+1}, \zeta_{m+1}, t_{m+1}) \\ & \times \bar{\mathcal{P}}(x_{m+1}, z_{m+1}, \zeta_{m+1} | x_m, z_m, \zeta_m) \\ = & \int_{-\infty}^{\infty} dx_{m+1} \int_0^{\infty} dz_{m+1} \int_0^{\infty} d\zeta_{m+1}\, \mathscr{P}_{Ber}(x_{m+1}, z_{m+1}, \zeta_{m+1}, t_{m+1}) \\ & \times {\sum_{n=0}^{N-1}}' \frac{2}{L} \mathrm{Re}\left\{\Phi\left(\frac{n\pi}{L}, \Delta t, z_{m+1}, \zeta_{m+1} \middle| z_m, \zeta_m\right) e^{in\pi\frac{x_m - a}{L}}\right\} \cos\left(n\pi \frac{x_{m+1} - a}{L}\right). \end{aligned} \tag{6.45}$$

Applying the J-point Gauss-Legendre quadrature integration rule, we can rewrite this formula as:

$$\begin{aligned}
& c\left(x_m, z_m, \zeta_m, t_m\right) \\
\approx\ & \sum_{j_z=0}^{J_z-1} w_{j_z} \sum_{j_\zeta=0}^{J_\zeta-1} w_{j_\zeta} \sum_{n=0}^{N-1}{}' \operatorname{Re}\left\{\Phi\left(\frac{n\pi}{L}, \Delta t, z_{j_z}, \zeta_{j_\zeta} \middle| z_m, \zeta_m\right) e^{in\pi\frac{x_m-a}{L}}\right\} V_{n,j_z,j_\zeta}\left(t_{m+1}\right) \\
=\ & \sum_{n=0}^{N-1}{}' \operatorname{Re}\left\{\beta_n\left(z_m, \zeta_m, t_m\right) e^{in\pi\frac{x_m-a}{L}}\right\}, \qquad (6.46)
\end{aligned}$$

where

$$V_{n,j_z,j_\zeta}\left(t_{m+1}\right) = \frac{2}{L}\int_a^b dx_{m+1} \mathscr{P}_{Ber}\left(x_{m+1}, z_{j_z}, \zeta_{j_\zeta}, t_{m+1}\right) \cos\left(n\pi\frac{x_{m+1}-a}{L}\right), \qquad (6.47)$$

$$\beta_n\left(z_m, \zeta_m, t_m\right) = \sum_{j_z=0}^{J_z-1} w_{j_z} \sum_{j_\zeta=0}^{J_\zeta-1} w_{j_\zeta} \Phi\left(\frac{n\pi}{L}, \Delta t, z_{j_z}, \zeta_{j_\zeta} \middle| z_m, \zeta_m\right) V_{n,j_z,j_\zeta}\left(t_{m+1}\right). \qquad (6.48)$$

Given the expressions (6.44) and (6.46), one can now determine the early-exercise points at every time $t_m$ ($m = M-1, M-2, \cdots, 1$) rapidly by solving the following equation with an efficient root finding procedure, for instance, Newton's method:

$$c\left(x_m, z_{j_z}, \zeta_{j_\zeta}, t_m\right) - g\left(x_m, t_m\right) = 0, \qquad (6.49)$$

for $j_z = 0, 1, \cdots, J_z - 1$ and $j_\zeta = 0, 1, \cdots, J_\zeta - 1$. When the early-exercise points $x^*\left(z_{j_z}, \zeta_{j_\zeta}, t_m\right)$ have been determined, procedure (6.43) can be used to compute the Bermudan call option price. More specifically:

- At $t_M$:

$$\mathscr{P}_{Ber}\left(x_M, z_M, \zeta_M, t_M\right) = g\left(x_M, t_M\right); \qquad (6.50)$$

- At $t_m$ ($m = M-1, M-2, \cdots, 2, 1$):

$$\mathscr{P}_{Ber}\left(x_m, z_m, \zeta_m, t_m\right) = \begin{cases} g\left(x_m, t_m\right) & \text{for} \quad x_m \in \left[a, x^*\left(z_{j_z}, \zeta_{j_\zeta}, t_m\right)\right]; \\ c\left(x_m, z_m, \zeta_m, t_m\right) & \text{for} \quad x_m \in \left[x^*\left(z_{j_z}, \zeta_{j_\zeta}, t_m\right), b\right]; \end{cases} \qquad (6.51)$$

- At $t_0$:

$$\mathscr{P}_{Ber}\left(x_0, z_0, \zeta_0, t_0\right) = c\left(x_0, z_0, \zeta_0, t_0\right). \qquad (6.52)$$

With the procedure above and expression (6.46), we can compute recursively $\mathscr{P}_{Ber}(x_0, z_0, \zeta_0, t_0)$ from $\mathscr{P}_{Ber}(x_M, z_M, \zeta_M, t_M)$, backwards in time. Another more efficient way is to recover the cosine series of $\mathscr{P}_{Ber}$, i.e. $V_n$, for each time point using backward recursion, and only at time $t_0$ we apply (6.46) to reconstruct $\mathscr{P}_{Ber}(x_0, z_0, \zeta_0, t_0)$. At $t_M$, one can derive an analytic expression for $V_{n,j_z,j_\zeta}(t_M)$ by using (6.47):

$$V_{n,j_z,j_\zeta}(t_M) = G_n(0, b), \tag{6.53}$$

where

$$\begin{aligned} G_n(l,u) &= \frac{2}{L}\int_l^u K\max(1-e^y, 0)\cos\left(n\pi\frac{y-a}{L}\right)dy \\ &= \frac{2}{L}K\left[\psi_n(\min(l,0), \min(u,0)) - \chi_n(\min(l,0), \min(u,0))\right]. \end{aligned} \tag{6.54}$$

At $t_{M-1}$, by inserting $V_{n,j_z,j_\zeta}(t_M)$ into (6.48), we obtain $\beta_n\left(z_{j_z}, \zeta_{j_\zeta}, t_{M-1}\right)$ for $j_z = 0, 1, \cdots, J_z - 1$ and $j_\zeta = 0, 1, \cdots, J_\zeta - 1$, thus $c(x_{M-1}, z_{M-1}, \zeta_{M-1}, t_{M-1})$ with (6.46). We then solve $c(x_{M-1}, z_{M-1}, \zeta_{M-1}, t_{M-1}) - g(x_{M-1}, t_{M-1}) = 0$ by Newton's method to derive the early-exercise point $x^*\left(z_{j_z}, \zeta_{j_\zeta}, t_{M-1}\right)$. Then we split the integral in (6.47) into two parts (for $j_z = 0, 1, \cdots, J_z - 1$ and $j_\zeta = 0, 1, \cdots, J_\zeta - 1$):

$$\begin{aligned} V_{k,j_z,j_\zeta}(t_{M-1}) &= \frac{2}{L}\int_a^b dx_{M-1}\mathscr{P}_{Ber}\left(x_{M-1}, z_{j_z}, \zeta_{j_\zeta}, t_{M-1}\right)\cos\left(k\pi\frac{x_{M-1}-a}{L}\right), \\ &= C_{k,j_z,j_\zeta}\left(x^*\left(z_{j_z}, \zeta_{j_\zeta}, t_{M-1}\right), b, t_{M-1}\right) + G_k\left(a, x^*\left(z_{j_z}, \zeta_{j_\zeta}, t_{M-1}\right)\right), \end{aligned} \tag{6.55}$$

where

$$\begin{aligned} C_{k,j_z,j_\zeta}(l,u,t_{M-1}) =& \frac{2}{L}\int_l^u \mathscr{P}_{Ber}\left(y, z_{j_z}, \zeta_{j_\zeta}, t_{M-1}\right)\cos\left(k\pi\frac{y-a}{L}\right)dy \\ =& \frac{2}{L}\int_l^u {\sum_{n=0}^{N-1}}' \mathrm{Re}\left\{\beta_n\left(z_{j_z}, \zeta_{j_\zeta}, t_{M-1}\right)\, e^{in\pi\frac{y-a}{L}}\right\}\cos\left(k\pi\frac{y-a}{L}\right)dy \\ =& \mathrm{Re}\left\{{\sum_{n=0}^{N-1}}' \mathcal{M}_{k,n}(l,u)\ \beta_n\left(z_{j_z}, \zeta_{j_\zeta}, t_{M-1}\right)\right\}, \end{aligned} \tag{6.56}$$

with

$$\mathcal{M}_{k,n}(l,u) = \frac{2}{L}\int_l^u e^{in\pi\frac{y-a}{L}}\cos\left(k\pi\frac{y-a}{L}\right)dy. \tag{6.57}$$

**Table 6.3:** Bermudan put option prices $\mathscr{P}_{Ber}(M)$ with $M$ early-exercise dates and American put option prices $\mathscr{P}_{Ame}(d)$ defined in expression (6.58). The rows "FD" and "COS" are prices by using the finite difference method and the COS method, respectively. The same parameter values are used here as those in Table 6.2. The reference value of the American put option price is 9.9950, cited from (223). The relative errors are indicated by RE.

| Method | $\mathscr{P}_{Ber}(M)$ | | | | | $\mathscr{P}_{Ame}(d)$ | | | |
|---|---|---|---|---|---|---|---|---|---|
| | $M=2$ | $M=4$ | $M=8$ | $M=16$ | $M=32$ | $d=1$ | RE | $d=2$ | RE |
| COS | 9.8203 | 9.9094 | 9.9542 | 9.9771 | 9.9873 | 10.0005 | 0.055% | 9.9961 | 0.011% |
| FD | 9.8172 | 9.9084 | 9.9542 | 9.9771 | 9.9885 | 10.0000 | 0.050% | 9.9998 | 0.048% |

The same computational procedure is repeated, backwards in time, until $V_{k,j_z,j_\zeta}(t_1)$ is recovered, which is then inserted into (6.48) and (6.46) to get the final option price $\mathscr{P}_{Ber}(x_0, z_0, \zeta_0, t_0) = c(x_0, z_0, \zeta_0, t_0)$. Note that at $t_0$, instead of computing a matrix $[N \times j_z \times j_\zeta]$, we only consider an array $[N \times 1]$ for $\beta_n(z_0, \zeta_0, t_1)$. And the initial value of asset price $S_0$ only appears at the final time step $t_0$. The row indicated by "COS" in Table 6.3 represents Bermudan put option prices by using the COS method (middle column). There are no reference values in the literature for these cases, so I check these results with those by using the finite difference method, in the row FD middle column. I will introduce the finite difference method in section 6.6. Comparing values in the middle column of Table 6.3, we see that results from these two methods are very close to each other.

## 6.5 American and discrete barrier options

The prices of American options can be obtained by applying a Richardson extrapolation on the prices of a few Bermudan options with small monitoring dates. Let $\mathscr{P}_{Ber}(M)$ being the value of a Bermudan option with $M$ early exercise dates, the approximated value of the American option is given by the following four-point Richardson extrapolation scheme (230):

$$\mathscr{P}_{Ame}(d) = \frac{1}{21}\left[64\mathscr{P}_{Ber}\left(2^{d+3}\right) - 56\mathscr{P}_{Ber}\left(2^{d+2}\right) + 14\mathscr{P}_{Ber}\left(2^{d+1}\right) - \mathscr{P}_{Ber}\left(2^{d}\right)\right]. \tag{6.58}$$

The row COS in Table 6.3 represents Bermudan put option prices by using the COS method as well as two corresponding American put option prices from (6.58). I choose a domain $[a, b] = [-1.5, 1.5]$ for $x$, a domain $[0, 0.5]$ for both $z$ and $\zeta$, and $N = 128$. Larger $d$ values give more accurate American option prices through the Richardson extrapolation (6.58). Relative errors illustrated in Table 6.3 are less than 0.1%, confirming our Bermudan option pricing formula. However, the COS method with Gauss-Legendre quadrature integration is time consuming for Bermudan and American put options under the HCIR model. Numerical results show that American call option prices are the same as European call option prices, which coincides with the conclusion in Table 1.1.

For discretely-monitored barrier options, the pricing procedure of the preceding section for Bermudan options can be applied directly. It is even easier for barrier options, no matter whether they have a fixed barrier level or with a floating one, as the barrier level is known in advance, and does not need to be determined inside the recursion loop. Also inside the recursion loop, no early-exercise scenarios exist, so $V_{k,j_z,j_\zeta} = C_{k,j_z,j_\zeta}$.

## 6.6 An ADI scheme for American put options

This section is devoted to the finite difference (FD) method with an alternating direction implicit (ADI) time discretization scheme, called the modified Craig-Sneyd (MCS) scheme (234), for pricing American put options in the HCIR model.

The FD method for option pricing starts from the Kolmogorov backward equation 2.7 for the risk-neutral option price with some initial and boundary conditions. Let $u(s, v, r, t)$ be the risk-neutral put option price under the HCIR model if at time $T - t$ the asset price, its variance as well as the interest rate are equal to $s$, $v$ and $r$, respectively. Then $u(t)$ satisfies the following partial differential equation (PDE):

$$\begin{aligned}\frac{\partial u}{\partial t} &= rs\frac{\partial u}{\partial s} + \kappa(\theta - v)\frac{\partial u}{\partial v} + \kappa_r(\theta_r - r)\frac{\partial u}{\partial r} \\ &\quad + \frac{1}{2}s^2 v\frac{\partial^2 u}{\partial s^2} + \frac{1}{2}\sigma^2 v\frac{\partial^2 u}{\partial v^2} + \frac{1}{2}\sigma_r^2 r\frac{\partial^2 u}{\partial r^2} + \rho\sigma s v\frac{\partial^2 u}{\partial s\partial v} - ru, \qquad (6.59)\end{aligned}$$

for $s > 0$, $v > 0$, $r > 0$ and $0 < t \leq T$. In numerical practice, a bounded spatial domain $[0, S_{max}] \times [0, V_{max}] \times [-R_{max}, R_{max}]$ is chosen with fixed values $S_{max}$, $V_{max}$ and $R_{max}$ taken sufficiently large. The PDE (6.59) is then complemented by the initial and boundary conditions:

$$\begin{aligned}
u(s, v, r, 0) &= \max(K - s, 0), & (6.60)\\
u(0, v, r, t) &= K, & (6.61)\\
\frac{\partial u}{\partial s}(S_{max}, v, r, t) &= 0, & (6.62)\\
\frac{\partial u}{\partial v}(s, V_{max}, r, t) &= 0, & (6.63)\\
\frac{\partial u}{\partial r}(s, v, \pm R_{max}, t) &= 0. & (6.64)
\end{aligned}$$

Condition (6.60) states the payoff function. Condition (6.61) to (6.63) have already been used in the literature for the put option pricing under the Heston model, see for instance (231, 233). Note that I have extended the domain of $r$ to $[-R_{max}, R_{max}]$ rather than on $[0, R_{max}]$ in order to treat the case when the Feller condition for the Cox-Ingersoll-Ross model, i.e. $2\kappa_r\theta_r > \sigma_r^2$, is not satisfied and to apply the condition (6.64) as performed in (224).

For the numerical solution of the put option pricing problems mentioned before, the PDE (6.59) is first semidiscretized on a nonuniform Cartesian spatial grid. With integers $m_1$, $m_2$, $m_3 \geq 1$ and parameters $d_1$, $d_2$, $d_3$, $d_4 > 0$, the meshes $0 = s_0 < s_1 < \cdots < s_{m_1} = S_{max}$, $0 = v_0 < v_1 < \cdots < v_{m_2} = V_{max}$ and $-R_{max} = r_0 < r_1 < \cdots < r_{m_3} = R_{max}$ are defined by (224, 234, 235):

$$\begin{aligned}
s_i &= K + d_1 \sinh\left(\sinh^{-1}(-K/d_1) + i\Delta\xi\right), & (6.65)\\
v_j &= d_2 \sinh(j\Delta\eta), & (6.66)\\
r_j &= d_4 + d_3 \sinh\left(\sinh^{-1}((-R_{max} - d_4)/d_3) + k\Delta\vartheta\right), & (6.67)
\end{aligned}$$

for $0 \leq i \leq m_1$, $0 \leq j \leq m_2$ and $0 \leq k \leq m_3$, and with

$$\begin{aligned}
\Delta\xi &= \frac{1}{m_1}\left[\sinh^{-1}((S_{max} - K)/d_1) - \sinh^{-1}(-K/d_1)\right], & (6.68)\\
\Delta\eta &= \frac{1}{m_2}\sinh^{-1}(V_{max}/d_2), & (6.69)\\
\Delta\vartheta &= \frac{1}{m_3}\left[\sinh^{-1}((R_{max} - d_4)/d_3) - \sinh^{-1}((-R_{max} - d_4)/d_3)\right]. & (6.70)
\end{aligned}$$

The parameter $d_1$, $d_2$ and $d_3$ control the fraction of mesh points $s_i$ that lie in the neighborhood of the strike $K$, the fraction of points $v_j$ that lie near $v_0$ and the fraction of points $r_k$ that lie near a given interest rate level $r = d_4$, respectively. In this section I set $S_{max} = 10K$, $V_{max} = 5$, $R_{max} = 1$, $d_1 = K/5$, $d_2 = V_{max}/500$, $d_3 = R_{max}/400$ and $d_4 = \theta_r$. In view of the Dirichlet condition (6.61), the relevant set of grid points is thus

$$\mathcal{G} = \{(s_i, v_j, r_k) : 1 \leq i \leq m_1, 0 \leq j \leq m_2, 0 \leq k \leq m_3\}. \tag{6.71}$$

As an illustration, Figure 6.1 displays the typical mesh grids defined by (6.65), (6.66) and (6.67) with $m_1 = 120$, $m_2 = m_3 = 60$, $K = 100$, $\theta_r = 0.04$.

To approximate the first and second derivatives of $u$ in (6.59), I employ the following well-known FD formulas ($c_i = x_i - x_{i-1}$):

$$u'(x_i) \approx \frac{c_i^2 u(x_{i-2}) - (c_{i-1} + c_i)^2 u(x_{i-1}) + c_{i-1}(c_{i-1} + 2c_i) u(x_i)}{c_{i-1} c_i (c_{i-1} + c_i)}, \tag{6.72}$$

$$u'(x_i) \approx \frac{-c_{i+1}^2 u(x_{i-1}) + \left(c_{i+1}^2 - c_i^2\right) u(x_i) + c_i^2 u(x_{i+1})}{c_i c_{i+1} (c_i + c_{i+1})}, \tag{6.73}$$

$$u'(x_i) \approx \frac{-c_{i+2}(2c_{i+1} + c_{i+2}) u(x_i) + (c_{i+1} + c_{i+2})^2 u(x_{i+1}) - c_{i+1}^2 u(x_{i-2})}{c_{i+1} c_{i+2} (c_{i+1} + c_{i+2})}, \tag{6.74}$$

$$u''(x_i) \approx \frac{2c_{i+1} u(x_{i-1}) - 2(c_i + c_{i+1}) u(x_i) + 2c_i u(x_{i+1})}{c_i c_{i+1} (c_i + c_{i+1})}. \tag{6.75}$$

The discretization of the mixed derivative term $\frac{\partial^2 u}{\partial s \partial v}$ in (6.59) can be obtained by applying (6.73) successively in the $s$- and $v$-directions. In view of conditions (6.62) to (6.64), we have $u(x_{m_1+1}, v_j, r_k) \approx u(x_{m_1}, v_j, r_k)$, $u(x_i, v_{m_2+1}, r_k) \approx u(x_i, v_{m_2}, r_k)$, $u(x_i, v_j, r_{-1}) \approx u(x_i, v_j, r_0)$ and $u(x_i, v_j, r_{m_3+1}) \approx u(x_i, v_j, r_{m_3})$ where $s_{m_1+1} = 2s_{m_1} - s_{m_1-1}$, $v_{m_2+1} = 2v_{m_2} - v_{m_2-1}$, $r_{-1} = 2r_0 - r_1$ and $r_{m_3+1} = 2r_{m_3} - r_{m_3-1}$ are virtual points. These virtual points are introduced such that central schemes (6.73) and (6.75) can be used for $u_{i,j,k}$ defined in (6.71), except in the region $v = 0$ and $v > \theta$. At $v = 0$, the derivative $\partial u/\partial v$ is approximated using the upwind scheme (6.74), and all terms in the $v-$direction vanish at $v = 0$ because the factor $v$ occurring in (6.59). In the region $v > \theta$ the upwind scheme (6.72) is applied in order to avoid spurious oscillations in the FD solution when $\sigma$ is close to zero (234).

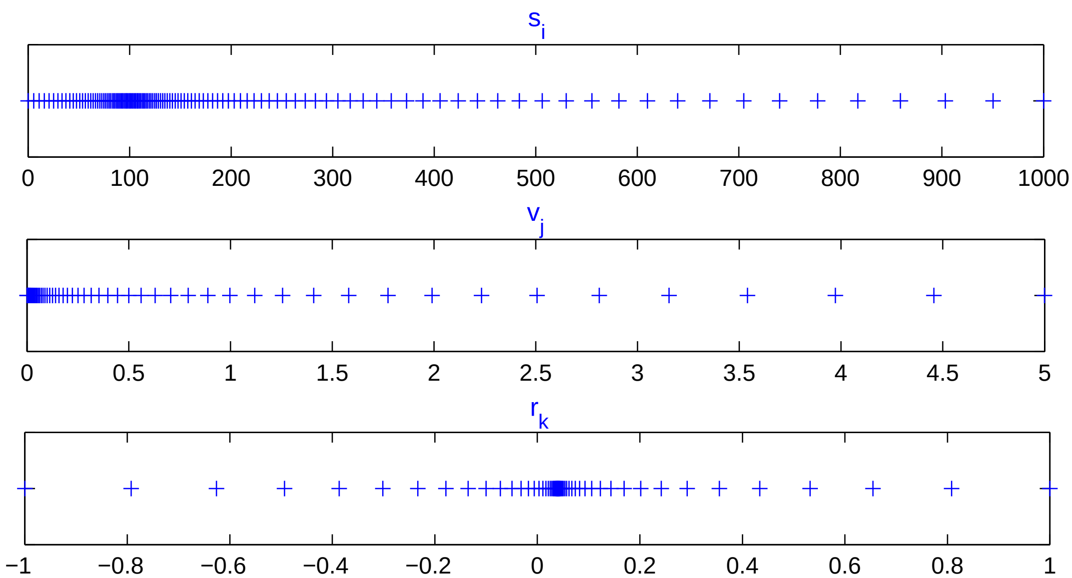


**Figure 6.1:** Sample meshes for $s$, $v$ and $r$ with $m_1 = 120$, $m_2 = m_3 = 60$, $K = 100$, $\theta_r = 0.04$.

The FD discretization described above of the initial-boundary put option pricing problem (6.59)-(6.64) for the HCIR model yields an initial value problem for a large system of ordinary differential equations:

$$U'(t) = AU(t) + g, \quad (0 \leq t \leq T), \quad U(0) = U_0. \tag{6.76}$$

Here $A$ is a given $m \times m$-matrix and $g$, $U_0$ are given $m$-vectors with $m = m_1(m_2 + 1)(m_3 + 1)$. The vector $U_0$ is directly obtained from the initial condition (6.60). For each given $t > 0$, the solution vector $U(t)$ to (6.76) approximates the exact solution values $u(s, v, r, t)$ of (6.59)-(6.64) at the spatial grid points $(s, v, r) \in \mathcal{G}$.

An effective numerical time-discretization method for the spatially discretized HCIR problem (6.76) is the modified Craig-Sneyd (MCS) scheme (231, 234, 236). MCS is a splitting scheme of the alternating direction implicit (ADI) type. In line with the ADI idea, the matrix $A$ is decomposed into four simpler matrices:

$$A = A_0 + A_1 + A_2 + A_3, \tag{6.77}$$

where the matrices $A_0$, $A_1$, $A_2$, $A_3$ represent the part of $A$ that stem from the FD discretization of the mixed derivative term, and all spatial derivatives in the $s$-,

$v$- and $r$- directions in (6.59), respectively. The $ru$ term in (6.59) is distributed evenly over $A_1$, $A_2$ and $A_3$.

Let $\hat{\theta} > 0$ be a given real parameter, $\Delta t = T/\widehat{N}$ with integer $\widehat{N} \geq 1$ be a given time step, and let temporal grid points be given by $t_n = n\Delta t$ for $n = 0, 1, 2, \cdots, \widehat{N}$. Then approximations $U_n \approx U(t_n)$ can be generated successively in a one-step manner for $n = 1, 2, \cdots, \widehat{N}$ by the MCS scheme:

$$\begin{cases} Y_0 = & \begin{cases} \text{for } \mathscr{P}_{Ber}: & U_{n-1} + \Delta t \left( A U_{n-1} + g \right), \\ \text{for } \mathscr{P}_{Ame}: & U_{n-1} + \Delta t \left( A U_{n-1} + g \right) + \Delta t \lambda_{n-1}, \end{cases} \\ Y_j = & Y_{j-1} + \hat{\theta} \Delta t A_j \left( Y_j - U_{n-1} \right) \qquad (j = 1, 2, 3), \\ \widehat{Y}_0 = & Y_0 + \hat{\theta} \Delta t A_0 \left( Y_3 - U_{n-1} \right), \\ \widetilde{Y}_0 = & \widehat{Y}_0 + \left( \frac{1}{2} - \hat{\theta} \right) \Delta t A \left( Y_3 - U_{n-1} \right), \\ \widetilde{Y}_j = & \widetilde{Y}_{j-1} + \hat{\theta} \Delta t A_j \left( \widetilde{Y}_j - U_{n-1} \right) \qquad (j = 1, 2, 3), \\ U_n = & \begin{cases} \text{for } \mathscr{P}_{Ber}: \begin{cases} \max\left( \widetilde{Y}_3, U_0 \right) & \text{at monitoring dates,} \\ \widetilde{Y}_3 & \text{at other dates,} \end{cases} \\ \text{for } \mathscr{P}_{Ame}: \begin{cases} \max\left( \widetilde{Y}_3 - \Delta t \lambda_{n-1}, U_0 \right), \\ \lambda_n = \max\left( \lambda_{n-1} + \left( U_0 - \widetilde{Y}_3 \right) / \Delta t, 0 \right). \end{cases} \end{cases} \end{cases} \tag{6.78}$$

Here we have used the splitting approach of Ikonen-Toivanen (232, 233) for the pricing of American option, where the auxiliary vector $\lambda_n$ is used with $\lambda_0$ the zero vector. Except for the monitoring dates, the MCS scheme for the pricing of the Bermudan option is the same as the one for the European vanilla option.

Note that in (6.78), the terms $Y_0$, $\widehat{Y}_0$ and $\widetilde{Y}_0$ are expressed explicitly. Nevertheless, solutions of the implicitly expressed terms $Y_j$ and $\widetilde{Y}_j$ involve the matrices $\left( I - \hat{\theta} \Delta t A_j \right)$ for $j = 1, 2, 3$, where $I$ denotes the $m \times m$ identity matrix. Since $A_j$'s are time independent, one can compute a $LU$ factorization of the matrices $\left( I - \hat{\theta} \Delta t A_j \right)$'s once.

Now we have two methods for pricing American put options. One is the approach of Ikonen-Toivanen mentioned in (6.78). We denote this method as FD-IT. The other one is by using the four-point Richardson extrapolation scheme mentioned in previous section. That is, four Bermudan put option prices with early-exercise dates $M = 2^d, 2^{d+1}, 2^{d+2}, 2^{d+3}$ are first calculated following (6.78), then used in (6.58). We denote this method as FD-Ex. The row FD in Table 6.3 already illustrated this method. More numerical results for these two methods

**Table 6.4:** American put option prices. The rows Ref. represent the reference values from Table 3 in (223). The rows FD-IT (FD-Ex) are values by using the FD method with Ikonen-Toivanen splitting (four-point Richardson extrapolation scheme with $d = 2$, see (6.58)), and the rows RE-IT (RE-Ex) are their relative errors with respect to the reference values Ref. The same parameter values are used as in Table 6.1.

| Method | $K = 90$ | | | $K = 100$ | | | $K = 110$ | | |
|---|---|---|---|---|---|---|---|---|---|
| | $T = \frac{1}{12}$ | $T = \frac{1}{4}$ | $T = \frac{1}{2}$ | $T = \frac{1}{12}$ | $T = \frac{1}{4}$ | $T = \frac{1}{2}$ | $T = \frac{1}{12}$ | $T = \frac{1}{4}$ | $T = \frac{1}{2}$ |
| | | | | $v_0 = 0.01,\ \kappa = 1.5,\ \sigma = 0.15,\ \rho = 0.1$ | | | | | |
| Ref. | 0.0001 | 0.0346 | 0.2040 | 1.0438 | 1.7379 | 2.3951 | 9.9950 | 9.9823 | 9.9796 |
| FD-IT | 0.0002 | 0.0348 | 0.2031 | 1.0340 | 1.7399 | 2.3977 | 10.0000 | 10.0000 | 10.0000 |
| RE-IT | 100% | 0.58% | -0.44% | -0.94% | 0.12% | 0.11% | 0.05% | 0.18% | 0.20% |
| FD-Ex | 0.0002 | 0.0344 | 0.2034 | 1.0492 | 1.7374 | 2.3950 | 9.9998 | 10.0003 | 9.9964 |
| RE-Ex | 100% | -0.58% | -0.29% | 0.52% | -0.03% | -0.004% | 0.05% | 0.18% | 0.17% |
| | | | | $v_0 = 0.04,\ \kappa = 0.75,\ \sigma = 0.3,\ \rho = 0.1$ | | | | | |
| Ref. | 0.0619 | 0.5303 | 1.1824 | 2.1306 | 3.4173 | 4.4249 | 10.0386 | 10.4271 | 11.0224 |
| FD-IT | 0.0612 | 0.5298 | 1.1827 | 2.1210 | 3.4140 | 4.4332 | 10.0159 | 10.4337 | 11.0480 |
| RE-IT | -1.13% | -0.09% | 0.03% | -0.45% | -0.10% | 0.19% | -0.23% | 0.06% | 0.23% |
| FD-Ex | 0.0622 | 0.5290 | 1.1832 | 2.1289 | 3.4126 | 4.4312 | 10.0167 | 10.4312 | 11.0488 |
| RE-Ex | 0.48% | -0.25% | 0.07% | -0.08% | -0.14% | 0.14% | -0.22% | 0.04% | 0.24% |
| | | | | $v_0 = 0.04,\ \kappa = 1.5,\ \sigma = 0.3,\ \rho = 0.1$ | | | | | |
| Ref. | 0.0592 | 0.4950 | 1.0752 | 2.1138 | 3.3478 | 4.2732 | 10.0372 | 10.3825 | 10.8964 |
| FD-IT | 0.0585 | 0.4940 | 1.0757 | 2.1048 | 3.3441 | 4.2792 | 10.0140 | 10.3919 | 10.9211 |
| RE-IT | -1.18% | -0.20% | 0.05% | -0.43% | -0.11% | 0.14% | -0.23% | 0.09% | 0.23% |
| FD-Ex | 0.0595 | 0.4932 | 1.0762 | 2.1128 | 3.3427 | 4.2771 | 10.0150 | 10.3893 | 10.9218 |
| RE-Ex | 0.51% | -0.36% | 0.09% | -0.05% | -0.15% | 0.09% | -0.22% | 0.07% | 0.23% |
| | | | | $v_0 = 0.04,\ \kappa = 1.5,\ \sigma = 0.15,\ \rho = -0.5$ | | | | | |
| Ref. | 0.0787 | 0.6012 | 1.2896 | 2.1277 | 3.4089 | 4.4103 | 10.0198 | 10.2512 | 10.6988 |
| FD-IT | 0.0777 | 0.5994 | 1.2855 | 2.1183 | 3.4019 | 4.4072 | 10.0010 | 10.2563 | 10.7189 |
| RE-IT | -1.27% | -0.30% | -0.32% | -0.44% | -0.21% | -0.07% | -0.19% | 0.05% | 0.19% |
| FD-Ex | 0.0787 | 0.5986 | 1.2861 | 2.1261 | 3.4008 | 4.4059 | 10.0022 | 10.2528 | 10.7211 |
| RE-Ex | 0% | -0.43% | -0.27% | -0.08% | -0.24% | -0.10% | -0.18% | 0.02% | 0.21% |

are shown in Table 6.4. The parameter values used here are the same as those in Table 6.1. The reference values of the American put options are from Table 3 in (223). Here I choose $d = 2$, $m_1 = 170$, $m_2 = m_3 = 80$, $\widehat{N} = 32$, $\hat{\theta} = \max\left\{\frac{1}{3}, \frac{2}{13}(2|\rho| + 1)\right\}$. Relative errors with respect to reference values are also calculated. We see that most of the absolute relative errors are less than 1%. MATLAB are used with sparse matrix. The CPU time per time step is about

0.35 second for both methods. That is about 60 (240) seconds for every value of method FD-IT (FD-Ex) in Table 6.4. Since the COS method for large $M = 32$ is time consuming, I did not compute the American put option by using the COS method for every case here, but with only one example shown in Table 6.3.

## 6.7 A short discussion about the computing time

As mentioned before, Fang and Oosterlee efficiently priced the Bermudan options under the Heston SV model by using the COS method plus Gauss-Legendre rule in (226). When the Feller condition for the Heston model is satisfied, the time cost for Bermudan options reported in their paper is about 8 seconds for 30 monitoring dates. For the HCIR model used in this chapter, the parameter values are chosen such that the Feller conditions for both the stochastic volatility and stochastic interest rate processes are satisfied. The Heston model is a two dimensional model, whereas the HCIR model has a third stochastic interest rate process, and I used about 200 points for this extra process while applying the Gauss-Legendre integration. Therefore the implement time for Bermudan options for 30 monitoring dates under the HCIR model is roughly about 1600 seconds, which is close to 30 minutes reported in this chapter. Of course maybe my MATLAB code is not efficient, and there is a large space to optimize it.

The characteristic function $\Phi\left(u, \Delta t, z_{m+1}, \zeta_{m+1} | z_m, \zeta_m\right)$ defined in expressions (6.17) through (6.21) involves two modified Bessel functions of the first kind $I_{\cdot}\left(\cdot\right)$, both of which have a complex argument. Moreover, the characteristic function changes at each time step as the values of $z$ and $\zeta$ at the endpoints of each interval change. Clearly, the hardest and numerically most time consuming part of option pricing is the evaluation of $\Phi\left(u, \Delta t, z_{m+1}, \zeta_{m+1} | z_m, \zeta_m\right)$, particularly the two modified Bessel functions of the first kind, at each time step for values of $u$, $z_{m+1}$ and $\zeta_{m+1}$.

If we consider a two dimensional stochastic model rather than a three dimensional one, then the pricing procedure would be much faster. Furthermore, if we use a model whose characteristic function does not involve special functions, such as the modified Bessel function, for example the Lévy model, then the pricing procedure would be extremely fast, in the order of milli-seconds. So it is the complexity of model that matters the computing time, and the COS method is among the most efficient method for option pricing.

For the pricing of exotic options under complex models, a combination of the COS method and other methods is meaningful. For instance, a hybrid of the COS method and the parallel computing technique on Graphics Process Units is worth trying. As reported in (237), at each time step, the COS algorithm can be decomposed into two steps, i.e. computations on each element of a vector which can be parallelized and the summation of vector elements. We can image that splitting a vector and performing the summation in parallel would shorten the computing time dramatically.

# 7

# Determining and benchmarking the implied risk-neutral asset price densities from option prices

> This chapter is based on the article (146), which is joint work with Oliver Salazar Celis, Damiaan Lemmens, Jacques Tempère and Annie Cuyt. Damiaan Lemmens is the initiator and the contributor of the calculations related to the DLN and the IVS methods in this article. The interpolation techniques were developed @ CANT and we apply it here to option pricing.

Stochastic models for option pricing implicitly assume a risk-neutral underlying asset price probability distribution. In order to calibrate these models as well as to identify limitations of these models, a comparison to the experimentally realized asset price probability distribution is required. In this context, the empirical asset price probability distribution is reconstructed from the time series data (40). The asset prices (or returns) at different time steps are collected, binned, and theoretical probability distributions are fitted and compared to this data. This approach has obvious limitations related to non-ergodicity (100): for many purposes the probability distribution function at a given time is needed, and this cannot be extracted from realized values drawn at different times when the probability distribution function itself can change in time.

This limitation can be overcome by implying the risk-neutral probability densities from option prices. We will use the acronym RND (the risk-neutral probability density function of the underlying asset price) henceforth. In this framework, a set of option prices (determined e.g. for different values of the strike $K$) at a given time are related to the RND at that given time. This is in essence the inverse problem to the option pricing problem. In that problem, when we calculate e.g. European vanilla options for a range of strikes $K$ with a certain maturity $T$, we determine the RND for a certain model such as Black-Scholes or Heston, and once the RND is found, the option price can be calculated as the expected value of its future payoff discounted back to the present with a discount rate being the risk-neutral interest rate. Now, we observe option prices for strike $K$ with maturity $T$, and from this we derive the $P(S_T)$ that the empirical set of market participants generated to produce these prices.

There exist a variety of approaches on extracting the RND in literature that can be followed. One can assume a functional form for the underlying distribution and determine its parameters doing a least squares fit to the observed prices. A popular choice for this functional form is a combination of log-normals (238, 239, 240, 241). We refer to this method as the "double log-normal" (DLN) method. Another approach is to use the relation first put forth in (242) that the implied RND can be obtained by taking the second derivative of the option price with respect to the strike price. A popular method based on this approach consists in constructing a smoothed volatility surface to calculate the second derivative (243, 244, 245). We refer to this method as the "implied volatility surface" (IVS) method. For a more thorough discussion of the possible methods to infer the implied density we refer to (246, 247, 248, 249, 250, 251, 252).

The main goal of the present chapter is to introduce a new global and nonlinear method to determine the implied RND. Such global approximations assume one functional form for the option prices, and the RND is thus related to the second derivative of that option price with respect to the strike price. Its (possibly nonlinear) parameters are usually determined from discrete observed bid and ask option prices. Our new method is designed to tackle the two main problems that arise in determining option implied densities. These problems are (1) that there are only option prices for discrete sets of strikes, and (2) that these prices contain errors (e.g. due to the bid-ask spread, there is an 'error bar' on the price of any given option). Such errors can cause unrealistic density approximations. We refer to our new method as the "Rational Interval Interpolation" (RII) method. This method overcomes the aforementioned drawbacks and takes into account the nature of the data.

Before the RII method is applied to real market data, we first compare it to the DLN and IVS methods using simulated data with added noise to show its superiority to them. Only a small part of the literature uses simulated data to test the performance of the methods used to derive the implied RND. In (252) simulated data are used to study the influence of the incomplete set of strikes and the presence of a bid-ask spread. In (239) the ability of the DLN and IVS methods to recover a distribution simulated with Heston's stochastic volatility model is investigated. However, an essential advantage of using the simulated data is that we precisely know the exact probability density function, which guarantees a comparison of the methods in a controlled environment. Here, we extend the test used in (239) to compare the proposed method to the DLN and IVS methods. More specifically, we use simulated data based on three known probability distribution functions, and add noise. This provides a better benchmark, and allows to accurately determine the robustness and accuracy of the methods. The probability distribution functions that we use for this benchmarking are the Black-Scholes density, the Heston density and the CGMY model density. This choice allows to probe the influence of specific market characteristics such as stochastic volatility and jumps on the various methods for option implied densities.

Then we look at real data, and apply our procedure to estimate the implied densities for the S&P 500 index options. A large part of the literature (for a typical example, see (246)) uses market data to test the performance of methods for the option implied density. In (247), the robustness of the DLN and IVS methods is investigated by comparing the implied densities obtained from real option prices to those obtained by adding a small error to these market prices. In (253), the S&P 500 index option quotes that are too deep in or out of the money are eliminated while the rest are smoothed using cubic spline interpolation when applying the IVS method. This implied risk-neutral density is then completed with tails drawn from a Generalized Extreme Value distribution. Here, as mentioned before, we propose to use global nonlinear approximations for both the implied RND and the implied put and call option prices based on this single implied RND in a straightforward way rather than using spline-based methods.

This chapter is structured as follows. In section 7.1 we review existing methods to extract the RND for the asset returns from the option price data, focusing on the DLN approach and the IVS approach. In section 7.2 we present our novel RII method to determine the implied RND. In section 7.3 we discuss how the simulated data are generated, and we present our benchmark, compare and discuss the results from the aforementioned three approaches. Section 7.4 is devoted to the application of our RII method to real data. And finally, a conclusion is drawn in Section 7.5.

## 7.1 Review of existing approaches

Suppose that at a certain time $t = T$ the asset price $S_T$ has a conditional RND $P(S_T, T|S_0)$, where the condition stipulates the initial value $S_0$ of the asset at time $t = 0$. Since the payoff of a plain vanilla European call option with strike $K$ and maturity $T$ is $\max[S_T - K, 0]$, the price $C$ of this call option can be calculated as

$$C(S_0, K, T) = e^{-rT} \int_K^{\infty} (S_T - K) P(S_T, T|S_0) dS_T, \tag{7.1}$$

where $e^{-rT}$ is a discount factor with interest rate $r$. Differentiating this formula twice with respect to $K$ we get

$$\begin{aligned} \left.\frac{\partial^2 C(S_0, K, T)}{\partial K^2}\right|_{K=S_T} &= e^{-rT} \frac{\partial}{\partial K} \left( - \int_K^{\infty} P(S_T, T|S_0) dS_T \right)\Bigg|_{K=S_T} \\ &= e^{-rT} P(S_T, T|S_0) \quad . \end{aligned} \tag{7.2}$$

The implied probability distribution is then straightforwardly given by (242)

$$P(S_T, T|S_0) = e^{rT} \left.\frac{\partial^2 C(S_0, K, T)}{\partial K^2}\right|_{K=S_T} . \tag{7.3}$$

As already mentioned there are some problems to bring this theoretical relation into practice, such as the fact that only a discrete set of strikes is available. Also, the market mechanism of bidding and asking results in a “measurement error” or uncertainty on the observed option prices, through the bid-ask spread.

### 7.1.1 Implied volatility surface (IVS) approach

A popular approach to cope with these problems is the one based on smoothing the volatility smile (243, 244, 245). For this method, option prices are first transformed to a certain volatility curve. As mentioned in section (1.2.2), in a Black-Scholes setting, one can convert the option prices $C(S_0, K, T)$ into an implied volatility surface $\sigma(S_0, K, T)$. This implied volatility surface is then smoothed with a cubic spline, and the smoothed surface is mapped back onto a smoothed option price function. This smoothed option price function allows for taking a second derivative and determining the (discounted) RND through expression (7.3).

### 7.1.2 Double log-normal (DLN) approach

Another commonly used approach is the DLN approach (238, 239, 240, 241). In this framework, one assumes that the RND of $S_T$ is given by a double log-normal distribution:

$$\begin{aligned} P(S_T) &= \frac{b}{S_T\sigma_1\sqrt{2\pi T}} \exp\left\{-\frac{1}{2\sigma_1^2 T}\left[\ln\left(S_T/S_0\right) - \left(m_1 - \frac{\sigma_1^2}{2}\right)T\right]\right\} \\ &\quad + \frac{1-b}{S_T\sigma_2\sqrt{2\pi T}} \exp\left\{-\frac{1}{2\sigma_2^2 T}\left[\ln\left(S_T/S_0\right) - \left(m_2 - \frac{\sigma_2^2}{2}\right)T\right]\right\}. \end{aligned} \tag{7.4}$$

In this expression, the fitting parameters $m_1, m_2$ are drifts, the fitting parameters $\sigma_1, \sigma_2$ are volatilities and the final fitting parameter $b$ determines the relative contribution of the two log-normal densities. The price of a European vanilla call option is then given by

$$\begin{aligned} C\left(S_0, K, T\right) &= be^{-rT}\left[e^{m_1 T} S_0 N(d_+^{(1)}) - KN(d_-^{(2)})\right] \\ &\quad + (1-b)\, e^{-rT}\left[e^{m_1 T} S_0 N(d_+^{(1)}) - KN(d_-^{(2)})\right], \end{aligned} \tag{7.5}$$

with

$$d_\pm^{(j)} = \frac{1}{\sigma_j\sqrt{T}} \ln\left(\frac{S_0}{K} + \left(m_j \pm \frac{\sigma_j^2}{2}\right)T\right). \tag{7.6}$$

The parameters $m_1, m_2, \sigma_1, \sigma_2, b$ and $r$ in (7.5) are then determined by minimizing the least squares distance to the observed market prices. Since this method requires six nonlinear parameters to be determined, it can easily strand in a local minimum and thus is prone to yield unreliable results.

## 7.2 Rational interval interpolation (RII) approach

The basic problem statement of RII starts from the following. Instead of an observed option price point value $\tilde{C}_i$, it is assumed that an interval $[\underline{c}_i, \overline{c}_i]$ is given at each (distinct) strike $K_i$ ($i = 0, \ldots, n$). The bounds $\underline{c}_i < \overline{c}_i$ are typically obtained from the market mechanism of bidding and asking, as illustrated in section 7.4.

We then look for an irreducible rational function $r_{\ell,m}(K) = p_\ell(K)/q_m(K)$ consisting of a numerator polynomial $p_\ell(K)$ of degree at most $\ell$ and a denominator polynomial $q_m(K)$ of degree at most $m$, with $\ell + m \ll n$ and such that the interval interpolation conditions

$$r_{\ell,m}(K_i) \in [\underline{c}_i, \overline{c}_i] \quad \Leftrightarrow \quad \underline{c}_i \leq r_{\ell,m}(K_i) \leq \overline{c}_i, \qquad i = 0, \ldots, n \tag{7.7}$$

are satisfied. Provided that $q_m(K_i) > 0$, it is detailed in (254) that the coefficients of $r_{\ell,m}(K)$ have to satisfy the linear inequalities

$$\begin{cases} -\overline{c}_i q_m(K_i) + p_\ell(K_i) \leq 0 \\ \underline{c}_i q_m(K_i) - p_\ell(K_i) \leq 0 \end{cases}, \qquad i = 0, \ldots, n. \tag{7.8}$$

Our goal is not merely to approximate option prices, but also to derive an approximation from it for the (discounted) RND using the relation (7.3), i.e. by differentiating an approximation $r_{\ell,m}(K)$ for the option price twice with respect to $K$. The advantage of using a rational approximation $r_{\ell,m}(K)$ is the fact that it is infinitely differentiable and its second derivative can easily be written down explicitly. However, by definition, derivatives are quite sensitive to small oscillations of the underlying function. Artificial oscillations typically appear in approximations constructed from data subject to (heavy) noise. This may result in inaccurate and unrealistic density approximations. Fortunately, the theoretical prices of European vanilla call options are known to be convex decreasing functions of $K$. Hence, in order to guide the approximations towards more realistic shapes, we add the following (discrete) conditions for the first and the second derivative.

First, it is not difficult to see that the theoretical price of a European vanilla call option is monotonically decreasing with respect to the strike $K$ and the value of its derivative is bounded between $-e^{-rT}$ and 0. After all, it can be shown that (242)

$$\frac{\partial C}{\partial K}(K) = -e^{-rT}\left(1 - \mathrm{CDF}(K)\right), \tag{7.9}$$

where $\mathrm{CDF}(K)$ is the cumulative distribution function corresponding to the underlying PDF. Therefore we add the conditions at the locations $K_i$ that

$$-e^{-rT} \le r'_{\ell,m}(K_i) \le 0, \qquad i = 0, \ldots, n. \tag{7.10}$$

Here $r'_{\ell,m}(K)$ denotes the first derivative of $r_{\ell,m}(K)$ with respect to $K$.

It is convenient to write

$$r'_{\ell,m}(K) = \frac{p'_\ell(K) - r_{\ell,m}(K)\, q'_m(K)}{q_m(K)}, \tag{7.11}$$

and provided that both $q_m(K_i) > 0$ and (7.7) are satisfied, (7.10) is also satisfied if

$$\begin{cases} p'_\ell(K_i) - \overline{c_i}\, q'_m(K_i) \le 0 \\ p'_\ell(K_i) - \underline{c_i}\, q'_m(K_i) \le 0 \\ -e^{-rT} q_m(K_i) - p'_\ell(K_i) + \overline{c_i}\, q'_m(K_i) \le 0 \\ -e^{-rT} q_m(K_i) - p'_\ell(K_i) + \underline{c_i}\, q'_m(K_i) \le 0 \end{cases}, \qquad i = 0, \ldots, n. \tag{7.12}$$

Second, because a CDF is monotonically increasing with respect to its random variable, the first (partial) derivative of the theoretical European call option price is also monotonically increasing with respect to $K$. Hence convexity of $r_{\ell,m}(K)$ – thus positivity of its second derivative $r''_{\ell,m}(K)$ – is required for it to imply a realistic PDF. The nonnegativity of the RND is also a natural constraint from the perspective of finance. Therefore we also add the discrete conditions

$$0 \le r''_{\ell,m}(K_i), \qquad i = 0, \ldots, n. \tag{7.13}$$

For this purpose, it is convenient to write

$$r''_{\ell,m}(K) = \frac{p''_\ell(K) - r_{\ell,m}(K)\, q''_m(K) - 2\, r'_{\ell,m}(K)\, q'_m(K)}{q_m(K)}. \tag{7.14}$$

Provided that (7.7), (7.10) and $q_m(K_i) > 0$ hold, (7.13) is satisfied if

$$\begin{cases} -p''_\ell(K_i) + \overline{c_i}\, q''_m(K_i) - 2\, e^{-rT}\, q'_m(K_i) \le 0 \\ -p''_\ell(K_i) + \overline{c_i}\, q''_m(K_i) \le 0 \\ -p''_\ell(K_i) + \underline{c_i}\, q''_m(K_i) - 2\, e^{-rT}\, q'_m(K_i) \le 0 \\ -p''_\ell(K_i) + \underline{c_i}\, q''_m(K_i) \le 0 \end{cases}, \qquad i = 0, \ldots, n. \tag{7.15}$$

Although the conditions (7.10) and (7.13) are merely imposed on a discrete set and therefore do not prevent violations in between given strikes, they seem to work very well in practice (255). Moreover, it can be shown that when discrete conditions are imposed at sufficiently many locations, the condition is implied in between all locations (256). Unfortunately, the theoretical number of discrete conditions needed for this implication to hold is often too high to be of practical use. Guaranteeing a rational approximation with a nonnegative second derivative on the entire real line is out of scope here, but the interested reader is referred to (257).

For fixed $\ell$ and $m$, the problem that remains, is to obtain nonzero values for the coefficients of $r_{\ell,m}(K)$ such that the homogeneous linear inequalities (7.8), (7.12) and (7.15) are satisfied. How this can be done is discussed next. Let $p_\ell(K)$ and $q_m(K)$ be polynomials of the form

$$p_\ell(K) = \sum_{i=0}^{\ell} \alpha_i K^i, \qquad q_m(K) = \sum_{i=0}^{m} \beta_i K^i, \tag{7.16}$$

denote the corresponding vector of coefficients by

$$\mathbf{c} = (\alpha_0, \ldots, \alpha_\ell, \beta_0, \ldots, \beta_m)^T \in \mathbb{R}^{\ell+m+2} \tag{7.17}$$

and denote by $\mathbf{A}$ the $(10n+10) \times (\ell+m+2)$ constraint matrix implied by the inequalities (7.8), (7.12) and (7.15). In order to obtain a nontrivial vector $\mathbf{c} \neq \mathbf{0}$ which strictly satisfies the component-wise inequalities $\mathbf{Ac} \leq 0$, we propose the computation of a Chebyshev direction (254) of the corresponding unbounded polyhedral cone (258). This requires solving the strictly convex quadratic programming (QP) problem:

$$\begin{aligned} &\arg \min_{\mathbf{c} \in \mathbb{R}^{\ell+m+2}} (\|\mathbf{c}\|_2)^2 \\ \text{subject to} \quad &\mathbf{A}_j \mathbf{c} \leq -\delta \|\mathbf{A}_j\|_2, \quad j = 1, \ldots, 10n+10. \end{aligned}$$

Here $\delta > 0$ is an arbitrary positive constant, $\mathbf{A}_j$ denotes the j-th row of the matrix $\mathbf{A}$ and $\|\cdot\|_2$ is the Euclidean norm. For a discussion on the geometrical interpretation of this QP formulation we refer to (254). Note that the involved optimization has – provided that a solution exists – a unique global minimum. The freely available MATLAB interface `qpas` (259) can for instance be used, which efficiently handles thousands of constraints. To improve the numerical conditioning of the optimization problem, it is advised to rescale the given strikes $K_i$ to the interval $[-1, 1]$ and to use orthogonal polynomials (e.g. Chebyshev polynomials) as basis functions rather than the monomials.

Concerning the values of $\ell$ and $m$, we remark the following. The total model complexity is determined by the total number of coefficients, i.e. $\ell + m + 2$. For a fixed model complexity of $\ell + m + 2$, nothing prevents us to choose arbitrary combinations of $\ell$ and $m$, like in (254). However, for $r_{\ell,m}(K)$ to have a slant asymptote resembling the linearity of option prices when $K$ becomes small, the choice $\ell = m + 1$ is more natural. This way, one can even fix the slope of the asymptote to $-e^{-rT}$. Hence we only consider $\ell = m+1$ and solve the QP problem above for increasing values of $m = 0, 1, 2, \ldots$ until a solution is found.

## 7.3 Benchmark

### 7.3.1 Simulated data and market models

Rather than using market data directly, with an essentially still uncertain RND, we use simulated data based on known RND first, and then add noise. This allows us to accurately test and benchmark the different approaches to imply a probability density function from noisy data.

Three different models of the market are used to test the existing methods (DLN and IVS), and the RII method proposed in this chapter. The first model to simulate market data is of course the Black-Scholes model (9), characterized by expression (1.21) for the asset price. We choose as risk-neutral interest rate $r = 0.05$, volatility $\sigma = 0.2$ and the initial asset price $S_0 = 925$. The same parameter values for $r$ and $S_0$ are used for the next two models.

The second model is the Heston model (76), characterized by two coupled stochastic differential equations

$$\begin{cases} dS(t) = rS(t)dt + \sqrt{v(t)}S(t)dW_1(t) \\ dv(t) = \kappa(\theta - v(t))dt + \sigma_v\sqrt{v(t)}dW_2(t) \end{cases}, \tag{7.18}$$

with $dW_1$ and $dW_2$ two Gaussian processes. The parameters for the Heston model are chosen so that the resulting distribution lies close to a log-normal distribution:

the mean reversion rate is $\kappa = 2$, the mean reversion level is $\theta = 0.04$ and the volatility is $\sigma_v = 0.1$. The correlation $\rho = \langle dW_1 dW_2 \rangle$ is chosen to be $\rho = 0.5$, and the variance at inception (at time $t = 0$) is set to $v_0 = 0.0437$. The second equation determines the stochastic nature of the volatility, and was originally introduced to incorporate the long memory of the volatility observed in realized time series. This model is used to check whether a relative small deviation from the log-normal model already influences the performance of the methods. That is why we use previous mentioned parameter values such that the Feller condition of the Heston model, i.e. $2\kappa\theta > \sigma_v^2$, is already satisfied.

The third model is the CGMY model (85), which is chosen to obtain fat tails in the asset price distribution. Its characteristic exponent is given in expression (2.105). In the mean-correcting martingale measure (109), see section (2.3.2.2), the new characteristic exponent

$$\hat{f}(\omega) = f(\omega) + i\omega \left(r - f(-i)\right) \tag{7.19}$$

is used, such that the asset price discounted by the bank account is a martingale: $\mathbb{E}[e^{-rT} S_T] = S_0 \, e^{-rT} \mathbb{E}[e^{x_T}] = S_0 \, e^{\hat{f}(-i)T - rT} = S_0$. We choose parameter values $C = 0.0244$, $G = 0.0765$, $M = 7.5515$, $Y = 1.2945$. The corresponding distribution differs substantially from the log-normal distribution as can be seen in Figure 7.1. Nevertheless the parameter values for this model are realistic since they are obtained by calibrating a set of European call options on the S&P500 index (109).

The Black-Scholes, Heston and CGMY models of the market belong to three very different classes, and capture different aspects of the market. With each of these market models, we first analytically generate European vanilla option prices for various strikes $K_i$ and time to maturities $T_i$. In total 56 distinct strikes are chosen at equidistant locations in the interval (including the endpoints) with mid-point equal to the forward value and radius equal to 4 times the standard deviation of the underlying PDF. At a single maturity time, such a number of strikes is typical. Figure 7.1 already followed this setup. Then noise is added to the corresponding exact option prices $C_i$ and we let loose the option implied density methods (DLN, IVS and RII) to see how well they perform in retrieving the original, known probability density function of the Black-Scholes, Heston and

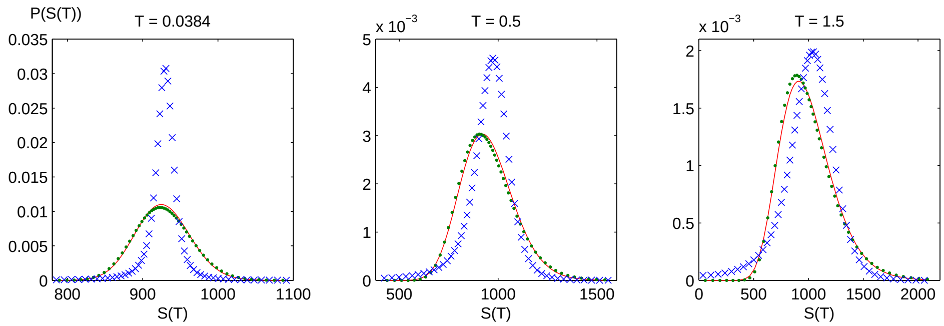


**Figure 7.1:** Illustration of the different distributions used to test the DLN, the IVS and the RII method. From left to right, time ranges from 0.0384 to 0.5 to 1.5 year. The full red curve represents the log-normal distribution, the green dots the Heston distribution and the blue crosses the CGMY distribution.

CGMY models, respectively. This allows us to learn how different aspects of the market (Lévy nature, stochastic volatility, etc.) and the durations influence the performance of the option implied density methods.

An important step in the benchmarking process, is the addition of noise to the exact option prices. The prices plus noise should be similar to market data. Different choices can be made for replicating option market data. One can choose to work with last trade data. The benefit of doing this is that there is one realistic price per strike. The downside is that data for different strikes can originate from trades at different times, and theoretically when comparing prices originating from different times one should discount them all to the same time. Another possibility is to use bid-ask price data, and have a vector of prices which is relevant at the same time. The problem there is that people can state unrealistic high ask prices, ask prices at which there will never be traded. The same can be said about bid prices. In the following we try to replicate last trade data. There are many assets for which options are traded actively enough for last trade data to be useful. We construct the noise in such a way that it replicates the fact that the noise of financial data is smallest around the forward value $F$ and largest in the tails. Here $F = S_0 e^{rT}$ for all three above mentioned models and the values $T = 0.0384$, $T = 0.5$ and $T = 1.5$ (year) are chosen. Hence $F = 926.78$, $F = 948.42$ and $F = 997.04$ respectively. To determine where the tails start we

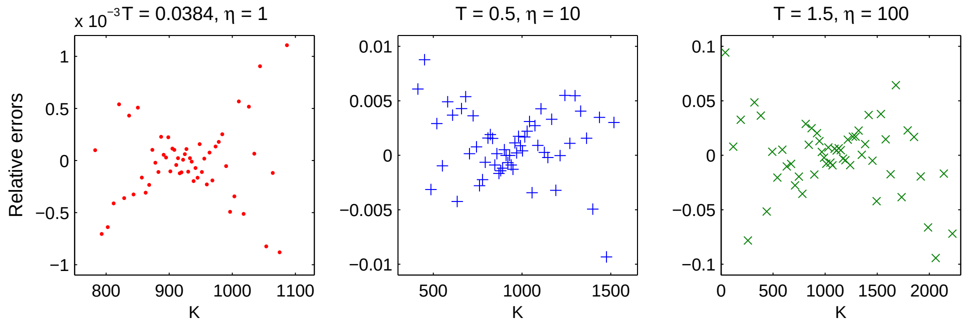


**Figure 7.2:** This figure represents a sample set of the relative errors for different values of $\eta$ and time to maturity $T$ in years. In the left panel $\eta = 1$, $T = 0.0384$, in the middle one $\eta = 10$, $T = 0.5$, and in the right one $\eta = 100$, $T = 1.5$. The relative errors increase as the value of $\eta$ grows (independent of $T$).

use the standard deviation $s$. For each option price a relative error is chosen from a uniform distribution on an interval $[-\beta, \beta]$ where $\beta$ is determined by

$$\beta(K) = \eta \left( 0.00025 \frac{|F - K|}{s} + 0.0001 \right). \tag{7.20}$$

If the control parameter $\eta$ is 1, then the relative error ranges from 0.0001 per unit in the center to 0.0011 per unit in the tails (four standard deviations away from the center). If $\eta$ is 100, then the relative error ranges from 0.01 per unit in the center to 0.11 per unit in the tails. Figure 7.2 illustrates the typical behavior of the relative errors.

For the RII method, intervals $[\underline{c}_i, \overline{c}_i] = [C_i\,(1 - \delta_i), C_i\,(1 + \epsilon_i)]$ are constructed for each of the strikes $K_i$ ($i = 0, \ldots, 55$). Like before, $C_i$ denotes the analytically obtained option price value at strike $K_i$. The relative errors $\epsilon_i = \delta_i > 0$ are chosen according to (7.20). Hence the widths of the intervals mimic the typical behavior of uncertainty in observed financial data: small for strikes close to the forward value and increasingly larger for strikes away from the forward value. In practice, the exact values $C_i$ are unknown and only observed values $\tilde{C}_i$ are given. But intervals $[\underline{c}_i, \overline{c}_i] = [\tilde{C}_i\,(1 - \delta_i), \tilde{C}_i\,(1 + \epsilon_i)]$ with $\delta_i$ and $\epsilon_i$ large enough can always be chosen such that $C_i \in [\underline{c}_i, \overline{c}_i]$.

### 7.3.2 Results and discussion

The obtained RII implied RNDs for different maturity times and values of the control parameter $\eta$ for the three market models are illustrated in Figure 7.3. The performance of the different methods is summarized in Table 7.1. In this table a method which renders a better implied distribution has more plus signs, if the implied distribution is unacceptable a minus sign is assigned to it. We discriminate between good and bad fits in the following way. If $d_i$ are the data points from the original distribution and $d'_i$ are the data points of the implied distribution then we calculate a normalized average error $ne$:

$$ne = \frac{1}{N \max(d_i)} \sum_i |d_i - d'_i| \,. \tag{7.21}$$

Absolute errors are used instead of relative errors because we want to concentrate on the center of the distribution. To be able to compare the average errors of different implied distributions the average error is divided by the maximum value of the original distribution. For example if $ne = 1$ then, on average, the absolute error in each point is as large as the maximum value of the distribution, and the corresponding implied distribution is obviously worthless. If the implied distribution is zero in every data point then $ne$ lies close to 0.5. When $ne \leq 0.1$ the implied distribution starts to look like the original distribution, and we assign a $-$ sign to the distributions for which $ne > 0.1$. If $0.02 \leq ne \leq 0.1$ a $+$ sign is assigned to the implied density, when $0.004 \leq ne \leq 0.02$ a $++$ sign and when $ne \leq 0.004$ a $+++$ sign.

Analyzing Figure 7.3 and Table 7.1 leads to the following conclusions regarding the three tested methods. First, it is apparent that only our newly introduced RII method delivers satisfactory PDF approximations for each scenario. Second, the DLN method is unstable due to the six-dimensional nonlinear optimization problem involved. It is very often in the literature assumed that the interest rate can be determined by other means (bond and future prices). One parameter is then eliminated and the minimization routine becomes much more stable. Although the RII method also relies on a many parameter function, it does not suffer from such effects because the involved optimization is convex. Third, the DLN method, entirely as expected, is least flexible concerning the reproduction

**Table 7.1:** Summary of the performances of the different methods to derive the implied RNDs. The double log-normal method is abbreviated by DLN, the method based on smoothing the volatility surface by IVS, and the method based on rational interval interpolation by RII. A better implied distribution has more plus signs, if the implied distribution is unacceptable a minus sign is assigned.

| $\eta$ | $T$ | Black Scholes | | | Heston | | | CGMY | | |
|---|---|---|---|---|---|---|---|---|---|---|
| | | DLN | IVS | RII | DLN | IVS | RII | DLN | IVS | RII |
| 1 | 0.038 | ++ | ++ | +++ | ++ | ++ | +++ | + | ++ | +++ |
| | 0.5 | − | ++ | +++ | + | ++ | +++ | − | ++ | +++ |
| | 1.5 | − | ++ | +++ | + | ++ | +++ | − | ++ | +++ |
| 10 | 0.038 | +++ | + | ++ | + | + | ++ | + | + | ++ |
| | 0.5 | − | + | +++ | + | − | +++ | − | + | ++ |
| | 1.5 | +++ | + | +++ | ++ | − | +++ | − | + | ++ |
| 100 | 0.038 | ++ | − | ++ | + | − | ++ | − | − | ++ |
| | 0.5 | + | − | ++ | − | − | ++ | − | − | ++ |
| | 1.5 | − | − | ++ | + | − | ++ | − | − | ++ |

of PDF's differing substantially from the log-normal one. The IVS method on the other hand, seems to be flexible as far as it concerns handling data coming from models differing from the log-normal one. Nevertheless also for this method, the data can be from a model with a PDF which is too far from the log-normal one to be tractable. Like the DLN method, also the IVS method might benefit from knowledge of the interest rate. Forth, it is seen that the IVS method is particularly sensitive to random errors, while the RII method is the most robust method in the presence of such errors.

Regarding the results of our RII method, we can say the following. First, for each market model and each time to maturity $T$, the deviation between the RII implied density and the original PDF understandably becomes larger as the value of the error control parameter $\eta$ grows. Second, almost for each $\eta$ and $T$, the performance of the RII method decays with increasing skewness and kurtosis of the underlying PDF. However, the final results are always satisfactory. Third, for each market model and each $\eta$, the values of the error criteria parameter $ne$ are fairly similar for different time to maturities. Hence the maturity time $T$ of the option hardly influences the performance of the method. Fourth, for each RII implied density, it is seen that the left tail approximation can be worse than the right tail approximation. This is mainly due to the fact that relative

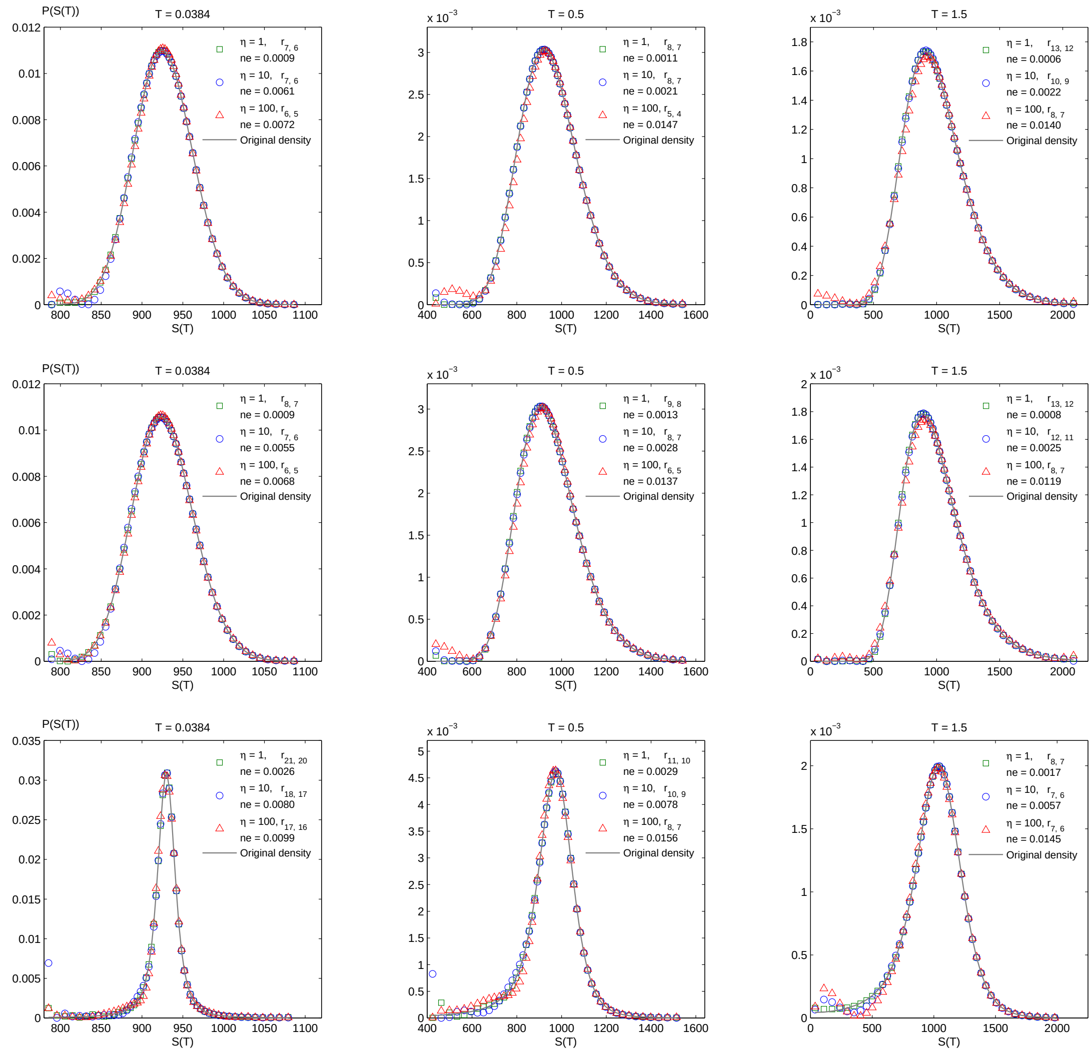


**Figure 7.3:** This figure illustrates the RII implied RNDs for the Black-Scholes data, the Heston data and the CGMY data, respectively, from top to bottom. From left to right, the time to maturity $T$ takes the value 0.0384, 0.5 and 1.5. In each panel, the full gray line is the exact PDF, while the green squares, the blue circles and the red triangles are the RII implied density approximations from the scenarios with control parameter $\eta = 1$, 10 and 100, respectively. The complexity of the rational function $r_{\ell,m}(K)$, as well as the value $ne$ from (7.21) are shown for each scenario.

errors on large option prices (for small strikes) result in much larger absolute deviations than on small option prices (for large strikes). However, for small relative deviations (i.e. $\eta = 1$) the RII method always performs outstanding.

The benchmark leads us to conclude that the commonly used DLN and IVS methods may lack reliability in a market that behaves more Heston-like or that has CGMY characteristics, and that the RII method outlined here is currently the most promising technique for implying RNDs from real option price data. Notably, though the simulated data are dependent on some special models, our RII method is model independent.

## 7.4 Application to market data

Now that it is demonstrated from simulated data that our RII implied density method produces reliable results, we are ready to apply the technique to real market data. We extract the implied RNDs from the daily closing bid and ask prices for Standard and Poor's 500 (S&P 500) Index options.

Unlike with simulated data, we now have no exact original density to benchmark, neither do we have the risk-neutral interest rate $r$ to discount the expected value to current time. By contrast, we have bid and ask prices from the market, which are quoted for all traded strikes no matter whether transactions occur or not. In (253), the average of bid and ask is taken as the best available measure of the option price. We use bid and ask prices directly to define the interval data for our RII method. In addition, we use bids and asks as a criterium to measure the goodness of the computed implied RND in the following way. If $[\underline{c}_i, \overline{c}_i]$ is the bid and ask interval at strike price $K_i$ and $\mathrm{ImpliedPrice}(K_i)$ is the implied European vanilla option price derived from the implied RND for that strike, then we define the relative position (RP) of this implied option price as:

$$RP(K_i) = \frac{\mathrm{ImpliedPrice}(K_i) - \underline{c}_i}{\overline{c}_i - \underline{c}_i}. \tag{7.22}$$

If $RP(K_i)$ equals 0.5, then the implied price is exactly in the middle between bid and ask at strike price $K_i$. We call the implied density good if $RP(K_i)$ lies in between 0 (at the bid price) and 1 (at the ask price). The further the distance between the value $RP(K_i)$ and the interval $[0, 1]$, the worse the achieved implied RND.

Another difference between real data and the previously considered simulated data is the availability of put option prices. Our RII method can be applied directly to derive an implied density from the put option prices after taking a few minor modifications into account, as we show next. Analogous to the price of a European vanilla call option, the price of a European vanilla put option is given by the basic pricing formula

$$P(S_0, K, T) = e^{-rT} \int_0^K (K - S_T) P(S_T, T|S_0) dS_T. \tag{7.23}$$

Because the theoretical price of a European vanilla put option is also convex, but now monotonically increasing with respect to the strike $K$, the inequalities (7.10) for calls are replaced by

$$0 \le r'_{\ell,m}(K_i) \le e^{-rT}, \qquad i = 0, \dots, n. \tag{7.24}$$

Consequently, the linear inequalities (7.12) are replaced by

$$\begin{cases} -p'_\ell(K_i) + \overline{c_i}\, q'_m(K_i) \le 0 \\ -p'_\ell(K_i) + \underline{c_i}\, q'_m(K_i) \le 0 \\ e^{-rT} q_m(K_i) + p'_\ell(K_i) - \overline{c_i}\, q'_m(K_i) \le 0 \\ e^{-rT} q_m(K_i) + p'_\ell(K_i) - \underline{c_i}\, q'_m(K_i) \le 0 \end{cases}, \quad i = 0, \dots, n. \tag{7.25}$$

The goal of this section is to find a single implied RND and verify whether it reproduces feasible implied call and put option prices, i.e. the ImpliedPrice from the basic pricing formulas (7.1) and (7.23). A good implied RND reproduces implied option prices that are within the given bids and asks. We start with a detailed description of one example to explain the improved procedure of our RII method. Other examples, following the same reasoning, are given at the end of this section.

For data, we take the S&P 500 index call option prices as well as the put option prices of January 5th, 2005 with maturity time on March 18th, 2005 (72 days). This is the same data as used in (253), see Table 1 of that paper. In total there are 22 strike prices for calls ranging between 1050 and 1500, and 35 strike prices for puts ranging between 500 and 1350. The S&P 500 index closing level is 1183.74, the interest rate is 2.69%, and the dividend yield is 1.7%. As mentioned

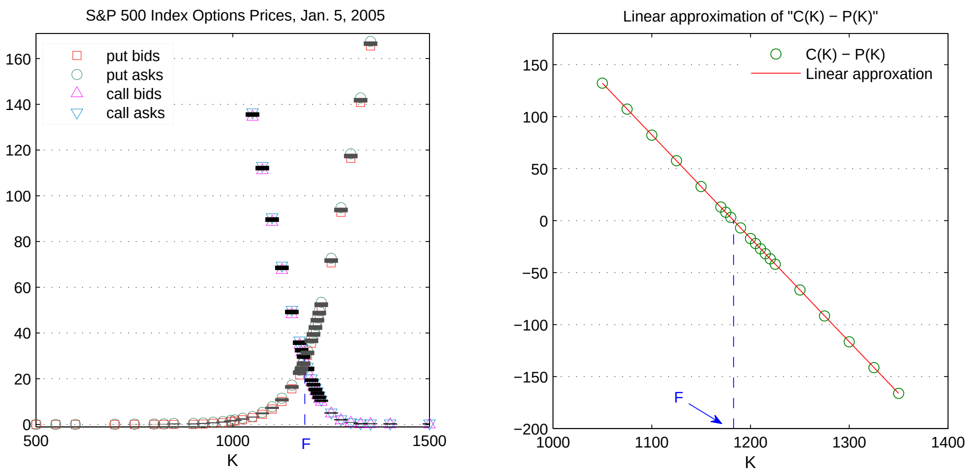


**Figure 7.4:** Left, the bid and ask call and put price intervals from the S&P 500 index options of January 5th, 2005 with maturity date on March 18th, 2005. Right, obtaining the forward value $F$ and the discount factor $e^{-rT}$ from the best linear $\ell_1$-norm approximation of $C - P$, with circles the data and line the linear approximation. The vertical blue dashed line indicates the location of the forward price $F$.

before, bid and ask prices from both puts and calls are used to define the interval data. These data intervals are shown in Figure 7.4 (left).

As demonstrated in (253), on average, option traders expect a risk-neutral return which is 21 basis points below the risk-neutral interest rate (using The London Interbank Offered Rate as a proxy for that rate). For this reason we do not use the interest rate 2.69% as mentioned above. Instead, to determine the value of the discount factor $e^{-rT}$, we rely on the put-call parity

$$C(S_0, K, T) - P(S_0, K, T) = e^{-rT}(F - K), \tag{7.26}$$

where the forward price $F$ is the expected price of $S_T$. The forward price $F$ together with the discount factor $e^{-rT}$ are obtained from a linear approximation of the values $\tilde{C}_i - \tilde{P}_i$ as a function of common strike prices $K_i$. Here we obtain them from a best linear $\ell_1$-norm approximation, using the midpoints of the given intervals as data values, i.e. $\tilde{C}_i$ and $\tilde{P}_i$. Such an $\ell_1$-approximation is least sensitive to outliers (for more details we refer to (258, Section 6.1)). The results of this approximation are shown in Figure 7.4 (right). We find $F = 1182.9$ and $e^{-rT} =$

0.9948. Since $T = 72/365$, we have the option traders' expected risk-neutralized return $r = 2.64\%$, which is a realistic value. Though the value $F$ is slightly smaller than the index closing level 1183.74, it is still realistic due to the large uncertainty of that single last trade price.

Given the value of the discount factor above, we apply the RII method to both the call price interval data and the put price interval data. We obtain two rational approximations $r_{5,4}^{\text{call}}(K)$ and $r_{5,4}^{\text{put}}(K)$. Note that, in general, the obtained numerator and denominator degrees need not be the same for puts and calls. The two resulting implied densities are shown in Figure 7.5 (left). We find that these two implied RNDs differ too much to be reliable. Our goal is to obtain a single implied RND, suitable for both call price data and put price data.

For this purpose, first, we note that we can bring both curves $r^{\text{call}}$ and $r^{\text{put}}$ in better agreement by forcing the denominator polynomials to be the same, and the degrees of the numerator polynomials to be equal. The details of this procedure are outlined in Appendix A. Basically, the coefficients of both rational approximations are obtained from a single QP problem, which combines the QP problem of the RII method for call with the QP problem of the RII method for put into one. This is a simultaneous call-put RII method.

The idea behind the next step is that we use the call curve in the region where call prices are most reliable, and the put curve in the region where put prices are most reliable, and then glue the two curves together at an intermediate value. For this intermediate value, we take the forward price F, at which point the European vanilla call option price coincides with the European vanilla put option price. Since most trading occurs for at-the-money and out-of-the-money contracts, we take the prices for these contracts to be more reliable. Put options are out-of-the-money when $K < F$, whereas for call options this is $K > F$. Then, we can propose to use the implied density curve $r^{\text{put}}(K)$ for $K < F$ and $r^{\text{call}}(K)$ for $K > F$. This choice is supported by practice: the CBOE also calculates the VIX index by combining only out-of-the-money call and put contracts. Another motivation for this choice is that from the basic pricing formulas (7.1) and (7.23) we know that for both the calls and puts, the option prices for all strikes are dominated by the out-of-the-money probability density functions. Moreover, we

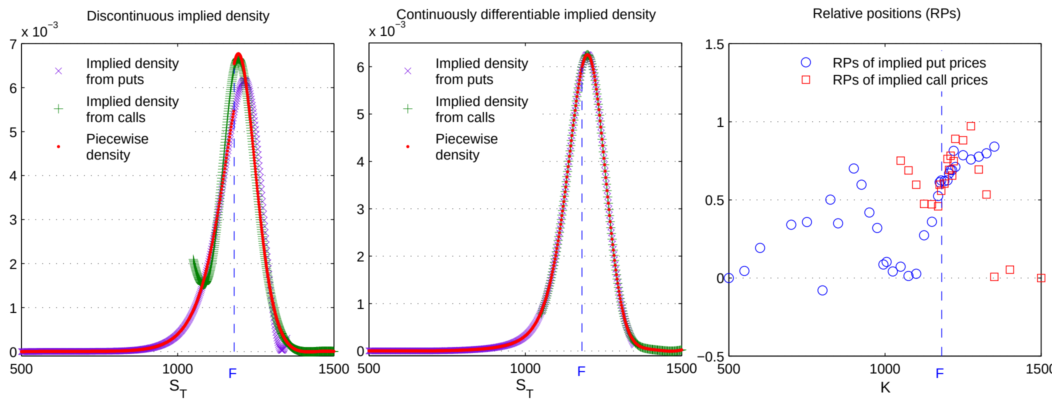


**Figure 7.5:** The purple crosses represent the implied RND derived from put option prices, the dark green plus signs represent the one from call option prices, and the red dots are the piecewise RNDs with basic RII method for the left panel, and final improved RII method for the middle panel. The right panel illustrates the relative positions of implied option prices, see expression (7.22). The vertical blue dashed line indicates the location of forward price $F$.

already obtain $F$ from the determination of the discount factor. The results of this procedure are shown in Figure 7.5 (left).

The remaining drawback of this procedure is that the implied density curve is in general not continuously differentiable at the value where we have stitched together $r^{\text{call}}$ and $r^{\text{put}}$. Within the RII formalism, this can be easily overcome by introducing some additional equations and inequalities that express the conditions of continuous differentiability at $F$. In Appendix B, the details of this improvement on the formalism are explained. The results for the (normalized) implied RND and for the relative positions (7.22) are shown in Figure 7.5 (middle and right). Almost all the implied prices calculated from the implied RND are within their bid and ask intervals, from which we conclude with confidence that the continuously differentiable implied RND derived from our final improved RII method, combining all available information from call and put prices into the best of both worlds, reliably represents the single implied RND we are looking for.

Finally, to illustrate the robustness of our RII method, we consider some additional S&P 500 index options. We arbitrarily choose the date of September 3rd,

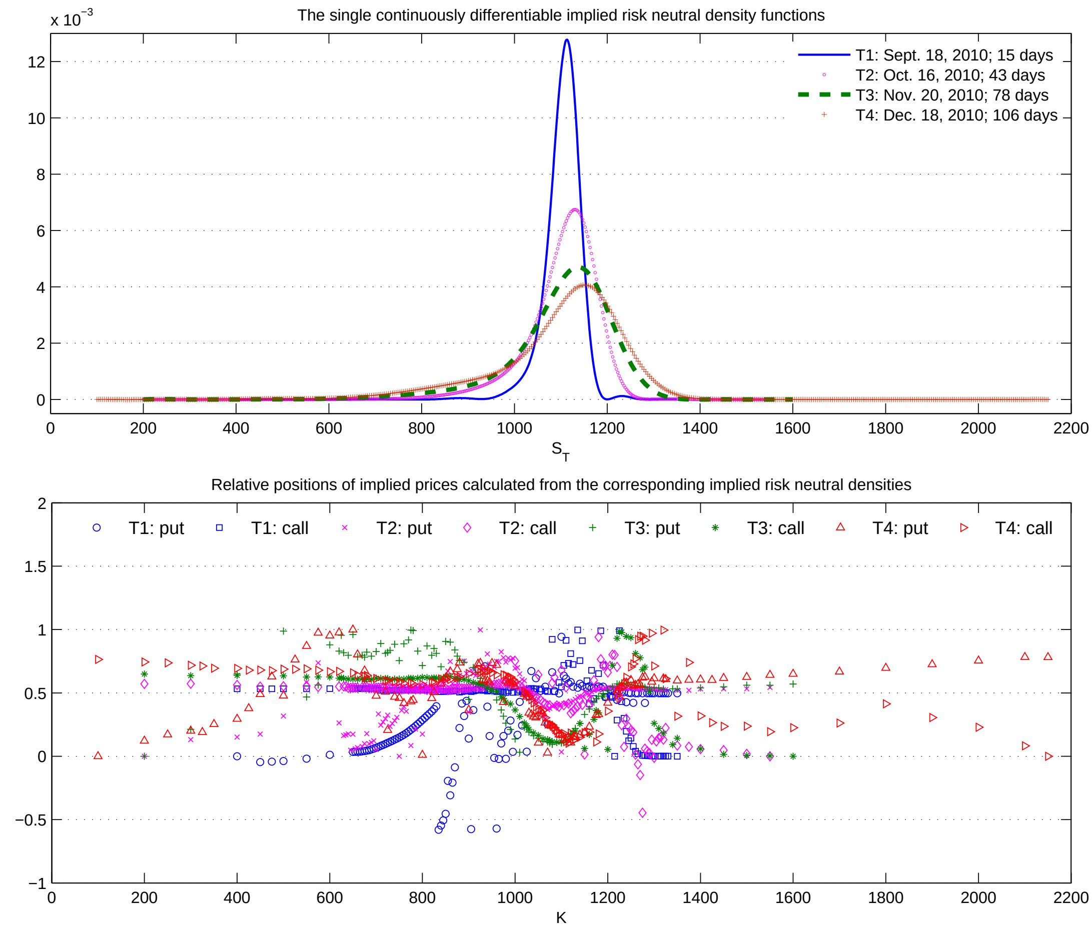


**Figure 7.6:** The top panel illustrates the single continuously differentiable implied RNDs derived from S&P 500 index option prices of September 3rd, 2010 with different maturity times by using our final improved RII method. The bottom panel represents their corresponding relative positions, defined in expression (7.22), for both European vanilla put option prices and call option prices with different maturity dates.

2010, then extract the single continuously differentiable implied RNDs from the closing bid and ask prices with maturity times ranging from 2 weeks to around 3 months, that is, with the maturity dates on September 18th, 2010 (15 days), October 16th, 2010 (43 days), November 20th, 2010 (78 days) and December 18th, 2010 (106 days). The obtained implied RNDs as well as their corresponding relative positions for both implied European vanilla put option prices and call option prices are shown in Figure 7.6. The worst result is in the scenario with 15 days to maturity. The probability density function of such short maturity contracts are often badly behaved because of the price effects from trading strategies related to contract expiration and rollover of hedge positions into later expirations (253). Even for this worst case, the relative positions are mostly within their bid and ask intervals, i.e. between $[0, 1]$ in Figure 7.6 (bottom). For other cases, results are better.

## 7.5 Conclusions

A rational interval interpolation (RII) method is presented to imply the risk-neutral probability density function of the underlying asset price (RND) from the observed option price as a function of the strike. This RII method is compared with existing techniques, in particular the commonly used implied volatility surface (IVS) approach and the double log-normal (DLN) approach. For this purpose, a benchmark is developed that evaluates how well a given method retrieves a RND from noisy option prices. This allows to assess the RII, IVS and DLN approaches in different settings. A method may be good at retrieving the Black-Scholes RND, but fail to obtain the correct RND in the case of a CGMY or Heston world. Since we know that realistic RND significantly differ from the Black-Scholes result, this is a concern that should be addressed when comparing methods.

We find that for any setting, the RII method presented here is more robust to increasing noise levels on the option prices than both the DLN and IVS method. Moreover, in contrast to the DLN and IVS method, the RII method retains the ability to retrieve the correct RND in the more realistic test cases of the Heston and CGMY model. The RII method is also better suited for working with longer maturity options, a property that may be related to its ability to recover distributions with fat tails. The only region where significant discrepancies between the option implied RND and the test RND can be found is for option prices well in-the-money: this tail of the distribution can be overestimated when the noise on the option price becomes large.

In order to overcome this difficulty when applying the method to real market data, we rely on both European vanilla call and put options, with different numbers of available strike prices, combining the complementary out-of-the-money regions where these contracts give reliable results. This results in a single, continuously differentiable implied RND compatible with both call and put option price intervals. For market data, the exact analytic expression for the underlying distribution is unknown and cannot be used to check the RII result, so we use the relative position of the result within the bid and ask interval as an indicator of the quality of the results. The method and techniques outlined here allow to determine the implied RNDs that are model-independent and do not suffer from time-dependent effects in historical data. This opens the way to study the role of the scale-free characteristics of these densities near critical points.

## 7.6 Appendix

### 7.6.1 The simultaneous call-put RII method

Of the same underlying, we assume to be given $n_1+1$ call intervals $[\underline{c}_i, \overline{c}_i]$ at strike locations $K_i^{\text{call}}$ $(i = 0, \cdots, n_1)$ and $n_2+1$ put intervals $[\underline{p}_i, \overline{p}_i]$ at strike locations $K_i^{\text{put}}$ $(i = 0, \cdots, n_2)$. Denote the common call-put denominator polynomial of degree $m$ by

$$q_m(K) = \sum_{i=0}^{m} \beta_i K^i. \tag{7.27}$$

We are looking for two rational functions $r_{\ell_1,m}^{\text{call}}(K) = p_{\ell_1}^{\text{call}}(K)/q_m(K)$ and $r_{\ell_2,m}^{\text{put}}(K)$ $= p_{\ell_2}^{\text{put}}(K)/q_m(K)$ with respective numerator polynomials

$$p_{\ell_1}^{\text{call}}(K) = \sum_{i=0}^{\ell_1} \alpha_i^{(1)} K^i, \qquad p_{\ell_2}^{\text{call}}(K) = \sum_{i=0}^{\ell_2} \alpha_i^{(2)} K^i, \tag{7.28}$$

for which the following conditions are satisfied:

$$\begin{cases} \underline{c}_i \leq r^{\text{call}}_{\ell_1,m}(K^{\text{call}}_i) \leq \overline{c}_i, & i = 0,\ldots,n_1, \\ \underline{p}_i \leq r^{\text{put}}_{\ell_2,m}(K^{\text{put}}_i) \leq \overline{p}_i, & i = 0,\ldots,n_2, \\ -e^{-rT} \leq r'^{\text{call}}_{\ell_1,m}(K^{\text{call}}_i) \leq 0, & i = 0,\ldots,n_1, \\ 0 \leq r'^{\text{put}}_{\ell_2,m}(K^{\text{put}}_i) \leq e^{-rT}, & i = 0,\ldots,n_2, \\ 0 \leq r''^{\text{call}}_{\ell_1,m}(K^{\text{call}}_i), & i = 0,\ldots,n_1, \\ 0 \leq r''^{\text{put}}_{\ell_2,m}(K^{\text{put}}_i), & i = 0,\ldots,n_2. \end{cases} \tag{7.29}$$

Denote the vector of combined coefficients by

$$\mathbf{c} = (\alpha^{(1)}_0, \cdots, \alpha^{(1)}_{\ell_1}, \alpha^{(2)}_0, \cdots, \alpha^{(2)}_{\ell_2}, \beta_0, \cdots, \beta_m)^T \in \mathbb{R}^{\ell_1+\ell_2+m+3} \tag{7.30}$$

and denote by $\mathbf{A}$ the $(10n_1 + 10n_2 + 20) \times (\ell_1 + \ell_2 + m + 3)$ constraint matrix composed of the linear inequalities ensuring (7.29). Note that this matrix has many zero entries. A nontrivial vector $\mathbf{c} \neq \mathbf{0}$ which strictly satisfies the component wise inequalities $\mathbf{Ac} \leq 0$, can then be obtained in a similar way as before. Hence by solving the strictly convex quadratic programming (QP) problem:

$$\begin{aligned} &\arg \min_{\mathbf{c}\in\mathbb{R}^{\ell_1+\ell_2+m+3}} (\|\mathbf{c}\|_2)^2 \\ &\text{subject to} \quad \mathbf{A}_j\mathbf{c} \leq -\delta \|\mathbf{A}_j\|_2, \quad j = 1,\ldots,10n_1+10n_2+20. \end{aligned} \tag{7.31}$$

A natural choice for $\ell_1$ and $\ell_2$ is

$$\ell_1 = \ell_2 = m + 1. \tag{7.32}$$

### 7.6.2 Ensuring continuous differentiability

At the location of the forward value $F$, we add to the simultaneous call-put RII method that the piecewise implied density derived from $r^{\text{call}}_{\ell_1,m}(K) = p^{\text{call}}_{\ell_1}(K)/q_m(K)$ and $r^{\text{put}}_{\ell_2,m}(K) = p^{\text{put}}_{\ell_2}(K)/q_m(K)$ is continuously differentiable at $K = F$. So we require

$$\begin{cases} r''^{\text{call}}_{\ell_1,m}(F) = r''^{\text{put}}_{\ell_2,m}(F), \\ r'''^{\text{call}}_{\ell_1,m}(F) = r'''^{\text{put}}_{\ell_2,m}(F). \end{cases} \tag{7.33}$$

Without any further consideration, these conditions are essentially nonlinear equations in the unknown coefficients. However, we show how (7.33) can be satisfied by the following linear conditions. Basically, the rational approximations $r_{\ell_1,m}^{\text{call}}(K)$ and $r_{\ell_2,m}^{\text{put}}(K)$ need to share some additional theoretical relations that exist between $C(S_0, K, T)$ and $P(S_0, K, T)$ at $K = F$.

First, it is known that at-the-money (hence when $K = F$) is the only status where the price of a call option and a put option are the same. Therefore we impose that

$$r_{\ell_1,m}^{\text{call}}(F) = r_{\ell_2,m}^{\text{put}}(F). \tag{7.34}$$

Provided that $q_m(F) \neq 0$, one readily obtains that (7.34) implies

$$p_{\ell_1}^{\text{call}}(F) - p_{\ell_2}^{\text{put}}(F) = 0. \tag{7.35}$$

Without loss of generality, we put

$$q_m(F) > 0. \tag{7.36}$$

At this point it is worth emphasizing that, when $\underline{c}_i < \overline{c}_i$ and if the linear inequalities

$$\begin{cases} -\overline{c}_i q_m\left(K_i^{\text{call}}\right) + p_{\ell_1}^{\text{call}}\left(K_i^{\text{call}}\right) \leq 0 \\ \underline{c}_i q_m\left(K_i^{\text{call}}\right) - p_{\ell_1}^{\text{call}}\left(K_i^{\text{call}}\right) \leq 0 \end{cases}, \qquad i = 0, \ldots, n. \tag{7.37}$$

are strictly satisfied, then it follows that $q_m\left(K_i^{\text{call}}\right) > 0$. A similar reasoning holds of course for $q_m\left(K_i^{\text{put}}\right)$. As a consequence, the denominator $q_m(K)$ obtained from solving the proposed QP problem(s) always satisfies $q_m\left(K_i^{\text{call}}\right) > 0$ and $q_m\left(K_i^{\text{put}}\right) > 0$ by construction. Because the forward value $F$ may not belong to either the given $K_i^{\text{call}}$ or the given $K_i^{\text{put}}$, a nonzero condition such as (7.36) needs to be added for (7.35) to imply (7.34).

Second, from the put–call parity (7.26) follows

$$\frac{\partial P(S_0, K, T)}{\partial K} = e^{-rT} + \frac{\partial C(S_0, K, T)}{\partial K}. \tag{7.38}$$

Therefore we also impose that

$$r_{\ell_1,m}^{\prime\,\text{put}}(F) = e^{-rT} + r_{\ell_2,m}^{\prime\,\text{call}}(F). \tag{7.39}$$

Given that $q_m(F) > 0$ and $r_{\ell_1,m}^{\text{call}}(F) = r_{\ell_2,m}^{\text{put}}(F)$, (7.39) is satisfied if and only if

$$p_{\ell_2}^{\prime\,\text{put}}(F) - p_{\ell_1}^{\prime\,\text{call}}(F) - e^{-rT} q_m(F) = 0. \tag{7.40}$$

Combining all the above, it is not difficult to find that (7.33) is satisfied if the linear inequality (7.36), the linear equalities (7.35), (7.40) and

$$p''^{\text{put}}_{\ell_2}(F) - p''^{\text{call}}_{\ell_1}(F) - 2e^{-rT}q'_m(F) \;=\; 0, \tag{7.41}$$

$$p'''^{\text{put}}_{\ell_2}(F) - p'''^{\text{call}}_{\ell_1}(F) - 3e^{-rT}q''_m(F) \;=\; 0, \tag{7.42}$$

are satisfied. The converse is also true after (re)normalizing such that $q_m(F) > 0$. Following a similar reasoning, even higher orders of smoothness can be imposed if desired.

# 8

# Conclusions

In this thesis, I investigated the pricing of financial derivatives and its inverse problem, deriving the probability density for the underlying asset from the observed prices of financial derivatives. Although the Balck-Scholes model is very simple, it already captures two most important things that are of concern to investors and speculators, namely the interest rate and the volatility. The interest rate determines the expected risk-neutral return of an investment, whereas the volatility measures its risk. Trading financial derivatives seems similar to exchanging cash flows, but in essence it is more accurate to describe it as *trading the return* or *trading the risk*. This is of course a simplified picture: some instriments trade both risk and return, and/or some other items of interest to investors. In view of the trading of returns, available financial instruments include interest rate derivatives, foreign exchange derivatives, and so called fixed income products (because the returns of these products are actually fixed at the beginning), etc. In view of the trading of volatility, there are variance options, timer options, VIX options, etc.

In order to describe the important financial parameters accurately, such as the interest rate and the underlying asset's volatility, researchers found in empirical studies that the Black-Scholes model is insufficient, and a host of more complicated models were established. Models with more free degrees are supposed to provide a more accurate description of the market. However, what characterizes a good model and makes it popular amongst practitioners, is not only its capability to capture the important features of the market, but also its numerical efficiency.

Succesful models must be able to produce fast and robust pricing formulas and allow for efficient calibration. As argued in this thesis, including diffusion and jumps (mainly through the Lévy process and Poisson jumps) is of importance for realistic models. Also the correlation between the underlying asset and its volatility is indispensable. Both jumps and stochastic volatility complicate pricing efficiency. Path integrals offer a new point of view to the formulation of these models and their pricing formulae, providing new closed form expressions for the prices and allowing for new types of estimators.

In this thesis, I have contributed to the path-integral formulation in the following ways:

- I have shown in chapter 3 (and reported in reference (144)) how the path-integral propagator for a model that does not include jumps can be extended straightforwardly so as to include jumps. The derivative prices obtained with the models, extended to include jumps, were compared our own Monte-Carlo simulations, and the technique was used in subsequent chapters every time jump-diffusion models were involved.

- I have applied in chapter 4 the path-integral Duru-Kleinert transformation to change from real time to time as measured by volatility (where the 'clock' ticks faster as volatility is higher). This is of particular use to trade timer options, and I have derived pricing formulae for timer options in different models. This was reported in reference (145). It also led to a "spin-off" result in the field of radioactive dosimetry, for which a publication is in preparation. As future prospects, this method opens up new avenues to study models that interpret stochastic volatility through a Brownian motion subordinated to a random clock.

- Very often path-dependent derivatives (such as Asian options) can be interpreted as partitioning the set of all paths, and offering a payoff that differs from partition to partition. Path integration over conditioned paths, the subject of chapter 5, is in essence a method to take the sum over all paths in a given partition. Some of this work was the subject of reference (229). Then, the full path integral can be rewritten as a sum over all partitions,

> so that the payoff can be straightforwardly taken into account. I developed and applied this technique to various Asian options, options on realized variance, VIX options and the dosimetry application mentioned earlier.

To enhance the numerical efficiency of the results, we have been inspired by the COS method (143). This method looks promising for the calculation of the propagators or the pricing formulas obtained in chapters 3-5, and I explore its use as well as the use of finite difference methods in chapter 6. We find that for some of the applications studied earlier, the COS method indeed allows a substantial increase in computing efficiency, and there is merit in combining these techniques. As a prospect for future research, we note that the implementation on a Graphics Processing Unit (237) is an appealing direction. It will hopefully speed up the numerical calculation efficiency, which is particularly important for high dimensional problems.

The final part of the thesis, in chapter 7, explores the possibility to derive the underlying probability density for the asset, given the prices, observed in the market, for options built on that asset. This work has been submitted for publication (reference (146)). There exist inversion formulae, but they suffer from noise and from inherent assumptions of the model (such as lognormality). We introduce our own technique, the rational interval interpolation, and compare it with some existing methods, finding that it is fast and robust. After benchmarking the technique, using simulated market data that emphasizes characteristics such as fat tails, we show the applicability of the technique to real market data.

In conclusion, I have presented several new techniques and pricing formulas based on path integration in this thesis. This was done for a variety of models. We also investigate the inverse problem, getting 'experimental observations' of model characteristics from the observed option prices. This is necessary to justify the use of a certain model. I believe this leads to a new starting point, from which we are ready to do more significant researches on financial derivatives and other related subjects.

# Samenvatting

In deze thesis wordt in essentie het prijzen van financiële instrumenten (opties en andere derivaten) bestudeerd. Ook bestudeer ik het inverse probleem dat er in bestaat om uit de prijzen die in de markt worden waargenomen de kansverdelingen van de onderliggende goederen te reconstrueren. Het belangrijkste instrument dat ik hierbij gebruik en verder ontwikkel is de padintegraalmethode. Deze laat toe om, gegeven een stochastisch model, de verwachte opbrengst te schrijven als een gewogen som over mogelijke geschiedenissen. Hiermee kunnen ook pad-afhankelijke contracten accuraat geprijsd worden op een natuurlijke manier.

Het eenvoudigste model is het Black-Scholes model. Ondanks de eenvoud ervan bevat het (voor speculanten alsook investeerders) reeds de twee belangrijkste aspecten van de markt, namelijk de interestvoet en de volatiliteit. De interestvoet bepaalt de risiconeutrale opbrengst van een investering, terwijl de volatiliteit een maat is voor het risico ervan. Het verhandelen van financiële derivaten lijkt gelijkaardig aan het uitwisselen van cash flows, maar mijns inziens is het juister om het te beschrijven als het verhandelen van opbrengst of het verhandelen van risico. Dit is natuurlijk een sterk vereenvoudigde opdeling, en gemengde produkten zijn mogelijk. Om opbrengst (return) te verhandelen wordt ondermeer gebruik gemaakt van interestvoet derivaten, foreign exchange derivaten, zogenaamde 'fixed income' produkten, enz. Om risico te verhandelen worden ondermeer variance opties, timer opties, VIX opties,... gebruikt.

Bij de studie van de belangrijkste financiële parameters (zoals interestvoet en volatiliteit) werd al snel duidelijk dat het Black-Scholes model (het 'standaardmodel' van de financiële derivaten) ontoereikend is. Vele nieuwe stochastische modellen werden vooropgesteld, met bijkomende vrijheidsgraden om het marktgedrag beter te vatten. Opdat een model succesvol is bij financiëel analysten, traders en andere gebruikers, is de capaciteit om het marktgedrag goed te beschrijven niet de enige belangrijke factor: ook de computationele efficiëntie is belangrijk. Succesvolle modellen moeten tot snelle en robuuste prijsformules leiden, waarvan de parameters efficiënt gecalibreerd kunnen worden. In deze thesis stellen we dat het combineren van diffusie (voor de volatiliteit) en sprongen (via Lévy processen en Poisson verdeelde sprongen) van belang zijn om de essentiële karakteristieken van de markt goed te beschrijven. Ook de correlatie tussen het proces van het onderliggend goed en het proces van de volatiliteit is onontbeerlijk. Maar, zowel stochastische volatiliteit als sprongen bemoeilijken het prijzen van opties: het gebrek aan analytische prijzingsformules maakt het prijzen numeriek minder efficiënt. Deze thesis stelt dat padintegralen een nieuwe invalshoek bieden voor de beschrijving van stochastische modellen, een invalshoek die in vele concrete gevallen leidt tot nieuwe uitdrukkingen voor optieprijzen en andere relevante verwachtingswaarden. Dit heb ik in mijn thesis op de volgende concrete derivaten en modellen toegepast:

- In hoofdstuk 3 toon ik hoe de padintegraalpropagator met sprongen kan geconstrueerd worden uit de kennis van de propagator voor het gelijkaardig model, maar zonder sprongen. Met deze nieuwe propagator worden optieprijsformules uitgewerkt, en geverifieerd met Monte-Carlo simulaties.

- In hoofdstuk 4 pas ik een methode uit de kwantum-padintegraaltheorie toe om timer opties te prijzen. De methode die hier vanuit de kwantumfysica naar de wereld van financiële instrumenten wordt overgebracht is de Duru-Kleinert transformatie. Deze transformatie laat toe om over te gaan van de echte tijd naar een tijd waarbij de klok sneller tikt naarmate de volatiliteit hoger is. In deze relatieve tijd kunnen prijsformules voor timeropties eenvoudig uitgewerkt worden. Dit deel van het werk leidde ook tot een terugkoppeling naar de kwantumfysica: het prijzen van timer opties blijkt analoog aan het zoeken van een maximale blootstellingstijd in een omgeving met fluctuerende radioactiviteit. In het algemeen kunnen met de techniek uit hoofdstuk 4 nieuwe modellen worden beschreven waarin de stochastische volatiliteit gesubordineerd is aan een random klok.

- In hoofdstuk 5 toon ik aan dat vele pad-afhankelijke derivaten (zoals Aziatische opties) in de padintegraalbeschrijving behandeld kunnen worden door de ruimte van de paden te partitioneren, waarbij alle paden binnen eenzelfde partitie ook dezelfde payoff hebben. Padintegratie over geconditioneerde paden laat toe om alle paden binnen een dergelijke partitie te sommeren. De uiteindelijke prijsformule en/of propagator wordt dan gevonden als een som over de partities. Deze techniek ontwikkel ik voor verschillende Aziatische opties, opties op gerealiseerde variantie, VIX opties en de eerder vermelde toepassing op radioactieve dosimetrie.

In het laatste deel van de thesis wordt het inverse prijzingsprobleem onderzocht. Bij de grote verscheidenheid aan modellen kan men zich terecht de vraag stellen waarom een bepaald model beter zou zijn dan een ander, gegeven de waargenomen prijzen in de markt. Verschillende modellen voorspellen verschillende waarschijnlijkheidsdichtheden voor de verdeling van de prijs van een onderliggend goed op een bepaalde tijd, maar uiteindelijk wordt op elk ogenblik slechts één prijs gerealiseerd. Hoe kunnen we dan toch uit het 'experiment' de waarschijnlijkheidsdichtheid distilleren? Het idee hierachter is dat, hoewel het onderliggend goed een bepaalde prijs heeft op een welbepaald ogenblik, er op datzelfde ogenblik ook een schare aan opties op datzelfde onderliggend goed verhandeld worden: opties met verschillende strike-prijs, call-opties en put-opties, ... De verzameling van deze produkten geeft evenzeer informatie over hoe de markt de waarschijnlijkheidsdichtheid voor de prijzen inschat. Er bestaan reeds een aantal methodes om de waarschijnlijkheidsdichtheid van de prijs van het onderliggende te reconstrueren, maar die zijn gevoelig voor ruis en zijn gebaseerd op een onderliggend model dat verondersteld wordt. Hier introduceren we onze eigen techniek, de rationele interval interpolatie toegepast op optieprijzen. We vergelijken deze techniek met de bestaande methodes en besluiten dat onze techniek robuuster is dan de meest courante methodes. Bovendien is de techniek modelonafhankelijk. We passen ten slotte de techniek toe op de echte marktdata.

Kortom, in deze thesis heb ik verschillende nieuwe technieken ontwikkeld – veelal gebaseerd op padintegralen– en prijsformules afgeleid voor een verscheidenheid aan modellen en contracten. Hierbij wordt duidelijk dat de padintegraalmethode een veelbelovende techniek is voor de financiële analyse. Ook heb ik het inverse probleem onderzocht om uit de waargenomen prijzen informatie te bekomen over de onderliggende kansverdelingen (die natuurlijk gelinkt zijn aan de padintegraalpropagatoren). Het potentieel van de padintegralen, getoond in deze thesis, zal mijns inziens blijven leiden tot een beter begrip, niet enkel van bestaande financiële produkten, maar ook van de eigenlijke werking van de financiële markten.

# Publications

- Lingzhi Liang, Damiaan Lemmens, Jacques Tempère, *Generalized pricing formulas for stochastic volatility jump diffusion models applied to the exponential Vašiček model*, The European Physical Journal B - Condensed Matter and Complex Systems, **75**(3):335-342, 2010.
- Damiaan Lemmens, Lingzhi Liang, Jacques Tempère, Ann De Schepper, *Pricing bounds for discrete arithmetic Asian options under Lévy models*, Physica A: Statistical Mechanics and its Applications, **389**(22):5193-5207, 2010.
- Lingzhi Liang, Damiaan Lemmens, Jacques Tempère, *Path integral approach to the pricing of timer options with the Duru-Kleinert time transformation*, Physical Review E, **83**(5):056112, 2011.
- Lingzhi Liang, Oliver Salazar Celis, Damiaan Lemmens, Jacques Tempère, Annie Cuyt, *Determining and benchmarking the implied risk-neutral asset price distributions from option prices*, submitted, 2012.

# References


[1] John C. Hull. *Options, Futures and Other Derivatives*. Prentice Hall, 7 edition, 2009. 5, 14

[2] CFA Institute. *Derivatives and portfolio management*, **6** of *CFA program curriculum Level II 2012*. Pearson, 2012. 5, 6, 20

[3] Greg Kuserk. *Financial derivatives: pricing and risk management*, chapter 3, pages 69–81. Kolb series in finance. John Wiley & Sons, 2010. 15

[4] CFA Institute. *Equity and fixed income*, **5** of *CFA program curriculum Level I 2011*. Pearson, 2011. 17

[5] Monetary and Economic Department. **OTC derivatives market activity in the first half of 2011**. Technical report, Bank for International Settlements, November 2011. 19

[6] Eugene F. Fama. **The Behavior of Stock-Market Prices**. *The Journal of Business*, **38**(1):34–105, 1965. 22

[7] Bachelier Louis. **Théorie de la spéculation**. *Annales Scientifiques de l'École Normale Supérieure*, **3**(17):21–86, 1900. 22

[8] Samuelson Paul. **Rational theory of warrant pricing**. *Industrial Management Review*, **6**(2):13–32, 1965. 23

[9] Black F. and Scholes M. **The pricing of options and corporate liabilities**. *Journal of Political Economy*, **81**:637–659, 1973. 23, 27, 183

[10] Merton R. C. **The theory of rational option pricing**. *The Bell Journal of Economics and Management Science*, **4**:141–183, 1973. 23

[11] Rama Cont and Peter Tankov. *Financial modelling with jump processes*. Chapman & Hall / CRC, 2004. 26, 33, 35, 36, 70, 83

[12] Roger Lee. **Implied Volatility: Statics, Dynamics, and Probabilistic Interpretation**. In *Recent Advances in Applied Probability*, pages 241–268. Springer US, 2005. 28

[13] Gatheral Jim. *The volatility surface: A practitioner's guide*. John Wiely & Sons, 2006. 28, 34, 35, 83

[14] Dupire Bruno. **A new approach for understanding the impact of volatility on option prices**. *ICBI Global Derivatives*, 1998. 28

[15] Yanhui Liu, Parameswaran Gopikrishnan, Cizeau, Meyer, Peng, and H. Eugene Stanley. **Statistical properties of the volatility of price fluctuations**. *Physical Review E*, **60**(2):1390–1400, 1999. 32, 74, 77, 87

[16] Yanhui Liu, Pierre Cizeaua, Martin Meyera, C.-K. Peng, and H. Eugene Stanley. **Correlations in economic time series**. *Physica A: Statistical Mechanics and its Applications*, **245**(3-4):437–440, 1997. 32

[17] F. Comte and E. Renault. **Long memory continuous time models**. *Journal of Econometrics*, **73**(1):101–149, 1996. 32

[18] F. Comte and E. Renault. **Long memory in continuous-time stochastic volatility models**. *Mathematical Finance*, **8**(4):291–323, 1998. 32

[19] Myron T. Greene and Bruce D. Fielitz. **Long-term dependence in common stock returns**. *Journal of Financial Economics*, **4**(3):339–349, 1977. 32

[20] Ser-Huang Poon and Clive W. J. Granger. **Forecasting volatility in financial markets: A review**. *Journal of Economic Literature*, **XLI**:478–539, 2003. 32

[21] Adrian Rodney Pagan. **The econometrics of financial markets**. *Journal of Empirical Finance*, **3**(1):15–102, 1996. 32

[22] Eugene F. Fama. **Efficient Capital Markets: A Review of Theory and Empirical Work**. *Journal of Finance*, **25**(2):383–417, 1970. 32, 34

[23] Eugene F. Fama. **Efficient Capital Markets: II**. *The Journal of Finance*, **46**(5):1575–1617, 1991. 32

[24] Rama Cont. **Empirical properties of asset returns: stylized facts and statistical issues**. *Quantitative Finance*, **1**:223–236, 2001. 32

[25] Rosario and Nunzio Mantegna. **Lévy walks and enhanced diffusion in Milan stock exchange**. *Physica A: Statistical Mechanics and its Applications*, **179**(2):232 – 242, 1991. 32

[26] M. Potters, R. Cont, and J.-P. Bouchaud. **Financial markets as adaptive systems**. *Europhysics Letters*, **41**(3):239–244, 1998. 32

[27] Rosario N. Mantegna and H. Eugene Stanley. **Scaling behaviour in the dynamics of an economic index**. *Nature*, **376**:46–9, 1995. 32

[28] P. Gopikrishnan, M. Meyer, L. A. N. Amaral, and H. E. Stanley. **Inverse cubic law for the distribution of stock price variations**. *The European Physical Journal B*, **3**(2):139–140, 1998. 32

[29] S. Ghashghaie, W. Breymann, J. Peinke, P. Talkner, and Y. Dodge. **Turbulent cascades in foreign exchange markets**. *Nature*, **381**:767–770, 1996. 32

[30] Dennis W. Jansen and Casper G. de Vries. **On the Frequency of Large Stock Returns: Putting Booms and Busts into Perspective**. *The Review of Economics and Statistics*, **73**(1):18–24, 1991. 32

[31] Francois M Longin. **The Asymptotic Distribution of Extreme Stock Market Returns**. *The Journal of Business*, **69**(3):383–408, 1996. 32

[32] Joseph Chen, Harrison Hong, and Jeremy C. Stein. **Forecasting crashes: trading volume, past returns, and conditional skewness in stock prices**. *Journal of Financial Economics*, **61**(3):345–381, 2001. 32

[33] J. Clay Singleton and John Wingender. **Skewness Persistence in Common Stock Returns**. *The Journal of Financial and Quantitative Analysis*, **21**(3):335–341, 1986. 32

[34] C.J. Adcock and K. Shutes. **An analysis of skewness and skewness persistence in three emerging markets**. *Emerging Markets Review*, **6**(4):396–418, 2005. 32

[35] Erik Van der Straeten and Christian Beck. **Superstatistical fluctuations in time series: Applications to share-price dynamics and turbulence**. *Physical Review E*, **80**(3):036108, 2009. 33, 77, 87

[36] Erik Van der Straeten and Christian Beck. **Dynamical modelling of superstatistical complex systems**. *Physica A Statistical Mechanics and its Applications*, **390**:591, 2011. 33

[37] Denis Nikolaevich Sob'yanin. **Generalization of the Beck-Cohen superstatistics**. *Physical Review E*, **84**:051128, 2011. 33

[38] Parameswaran Gopikrishnan, Vasiliki Plerou, Luís A. Nunes Amaral, Martin Meyer, and H. Eugene Stanley. **Scaling of the distribution of fluctuations of financial market indices**. *Phys. Rev. E*, **60**:5305–5316, 1999. 33

[39] **Fractional calculus and continuous-time finance**. *Physica A: Statistical Mechanics and its Applications*, **284**(1-4):376–384, 2000. 33

[40] Rosario N. Mantegna and H. Eugene Stanley. *Introduction to Econophysics: Correlations and Complexity in Finance*. Cambridge University Press, Cambridge, 2000. 33, 175

[41] Jean-Philippe Bouchaud and Marc Potters. *Theory of Financial Risk and Derivative Pricing: From Statistical Physics to Risk Management*. Cambridge University Press, 2 edition, 2004. 33, 37, 128

[42] John Y. Campbell and Andrew W. Lo. *The Econometrics of Financial Markets*. Princeton University Press, 1997. 33

[43] Ken Kiyono, Zbigniew R. Struzik, and Yoshiharu Yamamoto. **Criticality and Phase Transition in Stock-Price Fluctuations**. *Physical Review Letters*, **96**(6):068701, 2006. 33

[44] Cox J. C. **Note on option pricing I: constant elasticity of variance diffusions**. *Working paper*, 1975. 34

[45] John C. Cox and Stephen A. Ross. **The valuation of options for alternative stochastic processes**. *Journal of Financial Economics*, **3**(1-2):145–166, 1976. 34

[46] D.C. Emmanuel and J.D. MacBeth. **Further results on the constant elasticity of variance call option pricing model**. *Journal of Financial and Quantitative Analysis*, **17**(4):533–554, 1982. 34

[47] Rubinstein Mark. **Displaced Diffusion Option Pricing**. *Journal of Finance*, **38**(1):213–17, 1983. 34

[48] Ingersoll J. **Valuing foreign exchange options with a bounded exchange rate process**. *Review of Derivatives Research*, **1**:159–181, 1996. 34

[49] Rady S. **Option pricing in the presence of natural boundaries and a quadratic diffusion term**. *Finance and Stochastics*, **1**(4):331–344, 1997. 34

[50] Zuhlsdorff C. **The pricing of derivatives on assets with quadratic volatility**. *Working paper*, 1999. 34

[51] Lipton A. **Exact pricing formula for call and double-no-touch options in the universal volatility framework**. *Working paper*, 2000. 34

[52] E. Derman and I. Kani. **Riding on a Smile**. *Risk magazine*, **7**(2):32–39, 1994. 34

[53] M.E. Rubinstein. **Implied Binomial Trees**. *Journal of Finance*, **69**:771–818, 1994. 34

[54] Dupire B. **Pricing with a Smile**. *Risk magazine*, **7**(1):18–20, 1994. 34

[55] Benoit Mandelbrot. **The Variation of Certain Speculative Prices**. *The Journal of Business*, **36**:394, 1963. 34

[56] R R Officer. **The Variability of the Market Factor of the New York Stock Exchange**. *The Journal of Business*, **46**(3):434–53, July 1973. 34

[57] Fischer Black and Myron S Scholes. **The Valuation of Option Contracts and a Test of Market Efficiency**. *Journal of Finance*, **27**(2):399–417, 1972. 34

[58] Neil Shephard, editor. *Stochastic volatility: Selected readings*. Advanced Texts in Econometrics. Oxford University Press, New York, 2005. 34

[59] Ser-Huang Poon. *A Practical Guide to Forecasting Financial Market Volatility*. John Wiley & Sons, 2005. 34

[60] Riccardo Rebonato. *Volatility and Correlation: The Perfect Hedger and the Fox*. John Wiley & Sons, 2nd edition, 2004. 34

[61] Jean-Pierre Fouque, George Papanicolaou, and K. Ronnie Sircar. *Derivatives in Financial Markets with Stochastic Volatility*. Cambridge University Press, 2000. 34

[62] Antonio Mele and Fabio Fornari. *Stochastic Volatility in Financial Markets: Crossing the Bridge to Continuous Time*. Springer, 2000. 34

[63] Stephen J. Taylor. **Modeling Stochastic Volatility: A Review And Comparative Study**. *Mathematical Finance*, **4**(2):183–204, 1994. 34

[64] Peter K Clark. **A Subordinated Stochastic Process Model with Finite Variance for Speculative Prices**. *Econometrica*, **41**(1):135–55, 1973. 34

[65] Robert C. Blattberg and Nicholas J. Gonedes. **A Comparison of the Stable and Student Distributions as Statistical Models for Stock Prices**. *The Journal of Business*, **47**(2):244–280, 1974. 34

[66] George E Tauchen and Mark Pitts. **The Price Variability-Volume Relationship on Speculative Markets**. *Econometrica*, **51**(2):485–505, 1983. 34

[67] Torben G Andersen. **Return Volatility and Trading Volume: An Information Flow Interpretation of Stochastic Volatility**. *Journal of Finance*, **51**(1):169–204, 1996. 34

[68] Thierry Ané and Hélyette Geman. **Order Flow, Transaction Clock, and Normality of Asset Returns**. *Journal of Finance*, **55**(5):2259–2284, 2000. 34

[69] Stephen J. Taylor. **Conjectured Models for Trends in Financial Prices, Tests and Forecasts**. *Journal of the Royal Statistical Society. Series A (General)*, **143**(3):338–362, 1980. 34

[70] O. Vasicek. **An equilibrium characterization of the term structure**. *Journal of Financial Economics*, **5**(2):177–188, 1977. 34

[71] Herb Johnson and David Shanno. **Option Pricing when the Variance is Changing**. *The Journal of Financial and Quantitative Analysis*, **22**(2):143–151, 1987. 34

[72] James B. Wiggins. **Option values under stochastic volatility: Theory and empirical estimates**. *Journal of Financial Economics*, **19**(2):351 – 372, 1987. 34

[73] John C Hull and Alan D White. **The Pricing of Options on Assets with Stochastic Volatilities**. *Journal of Finance*, **42**(2):281–300, 1987. 34

[74] Louis O. Scott. **Option Pricing when the Variance Changes Randomly: Theory, Estimation, and an Application**. *The Journal of Financial and Quantitative Analysis*, **22**(4):419–438, 1987. 34

[75] Elias M Stein and Jeremy C Stein. **Stock Price Distributions with Stochastic Volatility: An Analytic Approach**. *Review of Financial Studies*, **4**(4):727–52, 1991. 34

[76] S. L. Heston. **A closed-form solution for options with stochastic volatility with applications to bond and currency options**. *The Review of Financial Studies*, **6**(2):327–343, 1993. 34, 84, 90, 91, 104, 120, 149, 183

[77] William Feller. **The Parabolic Differential Equations and the Associated Semi-Groups of Transformations**. *The Annals of Mathematics*, **55**(3):pp. 468–519, 1952. 35

[78] D. Duffie, D. Filipović, and W. Schachermayer. **Affine processes and applications in finance**. *The Annals of Applied Probability*, **13**(3):984–1053, 2003. 35

[79] Artur Sepp. *Affine models in mathematical finance: An analytical approach*. PhD thesis, University of Tartu, Tartu, 2007. 35, 41, 46

[80] Damiano Brigo and Fabio Mercurio. *Interest Rate Models - Theory and Practice: With Smile, Inflation and Credit*. Springer, 2006. 35

[81] Robert C. Merton. **Option pricing when underlying stock returns are discontinuous**. *Journal of Financial Economics*, **3**(1-2):125–144, 1976. 35, 82

[82] S. G. Kou. **A Jump-Diffusion Model for Option Pricing**. *Management Science*, **48**(8):1086–1101, 2002. 35, 82

[83] Lipton A. **Assets with jumps**. *Risk magazine*, **15**:149–153, 2002. 35

[84] Darrell Duffie, Jun Pan, and Kenneth Singleton. **Transform Analysis and Asset Pricing for Affine Jump-Diffusions**. *Econometrica*, **68**(6):1343–1376, 2000. 35, 74, 149

[85] Peter Carr, Hélyette Geman, Dilip B. Madan, and Marc Yor. **The Fine Structure of Asset Returns: An Empirical Investigation**. *The Journal of Business*, **75**(2):305–332, 2002. 35, 69, 184

[86] S. James Press. **A Compound Events Model for Security Prices**. *The Journal of Business*, **40**(3):317–335, 1967. 35

[87] Helyette Geman. **Pure jump Levy processes for asset price modelling**. *Journal of Banking & Finance*, **26**(7):1297–1316, 2002. 35

[88] H. Geman and M. Yor D. Madan. *Quantitative Analysis in Financial Markets*, **II**, chapter Asset Prices are Brownian Motion : only in Business Time. World Scientific, 2000. 35

[89] Dilip B. Madan, Peter P. Carr, and Eric C. Chang. **The Variance Gamma Process and Option Pricing**. *European Finance Review*, **2**(1):79–105, 1998. 35

[90] Dilip B. Madan and Eugene Seneta. **The Variance Gamma (V.G.) Model for Share Market Returns**. *The Journal of Business*, **63**(4):511–524, 1990. 35

[91] Dilip B. Madan and Frank Milne. **Option Pricing With V. G. Martingale Components**. *Mathematical Finance*, **1**(4):39–55, 1991. 35

[92] Peter Carr and Dilip B. Madan. **Option valuation using the fast Fourier transform**. *The Journal of Computational Finance*, **2**(4):61–73, 1998. 35, 41

[93] Tina Hviid Rydberg. **The normal inverse gaussian Lévy process: simulation and approximation**. *Stochastic Models*, **13**(4):887–910, 1997. 35

[94] OLE E. BARNDORFF-NIELSEN. **Normal Inverse Gaussian Distributions and Stochastic Volatility Modelling**. *Scandinavian Journal of Statistics*, **24**(1):1–13, 1997. 35

[95] OLE E. BARNDORFF-NIELSEN. **Processes of normal inverse Gaussian type**. *Finance and Stochastics*, **2**:41–68, 1997. 35

[96] ISMO KOPONEN. **Analytic approach to the problem of convergence of truncated Lévy flights towards the Gaussian stochastic process**. *Physical Review E*, **52**:1197–1199, 1995. 35

[97] **Tempering stable processes**. *Stochastic Processes and their Applications*, **117**(6):677–707, 2007. 35

[98] SVETLANA I. BOYARCHENKO AND SERGEI Z. LEVENDORSKII. *Non-Gaussian Merton-Black-Scholes Theory*. World Scientific, 2002. 35

[99] ANDREW MATACZ. **Financial modeling and option theory with the truncated Lévy process**. *International Journal of Theoretical and Applied Finance*, **3**(1):143–160, 2000. 35

[100] HAGEN KLEINERT. *Path Integrals in Quantum Mechanics, Statistics, Polymer Physics, and Financial Markets*. World Scientific, Singapore, 5th edition, 2009. 35, 37, 60, 62, 74, 90, 91, 94, 113, 175

[101] O. BARNDORFF-NIELSEN. **Exponentially Decreasing Distributions for the Logarithm of Particle Size**. *Proceedings of the Royal Society of London A: Mathematical Physical & Physical Sciences*, **353**(1674):401–419, 1977. 35

[102] E. EBERLEIN AND KELLER U. **Hyperbolic distributions in finance**. *Bernoulli*, **1**:281–299, 1995. 35

[103] ERNST EBERLEIN AND SEBASTIAN RAIBLE. **Term Structure Models Driven by General Lévy Processes**. *Mathematical Finance*, **9**(1):31–53, 1999. 35

[104] O. E. Barndorff-Nielsen. *Levy Processes: Theory and Applications*. Birkhauser, 2001. 35

[105] Ernst Eberlein, Ulrich Keller, and Karsten Prause. **New insights into smile, mispricing and value at risk: The hyperbolic model**. *Journal of Business*, **71**:371–406, 1998. 35

[106] N. H. Bingham and Rüdiger Kiesel. *Return distributions in finance*, chapter Modelling asset returns with hyperbolic distributions, pages 1–20. Butterworth-Heinemann, 2001. 35

[107] Peter Carr and Liuren Wu. **Time-Changed Levy Processes and Option Pricing**. *Journal of Financial Economics*, **17**(1):113–141, 2004. 36

[108] Peter Carr, Roger Lee, and Liuren Wu. **Variance Swaps on Time-Changed Levy Processes**. *Finance and Stochastics*, forthcoming. 36

[109] Wim Schoutens. *Levy Processes in Finance: Pricing Financial Derivatives*. Wiley, 2003. 36, 66, 67, 70, 184

[110] Andreas Kyprianou, Wim Schoutens, and Paul Wilmott, editors. *Exotic Option Pricing and Advanced Lévy Models*. Wiley, 2005. 36, 77

[111] Kyriakos Chourdakis. *Regime-Switching Models*. John Wiley & Sons, Ltd, 2010. 36

[112] Kaushik I. Amin and Victor K. Ng. **Option Valuation with Systematic Stochastic Volatility**. *The Journal of Finance*, **48**(3):881–910, 1993. 36

[113] Gurdip S. Bakshi and Zhiwu Chen. **An alternative valuation model for contingent claims**. *Journal of Financial Economics*, **44**(1):123–165, 1997. 36

[114] Louis O. Scott. **Pricing Stock Options in a Jump-Diffusion Model with Stochastic Volatility and Interest Rates: Applications of Fourier Inversion Methods**. *Mathematical Finance*, **7**(4):413–426, 1997. 36

[115] D. Lemmens, M. Wouters, J. Tempere, and S. Foulon. **Path integral approach to closed-form option pricing formulas with applications to stochastic volatility and interest rate models**. *Physical Review E*, **78**:016101, 2008. 36, 37, 74, 76, 77, 106, 149, 151

[116] Torben G. Andersen, Luca Benzoni, and Jesper Lund. **An Empirical Investigation of Continuous-Time Equity Return Models**. *The Journal of Finance*, **57**(3):1239–1284, 2002. 36

[117] David S. Bates. **Jumps and stochastic volatility: exchange rate processes implicit in deutsche mark options**. *The Review of Financial Studies*, **9**(1):69–107, 1996. 36, 75

[118] Charles Cao, Gurdip Bakshi, and Zhiwu Chen. **Empirical Performance of Alternative Option Pricing Models**. *The Journal of Finance*, **52**(5):2003–2049, 1997. 36

[119] Mikhail Chernov, A. Ronald Gallant, Eric Ghysels, and George Tauchen. **Alternative models for stock price dynamics**. *Journal of Econometrics*, **116**(1-2):225–257, 2003. 36

[120] B. Eraker, Michael Johannes, and Nicholas Polson. **The Impact of Jumps in Volatility and Returns**. *The Journal of Finance*, **58**(3):1269–1300, 2003. 36

[121] Jun Pan. **The jump-risk premia implicit in options: evidence from an integrated time-series study**. *Journal of Financial Economics*, **63**(1):3–50, 2002. 36

[122] Artur Sepp. **Pricing options on realized variance in the Heston model with jumps in returns and volatility**. *The Journal of Computational Finance*, **11**(4):33–70, 2008. 36, 74, 77, 87, 92, 120, 122, 141

[123] Belal E. Baaquie. *Quantum Finance: Path Integrals and Hamiltonians for Options and Interest Rates*. Cambridge University Press, 2004. 37, 74

[124] Belal E. Baaquie. *Interest Rates and Coupon Bonds in Quantum Finance*. Cambridge University Press, 2009. 37, 74

[125] Vadim Linetsky. **The Path Integral Approach to Financial Modeling and Options Pricing**. *Computational Economics*, **11**:129–163, 1998. 37, 114

[126] E. Bennati, M. Rosa-Clot, and S. Taddei. **A path integral approach to derivative security pricing I: Formalism and analytical results**. *International Journal of Theoretical and Applied Finance*, **2**(4):381–407, 1999. 37, 50

[127] Marc Goovaerts, Ann De Schepper, and Marc Decamps. **Closed-form approximations for diffusion densities: a path integral approach**. *Journal of Computational and Applied Mathematics*, **164-165**:337–364, 2004. 37

[128] W. Heisenberg. **Über quantentheoretische Umdeutung kinematischer und mechanischer Beziehungen**. *Zeitschrift für Physik*, **33**:879–893, 1925. 37

[129] M. Born and P. Jordan. **Zur Quantenmechanik**. *Zeitschrift für Physik*, **34**:858–888, 1925. 37

[130] M. Born, W. Heisenberg, and P. Jordan. **Zur Quantenmechanik II**. *Zeitschrift für Physik*, **35**:557–615, 1926. 37

[131] E. Schrödinger. **An Undulatory Theory of the Mechanics of Atoms and Molecules**. *Physical Review*, **28**(6):1049–1070, 1926. 37

[132] E. Schrödinger. **Quantisierung als Eigenwertproblem; von Erwin Schrödinger**. *Annalen der Physik*, pages 361–377, 1926. 37

[133] R. P. Feynman. *A Principle of Least Action in Quantum Mechanics*. PhD thesis, Princeton University, 1942. 37

[134] R. P. Feynman. **Space-time Approach to Non-relativistic Quantum Mechanics**. *Reviews of Modern Physics*, **20**:367, 1948. 37, 62

[135] R. P. Feynman and A. R. Hibbs. *Quantum Mechanics and Path Integral*. McGraw-Hill, 1965. 37

[136] R. P. Feynman. **The Development of the Space-Time View of Quantum Electrodynamics (Nobel Lecture in Physics, 1965)**. *Science*, **153**:699–708, 1966. 37

[137] J. von Neumann. **Die Eindeutigkeit der Schrödingerschen Operatoren**. *Mathematische Annalen*, **104**:570–578, 1931. 38

[138] A. Truman. **Feynman path integrals and quantum mechanics as** $\hbar \to 0$. *Journal of Mathematical Physics*, **17**:1852, 1976. 39

[139] A. Truman. **Classical mechanics, the diffusion (heat) equation, and the Schorödinger equation**. *Journal of Mathematical Physics*, **18**:2308, 1977. 39

[140] A. Truman. **The Feynman maps and the Wiener integral**. *Journal of Mathematical Physics*, **19**:1742, 1978. 39

[141] Paul Glasserman. *Monte Carlo Methods in Financial Engineering*. Springer, 2003. 40

[142] G. Petrella and S. G. Kou. **Numerical pricing of discrete barrier and lookback options via Laplace transforms**. *Journal of Computational Finance*, **8**:1–37, 2004. 41

[143] F. Fang and C. W. Oosterlee. **A Novel Pricing Method for European Options Based on Fourier-Cosine Series Expansions**. *SIAM J. Sci. Comput.*, **31**:826–848, November 2008. 41, 43, 150, 154, 203

[144] L. Z.J. Liang, D. Lemmens, and J. Tempere. **Generalized pricing formulas for stochastic volatility jump diffusion models applied to the exponential Vasicek model**. *The European Physical Journal B - Condensed Matter and Complex Systems*, **75**:335–342, 2010. 41, 73, 202

[145] L. Z.J. Liang, D. Lemmens, and J. Tempere. **Path integral approach to the pricing of timer options with the Duru-Kleinert time transformation**. *Physical Review E*, **83**:056112, 2011. 42, 89, 114, 133, 138, 202

[146] L. Z.J. Liang, O. Salazar Celis, D. Lemmens, J. Tempere, and A. Cuyt. **Determining and benchmarking the implied risk neutral asset price distributions from option prices**. *Submitted*, 2012. 44, 175, 203

[147] C. W. Gardiner. *Handbook of Stochastic Methods for Physics, Chemistry and the Natural Sciences*. Springer, 3nd, 2004. 46, 48, 76

[148] U. Deininghaus and R. Graham. **Nonlinear point transformations and covariant interpretation of path integrals**. *Zeitschrift für Physik B*, **34**(2):211–219, 1979. 50

[149] Flor Langouche, D. Roekaerts, and E. Tirapegui. *Functional Integration and Semiclassical Expansions*. D. Reidel Publishing Company, Holland, 2010. 50

[150] John C. Cox, Jr. Ingersoll, Jonathan E., and Stephen A. Ross. **A Theory of the Term Structure of Interest Rates**. *Econometrica*, **53**(2):385–407, 1985. 54, 149

[151] I. S. Gradshteyn and I. M. Ryzhik. *Table of integrals, series, and products*. Elsevier Inc., 7th edition, 2007. 56

[152] M. J. Goovaerts and J. T. Devreese. **Analytic Treatment of the Coulomb Potential in the Path Integral Formalism by Exact Summation of a Perturbation Expansion**. *Journal of Mathematical Physics*, **7**:1070–1082, 1972. 59

[153] I. H. Duru and H. Kleinert. **Solution of the path integral for the H-atom**. *Physics letters*, **84B**(2), 1979. 59, 90

[154] Christian Grosche. **An Introduction into the Feynman Path Integral**. *arXiv:hep-th/9302097v1*, 1993. 62, 102

[155] Christian Grosche and Frank Steiner. *Handbook of Feynman Path Integrals*. Springer-Verlag, Berlin Heidelberg, 1998. 62, 101, 105, 123

[156] Frank Steiner. **Space-time transformations in radial path integrals**. *Physics Letters*, **106A**(8), 1984. 62

[157] H. U. Gerber and E. S. W. Shiu. **Option pricing by Esscher-transforms**. *Transactions of the Society of Actuaries*, **46**:99–191, 1994. 70

[158] H. U. Gerber and E. S. W. Shiu. **Actuarial bridges to dynamic hedging and option pricing**. *Insurance: Mathematics and Economics*, **18**(3):183–218, 1996. 70

[159] Guoqing Yan and Floyd B. Hanson. **Option Pricing for a Stochastic-Volatility Jump-Diffusion Model with Log-Uniform Jump-Amplitudes**. *Proceedings of the 2006 American Control Conference*, 2006. 74

[160] Salvatore Micciche, Giovanni Bonanno, Fabrizio Lillo, and Rosario N Mantegna. **Volatility in financial markets: stochastic models and empirical results**. *Physica A: Statistical Mechanics and its Applications*, **314**(1-4):756–761, 2002. 74, 77, 87

[161] Marc Chesney and Louis Scott. **Pricing European Currency Options: A Comparison of the Modified Black-Scholes Model and a Random Variance Model**. *Journal of Financial and Quantitative Analysis*, **24**(3):267–284, 1989. 77, 79

[162] P. Nozieres and S. Schmitt-Rink. **Bose condensation in an attractive fermion gas: From weak to strong coupling superconductivity**. *Journal of Low Temperature Physics*, **59**:195–211, 1985. 79

[163] C. A. R. Sá de Melo, Mohit Randeria, and Jan R. Engelbrecht. **Crossover from BCS to Bose superconductivity: Transition temperature and time-dependent Ginzburg-Landau theory**. *Physical Review Letters*, **71**:3202–3205, 1993. 79

[164] Hagen Kleinert. **Option pricing for non-Gaussian price fluctuations**. *Physica A: Statistical Mechanics and its Applications*, **338**(1-2):151–159, 2004. 82, 98

[165] Yacine Aït-Sahalia and Robert Kimmel. **Maximum likelihood estimation of stochastic volatility models**. *Journal of Financial Economics*, **83**(2):413–452, 2007. 84

[166] Ignacio Pena, Gonzalo Rubio, and Gregorio Serna. **Smiles, Bid-ask Spreads and Option Pricing**. *European Financial Management*, **7**(3):351–374, 2001. 86

[167] Nick Sawyer. SG CIB **Launches timer options**. *Risk magazine*, **20**:6, 2007. 89, 133

[168] E. d. Fontenay. **Hedge fund replication and structured products**. *Societe Generale Asset Management*, 2007. 89

[169] J. B. Roberts. *Stochastic Problems in Dynamics*. Pitman, London, 1977. 89

[170] Katja Lindenberg and Bruce J. West. *Journal of Statistical Physics*, **42**:201–243, 1986. 89

[171] George H. Weiss. **Overview of theoretical models for reaction rates**. *Journal of Statistical Physics*, **42**:3–36, 1986. 90

[172] Peter Hänggi, Peter Talkner, and Michal Borkovec. **Reaction-rate theory: fifty years after Kramers**. *Reviews of Modern Physics*, **62**(2):251–341, 1990. 90

[173] Susanne Ditlevsen and Petr Lansky. **Parameters of stochastic diffusion processes estimated from observations of first-hitting times: Application to the leaky integrate-and-fire neuronal model**. *Physical Review E*, **76**(4):041906, 2007. 90

[174] Adi R. Bulsara, Tim C. Elston, Charles R. Doering, Steve B. Lowen, and Katja Lindenberg. **Cooperative behavior in periodically driven noisy integrate-fire models of neuronal dynamics**. *Physical Review E*, **53**(4):3958–3969, 1996. 90

[175] Enrico Bibbona, Petr Lansky, and Roberta Sirovich. **Estimating input parameters from intracellular recordings in the Feller neuronal model**. *Physical Review E*, **81**(3):031916, 2010. 90

[176] Hari Krovi, Maris Ozols, and Jérémie Roland. **Adiabatic condition and the quantum hitting time of Markov chains**. *Physical Review A*, **82**(2):022333, 2010. 90

[177] Martin Varbanov, Hari Krovi, and Todd A. Brun. **Hitting time for the continuous quantum walk**. *Physical Review A*, **78**(2):022324, 2008. 90

[178] Jaume Masoliver and Josep Perelló. **First-passage and risk evaluation under stochastic volatility**. *Physical Review E*, **80**(1):016108, 2009. 90

[179] Yuri A. Katz and Nikolai V. Shokhirev. **Default risk modeling beyond the first-passage approximation: Extended Black-Cox model**. *Physical Review E*, **82**(1):016116, 2010. 90

[180] S. Redner. *A Guide to First-Passage Processes*. Cambridge University Press, England, 2001. 90

[181] G. H. Weiss. *Aspects and Applications of the Random Walk*. North-Holland, Amsterdam, 1994. 90

[182] Daniel Hawkins and Sebastien Krol. **Product Overview: Timer Options**. *Lehman Brothers Equity Derivatives Strategy*, 2008. Available online at http://www.scribd.com/doc/19601860/Lehman-Brothers-Product-Overview-Timer-Options. 90

[183] A. Neuberger. **Volatility trading**. *London business school working paper*, 1990. 90

[184] Avi Bick. **Quadratic-Variation-Based dynamic strategies**. *Management Science*, **41**:4, 1995. 90

[185] Chengxu Li. **Bessel process, Heston's stochastic volatility model and timer options**. *SSRN eLibrary*, 2010. Available online at http://ssrn.com/paper=1402463. 90, 91, 92, 106, 120

[186] Carole Bernard and Zhenyu Cui. **Pricing of timer options**. *SSRN eLibrary*, 2010. Available online at http://ssrn.com/paper=1612014. 90

[187] David Saunders. **Pricing timer options under fast mean-reverting stochastic volatility**. *To appear, Canadian Applied Mathematics Quarterly*, 2010. 90

[188] Dong Hyun Ahn and Bin Gao. **A parametric nonlinear model of term structure dynamics**. *Review of Financial Studies*, **12**(4):721–762, 1999. 90, 91, 99, 122

[189] I. H. Duru and H. Kleinert. **Quantum Mechanics of H-Atom from Path Integrals**. *Fortschritte der Physik*, **30**:401–435, 1982. 90

[190] Marc Decamps and Ann De Schepper. **Atomic Implied Volatilities**. *SSRN eLibrary*, 2008. Available online at http://ssrn.com/paper=1279363. 90

[191] R. P. Feynman and H. Kleinert. **Effective classical partition functions**. *Physical Review A*, **34**(6):5080–5084, 1986. 91, 113

[192] Jesper Andreasen. *Dynamite dynamics*, chapter 17. Risk Books in association with Application Networks, 2003. 91

[193] Gabriel G. Drimus. **Options on Realized Variance by Transform Methods: A Non-Affine Stochastic Volatility Model**. *SSRN eLibrary*, 2009. Available online at http://ssrn.com/paper=1485648. 91, 108, 109

[194] Christopher S. Jones. **The dynamics of stochastic volatility: evidence from underlying and options markets**. *Journal of Econometrics*, **116**(1-2):181–224, 2003. 91

[195] Gurdip Bakshi, Nengjiu Ju, and Hui Ou-Yang. **Estimation of continuous-time models with an application to equity volatility dynamics**. *Journal of Financial Economics*, **82**(1):227 – 249, 2006. 91

[196] Peter Carr and Jian Sun. **A new approach for option pricing under stochastic volatility**. *Review of Derivatives Research*, **10**:87–150, 2007. 91, 104

[197] Mark Broadie and Ozgur Kaya. **Exact Simulation of Stochastic Volatility and Other Affine Jump Diffusion Processes**. *Operations Research*, **54**(2):217–231, 2006. 109

[198] Paul Glasserman and Kyoung-Kuk Kim. **Gamma expansion of the Heston stochastic volatility model**. *Finance and Stochastics*, **15**:267–296, 2011. 109

[199] Christian Kahl and Peter Jackel. **Fast strong approximation Monte Carlo schemes for stochastic volatility models**. *Quantitative Finance*, **6**(6):513–536, 2006. 109

[200] H. Kleinert. **Systematic corrections to the variational calculation of the effective classical potential**. *Physics Letters A*, **173**(4-5):332–342, 1993. 113

[201] J. P. A. Devreese, D. Lemmens, and J. Tempere. **Path integral approach to** Asian options in the Black-Scholes mode. *Physica A: Statistical Mechanics and its Applications*, **389**(4):780 – 788, 2010. 114

[202] Edward J. Calabrese and Linda A. Baldwin. **Toxicology rethinks its central belief**. *Nature*, **421**:691–692, 2003. 132

[203] Jocelyn Kaiser. **Hormesis: sipping from a poisoned chalice**. *Science*, **302**(5644):376–379, 2003. 132

[204] L. E. Feinendegen. **Evidence for beneficial low-level radiation effects and radiation hormesis**. *British Journal of Radiology*, **78**(925):3–7, 2005. 132

[205] G. Annex. **Biological effects at low radiation doses**. *UNSCEAR 2000 report*, **II**:160, 2000. 132

[206] J. W. Muller. **Counting statistics of short-lived nuclides**. *Journal of Radioanalytical and Nuclear Chemistry*, **61**:345–359, 1981. 132

[207] A. V. Nero, M. B. Schwehr, W. W. Nazaroff, and K. L. Revzan. **Distribution of airborne radon-222 concentrations in U.S. homes**. *Science*, **234**(4779):992–997, 1986. 132, 133

[208] T. Tollefsen, V. Gruber, P. Bossew, and M. De Cort. **Status of the European indoor radon map**. *Radiation Protection Dosimetry*, **145**(2-3):110–116, 2011. 132

[209] P. Bossew. **Radon: exploring the log-normal mystery**. *Journal of Environmental Radioactivity*, **101**(10):826 – 834, 2010. 132

[210] Krisztian Hamori, Eszter Toth, Lenard Pal, George Koteles, Andras Losonci, and Mihaly Minda. **Evaluation of indoor radon measurements in Hungary**. *Journal of Environmental Radioactivity*, **88**(2):189 – 198, 2006. 132

[211] Devis Tuia and Mikhail Kanevski. **Indoor radon distribution in Switzerland: lognormality and Extreme Value Theory**. *Journal of Environmental Radioactivity*, **99**(4):649 – 657, 2008. 132

[212] A. Clouvas, S. Xanthos, and G. Takoudis. **Indoor radon levels in Greek schools**. *Journal of environment radioactivity*, **102**(9):881–5, 2011. 132

[213] I. Janssen and J. H. Stebbings. **Gamma distribution and house 222Rn measurements**. *Health Physics*, **63**(2):205–8, 1992. 132, 133

[214] Patrick Murphy and Catherine Organo. **A comparative study of lognormal, gamma and beta modelling in radon mapping with recommendations regarding bias, sample sizes and the treatment of outliers**. *Journal of Radiological Protection*, **28**(3):293, 2008. 132

[215] G. Salvadori, S. P. Ratti, and G. Belli. **Modelling the chernobyl radioactive fallout (II): A multifractal approach in some European countries**. *Chemosphere*, **33**(12):2359 – 2371, 1996. 132

[216] Adrian A Drăgulescu and Victor M Yakovenko. **Probability distribution of returns in the Heston model with stochastic volatility**. *Quantitative Finance*, **2**(6):443–453, 2002. 133

[217] Peter Hanggi, Kurt E. Shuler, and Irwin Oppenheim. **On the relations between Markovian master equations and stochastic differential equations**. *Physica A: Statistical and Theoretical Physics*, **107**(1):143 – 157, 1981. 139

[218] Helyette Geman and Marc Yor. **Bessel processes, Asian options, and perpetuities**. *Mathematical Finance*, **3**(4):349–375, 1993. 141

[219] Vadim Linetsky. **Spectral Expansions for Asian (Average Price) Options**. *Operations Research*, **52**(6):856–867, 2004. 141

[220] M. Muskulus, K. in 't Hout, J. Bierkens, A. P. C. Van Der Ploeg, J. In't Panhuis, F. Fang, B. Janssens, and C. W. Oosterlee. **The ING problem - a problem from financial industry; three papers on the Heston-Hull-White model**. In *The 58th European Study Group Mathematics with Industry*, Utrecht, The Netherlands, 2007. 149

[221] Lech A. Grzelak and Cornelis W. Oosterlee. **On the Heston Model with Stochastic Interest Rates**. *SIAM Journal on Financial Mathematics*, **2**:255–286, 2011. 149

[222] Lech A. Grzelak and Cornelis W. Oosterlee. **An Equity-Interest Rate Hybrid Model With Stochastic Volatility and the Interest Rate Smile**. MPRA Paper 20574, University Library of Munich, Germany, 2010. 149

[223] Alexey Medvedev and Olivier Scaillet. **Pricing American options under stochastic volatility and stochastic interest rates**. *Journal of Financial Economics*, **98**(1):145–159, 2010. 149, 156, 157, 161, 165, 171

[224] Tinne Haentjens and Karel J. in 't Hout. **ADI finite difference discretization of the Heston-Hull-White PDE**. *AIP conference proceedings / American Institute of Physics*, **1281**:1995–1999, 2010. 149, 150, 167

[225] F. Fang and C. Oosterlee. **Pricing early-exercise and discrete barrier options by fourier-cosine series expansions**. *Numerische Mathematik*, **114**:27–62, 2009. 150, 162

[226] F. Fang and C. W. Oosterlee. **Pricing Options Under Stochastic Volatility with Fourier-Cosine Series Expansions**. In *Progress in Industrial Mathematics at ECMI 2008*, **15**, pages 833–838. 2010. 150, 162, 172

[227] B. Zhang and C. W. Oosterlee. **Efficient pricing of Asian options under Lévy processes based on Fourier cosine expansions. Part I: European-style products**. *Submitted*, 2011. 150, 157

[228] M. J. Ruijter and C. W. Oosterlee. **Two-dimensional Fourier cosine series expansion method for pricing financial options**. *Submitted*, 2012. 150

[229] D. Lemmens, L. Z.J. Liang, J. Tempere, and A. De Schepper. **Pricing bounds for discrete arithmetic Asian options under Lévy models**. *Physica A: Statistical Mechanics and its Applications*, **389**(22):5193–5207, 2010. 150, 202

[230] Chuang-Chang Chang, San-Lin Chung, and Richard C. Stapleton. **Richardson extrapolation techniques for the pricing of American-style options**. *Journal of Futures Markets*, **27**(8):791–817, 2007. 150, 165

[231] Tinne Haentjens, Karel in 't Hout, and Kim Volders. **ADI schemes with Ikonen-Toivanen splitting for pricing American put options in the Heston model**. *AIP conference proceedings / American Institute of Physics - ISSN 0094-243X - 1281*, pages 231–234, 2010. 150, 167, 169

[232] S. Ikonen and J. Toivanen. **Operator splitting methods for American option pricing**. *Applied Mathematics Letters*, **17**(7):809–814, 2004. 150, 170

[233] Samuli Ikonen and Jari Toivanen. **Operator splitting methods for pricing American options under stochastic volatility**. *Numerische Mathematik*, **113**(2):299–324, 2009. 150, 167, 170

[234] K. J. in 't Hout and S. Foulon. **ADI finite difference schemes for option pricing in the Heston model with correlation**. *International Journal of Numerical Analysis and Modeling*, **7**(2):303–320, 2010. 150, 166, 167, 168, 169

[235] Domingo Tavella and Curt Randall. *Pricing Financial Instruments: The Finite Difference Method*. Wiley, 2000. 167

[236] K.J. in 't Hout and B.D. Welfert. **Unconditional stability of second-order ADI schemes applied to multi-dimensional diffusion equations with mixed derivative terms**. *Applied Numerical Mathematics*, **59**(3-4), 2009. 169

[237] Bowen Zhang and Cornelis W. Oosterlee. **Acceleration of option pricing technique on graphics processing units**. *Concurrency and Computation: Practice and Experience*, 2012. 173, 203

[238] Bhupinder Bahra. **Implied Risk-neutral Probability Density Functions From Option Prices: Theory and Application**. *SSRN eLibrary*, 1997. 176, 179

[239] N. Cooper. **Testing techniques for estimating implied RNDs from the prices of European-style options**. Basel, Switzerland, Jun 1999. Proceedings of the Bank for International Settlements Workshop on Estimating and Interpreting Probability Density Functions. 176, 177, 179

[240] Ernst Glatzer and Martin Scheicher. **Modelling the Implied Probability of Stock Market Movements**. *SSRN eLibrary*, 2003. 176, 179

[241] Magnus Andersson and Magnus Lomakka. **Evaluating implied RNDs by some new confidence interval estimation techniques**. *Journal of Banking and Finance*, **29**(6):1535–1557, 2005. 176, 179

[242] Douglas T. Breeden and Robert H. Litzenberger. **Prices of State-Contingent Claims Implicit in Option Prices**. *The Journal of Business*, **51**(4):621–651, 1978. 176, 178, 181

[243] Allan M . Malz. **Estimating the Probability Distribution of the Future Exchange Rate from Option Prices**. *The Journal of Business*, **5**(2):18–36, 1997. 176, 179

[244] Matthias Fengler. **Arbitrage-free smoothing of the implied volatility surface**. *Quantitative Finance*, **9**(04):417–428, 2009. 176, 179

[245] Bernhard Brunner and Reinhold Hafner. **Arbitrage-free estimation of the risk-neutral density from the implied volatility smile**. *The Journal of Computational Finance*, **7**(1), 2003. 176, 179

[246] Eric Jondeau and Michael Rockinger. **Reading the smile: the message conveyed by methods which infer risk neutral densities**. *Journal of International Money and Finance*, **19**(6):885 – 915, 2000. 176, 177

[247] Robert R. Bliss and Nikolaos Panigirtzoglou. **Testing the stability of implied probability density functions**. *Journal of Banking & Finance*, **26**(2-3):381–422, 2002. 176, 177

[248] Rama Cont. **Beyond Implied Volatility: Extracting Information From Option Prices**. *SSRN eLibrary*, 1997. 176

[249] Jose M. Campa, P. H. Kevin Chang, Robert L. Reider, Willem H. Buiter, and Barry Eichengreen. **ERM Bandwidths for EMU and after: Evidence from Foreign Exchange Options**. *Economic Policy*, **12**(24):53–89, 1997. 176

[250] Amine Bouden. **Comparing Risk Neutral Density Estimation Methods using Simulated Option Data**. In *World Congress on Engineering*, pages 1029–1037, 2007. 176

[251] Jens Carsten Jackwerth and Mark Rubinstein. **Recovering Probability Distributions from Option Prices**. *The Journal of Finance*, **51**(5):1611–1631, 1996. 176

[252] Xiaoquan Liu. **Bid-ask spread, strike prices and risk-neutral densities**. *Applied Financial Economics*, **17**(11):887–900, 2007. 176, 177

[253] Stephen Figlewski. *Volatility and Time Series Econometrics: Essaays in Honor of Robert F. Engle*, chapter Estimating the Implied Risk-Neutral Density for the U.S. Market Portfolio, pages 323–353. Oxford University Press, 2010. 177, 190, 191, 192, 196

[254] O. Salazar Celis, A. Cuyt, and B. Verdonk. **Rational approximation of vertical segments**. *Numerical Algorithms*, **45**:375–388, 2007. 180, 182, 183

[255] R. Pacanowski, O. Salazar Celis, C. Schlick, X. Granier, P. Poulin, and A. Cuyt. **Rational BRDF**. *IEEE Transactions on Visualization and Computer Graphics*, 2011. 182

[256] T. Pomentale. **On discrete rational least squares approximation**. *Numerische Mathematik*, **12**(1):40–46, 1968. 182

[257] Hoa Nguyen, Annie Cuyt, and Oliver Salazar Celis. **Comonotone and coconvex rational interpolation and approximation**. *Numerical Algorithms*, **58**:1–21, 2011. 182

[258] S.P. Boyd and L. Vandenberghe. *Convex optimization*. Cambridge University Press, 2004. 182, 192

[259] Adrian Wills. **Quadratic Programming in C - MATLAB interface**. http://sigpromu.org/quadprog/. 182